# PHYTOALEXINS FROM CRUCIFERS: PROBING DETOXIFICATION PATHWAYS IN *SCLEROTINIA SCLEROTIORUM*

A Thesis Submitted to the
College of Graduate Studies and Research
in Partial Fulfillment of the Requirements
for the Degree of
Doctor of Philosophy
in the
Department of Chemistry
University of Saskatchewan
Saskatoon
By

**Mohammad Hossain**

# PERMISSION TO USE

In presenting this thesis in partial fulfillment of the requirements for a Postgraduate degree from the University of Saskatchewan, I agree that the Libraries of this University may make it freely available for inspection. I further agree that permission for copying of this thesis in any manner, in whole or in part, for scholarly purposes may be granted by the professor or professors who supervised my thesis work or, in their absence, by the Head of the Department or the Dean of the College in which my thesis work was done. It is understood that any copying or publication or use of this thesis or parts thereof for financial gain shall not be allowed without my written permission. It is also understood that due recognition shall be given to me and to the University of Saskatchewan in any scholarly use which may be made of any material in my thesis.

Requests for permission to copy or to make other use of material in this thesis in whole or part should be addressed to:

Head of the Department of Chemistry
University of Saskatchewan
Saskatoon, Saskatchewan (S7N 5C9)

# ABSTRACT

This thesis investigates two aspects of phytoalexin metabolism by the phytopathogenic fungus *Sclerotinia sclerotiorum* (Lib) de Bary: (i) determination of detoxification pathways of structurally different molecules; (ii) design and synthesis of potential inhibitors of enzyme(s) involved in detoxification steps.

First, the transformations of important cruciferous phytoalexins by the economically important stem rot fungus, *S. sclerotiorum*, were investigated. During these studies a number of new metabolic products were isolated, their chemical structures were determined using spectroscopic techniques, and further confirmed by synthesis. The metabolic products did not show detectable antifungal activity against *S. sclerotiorum* which indicated that these metabolic transformations were detoxification processes. Overall, the results of these transformations suggested that *S. sclerotiorum* produces various enzymes that can detoxify cruciferous phytoalexins via different pathways. While the detoxifications of strongly and moderately antifungal phytoalexins such as brassilexin, sinalexin, and 1-methoxybrassinin were fast and led to glucosylated products, the transformations of the weakly antifungal phytoalexins brassicanal A, spirobrassinin and 1-methoxyspirobrassinin were very slow and yielded non-glucosylated compounds.

Next, the design of potentially selective inhibitors of the brassinin detoxification enzyme, BGT, was sought. Two sets of potential inhibitors of BGT were designed: (i) a group was based on the structure of brassinin, where the indole ring of brassinin was replaced with benzofuran, thianaphthene, 7-azaindole and pyrazolo[1,5-a]pyridine and/or the position of side chain was changed from C-3 to C-2; and (ii) another group based on the structure of camalexin where the thiazole ring of camalexin was replaced with a phenyl group. The syntheses and chemical characterization of

these potential detoxification inhibitors, along with their antifungal activity, as well as screening using fungal cultures and cell-free extracts of *S. sclerotiorum*, were examined. The results of these screening indicated that 3-phenylindoles, 3-phenylbenzofuran, 5-fluorocamalexin, methyl (indol-2-yl)methyl-dithiocarbamate, methyl (benzofuran-3-yl)methyldithiocarbamate and methyl (benzo-furan-2-yl)methyldithiocarbamate could slow down the rate of detoxification of brassinin in fungal cultures and also in cell-free extracts of *S. sclerotiorum*. Among the designed compounds, 3-phenylindole appeared to be the best inhibitor both in fungal cultures and in cell-free extracts. Metabolism studies of all the designed compounds using fungal cultures of *S. sclerotiorum* indicated that they were metabolized by *S. sclerotiorum* to glucosyl derivatives, although at much slower rates.

It is concluded that some inhibitors that can slow down the rate of metabolism of brassinin could be good leading structures to design more active inhibitors of BGT.

# ACKNOWLEDGEMENTS

I would like to express my deep and sincere gratitude to my supervisor, Dr. M. Soledade C. Pedras, Throvaldson Professor, Department of Chemistry, University of Saskatchewan. Her wide knowledge and her logical way of thinking have been of great value for me. Her understanding, encouraging and personal guidance have provided a good basis for the present thesis.

I wish to express my warm and sincere thanks to my advisory committee members: Dr. Marek Majewski, Professor and Head, Department of Chemistry; Dr. Ed S. Krol, Assistant Professor, College of Pharmacy and Nutrition; and Dr. Art Davis, Professor, Department of Biology, for their constructive criticism, valuable advice and friendly help during my Ph. D. work.

I would also like to extend my thanks to the external examiner, Dr. Romas Kazlauskas, Professor, Department of Biochemistry, Molecular Biology & Biophysics & the Biotechnology Institute, University of Minnesota, for his detailed review of my thesis and excellent advice during my Ph. D. defence.

I wish to extend my warmest thanks to Dr. Keith Brown, Dr. Gabrielle Schatte and Mr. Ken Thoms for their help with NMR and Mass spectrometry instrumentations and to all those who have helped me with my work during my graduate study in the Department of Chemistry.

I wish to express my gratitude to all past and present members of Pedras group: Dr. N. Ismail, Dr. V. Uppala, Dr. S. Montaut, Dr. P. W. K. Ahiahonu, Dr. P. B. Chumala, Dr. M. Jha, Dr. M. Suchy, Dr. R. Gadagi, Dr. O. Okeola, Dr. Q. A. Zheng, Dr. A. Adio, V. Cekic, J. Liu, G. Sarwar, D. Okinyo, Y. Yu, V. K. Sarma, S. Hossain, S. Islam, I. Khalaff, and W. Jin.

I owe my loving thanks to my wife Farhana Mitul and to my sweet little daughter Ilana Hossain. Without their encouragement and understanding it would have been impossible for me to finish this work. I also express my heart felt gratitude to my parents and brothers for their loving support.

The financial support of the Department of Chemistry and the Graduate Studies and Research is gratefully acknowledged.

# Dedication:

*To my parents,*

*Mohd. Awlad Hossain and Shahida Hossain*

*and*

*To my wife,*

*Farhana Arman Mitul*

# TABLE OF CONTENTS

**Permission to use…… ..i**

**Abstract……. ii**

**Acknowledgements……iv**

**Dedication……v**

**Table of contents……vi**

**List of figures……xiii**

**List of tables……..xvi**

**List of abbreviations……....xvii**

***Chapter 1: INTRODUCTION*** ..... *1*

**1.1 General objectives** ..... **1**

**1.2 Cruciferous plants** ..... **2**

**1.3 Fungal pathogens of cruciferous crops** ..... **3**

1.3.1 Blackleg disease ..... 5

1.3.2 Alternaria blackspot disease ..... 5

1.3.3 Root rot disease ..... 6

1.3.4 Stem rot disease ..... 7

**1.4 Chemical defenses of plants** ..... **9**

1.4.1 Constitutive chemical defenses ..... 10

1.4.2 Induced chemical defenses ..... 11

1.4.2.1 Phytoalexins ..... 12

1.4.2.2 Phytoalexin from Cruciferae ..... 13

**1.5 Metabolic detoxification of phytoalexins ..... 15**
**1.6 Glucosyltransferases ..... 23**
1.6.1 Plant glucosyltransferases ..... 25
1.6.1.1 Biosynthesis of secondary metabolites ..... 26
1.6.1.2 Detoxification of secondary metabolites ..... 41
1.6.2 Microbial glucosyltransferases ..... 60
**1.7 Conclusions ..... 63**

***Chapter 2: RESULTS ..... 65***
**2.1 Synthesis and antifungal activity of phytoalexins and analogues ..... 65**
2.1.1 Synthesis ..... 65
2.1.2 Antifungal activity ..... 70
**2.2 Metabolism of phytoalexins and analogues in *Sclerotinia sclerotiorum* .... 73**
2.2.1 1-Methoxybrassinin (**11**) ..... 73
2.2.2 Cyclobrassinin (**18**) ..... 75
2.2.3 Brassilexin (**24**) ..... 77
2.2.3.1 Biotransformation ..... 77
2.2.3.2 Chemical synthesis of 1-β-D-glucopyranosylbrassilexin (**222**) ..... 79
2.2.4 Sinalexin (**25**) ..... 81
2.2.5 1-Methylbrassilexin (**215**) ..... 84
2.2.6 Brassicanal A (**34**) ..... 86
2.2.7 Spirobrassinin (**27**) ..... 87
2.2.8 1-Methoxyspirobrassinin (**28**) ..... 89
2.2.9 1-Methylspirobrassinin (**216**) ..... 91
2.2.10 Determination of the enantiomeric excess of spirobrassinins **27**, **28**, **216**, and metabolites **232**, **233**, and **234** ..... 94
2.2.11 Summary ..... 98

**2.3 Design and synthesis of potential brassinin detoxification inhibitors ..... 100**

2.3.1 Synthesis of methyl (indol-2-yl)methyldithiocarbamate (**240**), fluorocamalexins (**75**, **244**) and 3-(*N*-acetylamino)quinoline (**243**) ..... 103

2.3.2 Synthesis of methyl (benzofuran-3-yl)methyldithiocarbamate (**236**) ..... 104

2.3.3 Synthesis of methyl (benzofuran-2-yl)methyldithiocarbamate (**241**) ..... 105

2.3.4 Synthesis of methyl (thianaphthen-3-yl)methyldithiocarbamate (**237**) ..... 106

2.3.5 Synthesis of methyl (7-azaindole-3-yl)methyldithiocarbamate (**238**) ..... 107

2.3.6 Synthesis of methyl (5-methoxypyrazolo[1,5-a]pyridin-3-yl)methyldithiocarbamate (**239**) ..... 108

2.3.7 Synthesis of 3-phenylindoles (**245**, **246**, **247**) ..... 110

2.3.8 Synthesis of 3-phenylbenzofuran (**248**) ..... 110

**2.4 Antifungal activity of potential brassinin detoxification inhibitors against *Sclerotinia sclerotiorum* ..... 111**

**2.5 Metabolism of potential inhibitors of brassinin detoxification in *Sclerotinia sclerotiorum* ..... 114**

2.5.1 Methyl (indol-2-yl)methyldithiocarbamate (**240**) ..... 114

2.5.2 Methyl (thianaphthen-3-yl)methyldithiocarbamate (**237**) ..... 116

2.5.3 Metabolism of 3-phenylindole (**245**) ..... 118

2.5.4 Summary ..... 120

**2.6 Co-metabolism of brassinin, camalexins and potential brassinin detoxification inhibitors in *Sclerotinia sclerotiorum* ..... 120**

**2.7 Screening of potential brassinin detoxification inhibitors using crude cell-free extracts ..... 128**

***Chapter 3: DISCUSSION ..... 137***

**3.1 Antifungal activity ..... 137**

**3.2 Synthesis and metabolic detoxification of phytoalexins and analogues in *Sclerotinia sclerotiorum* ..... 141**

3.2.1 Synthesis ..... 142

3.2.2 Metabolism ..... 143

**3.3 Synthesis and metabolism of potential brassinin detoxification inhibitors in *Sclerotinia sclerotiorum* ..... 148**
3.3.1 Synthesis ..... 149
3.3.2 Metabolism ..... 151
**3.4 Effect of potential inhibitors on brassinin detoxification ..... 154**
**3.5 Overall conclusions and future work ..... 155**

***Chapter 4: EXPERIMENTAL ..... 158***
**4.1 General methods ..... 158**
**4.2 Synthesis of phytoalexins and analogues ..... 160**
4.2.1 Brassinin (**9**) ..... 160
4.2.2 Cyclobrassinin (**18**) ..... 162
4.2.3 1-Methoxybrassinin (**11**) ..... 163
4.2.4 Brassilexin (**24**) ..... 165
4.2.5 1-Methylbrassilexin (**215**) ..... 166
4.2.6 Sinalexin (**25**) ..... 167
4.2.7 Brassicanal A (**34**) ..... 169
4.2.8 Spirobrassinin (**27**) ..... 170
4.2.8.1 Synthesis ..... 170
4.2.8.2 Enantioresolution ..... 172
4.2.9 1-Methylspirobrassinin (**216**) ..... 174
4.2.10 1-Methoxyspirobrassinin (**28**) ..... 175
4.2.11 Camalexin (**31**) ..... 177
4.2.12 5-Fluorocamalexin (**244**) ..... 178
4.2.13 6-Fluorocamalexin (**75**) ..... 179
**4.3 Synthesis of potential brassinin detoxification inhibitors ..... 180**
4.3.1 Methyl (indol-2-yl)methyldithiocarbamate (**240**) ..... 180
4.3.2 Methyl (benzofuran-3-yl)methyldithiocarbamate (**236**) ..... 182
4.3.2.1 Synthesis of ethyl (2-acetylphenoxy)acetate (**260**) ..... 182
4.3.2.2 Synthesis of 2-acetylphenoxyacetic acid (**261**) ..... 183
4.3.2.3 Synthesis of 3-methylbenzofuran (**262**) ..... 184
4.3.2.4 Synthesis of benzofuran-3-carboxaldehyde (**263**) and benzofuran-3-methanol (**264**) ..... 185

4.3.2.5 Synthesis of benzofuran-3-carboxalde oxime (**265**) ..... 186
4.3.2.6 Synthesis of benzofuran-3-methanamine (**266**) ..... 187
4.3.2.7 Synthesis of methyl (benzofuran-3-yl)methyldithiocarbamate (**236**) ..... 188
4.3.3 Methyl (benzofuran-2-yl)methyldithiocarbamate (**241**) ..... 189
4.3.3.1 Synthesis of benzofuran-2-carboxaldehyde (**268**) ..... 189
4.3.3.2 Synthesis of benzofuran-2-carboxaldehyde oxime (**269**) ..... 190
4.3.3.3 Synthesis of benzofuran-2-methanamine (**270**) ..... 190
4.3.3.4 Synthesis of methyl (benzofuran-2-yl)methyldithiocarbamate (**241**) ..... 191
4.3.4 Methyl (thianaphthen-3-yl)methyldithiocarbamate (**237**) ..... 192
4.3.4.1 Synthesis of thianaphthene-3-carboxaldehyde (**272**) ..... 192
4.3.4.2 Synthesis of thianaphthene-3-carboxaldehyde oxime (**273**) ..... 193
4.3.4.3 Synthesis of thianaphthene-3-methanamine (**274**) ..... 194
4.3.4.4 Synthesis of methy (thianaphthen-3-yl)methyldithiocarbamate (**237**) ..... 195
4.3.5 Methyl (7-azaindol-3-yl)methyldithiocarbamate (**238**) ..... 196
4.3.5.1 Synthesis of 7-azaindole-3-carboxaldehyde (**276**) ..... 196
4.3.5.2 Synthesis of 7-azaindole-3-carboxaldehyde oxime (**277**) ..... 197
4.3.5.3 Synthesis of 7-azaindole-3-methanamine (**278**) ..... 197
4.3.5.4 Synthesis of methyl (7-azaindol-3-yl)methyldithiocarbamate (**238**) ..... 198
4.3.6 Methyl (5-methoxypyrazolo[1,5-a]pyridin-3-yl)methyldithiocar-bamate (**239**) . 199
4.3.6.1 Synthesis of 2-(2,4-dinitrophenoxy)-1H-isoindole-1,3(2H)-dione (**281**) ..... 199
4.3.6.2 Synthesis of *O*-(2,4-dinitrophenyl)hydroxylamine (**282**) ..... 200
4.3.6.3 Synthesis of N-amino-(4-methoxy)pyridinium 2,4-dinitrophenolate (**283**) . 201
4.3.6.4 Synthesis of methyl 5-methoxypyrazolo[1,5-a]pyridine-3-carboxylate (**242**) ... ..... 202
4.3.6.5 Synthesis of 5-methoxypyrazolo[1,5-a]pyridine-3-methanol (**284**) ..... 203
4.3.6.6 Synthesis of 5-methoxypyrazolo[1,5-a]pyridine-3-carboxaldehyde (**285**) ... 204
4.3.6.7 Synthesis of 5-methoxypyrazolo[1,5-a]pyridine-3-carboxaldehyde oxime (**286**) ..... 205
4.3.6.8 Synthesis of 5-methoxypyrazolo[1,5-a]pyridine-3-methanamine (**287**) ..... 205
4.3.6.9 Synthesis of methy (5-methoxypyrazolo[1,5-a]pyridin-3-yl)methyldi-thiocarbamate (**239**) ..... 206
4.3.7 3-Phenylindole (**245**) ..... 207
4.3.8 4-Fluoro-3-phenylindole (**246**) and 6-fluoro-3-phenylindole (**247**) ..... 208

4.3.9 3-Phenylbenzofuran (**248**) ..... 210
4.3.9.1 Synthesis of 1-phenyl-1-(2-hydroxyphenyl)ethanol (**293**) ..... 210
4.3.9.2 Synthesis of o-(1-phenylvinyl)phenol (**294**) ..... 210
4.3.9.3 Synthesis of 3-phenylbenzofuran (**248**) ..... 211
**4.4 Metabolic detoxification of phytoalexins, analogues and potential inhibitors ..... 212**
4.4.1 Preparation of minimal media ..... 212
4.4.2 Preparation of fungal cultures ..... 213
4.4.3 Time-course experiments ..... 213
4.4.4 Scale up experiments: isolation of metabolites ..... 213
4.4.5 Synthesis ..... 214
4.4.5.1 1-β-D-Glucopyranosylbrassilexin (**222**) ..... 214
4.4.5.2 Brassicanal A sulfoxide (**229**) ..... 217
4.4.5.3 3-(Hydroxymethyl)indole-2-methylsulfoxide (**230**) ..... 218
4.4.5.4 Methyl (thianaphthen-3-yl-1-*S*-oxide)methyldithiocarbamate (**296**) ..... 219
4.4.6 Spectral data of metabolites ..... 220
4.4.6.1 7-Oxy-(*O*-β-D-glucopyranosyl)-1-methoxybrassinin (**220**) ..... 220
4.4.6.2 1-(β-D-glucopyranosyl)cyclobrassinin (**221**) ..... 221
4.4.6.3 6-Hydroxysinalexin (**226**) ..... 222
4.4.6.4 6-Oxy-(*O*-β-D -glucopyranosyl)sinalexin (**227**) ..... 222
4.4.6.5 1-Methyl-(oxy-*O*-β-D-glucopyranosyl)brassilexin (**228**) ..... 223
4.4.6.6 Spiro[3H-indole-3,5′-thiazolidin]-2(1H),2′-dione (**231**) ..... 224
4.4.6.7 1-Methoxyspiro[3H-indole-3,5′-thiazolidin]-2(1H),2′-dione (**232**) ..... 225
4.4.6.8 1-Methoxy-2′-thioxospiro[3H-indole-3,5′-thiazolidin]-2(1H)-one (**233**) ..... 226
4.4.6.9 1-Methylspiro[3H-indole-3,5′-thiazolidin]-2(1H),2′-dione (**234**) ..... 227
4.4.6.10 1-Hydroxymethylspirobrassinin (**235**) ..... 228
4.4.6.11 1-β-D-glucopyranosyl-3-phenylindole (**299**) ..... 229
4.4.6.12 Methyl (7-oxy-*O*-β-D-glucopyranosylthianaphthen-3-yl)methyl-dithiocarbamate (**297**) ..... 230
4.4.6.13 Methyl (1-β-D-glucopyranosyl-3-hydroxylindol-2-yl)methyldi-thiocarbamate (**295**) ..... 231
**4.5 Antifungal activity ..... 232**

**4.6 Co-metabolism of brassinin, camalexins and potential brassinin detoxification inhibitors in *Sclerotinia sclerotiorum* .....232**

**4.7 Screening of potential brassinin detoxification inhibitors using crude cell free extracts .....233**

4.7.1 Preparation of crude cell free extracts.....233

4.7.2 Protein measurements .....234

4.7.2.1 Preparation of BSA calibration curve .....234

4.7.2.2 Protein measurements .....234

4.7.3 Enzyme assays .....234

***Chapter 5: REFERENCES*.....*236***

# LIST OF FIGURES

**Figure 1.1** Major phytotoxins of some important necrotrophic fungi of crucifers: sirodesmin PL (**1**); phomalide (**2**); depsilairdin (**3**); destruxin B (**4**); sclerin (**5**) ..... 7

**Figure 1.2** Chemical structure of major oat root saponin avenacin A-1 (**6**). ..... 11

**Figure 1.3** Chemical structures of rishitin (**7**) and pisatin (**8**) ..... 12

**Figure 1.4** Phytoalexins from crucifers: brassinin (**9**); brassitin (**10**); 1-methoxybrassinin (**11**); 4-methoxybrassinin (**12**); 1-methoxybrassitin (**13**); 1-methoxybrassenin A (**14**); 1-methoxybrassenin B (**15**); wasalexin A (**16**); wasalexin B (**17**); cyclobrassinin (**18**); cyclobrassinin sulfoxide (**19**); sinalbin B (**20**); sinalbin A (**21**); cyclobrassinone (**22**); dehydro-4-methoxybrassinin (**23**); brassilexin (**24**); sinalexin (**25**); dioxibrassinin (**26**); spirobrassinin (**27**); 1-methoxyspirobrassinin (**28**); 1-methoxyspirobrassinol (**29**); 1-methoxyspirobrassinol methyl ether (**30**); camalexin (**31**); 1-methylcamalexin (**32**); 6-methoxycamalexin (**33**); brassicanal A (**34**); brassicanal C (**35**); methyl 1-methoxyindole-3-carboxylate (**36**); brassicanal B (**37**); indolyl-3-acetonitrile (**38**) (Pedras et al., 2003a). ..... 14

**Figure 1.5** New phytoalexins from crucifers: arvelexin (**39**) (Pedras et al., 2003b); isalexin (**40**); brassicanate A (**41**); rutalexin (**42**) (Pedras et al., 2004b); erucalexin (**43**) (Pedras et al., 2006a); caulilexin A (**44**); caulilexin B (**45**); caulilexin C (**46**) (Pedras et al., 2006b) ..... 15

**Figure 1.6** Structure of potential brassinin detoxification inhibitors **55**-**61**, biotransformed in mycelial cultures of *Leptosphaeria maculans* (Pedras and Jha, 2006). ..... 18

**Figure 1.7** Biotransformation products of potential brassinin detoxification inhibitors obtained from mycelial cultures of *Leptosphaeria maculans* (Pedras and Jha, 2006). ..... 19

**Figure 1.8** Formation of glucoside by glucosyltransferases (GTs) (R is the aglycone). ..... 25

**Figure 1.9** Phenylpropanoids and formation of their 4-*O*-glucosides and glucose esters. ..... 28

**Figure 1.10** Chemical structures of steroidal alkaloids: solanidine (**140**), solasodine (**141**) and tomatidine (**142**). ..... 38

**Figure 1.11** Chemical structures of steroidal sapogenins: diosgenin (**144**), nuatigenin (**145**) and tigogenin (**146**). ..... 38

**Figure 1.12** Structure of 15-acetyl-4-deoxynivalenol (**157**) and nivalenol (**158**). ..... 45

**Figure 1.13** Structure and glycosylation pattern of vancomycin (**188**) and chloroeremomycin (**189**); the enzymes reponsible for the glycosyl transfer are shown above the indicated carbohydrate (Mulichak et al., 2001)..... 61

**Figure 2.1** Selected NOE (dashed lines) and HMBC (solid line) correlations for 7-oxy-(*O*-β-D-glucopyranosyl)-1-methoxybrassinin (**220**)..... 75

**Figure 2.2** Progress curves of the metabolism of brassilexin (**24**), sinalexin (**25**) and 1-methylbrassilexin (**215**) in *Sclerotinia sclerotiorum*. Cultures were extracted and extracts were analyzed by HPLC; concentrations were determined using calibration curves; each point is an average of experiments conducted in triplicate ± standard deviation (Pedras and Hossain, 2006). ..... 83

**Figure 2.3** X-ray structure of 6-oxy-(*O*-β-D-glucopyranosyl)sinalexin (**227**): general ORTEP-3 view with non-H atom displacement ellipsoids drawn at the 50% probability level. The H atoms are drawn as small spheres of arbitrary size (Pedras and Hossain, 2006)..... 84

**Figure 2.4** Progress curves of the metabolism of brassicanal A (**34**), spirobrassinin (**27**), 1-methoxyspirobrassinin (**28**) and 1-methylspirobrassinin (**216**) in *Sclerotinia sclerotiorum*. Cultures were extracted and the extracts were analyzed by HPLC; concentrations were determined using calibration curves; each point is an average of experiments conducted in triplicate ± standard deviation (Pedras and Hossain, 2006). ..... 89

**Figure 2.5** $^1$H NMR spectra of spirobrassinin (**27**): A – racemic mixture (1.8 mg) in $C_6D_6$ (500 μl); B – racemic mixture containing six equivalents of (*R*)-TFAE in $C_6D_6$ and $D_2O$ (*ca.* 20 μl); C – synthetic *S* enantiomer containing six equivalents of TFAE in $C_6D_6$ and $D_2O$ (*ca.* 20 μl); naturally occurring from cauliflower containing six equivalents of TFAE in $C_6D_6$ and $D_2O$ (*ca.* 20 μl) (Pedras et al., 2004d)..... 97

**Figure 2.6** $^1$H NMR spectra of 1-methoxyspirobrassinin (**28**): A – racemic mixture (1.5 mg) in $C_6D_6$ (500 μl); B – racemic mixture containing six equivalents of (*R*)-TFAE in $C_6D_6$ and $D_2O$ (*ca.* 20 μl) (Pedras et al., 2004d). ..... 97

**Figure 2.7** $^1$H NMR spectra of 1-methylspirobrassinin (**216**): A – racemic mixture (1.4 mg) in $C_6D_6$ (500 μl); B – racemic mixture containing six equivalents of (*R*)-TFAE in $C_6D_6$ and $D_2O$ (*ca.* 20 μl) (Pedras et al., 2004d). ..... 98

**Figure 2.8** Potential brassinin detoxification inhibitors with structures based on brassinin (**9**)..... 102

**Figure 2.9** Potential brassinin detoxification inhibitors with structures based on camalexin (**31**).....102

**Figure 2.10** Curves for transformation of brassinin (9, 0.05 and 0.1 mM) to 1-β-D-glucopyranosylbrassinin (**66**) in culture of *Sclerotinia sclerotiorum*. .....121

**Figure 2.11** Chemical structure of compounds that slowed down the rate of metabolism of brassinin (**9**) in mycelial cultures of *Sclerotinia sclerotiorum*. .....123

**Figure 2.12** Chemical structure of compounds that did not affect the rate of metabolism of brassinin (**9**) in mycelial cultures of *Sclerotinia sclerotiorum*. .....123

**Figure 2.13** Transformation of brassinin (**9**, 0.05 mM) in the presence of methyl (benzofuran-3-yl)methyldithiocarbamate (**236**, 0.05 and 0.1 mM) in cultures of *Sclerotinia sclerotiorum*. .....125

**Figure 2.14** Transformation of brassinin (**9**, 0.05 mM) in the presence of methyl (benzofuran-2-yl)methyldithiocarbamate (**241**, 0.05 and 0.1 mM) in cultures of *Sclerotinia sclerotiorum*. .....125

**Figure 2.15** Transformation of brassinin (**9**, 0.05 mM) in the presence of methyl (indol-2-yl)methyldithiocarbamate (**240**, 0.05 and 0.1 mM) in cultures of *Sclerotinia sclerotiorum*.....126

**Figure 2.16** Transformation of brassinin (**9**, 0.05 mM) in the presence of 3-phenylindole (**245**, 0.05 and 0.1 mM) in cultures of *Sclerotinia sclerotiorum*. .....127

**Figure 2.17** Transformation of brassinin (**9**, 0.05 mM) in the presence of 6-fluoro-3-phenylindole (**247**, 0.05 and 0.1 mM) in cultures of *Sclerotinia sclerotiorum*. .....128

**Figure 2.18** Specific activity of brassinin glucosyltransferase (BGT) in crude cell-free extracts of *Sclerotinia Sclerotiorum* at different brassinin (**9**) concentrations (two independent experiments conducted in triplicate). .....130

**Figure 2.19** Curves for the transformation of brassinin (**9**) at different concentrations in crude cell-free extracts of *Sclerotinia sclerotiorum*. 1. with no inhibitor; 2. with 0.01 mM 3-phenylindole (**245**); 3. with 0.05 mM 3-phenylindole (**245**); 4. with 0.1 mM 3-phenylindole (**245**); 5. with 0.2 mM 3-phenylindole (**245**). .....134

**Figure 2.20** Inhibitory effect of compounds **236**, **237**, **238**, **239**, **240**, and **241** on brassinin glucosyltransferase (BGT) in cell-free extracts of mycelia of *Sclerotinia sclerotiorum*……..135

**Figure 2.21** Inhibitory effect of compounds **75**, **244**, **245**, **247**, **248**, and **249** on brassinin glucosyltransferase (BGT) in cell-free extracts of mycelia of *Sclerotinia sclerotiorum*……..……..136

**Figure 3.1** Structure of compounds discussed in Section 3.1. ……138

**Figure 3.2** Structure of compounds discussed in Section 3.2. ……141

**Figure 3.3** Structure of compounds discussed in Section 3.3. ……148

# LIST OF TABLES

**Table 2.1** Percentage of growth inhibition[a] of *Sclerotinia sclerotiorum* incubated with phytoalexins (**9**, **11**, **18**, **24**, **25**, **27**, **28**, **31**, **34**) and derivatives (**215**, **216**) (48 h, constant light). ..... 72

**Table 2.2** Enantiomeric excess (ee) and optical rotation of spirobrassinins **27**, **28**, **216**, and metabolites **231**, **232**, **233**, and **234** (Pedras and Hossain, 2006)..... 91

**Table 2.3** Chemical shift non-equivalence observed between two enantiomers of each spirobrassinins **27**, **28**, **216** and metabolites **232**, **233**, **234** treated with 6-equiv of *R*-TFAE in $C_6D_6$ and $D_2O$ (*ca.* 20 μl) (Pedras et al., 2004d)..... 96

**Table 2.4** Products of metabolism of phytoalexins **11**, **18**, **24**, **25**, **27**, **28** and **34** and their analogues **215**, and **216** (0.1 mM) in cultures of *Sclerotinia sclerotiorum* (Pedras et al., 2004c; Pedras and Hossain, 2006). ..... 99

**Table 2.5** Percentage of growth inhibition[a] of *Sclerotinia sclerotiorum* incubated with potential brassinin detoxification inhibitors (**236**, **237**, **238**, **239**, **240**, **241**, **242**, **243**, **244**, **245**, **246**, **247**, **248**, **249**, and **250**) (48 h, constant light). . 112

**Table 2.6** Effect of compounds on brassinin glucosyltransferase (BGT) in cell-free extracts of mycelia of *Sclerotinia sclerotiorum*. ..... 132

# LIST OF ABBREVIATIONS

| | |
|---|---|
| Ac | Acetyl |
| $Ac_2O$ | Acetic anhidride |
| AcOH | Acetic acid |
| *A. brassicae* | *Alternaria brassicae* |
| *B.* | *Brassica* |
| br | Broad |
| BGT | Brassinin glucosyltransferase |
| BSA | Bovin serum albumin |
| $^{13}C$ NMR | Carbon-13 nuclear magnetic resonance |
| calcd. | Calculated |
| cv | Cultivar |
| DBU | 1,8-Diazabicyclo[5.4.0]undec-7-ene |
| DMF | Dimethylformamide |
| DMSO | Dimethylsulfoxide |
| EI | Electron impact |
| ESI | Electronspray ionization |
| Et | Ethyl |
| EtOAc | Ethyl acetate |
| EtOH | Ethanol |
| FAB | Fast atom bombardment |
| FCC | Flash column chromatography |
| FTIR | Fourier transformed infrared |
| GT | Glucosyltransferase |
| $^{1}H$ NMR | Proton nuclear magnetic resonance |
| HMBC | Heteronuclear multiple bond correlation |
| HMQC | Heteronuclear multiple quantum correlation |
| HPLC | High performance liquid chromatography |
| HR | High resolution |
| Hz | Hertz |

| | |
|---|---|
| *J* | Coupling constant |
| *L. maculans* | *Leptosphaeria maculans* |
| *m*/*z* | Mass/charge ratio |
| *m*-CPBA | *meta*-chloroperbenzoic acid |
| Me | Methyl |
| MeI | Methyl iodide |
| MeOH | Methanol |
| MHz | Megahertz |
| min | Minute(s) |
| MS | Mass spectrum |
| NOE | Nuclear Overhauser enhancement |
| *P. parasitica* | *Peronospora parasitica* |
| PDA | Potato dextrose agar |
| PDB | Potato dextrose broth |
| PMSF | Phenyl methylsulphonyl fluoride |
| Py | Pyridine |
| *R. solani* | *Rhizoctonia solani* |
| rt | Room temperature |
| $t_R$ | Retention time |
| TFA | Trifluoroacetic acid |
| TFAE | (*R*)-2,2,2-Trifluoro-1-(9-anthryl)ethanol |
| THF | Tetrahydrofuran |
| TLC | Thin layer chromatography |
| UDP | Uridine diphosphate |
| UDPG | Uridine diphosphate glucose |
| UV | ultraviolet |

# Chapter 1: INTRODUCTION

## 1.1 General objectives

*Sclerotinia sclerotiorum* (Lib.) de Bary causes stem rot disease in a wide range of plant families, including Brassicaceae (syn. Cruciferae). The disease is an important problem and prevalent in many regions of the world. *S. sclerotiorum* attack affects plant development and may lower the quality and production of crops (Pedras and Ahiahonu, 2004). Common practices to prevent the spread of fungal diseases are crop rotations, use of certified seeds, removal of infected stubble, and application of fungicides. However, these approaches are expensive and the use of fungicides is environmentally detrimental. Due to increasing problems and concerns over the use of fungicides, there is a great interest in chemical defenses produced by plants. Plants produce secondary metabolites that may have antifungal activity and are part of their defense mechanisms against fungal attack. Some of these compounds are biosynthesized de novo by plants in response to pathogen attack, and are known as phytoalexins (Brooks and Watson, 1985). These phytoalexins are effective only as long as they are not metabolized and detoxified by the pathogen. It is well established that certain microorganisms that are pathogenic to plants are able to overcome these plant chemical defenses through metabolism and detoxification by utilizing a variety of enzymatic reactions (Pedras and Ahiahonu, 2005). A number of economically important pathogens of crucifers has been reported that can successfully detoxify many cruciferous phytoalexins (Pedras and Ahiahonu, 2005). The metabolic detoxification of phytoalexins can potentially deplete cruciferous plants from important inducible

chemical defenses and render plants susceptible to pathogenic attack. It is thus important to understand the detoxification pathway of phytoalexins by phytopathogenic fungi and to inhibit these degradation processes. The possibility of controlling plant pathogens by selectively inhibiting the phytoalexin detoxification enzymes is an attractive and new approach (Pedras and Jha, 2006). This inhibition might allow the plant to accumulate naturally occurring phytoalexins to a level at which the pathogen would not develop or spread.

In order to control the stem rot fungus a project dedicated to the determination of detoxification pathways of phytoalexins in *S. sclerotiorum* and the design and synthesis of potential phytoalexin detoxification inhibitors was undertaken. Altogether the following aspects were investigated:

- Synthesis and evaluation of the antifungal activity of some important phytoalexins to *Sclerotinia sclerotiorum*;
- Biotransformation studies of cruciferous phytoalexins and their analogues by *S. sclerotiorum*;
- Design and synthesis of phytoalexin detoxification inhibitors;
- Co-transformation of brassinin with potential inhibitors by *S. sclerotiorum*;
- Screen for inhibitors using cell-free extracts containing BGT and compare with in *vivo* studies.

## 1.2 Cruciferous plants

Cruciferous plants are cultivated worldwide and are important sources of edible roots, stems, leaves, buds and inflorescences, as well as of edible or industrial oils, condiments and forage. Many well known vegetables such as kale (*Brassica oleracea* var. *acephala*), cabbage (*B. oleracea* var. *capitata*), broccoli (*B. oleracea* var. *botrytis*), cauliflower (*B. oleracea* var. *italica*), Brussels sprouts (*B. oleracea* var. *gemmifera*),

kohlrabi (*B. oleracea* var. *gongylodes*), Chinese cabbage (*B. campestris* var *pekinensis*), turnip (*B. campestris* var. *rapifera)*, rutabaga (*B. napus* var. *napobrassica*), etc. are part of this botanical family, the Brassicaceae (Gomez-Campo, 1999). Oilseed crucifers (*Brassica* spp.) are the third largest source of edible vegetable oils, and brown (*B. juncea*) and white (*Sinapis alba*) mustard seeds, as well as wasabi (*Wasabiae japonica*) are well-known condiments (Pedras, 1998). Varieties of *B. napus* and *B. rapa* whose seeds meet certain defined standards, i.e. low-erucic acid content in the oil and low-glucosinolate content in the residual seed meal were named "canola" by Canadian researchers. The meal of oilseed brassicas is an important source of protein for animal feed. Historically, most cultivated cruciferous plants and some of their wild relatives were used in medicine as anti-escorbutic; a modern version of their medicinal value is the anti-carcinogenic effect of some of their constituents (Gomez-Campo, 1999). The scientific interest for cruciferous plants and its economical importance is best assessed by the tremendous number and variety of scientific articles published annually. The wild crucifer, *Arabidopsis thaliana*, whose genome sequence was published in 2000 (Theologis et al., 2000), is a model plant for carrying out research on plant-pathogen interactions.

## 1.3 Fungal pathogens of cruciferous crops

Pathogens affect plant communities in many ways, with widely different consequences. Plant pathogenic fungi are ubiquitous in plant communities, and their impacts are diverse and often profound. Similar to other plants, crucifers have a whole host of fungal pathogens that cause a variety of diseases. These fungal infections result in large losses of crop yields worldwide. The increase in economic importance of *Brassica* crops, and in particular of oilseed rape, has led to an increase in research on host-pathogen interactions. Similar to other plant fungi, the fungal pathogens of

crucifers are categorized depending on parasitism into two distinct groups: biotrophic and necrotrophic fungi.

Biotrophic lifestyle of fungi is defined as deriving energy from living plant cells (Schulze-Lefert and Panstruga, 2003). Most biotrophic fungi are obligatory parasites surviving only limited saprophytic phases; especially the development of a fruiting body is dependent on the presence of a host. The cultivation of single (vegetative) stages of these fungi in cell-free nutrient medium succeeded only in a few cases. Several biotrophic fungi are known to be important pathogens of crucifers. *Albugo candida* (Pers.) Kuntze is one of the important biotrophic fungi that causes white rust and staghead diseases in numerous members of Brassicaceae and some other families (Goyal et al., 1995). Among the crucifers, the host list includes many oleiferous, vegetable, ornamental, and wild types. *Peronospora parasitica* (Pers. Ex Fr.) Fr. is another important biotrophic fungus of crucifers that causes downy mildew disease and is distributed almost all over the world (Casimiro et al., 2006) in parallel with *A. candida*. Clubroot is also a major disease of crucifers caused by a biotrophic fungus, *Plasmodiophora brassicae* Wor. This fungus infects the majority of cruciferous species and causes significant damage in all temperate areas (Manzanares-Dauleux et al., 2000).

Necrotrophic fungi are a destructive group of plant pathogens that have pathogenesis strategies distinct from biotrophic fungi (Veronese et al., 2006). Whereas necrotrophic pathogens induce cell death in their hosts by secreting phytotoxins and/or enzymes into host tissue before and during colonization, biotrophic pathogens require living cells to complete their life cycle. *Leptosphaeria maculans* (Desm.) Ces. and de Not, *Alternaria brassicae* (Berk.) Sacc., *Sclerotinia sclerotiorum* (Lib.) de Bary and *Rhizoctonia solani* Khun are some important necrotrophic fungi of crucifers. They cause different diseases in crucifers which have large negative impact on quality and

production of crops. Some of the important diseases of crucifers caused by necrotrophic fungi are described below.

### 1.3.1 Blackleg disease

*Leptosphaeria maculans* (Desm.) Ces. and de Not is the most important nectrophic pathogen of oilseed *Brassica* crops, causing stem canker or blackleg disease (Pedras, 1998). Crop losses caused by *L. maculans*, in Canada alone, exceeds tens of millions of dollars annually. The role of toxins in the development of diseases by this pathogen has been investigated by several researchers. Ferezou et al. (1977) first described the production of the toxin sirodesmin PL (**1**) in liquid cultures of *L. maculans* (Pedras, 1998). Pedras et al. (1988, 1989) subsequently reported the occurrence of other structurally related toxins (Pedras, 2001). Although the blackleg fungus is a host-selective pathogen, these toxins are host non-specific, that is, they cause necrosis and cell death of both host and non-host plants. However, the role of these toxins in the infection process is not clear and remains to be clarified. It was later reported that phomalide (**2**) was a host selective toxin isolated from 30 to 60-hour-old cultures of blackleg fungus (Pedras et al., 1993). Recently, depsilairdin (**3**), produced by isolate Laird 2, was found to cause strong necrotic lesions only on brown mustard leaves that host the fungal isolate (Pedras et al., 2004a).

### 1.3.2 Alternaria blackspot disease

Alternaria blackspot, caused by *A. brassicae* and other related species, are widespread and found around the world especially where crucifers are commercially grown (Gomez-Campo, 1999). *A. brassicae* is common in many temperate parts of the world during the summer and in many subtropical and tropical parts during the winter. All commercial brassicas are essentially susceptible to *A. brassicae*. However, there are some differences in their degrees of susceptibility (Jasalavich et al., 1993). Crucifers

such as *B. napus* and *B. carinata* are less susceptible to *A. brassicae* than *B. rapa* and *B. juncea*. *A. brassicae* produces phytotoxic compounds which may be important in pathogenesis by these fungi. The major phytotoxic compounds produced by *A. brassicae* have been chemically characterized and consist of destruxin B (**4**) and related compounds (Pedras, 1998). Destruxin B (**4**) causes chlorotic and necrotic foliar lesions on diverse *Brassica* species and other cruciferous host-plants. However, the molecular basis for the selective phytotoxicity of destruxin B and related toxins is not understood.

### 1.3.3 Root rot disease

Damping off and root rot diseases caused by *Rhizoctonia solani* Kuhn are widespread in western Canada especially in the northern prairies and are usually caused by anastomosis group AG 2-1 (Sippell et al., 1985). The disease also appears to be of some importance in Germany. To date no phytotoxic compounds were reported from *R. solani* which showed toxicity on crucifers (Pedras et al., 2005a). However, some secondary metabolites such as phenylacetic acid, *m*- and *p*-hydroxyphenylacetic acid were reported from *R. solani*, which were considered to be phytotoxins due to their toxicity to roots of sugar beet.

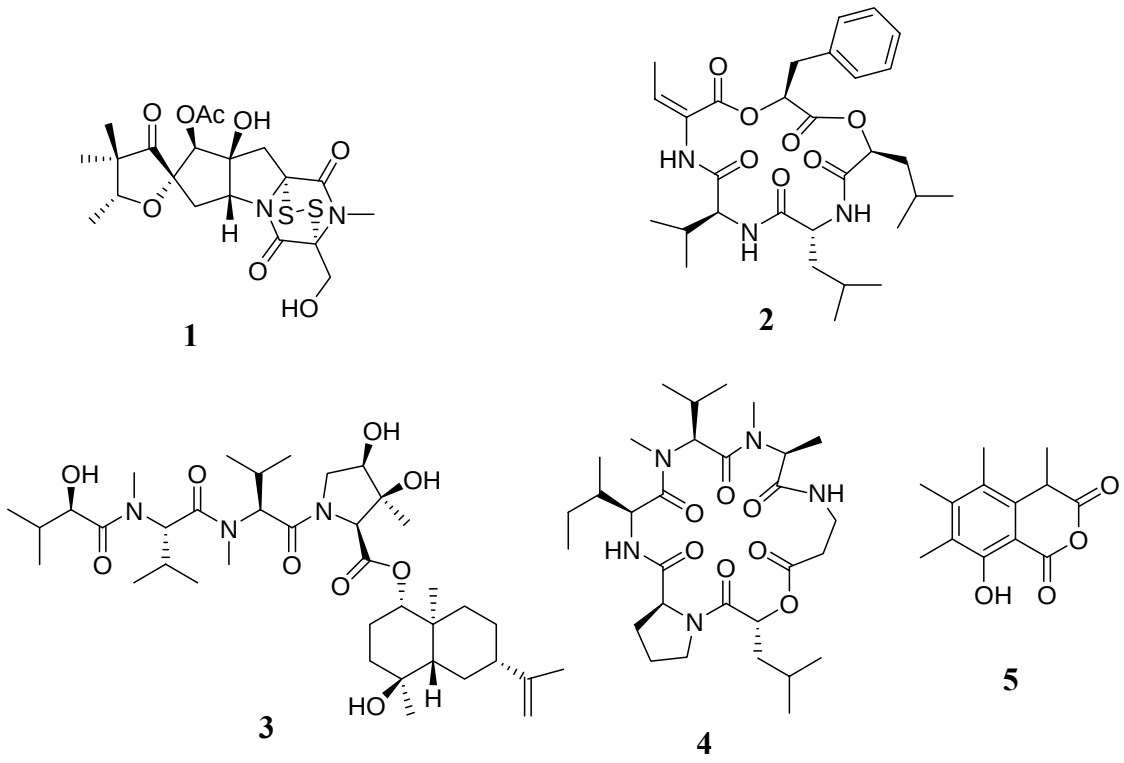


**Figure 1.1** Major phytotoxins of some important necrotrophic fungi of crucifers: sirodesmin PL (**1**); phomalide (**2**); depsilairdin (**3**); destruxin B (**4**); sclerin (**5**).

### 1.3.4 Stem rot disease

Sclerotinia stem rot or cottony soft rot is caused by *S. sclerotiorum* (Lib.) de Bary and is common around the world in the temperate regions (Boland and Hall, 1994). The disease is also serious during storage of cruciferous vegetables. *S. sclerotiorum* has a very broad host range consisting of 42 subspecies or varieties, 408 species, 278 genera, and 75 families of plants. This includes 48 members of Brassicaceae consisting of oleiferous, vegetable, ornamental and wild types (Boland and Hall, 1994).

During its life cycle, *S. sclerotiorum* produces many black fleshy structures called sclerotia which allow the fungus to survive in soil for many years (Adams and

Ayers, 1979). Infection of susceptible host plants can occur from mycelium originating from eruptive germination of sclerotia in the soil. Sclerotia on or near the soil surface germinate to form fruiting bodies called apothecia (stalks with funnels on the end, like tiny mushrooms) (Dillard et al., 1995). The apothecia produce and eject ascospores (Huang and Dueck, 1980) which are carried by the wind and settle on non-living or senescent plant parts where, if there is sufficient moisture and temperatures are cool (5-20 ˚C), they germinate. The fungus then invades the green tissue. White cottony mycelia may develop and sclerotia subsequently produced externally on affected plant parts and internally in stem pith cavities. The black sclerotial bodies reach the soil, where they remain on the surface or become buried as a result of farming practices, so completing the life-cycle of the fungus.

In oleiferous brassicas, infection due to *S. sclerotiorum* is usually seen starting from the early flowering stage (Boland and Hall, 1994). Yield loss in oleiferous brassicas varies considerably based on stage of plant when infection took place, maximum loss taking place when the plants get infected during early bloom stage. Yield losses due to *Sclerotinia* stem rot in the canola and rapeseed (*B. napus*, *B. rapa*) can cause losses up to 50% depending on environmental and weather conditions (Pedras and Ahiahonu, 2004; Lefol et al., 1997). Appreciable degrees of resistance to *S. sclerotiorum* in cultivated crucifers are not known. A wild crucifer *Erucastrum gallicum* was discovered recently to be resistant to *S. sclerotiorum* (Lefol et al., 1997).

Oxalic acid was known to be the pathogenicity determinant for *S. sclerotiorum* and oxalic acid minus mutants were non-pathogenic (Godoy et al., 1990). The role of oxalic acid in the pathogenicity of *S. sclerotiorum* has been confirmed by using *A. thaliana* (L.) Heynh. as a model system (Dickman and Mitra, 1992). Although oxalic acid was reported to cause wilt damage to sunflower (*Helianthus annuus*) and other plant species (Hu et al., 2003), it did not cause any macroscopic damage to *B. napus*, *B.*

*juncea*, *S. alba*, and *E. gallicum* (Pedras and Ahiahonu, 2004). However, it has been reported that *S. sclerotiorum* produces sclerin (**5**) that is phytotoxic to three cruciferous species (*B. napus*, *B. juncea*, *S. alba*) susceptible to *Sclerotinia* stem rot disease but not to resistant species (*E. gallicum*) (Pedras and Ahiahonu, 2004).

## 1.4 Chemical defenses of plants

Due to fungal diseases, every year enormous crop losses take place in Cruciferae or Brassicaceae. The approaches that have been used to control fungal diseases are non-chemical control and chemical control. Chemical control (such as fungicides) has been very successful to control fungal diseases. However, because of their negative environmental impact, fungicides are posing major concerns over the last 40 years. Therefore, there is a strong interest in chemical defenses produced by plants to prevent fungal attack. In order to effectively manipulate these defenses, it is very important to understand plant-pathogen interactions in detail.

A multitude of potential microbial pathogens are present in cultivated fields. Most of these pathogens, however, are unable to breach structural barriers or withstand chemical defenses of the plant (Huang, 2001). Only pathogens with the ability to circumvent the defense mechanisms are able to successfully infect and colonize the plant. Upon invasion, some plants build defenses by reinforcing cell walls with callose, lignin, hydroxyproline-rich glycoproteins, antimicrobial secondary metabolites, and hydrolytic enzymes to confine the pathogen. Plant disease resistance may be divided into two categories: preformed or constitutive resistance, and induced resistance. Preformed resistance is dependent upon the characteristics of normal, uninfected plants, such as thickness of cuticle and presence of constitutive antimicrobial compounds (Grayer and Harborne, 1994). The induced resistance is expressed after microbial

attack in the form of fortification of cell walls, biosynthesis of phytoalexins, and accumulation of pathogenesis-related proteins (Grayer and Harborne, 1994). In this section, constitutive and induced chemical defenses as a part of plant resistance mechanisms will be discussed.

### 1.4.1 Constitutive chemical defenses

Constitutive chemical defenses are preformed antifungal compounds of low molecular weight or macromolecules produced by plants (Grayer and Harborne, 1994). The preformed antifungal compounds of low molecular weight are called preinfectional metabolites, prohibitins or phytoanticipins. It has become apparent that the presence of antifungal macromolecules such as proteins may play an important role in the defense systems of higher plants against pathogens (Grayer and Harborne, 1994). The distinction between phytoanticipins and phytoalexins is not always clear. It has been found that some secondary metabolites are constitutive in one plant species but are induced in another plant species (Grayer and Harborne, 1994).

A large number of constitutive plant compounds have been reported to have antifungal activity. Well-known examples include phenols and phenolic glycosides, unsaturated lactons, saponins, cyanogenic glycosides, and glucosinolates (Osbourn, 1996; Grayer and Harborne, 1994; Bennett and Wallsgrove, 1994). Glucosinolates, sulfur-containing glucosides, are important phytoanticipins of the family Cruciferae, including the agronomically important genus *Brassica* and the cruciferous weed *Arabidopsis*. High glucosinolate levels have been associated with resistance of oilseed rape and Indian mustard to *L. maculans* (Mithen and Magrath, 1992; Osbourn, 1996) and with resistance of cabbage to *P. parasitica* (Osbourn, 1996, Greenhalgh and Mitchell, 1976). The oat saponins, avenacins (e.g., **6**), are representatives of the glycosylated triterpenoid saponins and include four structurally-related molecules that are found in oat roots (Osbourn, 2003). The avenacins are involved in defense against a

variety of pathogens. The soilborne pathogen *Gaeumannomyces graminis* var. *avenae* relies on the enzymatic detoxification of these compounds in order to infect oat roots. A mutant of *G. graminis* that was obtained by transformation-mediated targeted disruption of the gene encoding the saponin-detoxifying enzyme avenacinase was unable to sucessfully infect oat roots, but retained full pathogenicity on wheat, which does not produce avenacins (Bowyer et al., 1995). This work is a clear demonstration of the significance of detoxification reactions in successful fungal invasion.

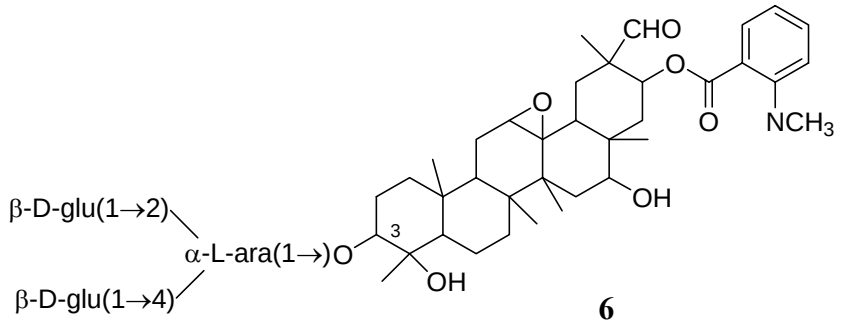


**6**

**Figure 1.2** Chemical structure of major oat root saponin avenacin A-1 (**6**).

### 1.4.2 Induced chemical defenses

Some of the important induced chemical defenses of plants include phytoalexins and pathogenesis-related (PR) proteins. By definition, phytoalexins are low molecular weight antimicrobial compounds biosynthesized by plants from remote precursors in response to pathogen attack, probably as a result of de novo synthesis of enzymes (Osbourn, 1996). On the other hand, PR proteins are plant proteins that respond hypersensitively and whose syntheses are induced in pathological or related situations (Huang, 2001). Enzymes involved in phytoalexin biosyntheses and other metabolic pathways induced by pathogenic infection are generally not considered to be

PR proteins. In this section, the discussion will be restricted to phytoalexins, particularly to cruciferous phytoalexins because of the subject matter of this thesis.

### *1.4.2.1 Phytoalexins*

The phytoalexin theory was first given by Müller and Börger (1940) based on their studies of interactions between *Phytophthora infestans* and *Solanum tuberosum* (potato) (Hammerschmidt, 1999). Müller and Börger showed that the virulent race of *P. infestans* developed freely all over the potato tuber with the exception of the area that was pre-inoculated with an avirulent race of the same fungus. From these results, they suggested that tuber cells, when inoculated with an avirulent race of *P. infestans*, produced an inhibitory substance or phytoalexin that inhibited mycelial growth of the virulent race. The putative phytoalexin was latter discovered by Tomiyama et al. (1968) and named rishitin (**7**) although the first known phytoalexin was pisatin (**8**) and isolated by Perrin and Bottomley (1962) from the seed cavities of pea.

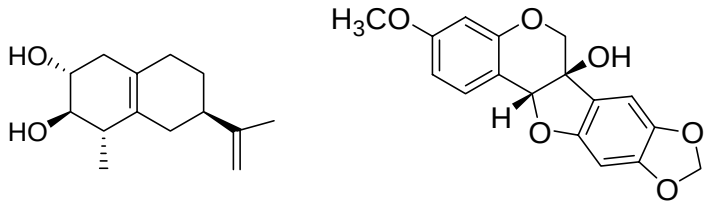


**7** **8**

**Figure 1.3** Chemical structures of rishitin (**7**) and pisatin (**8**).

To date a large number of phytoalexins have been isolated from different plant families. Interestingly, closely related plants synthesize phytoalexins of similar chemical structures. For example, plants from Leguminosae produce predominantly isoflavonoid phytoalexins (Harborne, 1999; Ingham, 1982); plants from Solanaceae synthesize mostly terpenoid phytoalexins (Brooks and Watson, 1991; Jadhav et al.,

1991); plants from Caryophyllaceae accumulate phytoalexins derived from anthranilamide (Niemann, 1993); and cruciferous plants accumulate sulfur-containing indole phytoalexins (Pedras et al., 2003a). However, exceptions have been noted in some cases. Phytoalexins play an important role in disease resistance and the importance in defense mechanisms has been reviewed by Smith (1996).

### *1.4.2.2 Phytoalexins from Cruciferae*

Phytoalexins from the family Cruciferae have structural uniqueness and contain an indole ring with substitution at the C-3 position and additional nitrogen and sulfur atoms. Close to 35 phytoalexins (Figs. 1.4 and 1.5, compounds **9**-**46**) from crucifers have been isolated and their structures elucidated since they were first reported in 1986 by Takasugi and co-workers (Takasugi et al., 1986). The first reported cruciferous phytoalexins were brassinin (**9**), 1-methoxybrassinin (**11**) and cyclobrassinin (**18**) isolated from Chinese cabbage (*B. campestris* L. ssp. pekinensis) heads after inoculating with *Pseudomonas cichorii* (Takasugi et al., 1986). Phytoalexins from crucifers have been reviewed several times (Gross, 1993; Rouxel et al., 1995; Pedras et al., 2000 and 2003a). Since the last review (Pedras et al., 2003a), eight new phytoalexins have been reported from crucifers (Fig. 1.5). Arvelexin (**39**) was isolated from *Thlaspi arvense* (stinkweed) (Pedras et al., 2003b); isalexin (**40**), brassicanate A (**41**), and rutalexin (**42**) were isolated from *B. napus*, ssp. *rapifera* (rutabaga) (Pedras et al., 2004b); erucalexin (**43**) was isolated from *Erucastrum gallicum* (dog mustard) (Pedras et al. 2006a); and caulilexin A (**44**), caulilexin B (**45**) and caulilexin C (**46**) were reported from the flower of *B. oleracea* var. *botrytis* (cauliflower) (Pedras et al., 2006b).

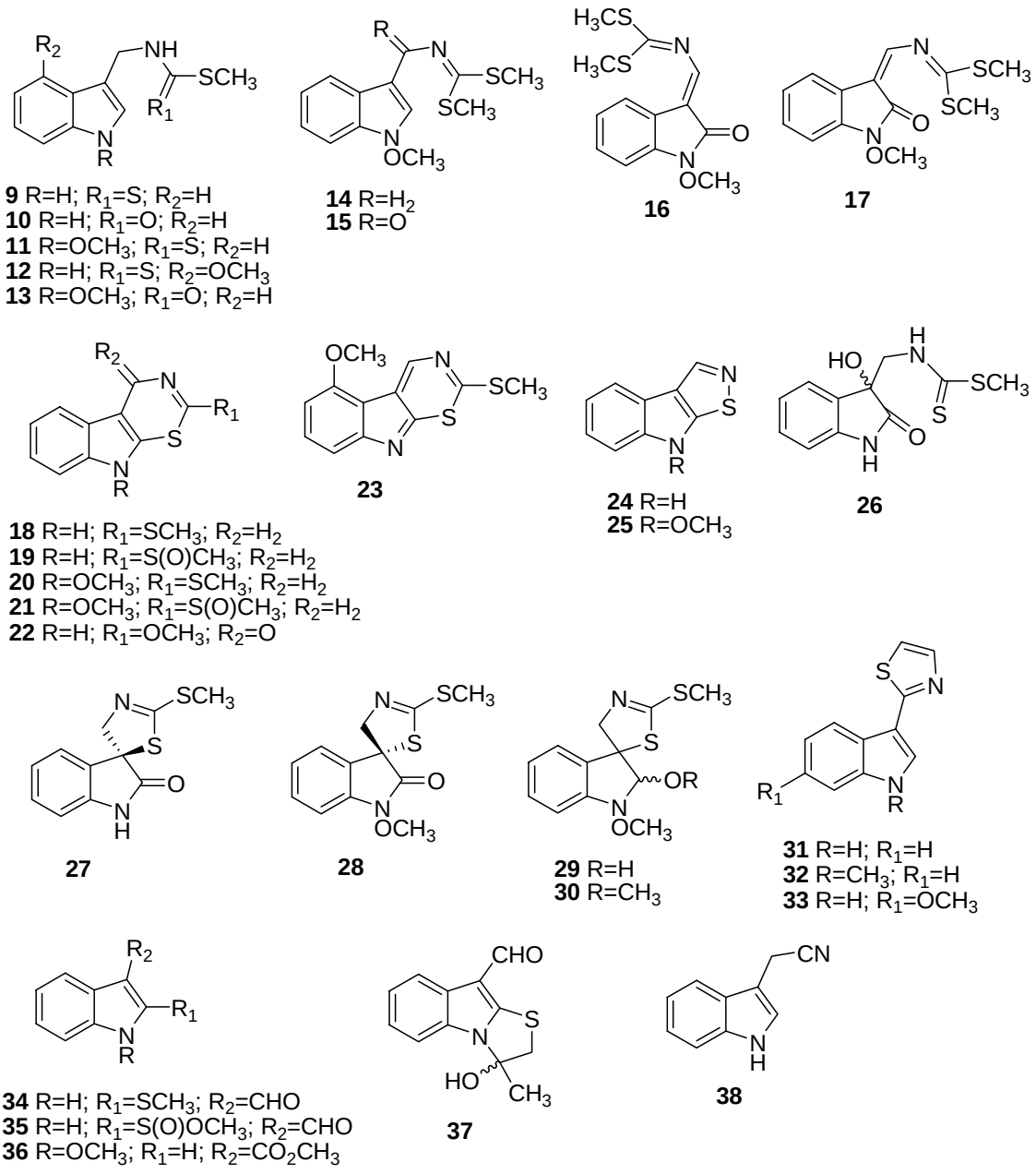


**Figure 1.4** Phytoalexins from crucifers: brassinin (**9**); brassitin (**10**); 1-methoxybrassinin (**11**); 4-methoxybrassinin (**12**); 1-methoxybrassitin (**13**); 1-methoxybrassenin A (**14**); 1-methoxybrassenin B (**15**); wasalexin A (**16**); wasalexin B (**17**); cyclobrassinin (**18**); cyclobrassinin sulfoxide (**19**); sinalbin B (**20**); sinalbin A (**21**); cyclobrassinone (**22**); dehydro-4-methoxybrassinin (**23**); brassilexin (**24**); sinalexin (**25**); dioxibrassinin (**26**); spirobrassinin (**27**); 1-methoxyspirobrassinin (**28**); 1-methoxyspirobrassinol (**29**); 1-methoxyspirobrassinol methyl ether (**30**); camalexin (**31**); 1-methylcamalexin (**32**); 6-methoxycamalexin (**33**); brassicanal A (**34**);

brassicanal C (**35**); methyl 1-methoxyindole-3-carboxylate (**36**); brassicanal B (**37**); indolyl-3-acetonitrile (**38**) (Pedras et al., 2003a).

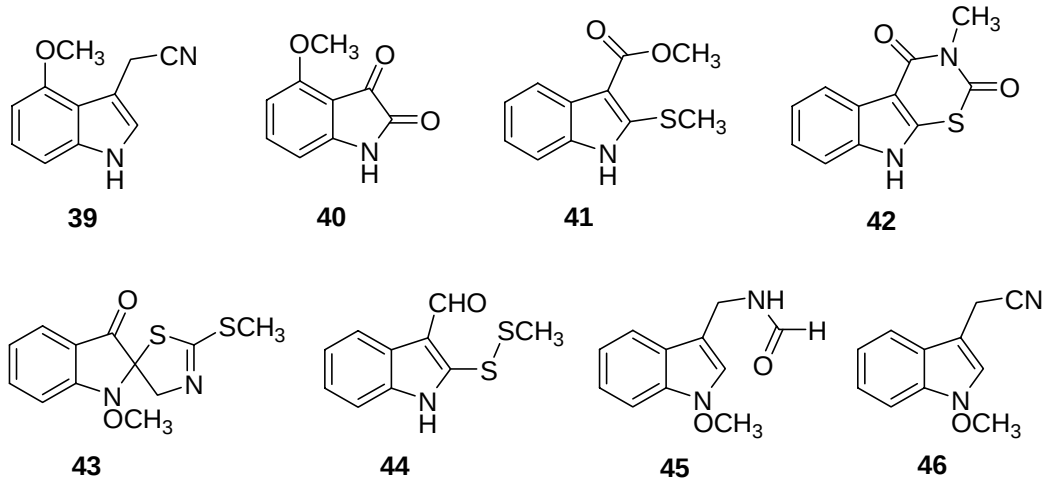


**Figure 1.5** New phytoalexins from crucifers: arvelexin (**39**) (Pedras et al., 2003b); isalexin (**40**); brassicanate A (**41**); rutalexin (**42**) (Pedras et al., 2004b); erucalexin (**43**) (Pedras et al., 2006a); caulilexin A (**44**); caulilexin B (**45**); caulilexin C (**46**) (Pedras et al., 2006b).

## 1.5 Metabolic detoxification of phytoalexins

Phytoalexins are effective in the defense mechanism of plants only as long as they are not metabolized and detoxified by the pathogen. It is well established that certain microorganisms that are pathogenic to plants are able to overcome these plant chemical defenses through metabolism and detoxification (Pedras and Ahiahonu, 2005). The outcome of this detoxification favors the pathogen and is unfavorable to plants. To date, there are many examples that show phytoalexins can be detoxified to less toxic compounds by phytopathogenic fungi. The pathways used by plant pathogenic fungi to metabolize and detoxify phytoalexins have been recently reviewed (Pedras and Ahiahonu, 2005). This review covered the phytoalexin detoxifications that had been investigated to date. Therefore, this topic is not reviewed in this thesis introduction, although the subject mater is relevant to my research project. Only new works on the metabolism and detoxification of phytoalexins, which were reported after the last review, are reviewed here. As well, the transformations of cruciferous

phytoalexins that have been studied using the fungus, *S. sclerotiorum*, are summarized in this section. Although the biotransformation of the pea (*Pisum sativum*) phytoalexin (+)-pisatin (**8**) was reviewed (Pedras and Ahiahonu, 2005), it is an important example to show the significance of phytoalexin detoxification in successful fungal invasion. Pisatin (**8**) was detoxified by the pea fungal pathogen, *Nectria haematococca*, through a demethylation reaction, which was catalyzed by a microsomal cytochrome P-450 monooxygenase, pisatin demethylase (PDA). The virulence of *N. haematococca* isolates on pea depended on their ability to detoxify pisatin (**8**) through demethylation. Only those isolates that had PDA were virulent on pea. Results with specific mutants of *N. haematococca* confirmed this hypothesis and showed that phytoalexin detoxification can be a virulence trait (VanEtten et al. 2001).

The metabolism of crucifer phytoalexins have been studied mainly using three economically important cruciferous fungal pathogens, namely *Leptosphaeria maculans*, *Sclerotinia sclerotiorum*, and *Rhizoctonia solani* (Pedras and Ahiahonu, 2005). Recently, the biotransformation pathway of brassilexin (**24**), sinalexin (**25**) and their analogues by the fungus, *L. maculans*, was described (Pedras and Suchy, 2005). It was discovered that *L. maculans* transformed brassilexin (**24**) to the very polar metabolite 3-formylindolyl-2-sulfonic acid (**49**) as shown in Scheme 1.1. The first step in the transformation of brassilexin (**24**) involved reduction of its isothiazole ring yielding 3-aminomethyleneindole-2-thione (**47**), which was subsequently hydrolyzed to 2-sulfanylindolyl-3-carbaldehyde (**48**) followed by oxidation to 3-formylindolyl-2-sulfonic acid (**49**). Although aldehyde **48** was not detected in the fungal cultures incubated with brassilexin (**24**) or 3-aminomethyleneindole-2-thione (**47**), an incubation experiment with **48** showed its complete metabolism to sulfonic acid **49**. The biotransformation of brassilexin (**24**) was shown to be a detoxification, since the antifungal activities of brassilexin (**24**) and its metabolites indicated that brassilexin

(**24**) was more antifungal to *L. maculans* than any of the products **47**-**49**. Investigation of the metabolism of sinalexin (**25**) and its analogues 1-methylbrassilexin (**50**) and 1-acetylbrassilexin (**51**) in *L. maculans* suggested that sinalexin (**25**) and 1-methylbrassilexin (**50**) were detoxified to enamines **52** and **53** (Scheme 1.2), respectively, whereas 1-acetylbrassilexin (**51**) was transformed to brassilexin (**24**), whose biotransformation followed the pathway depicted in Scheme 1.1 (Pedras and Suchy, 2005). Enamine **52** was found to decompose in aqueous solution and **53** was biotransformed slowly to undetermined products.

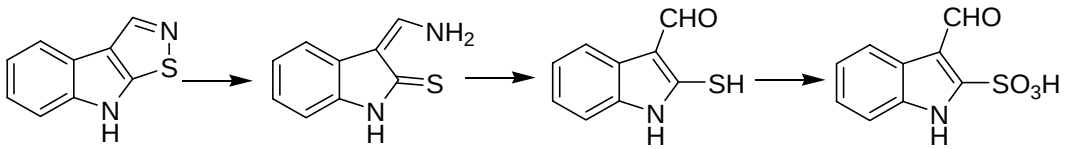


**24** **47** **48** **49**

**Scheme 1.1** Detoxification pathway of brassilexin (**24**) in *Leptosphaeria maculans* (Pedras and Suchy, 2005).

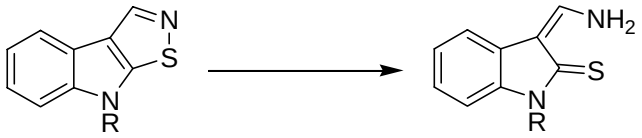


**25** R=$OCH_3$
**50** R=$CH_3$
**51** R=$COCH_3$

**47** R=H
**52** R=$OCH_3$
**53** R=$CH_3$

**Scheme 1.2** Detoxification pathway of sinalexin (**25**), 1-methylbrassilexin (**50**) and 1-acetylbrassilexin (**51**) in *Leptosphaeria maculans* (Pedras and Suchy, 2005).

It was reported (Scheme 1.3) that brassinin (**9**) was detoxified in mycelial cultures or cell free extracts of *L. maculans* to less toxic indole-3-carboxaldehyde (**54**) (Pedras et al., 2005b). In order to inhibit this detoxification in *L. maculans*, a large number of potential brassinin detoxification inhibitors was designed by replacement of its dithiocarbamate group (toxophore) with carbamate, dithiocarbonate, urea, thiourea,

sulfamide, sulfonamide, dithiocarbazate, amide, and ester functional groups and by substituting the indolyl moiety with naphthalenyl and phenyl moiety (Pedras and Jha, 2006). Among all these designed compounds, compounds **55-61** were reported to be biotransformed in mycelial cultures of *L. maculans* (Fig. 1.6). Although methyl 3-phenyldithiocarbazate (**56**) and tryptophol dithiocarbonate (**57**) could slow down the rate of detoxification of brassinin (**9**), they were metabolized to methyl 3-phenylthiocarbazate (**63**) and tryptophol (**62**), respectively, by *L. maculans*. On the other hand, methyl *N*-benzyldithiocarbamate (**55**) and *N*-(indol-3-ylmethyl)-*N*′-methylthiourea (**58**) did not affect the rate of detoxification of brassinin (**9**) but they were metabolized to benzoic acid and indole-3-carboxaldehyde (**54**), respectively. Compounds **59-61** were metabolized to 3-(indol-3-yl)propanoic acid (**64**) by *L. maculans* without affecting the metabolism of brassinin (**9**).

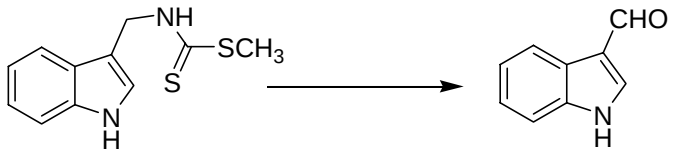


**9** **54**

**Scheme 1.3** Detoxification of brassinin (**9**) in mycelial cultures or cell free extracts of *Leptosphaeria maculans* (Pedras et al., 2005b).

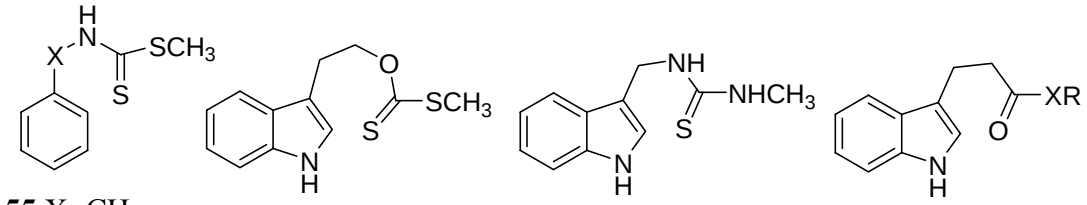


**55** X=$CH_2$
**56** X=NH

**57**

**58**

**59** XR=$OCH_3$
**60** XR=$NH_2$
**61** XR=$NHCH_3$

**Figure 1.6** Structure of potential brassinin detoxification inhibitors **55-61**, biotransformed in mycelial cultures of *Leptosphaeria maculans* (Pedras and Jha, 2006).

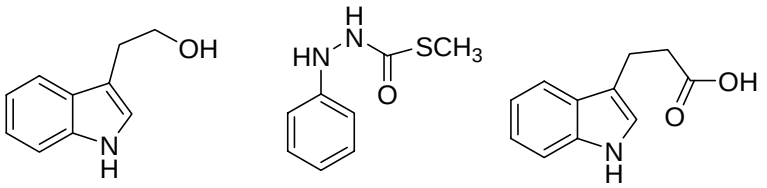


**62** **63** **64**

**Figure 1.7** Biotransformation products of potential brassinin detoxification inhibitors obtained from mycelial cultures of *Leptosphaeria maculans* (Pedras and Jha, 2006).

The biotransformation of brassinin (**9**) was also investigated by the stem rot fungus, *S. sclerotiorum* (Pedras et al., 2004c). It was reported that *S. sclerotiorum* metabolized brassinin (**9**) to 1-β-D-glucopyranosylbrassinin (**66**), an unusual pathway, as shown in Scheme 1.4. The antifungal activity of brassinin (**9**) and its metabolite **66** was compared using radial mycelial growth assay, which indicated that the metabolism of brassinin (**9**) by *S. sclerotiorum* was a detoxification, as the glucoside **66** had no significant antifungal activity. Furthermore, the transformation of brassinin (**9**) to glucoside **66** was also observed in the crude cell-free extracts of mycelia of *S. sclerotiorum* when the mycelia were grown in the presence of compounds related to brassinin (**9**) such as camalexin (**31**), methyl tryptaminedithiocarbamate (**65**), methyl 1-methyltryptaminedithiocarbamate (**68**), or spirobrassinin (**27**) (Pedras et al., 2004c). Without stimulating the fungus with these compounds, the transformation of brassinin (**9**) to **66** was not observed in the cell-free extracts. These results suggested that an inducible brassinin glucosyltransferase (BGT) was responsible for the detoxification of brassinin (**9**) in *S. sclerotiorum*. The BGT activity was found to be UDP-glucose dependent as no BGT activity was observed in the absence of UDP-glucose.

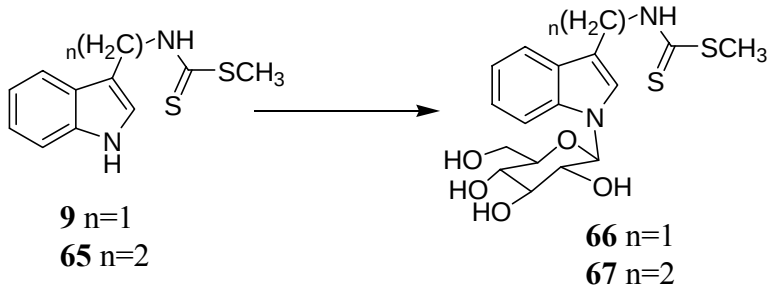


**Scheme 1.4** Detoxification of the phytoalexin brassinin (**9**) and its analogues methyl tryptaminedithiocarbamate (**65**) by the fungus *Sclerotinia sclerotiorum* (Pedras et al., 2004c).

To probe the selectivity of the BGT involved in the detoxification of brassinin, the metabolism of brassinin analogues such as methyl tryptaminedithiocarbamate (**65**), methyl 1-methyltryptaminedithiocarbamate (**68**) and methyl 2-naphthylmethyl dithiocarbamate (**70**) was investigated in mycelial cultures of *S. sclerotiorum* (Pedras et al., 2004c). It was reported that compounds **65**, **68** and **70** were metabolized by *S. sclerotiorum* to their respective glucosides **67**, **69** and **71** as shown in Schemes 1.4-1.6. When the *N*-1 position was blocked as in **68**, the metabolism involved in the oxidation of C-7 followed by *O*-glucosylation. 2-Naphthylmethyl dithiocarbamate **70** was also *O*-glucosylated at C-5, similar to the *N*-1 protected indole **68**.

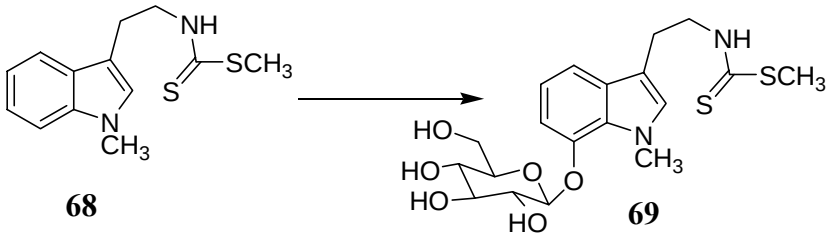


**Scheme 1.5** Detoxification of the phytoalexin analogue methyl 1-methyltryptamine dithiocarbamate (**68**) by *Sclerotinia sclerotiorum* (Pedras et al., 2004c).

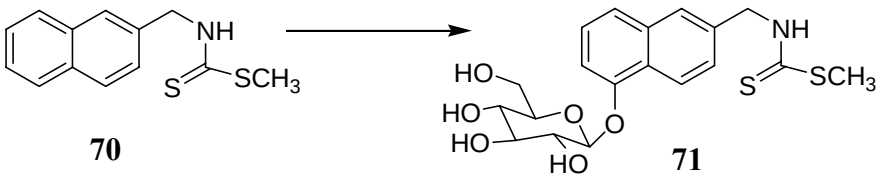


**70** **71**

**Scheme 1.6** Detoxification of the phytoalexin analogue methyl 2-naphthylmethyl dithiocarbamate (**70**) by *Sclerotinia sclerotiorum* (Pedras et al., 2004c).

The biotransformation of camalexin (**31**) and 6-methoxycamalexin (**33**) were investigated in the mycelial cultures of *S. sclerotiorum* (Pedras and Ahiahonu, 2002). The results of these investigations suggested that *S. sclerotiorum* metabolized camalexin (**31**) to 6-oxy-(*O*-β-D-glucopyranosyl)camalexin (**73**) via 6-hydroxycamalexin (**72**) (Scheme 1.7). Similar to this metabolism, the phytoalexin 6-methoxycamalexin (**33**) was also metabolized by *S. sclerotiorum* to **73** via **72** (Schemes 1.7 and 1.8). In addition, 6-methoxycamalexin (**33**) was partly transformed to the minor metabolite **74**. Therefore, the metabolism of 6-methoxycamalexin (**33**) in *S. sclerotiorum* occurred via two pathways, with the major product **73** resulting from demethylation of the methoxy group at C-6, followed by glucosylation (Pedras and Ahiahonu, 2002). Interestingly, similar to brassinin (**9**) detoxification, the minor product **74** resulted from direct *N*-glucosylation (Scheme 1.8). The metabolism of camalexin (**31**) and 6-methoxycamalexin (**33**) by *S. sclerotiorum* were also detoxification processes as their metabolites had no significant antifungal activity.

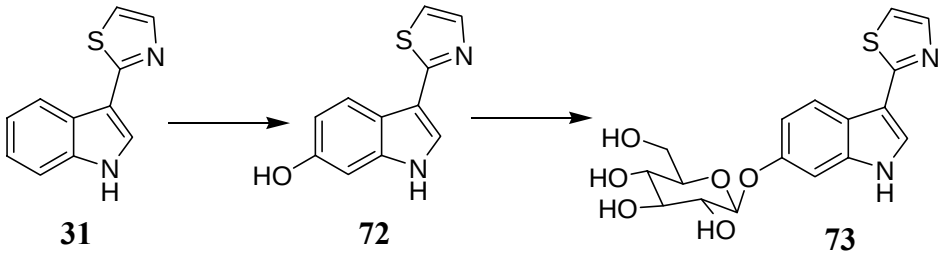


**31** **72** **73**

**Scheme 1.7** Detoxification of the phytoalexin camalexin (**31**) by *Sclerotinia sclerotiorum* (Pedras and Ahiahonu, 2002).

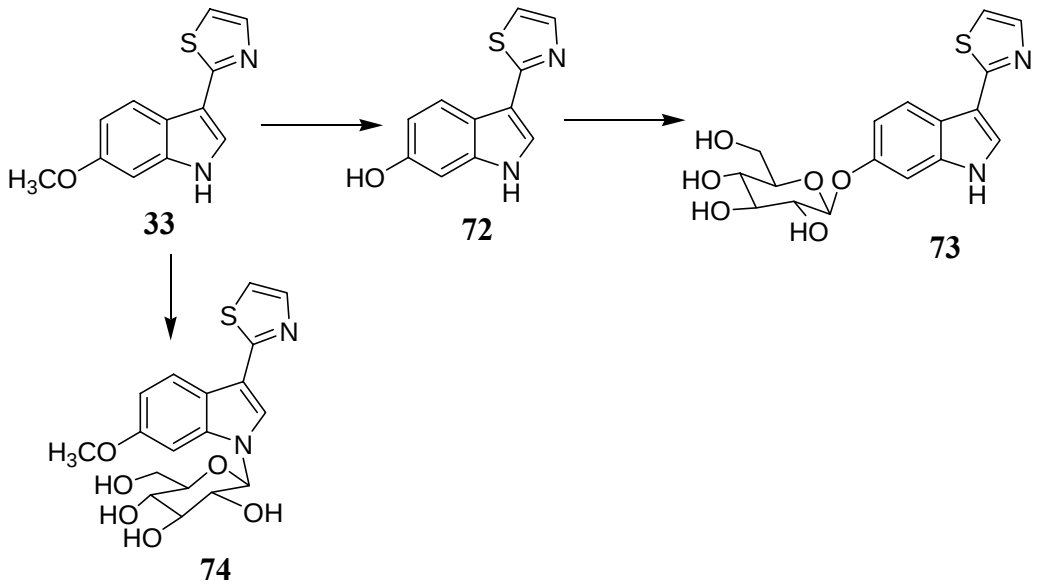


**Scheme 1.8** Detoxification of the phytoalexin 6-methoxycamalexin (**33**) by *Sclerotinia* s*clerotiorum* (Pedras and Ahiahonu, 2002).

To probe the detoxification pathway of camalexins in *S. sclerotiorum*, camalexins **75** and **77** were synthesized and separately fed to mycelial cultures of *S. sclerotiorum*. 6-Fluorocamalexin (**75**) was transformed to *N*-1 glucosylated compound **76**, as expected since the C-6 position was blocked (Scheme 1.9) (Pedras and Ahiahonu, 2002). Interestingly, when both C-6 and *N*-1 positions were blocked, as in **77**, transformation involved the oxidation of C-7 followed by glucosylation to **78** (Scheme 1.10). In addition, compound **79** was formed from the transformation of camalexin **77**. However, the rates of transformation of **75** and **77** were significantly slower than that of camalexins **31** and **33**.

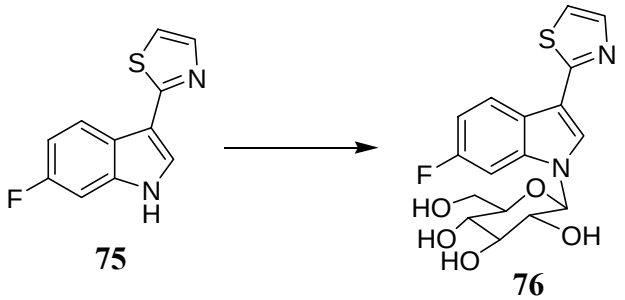


**Scheme 1.9** Detoxification of the phytoalexin analogue 6-fluorocamalexin (**75**) by *Sclerotinia* s*clerotiorum* (Pedras and Ahiahonu, 2002).

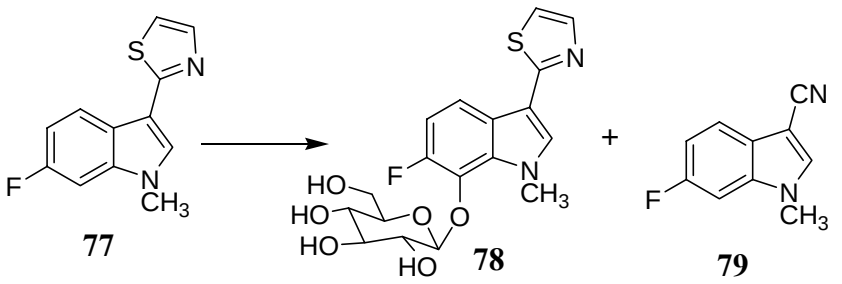


**Scheme 1.10** Detoxification of the phytoalexin analogue 6-fluoro-1-methylcamalexin (**77**) by *Sclerotinia* s*clerotiorum* (Pedras and Ahiahonu, 2002).

In conclusion, plants can synthesize phytoalexins as part of the defense mechanisms against fungal attack, while fungi may utilize enzymes that metabolize and detoxify phytoalexins (Pedras and Ahiahonu, 2005). Therefore, investigation of phytoalexin detoxification mechanisms, followed by isolation of fungal enzymes involved in the crucial detoxification steps will assist the biorational design of inhibitors of phytoalexin detoxification enzymes that may selectively control the particular pathogen.

## 1.6 Glucosyltransferases

From the above description of published work, it is clear that the phytopathogenic fungus, *S. sclerotiorum*, is an exceptional pathogen that utilizes glucosyltransferases for the detoxification of phytoalexins. To the best of my knowledge, confirmed by a recent publication (Pedras and Ahiahonu, 2005), there are no other phytopathogenic fungi that detoxify phytoalexins through glucosylation. Glucosylation reactions are very common in plants. Therefore, it was suggested that *S. sclerotiorum* has obtained proficient glucosyltransferases due to continuous adaptation and co-evolution with plants (Pedras et al., 2004c). Since glucosyltransferases of *S. sclerotiorum* play an important role in detoxification of phytoalexins, it was of great

interest to survey glucosyltransferases of other living systems to compare their substrate specificity, reaction mechanisms and potential inhibitors. Information from this literature survey contextualizes the glucosyltransferases of *S. sclerotiorum*. Therefore, in this section, glucosyltransferases (plant and microbial) that are involved in glucosylation of secondary metabolites and also in the detoxification of bioactive secondary metabolites are reviewed.

The glycosylation reaction that conjugates a carbohydrate molecule with endogenous and exogenous organic molecules is an important tool for all organisms (Jones and Vogt, 2001). Glycosylation can increase water solubility, reduce chemical reactivity and alter biological activity of compounds. Secondary metabolites are glycosylated at O (-OH and –COOH), N, S and C atoms by glycosyltransferases using nucleotide-activated sugars as donor substrates (Fig. 1.8). The glycosyltransferases involved in glycosylation of small molecules have been grouped into family 1 of the 78 families that are classified on the basis of substrate recognition and sequence relatedness (Lim and Bowles, 2004; http://afmb.cnrs-mrs.fr/CAZY/). In plants, these transfer reactions generally use UDP-glucose with acceptors that include hormones such as auxins and cytokinins, secondary metabolites such as flavonoids, and foreign compounds such as pesticides and secondary metabolites (e.g., phytotoxins, allelochemicals) from other organisms (Lim and Bowles, 2004). When glycosyltransferases transfer a glucose molecule to an acceptor molecule they are called glucosyltransferases. Although glucosylation is a very common detoxification mechanism among plants, it is less usual in microorganisms (Hall et al., 2000). Glucosyltransferases are also uncommon in mammalian organisms; however, typically UDP-glucuronosyltransferases are used to transfer glucuronic acid from UDP-glucuronic acid to endogenous (e.g. steroids, bilirubin and bile acids) and exogenous

(e.g., dietary flavonoids, and drugs) acceptors in mammalian systems (Radominska-Pandya et al., 2001).

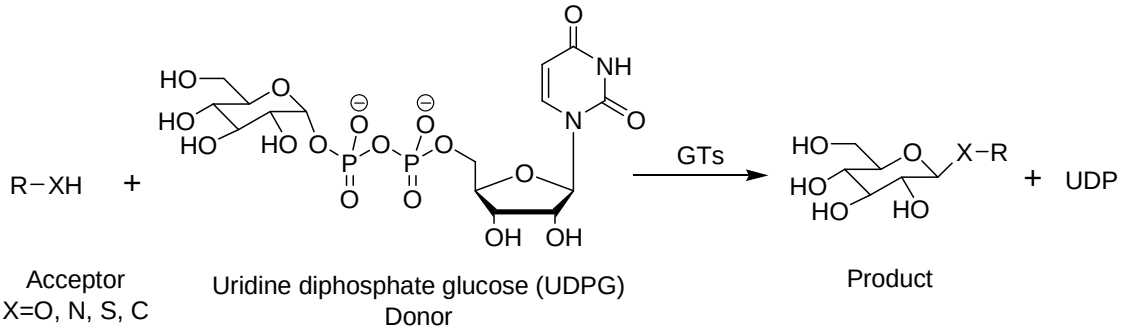


**Figure 1.8** Formation of glucoside by glucosyltransferases (GTs) (RX is the aglycone).

### 1.6.1 Plant glucosyltransferases

Plants are capable of synthesizing a great diversity of low-molecular-weight compounds, defined as secondary plant metabolites. Part of this diversity arises from multiple reactions of a common skeleton such as hydroxylation, methylation, acylation or conjugation with small molecules. For instance, the diversity of more than 5000 known flavonoids originates from such combinatorial modifications of their common aromatic structure (Gachon et al., 2005). Glucosylation is one of the most widespread of these modifications. Foreign compounds originating from other organisms and man-made chemicals, defined as xenobiotics, are also glucosylated by plants (Pflugmacher and Sandermann, 1998). Overall, glucosylating activities in any given individual plants must therefore be regarded as broad. However, the number of expressed glucosyltransferases involved in secondary plant metabolism and the substrate specificities of these enzymes remain largely unknown (Jones and Vogt, 2001). In this section, the substrate specificities of glucosyltransferases involved in the biosynthesis of plant secondary metabolites are discussed first. Subsequently, glucosyltransferases

involved in detoxification of foreign compounds that originate from organisms that co-habit (i.e. share the same space) are discussed. However, the detoxification of man-made chemicals such as herbicides, insecticides and other that occur also through glucosylation (Cole and Edwards, 2000; Hall et al., 2000) will not be covered.

### *1.6.1.1 Biosynthesis of secondary metabolites*

**Phenylpropanoids**

The phenylpropanoid pathway in plants leads to the synthesis of a wide range of secondary metabolites, many of which accumulate as glucosides. Many researchers are investigating glucosyltransferases (GTs) and genes encoding GTs that are capable of transferring a glucose moiety to phenylpropanoids. Most phenylpropanoids are known to form 4-*O*-glucosides through glucosylation; in addition, phenylpropanoids containing a carboxylic acid group also form glucose esters (Fig. 1.9). The glucose ester of sinapic acid (**90**), 1-*O*-sinapoylglucose (**96**) is formed by a GT and genes encoding enzymes capable of this transfer reaction have been identified in both *Brassica napus* and in *Arabidopsis* (Lim et al., 2001; Milkowski et al., 2000a, 2000b, 2004).

Five closely related genes (*UGT84A1-3* and *UGT72E2-3*) from *Arabidopsis* encoding enzymes that can glucosylate sinapic acid (**90**), sinapyl alcohol (**83**) and their related phenyl propanoids in vitro have been identified (Lim et al., 2001). The UGT84A1 and UGT84A3 glucosyltransferases showed significant activity in forming glucose ester conjugates with cinnamic acid, *p*-coumaric acid, caffeic acid (**88**), ferulic acid (**89**) and sinapic acid (**90**) whereas UGT84A2 displayed activity only towards sinapic acid (**90**). The enzyme UGT72E2, which produced 4-*O*-glucoside, showed activity towards ferulic acid (**89**), sinapic acid (**90**), coniferyl alcohol (**82**) and sinapyl alcohol (**83**), where high specific activity was found. The UGT72E3

glucosyltransferase was able to form 4-*O*-glucosides **87** and **93** only with sinapyl alcohol (**83**) and sinapic acid (**90**) respectively. Recently, it was reported that UGT72E2 glucosyltransferase was responsible for the accumulation of coniferyl and sinapyl alcohol 4-*O*-glucosides **86** and **87** in *A. thaliana* (Lanot et al., 2006). They have shown that transgenic plants in which *UGT72E2* was downregulated produced 50% less glucosides (**86** and **87**), whereas glucoside levels were increased in leaves and roots of transgenic plants containing elevated expression of *UGT72E2*. A glucosyltransferase was isolated from *B. napus* that showed highest relative activity towards sinapic acid (**90**) in vitro to give 1-*O*-sinapoylglucose (**96**) (Milkowski et al., 2000a).

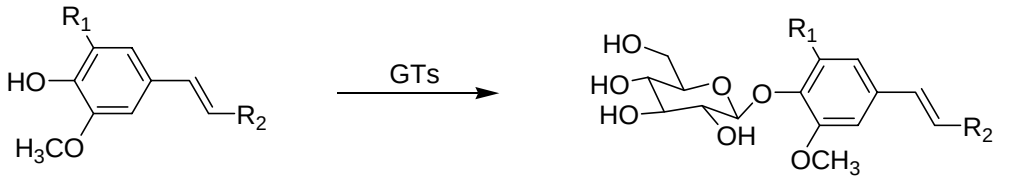


**80** $R_1$=H; $R_2$=CHO
**81** $R_1$=$OCH_3$; $R_2$=CHO
**82** $R_1$=H; $R_2$=$CH_2OH$
**83** $R_1$=$OCH_3$; $R_2$= $CH_2OH$

**84** $R_1$=H; $R_2$=CHO
**85** $R_1$=$OCH_3$; $R_2$=CHO
**86** $R_1$=H; $R_2$=$CH_2OH$
**87** $R_1$=$OCH_3$; $R_2$= $CH_2OH$

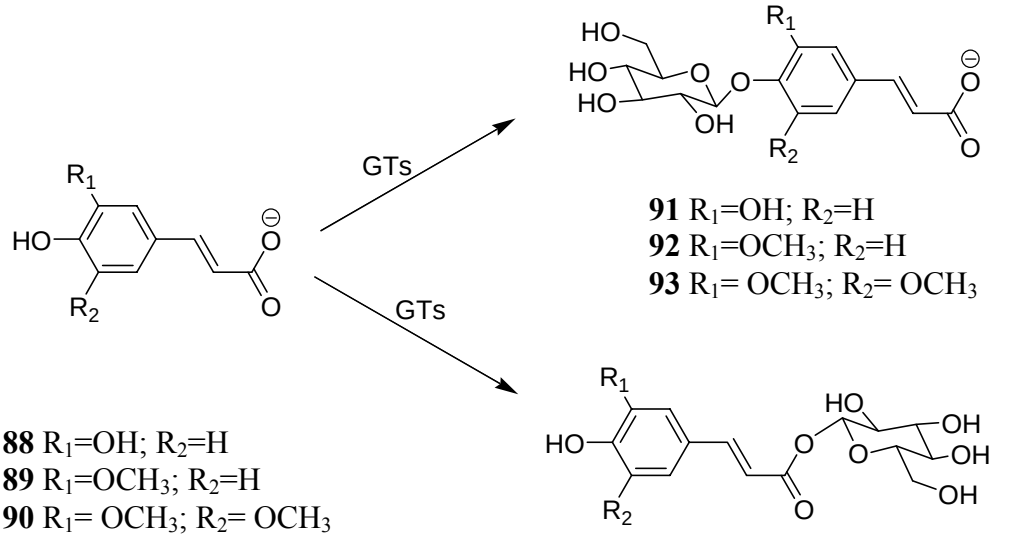


**88** $R_1$=OH; $R_2$=H
**89** $R_1$=$OCH_3$; $R_2$=H
**90** $R_1$= $OCH_3$; $R_2$= $OCH_3$

**91** $R_1$=OH; $R_2$=H
**92** $R_1$=$OCH_3$; $R_2$=H
**93** $R_1$= $OCH_3$; $R_2$= $OCH_3$

**94** $R_1$=OH; $R_2$=H
**95** $R_1$=$OCH_3$; $R_2$=H
**96** $R_1$= $OCH_3$; $R_2$= $OCH_3$

**Figure 1.9** Phenylpropanoids and formation of their 4-*O*-glucosides and glucose esters.

An *Arabidopsis* glucosyltransferase (UGT71C1) that can regioselectively glucosylate the 3-OH of caffeic acid (**88**) has been expressed in *Escherichia coli*, purified and assayed against a range of substrates in vitro (Lim et al., 2003) (Scheme 1.11). The enzyme did not show any activity towards the 4-OH position on the other phenylpropanoids, but the enzyme could recognize the 3-OH of *m*-coumaric acid (**98**) and the 2-OH of *o*-coumaric acid. The UGT71C1 enzyme was also able to glucosylate the 3-OH position of isoferulic acid (**97**).

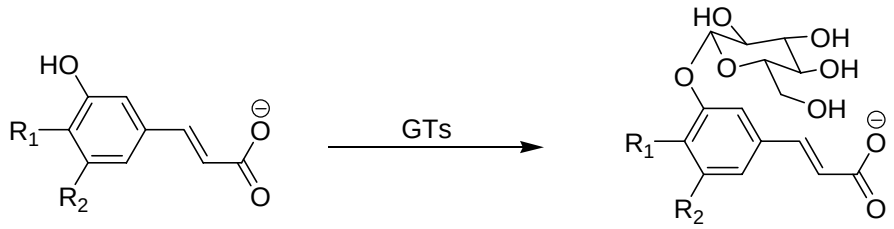


**88** $R_1$= OH; $R_2$=H
**97** $R_1$=$OCH_3$; $R_2$=H
**98** $R_1$=$R_2$=H

**99** $R_1$=OH; $R_2$=H
**100** $R_1$=$OCH_3$; $R_2$=H
**101** $R_1$=$R_2$=H

**Scheme 1.11** Glucosylation at 3-OH position of different hydroxycinamic acids: caffeic acid (**88**), isoferulic acid (**97**), *m*-coumaric acid (**98**).

Recently, Lunkenbein et al. (2006) have reported the isolation of a cDNA encoding glucosyltransferase (FaGT2) from ripe strawberry cv. Elsanta that catalyzes the formation of glucose esters of cinnamic acid and their derivatives in vitro. The enzyme FaGT2 could accept compounds containing a carboxylic group and an aromatic ring structure as substrates. Substituents at the aromatic ring were tolerated as long as they were not located in the ortho position. Thus *p*-coumaric acid, caffeic acid (**88**), ferulic acid (**89**), sinapic acid (**90**), and 5-hydroxyferulic acid were glucosylated.

**Flavonoids**

Flavonoids represent a very interesting group of plant secondary metabolites that are ubiquitous in plants. Many flavonoids exist as glucosides in plants. To date, an

overwhelming number of flavonoid glycosides have been identified. For example, out of a total of 5,000 different flavonoids, 300 different glycosides of one single flavonol, quercetin, have already been identified (Harborne and Baxter, 1999). Although flavonoid glucosides are abundant in plants, there are not many studies on the glucosyltransferases that are responsible for the glucosylation of this huge number of flavonoid glucosides. Substrate specificity tests with flavonoids and heterologously expressed (e.g. in *E. coli* or yeast) GTs were conducted by a few groups and were reviewed by Vogt and Jones (2000). Some flavonoid glucosyltransferases showed a wide range of substrate specificity with poor regioselectivity in vitro. However, some glucosyltransferases showed regioselectivity for particular hydroxyl groups. For example, flavonoid 3-*O*-glucosyltransferase, that transfers a glucose moiety to the 3-OH position of a flavonoid, have been studied by several researchers (Suzuki et al., 2005; Kim et al., 2006; Offen et al., 2006; Tohge et al., 2005). Suzuki et al (2005) isolated and purified a flavonoid 3-*O*-glucosyltransferase from buckwheat (*Fagopyrum esculentum*) cotyledons that can regioselectively glucosylate quercetin (**102**) at the 3-OH position (Scheme 1.12). The enzyme showed little affinity towards kaempferol (**103**), although it has a free 3-OH group. Apigenin (**110**) and luteolin (**111**) containing no 3-OH group were not active substrates for this buckwheat GT and only UDP-glucose was found to be a good sugar donor. It has been reported that a UGT73B2 glucosyltransferase from *Arabidopsis* was able to transfer a glucose unit to 3-OH preferentially when both 3-OH and 7-OH were available (Scheme 1.12) (Kim et al., 2006). However, glucosylation occurred at the 7-OH when the 3-OH was absent (Schemes 1.13 and 1.14). For example, quercetin (**102**), kaempferol (**103**), and isorhamnetin (**104**) were glucosylated by UGT73B2 at 3-OH position, whereas apigenin (**110**), luteolin (**111**), naringenin (**114**), and eriodictyol (**115**), where 3-OH were not available, were glucosylated at 7-OH. Another recombinant *Arabidopsis* glucosyltransferase (UGT78D2) was reported that glucosylate both flavonols and

anthocyanidins at the 3-OH position (Tohge et al., 2005). Three flavonols such as quercetin (**102**), kaempferol (**103**), and myricetin (**105**) (Scheme 1.12) and three anthocyanidins such as cyanidin (**126**), delphinidin (**127**), and pelargonidin (**128**) were tested as substrates for the reaction catalyzed by recombinant UGT78D2. All of them were suitable substrates for the reaction catalyzed by recombinant UGT78D2 to yield the corresponding 3-*O*-glucosides.

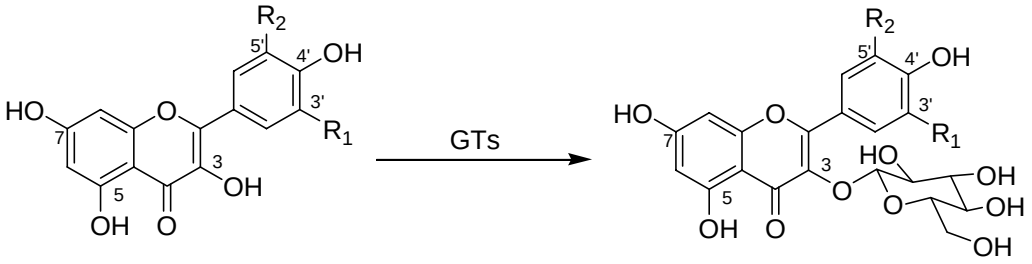


**102** $R_1$= OH; $R_2$=H
**103** $R_1$=$R_2$=H
**104** $R_1$=$OCH_3$; $R_2$=H
**105** $R_1$=$R_2$=OH

**106** $R_1$= OH; $R_2$=H
**107** $R_1$=$R_2$=H
**108** $R_1$=$OCH_3$; $R_2$=H
**109** $R_1$=$R_2$=OH

**Scheme 1.12** Glucosylation at 3-OH position of different flavonols: quercetin (**102**), kaempferol (**103**), isorhamnetin (**104**), myricetin (**105**).

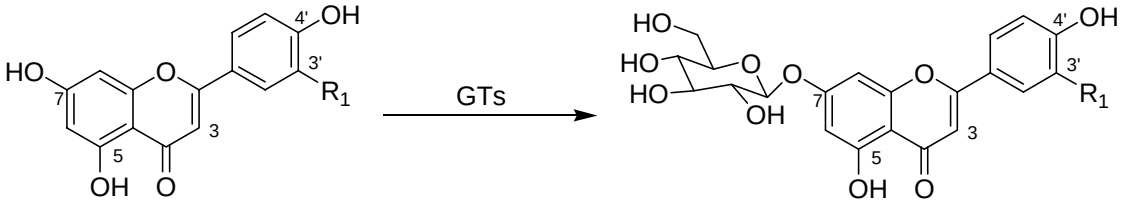


**110** $R_1$= H
**111** $R_1$= OH

**112** $R_1$=H
**113** $R_1$=OH

**Scheme 1.13** Glucosylation at 7-OH position of different flavones: apigenin (**110**), luteolin (**111**).

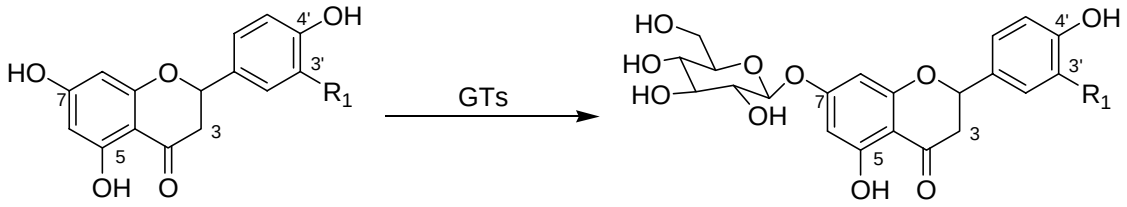


**114** $R_1$= H
**115** $R_1$= OH

**116** $R_1$=H
**117** $R_1$=OH

**Scheme 1.14** Glucosylation at 7-OH position of different flavanones: naringenin (**114**), eriodictyol (**115**).

Although the 7-*O*-glucoside flavonoid is one of the major flavonoid glycosides naturally produced in plants, there are few studies on the enzyme activity and genes of flavonoid 7-*O*-glucosyltransferases. Hirotani et al. (2000) reported the cloning, characterization and high-level expression in *E. coli* of a cDNA encoding glucosyltransferase from hairy roots (*Scutellaria baicalensis*), which is responsible for the glucosylation of flavonoids at the 7-*O*-position. The substrate specificity of this recombinant GT was examined using different flavonoids as acceptor substrate and UDPG as glucose donor. As shown in Scheme 1.15, the flavones such as baicalein (**118**), wogonin (**119**), apigenin (**110**), scutellarein (**120**), and 7-4′-dihydroxyflavone (**121**) and the flavonols, kaempferol (**103**) were accepted by the recombinant hairy root GT. The GT showed high specific activity towards **118**, **110**, and **103**. In a different study, another glucosyltransferase (NTGT2) from tobacco cells (*Nicotiana tabacum* L.) that transferred a glucose unit on the 7-OH group of flavonol and 3-OH group of coumarin was cloned in *E. coli* and characterized (Taguchi et al., 2003). The recombinant NTGT2 displayed high specific activity towards kaempferol (**103**) and 3-hydroxycoumarin, although it had broad substrate specificities.

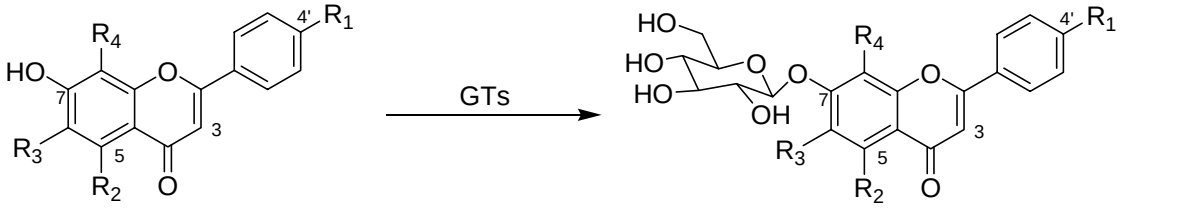


**118** $R_1$= $R_4$=H; $R_2$= $R_3$=OH
**119** $R_1$= $R_3$=H; $R_2$=OH; $R_4$=$OCH_3$
**110** $R_1$= $R_2$=OH; $R_3$= $R_4$=H
**120** $R_1$= $R_2$=$R_3$=OH; $R_4$=H
**121** $R_1$=OH; $R_2$=$R_3$=$R_4$=H

**122** $R_1$= $R_4$=H; $R_2$= $R_3$=OH
**123** $R_1$= $R_3$=H; $R_2$=OH; $R_4$=$OCH_3$
**112** $R_1$= $R_2$=OH; $R_3$= $R_4$=H
**124** $R_1$= $R_2$=$R_3$=OH; $R_4$=H
**125** $R_1$=OH; $R_2$=$R_3$=$R_4$=H

**Scheme 1.15** Glucosylation at 7-OH position of different flavones: baicalein (**118**), wogonin (**119**), apigenin (**110**), scutellarein (**120**), 7,4′-dihydroxyflavone (**121**).

Recently, different flavonoids, such as **102**, **103**, **110**, **111**, **114**, and **115** were tested as substrates with a cloned glucosyltransferase (RUGT-5) from rice (Ko et al., 2006). The enzyme showed very poor regioselectivity; at least two products were obtained from each flavonoid. Glucosylation occurred at the hydroxyl groups at C-3, C-7 or C-4′ positions of flavonoids. The most efficient substrate was kaempferol (**103**), followed by apigenin (**110**), and luteolin (**111**). Two flavonoid glucosyltransferases (UGT73A4 and UGT71F1) from *Beta vulgaris* were reported to exhibit a broad substrate specificity, but a distinct regioselectivity, glucosylating a variety of flavonols, flavones, flavonones, and coumarins (Isayenkova, et al., 2006). UGT73A4 showed a preference for the 4′- and 7-OH position in the flavonoids, whereas UGT71F1 preferentially glucosylated the 3- or the 7-OH position.

Anthocyanins are the principal pigments in flowers, conferring intense red-to-blue cyanic colors on petals and helping to attract pollinators (Ogata et al., 2005). Its biosynthesis involves glucosylation steps that are important for the stability of the pigment and for its aqueous solubility in vacuoles. 3-*O*-Glucosyltransferases that catalyze the first 3-*O*-glucosylation event are common to the biosynthetic pathway of all anthocyanins (Yamazaki et al., 1999). Ford et al. (1998) reported the cloning of a

cDNA encoding 3-*O*-glucosyltransferase (V*v*GT1) from grapes of *Vitis vinifera* that is responsible for the biosynthesis of cyanidin 3-*O*-glucoside (**129**) from cyanidin (**126**) (Scheme 1.16). The recombinant V*v*GT1 accepted only UDP-glucose as a donor substrate but it could transfer a glucose moiety to flavonols such as quercetin (**102**) and kaempferol (**103**) at the 3-hydroxyl position as well. Kinetic analyses showed that $k_{cat}$ for glucosylation of cyanidin (**126**) is 48 times higher than for glucosylation of the flavonol, quercetin (**102**). The enzyme V*v*GT1 also showed activity towards other anthocyanidins such as delphinidin (**127**) and pelargonidin (**128**). Recently, the 3-D structure of V*v*GT1 has been solved at 1.9 Å resolution in a UDP (product) bound form and, subsequently, in its 'Michaelis' complex with both an intact UDP-glucose donor and the acceptor kaempferol (**103**), also at 1.9 Å resolution and in 'nonproductive' complex with UDP and quercetin (**102**), at 2.1 Å (Offen et al., 2006). 3-*O*-glucosyltransferase from *Gentiana triflora* was also expressed in *E. coli* and its substrate specificity was determined using various anthocyanidins and flavonols (Tanaka et al., 1996). The enzyme showed higher substrate specificity towards anthocyanidins (**126**, **127**, **128**) than that of flavonols (**102**, **103**, **105**). Delphinidin (**127**) was found to be the best substrate for the Gentian 3GT.

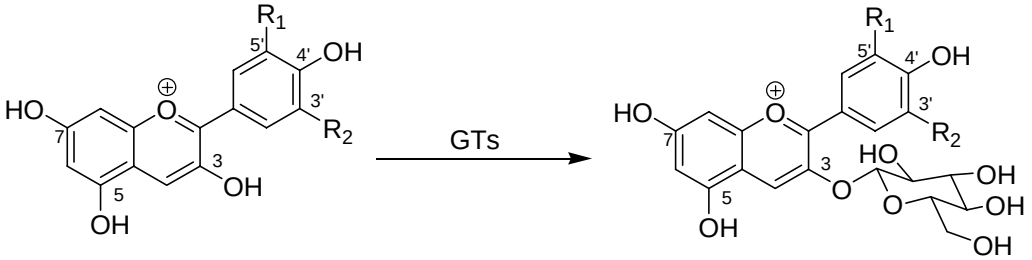


**126** $R_1$= OH; $R_2$=H
**127** $R_1$=$R_2$=OH
**128** $R_1$=$R_2$=H

**129** $R_1$= OH; $R_2$=H
**130** $R_1$=$R_2$=OH
**131** $R_1$=$R_2$=H

**Scheme 1.16** Glucosylation at 3-OH position of different anthocyanidins: cyanidin (**126**), delphinidin (**127**), pelargonidin (**128**).

Formation of anthocyanidin 3-*O*-glucoside is known to be an early-stage reaction, common to most anthocyanin biosynthesis (Yamazaki et al., 1999). The late stage involves the reactions of further modifications such as glycosylation, acylation and methylation. The late-stage transformations of the biosynthetic pathway involving 5-*O*-glucosyltransferase have been studied in the plant *Perilla frutescens* var. *crispa* (Gong et al. 1997, Yamazaki et al., 1999). The cDNA encoding 5-*O*-glucosyltransferases from *P. frutescens* and *Verbena hybrida* (verbena) were isolated by over expressing in yeast cells and their molecular and biochemical properties were characterized (Yamazaki et al., 1999). Both the recombinant enzymes in the yeast extracts catalyzed the conversion of anthocyanidin 3-*O*-glucosides (**129**, **130**, **131**) into the corresponding anthocyanidin 3,5-di-*O*-glucosides (**132**, **133**, **134**) using UDP-glucose as a cofactor (Scheme 1.17). Recently, a single glucosyltransferase that synthesized the cyanidin 5-*O*-glucoside (**135**) first, followed by the cyanidin 3,5-di-*O*-glucoside (**132**) was identified in *Rosa hybrida* (Scheme 1.18) (Ogata et al., 2005). The activity was confirmed to reside in a single gene product by in vitro assay of the recombinant enzyme (RhGT1), which could use either cyanidin (**126**) or cyanidin 5-*O*-glucoside (**135**) as an acceptor, but not the cyanidin 3-*O*-glucoside (**129**).

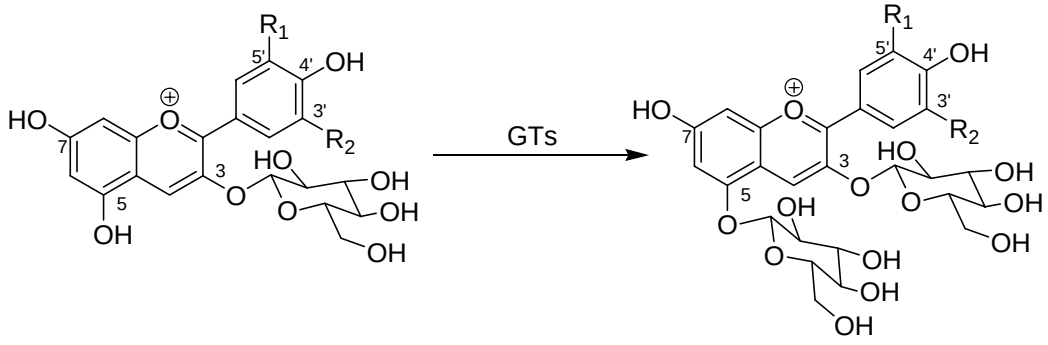


**129** $R_1$= OH; $R_2$=H
**130** $R_1$=$R_2$=OH
**131** $R_1$=$R_2$=H

**132** $R_1$= OH; $R_2$=H
**133** $R_1$=$R_2$=OH
**134** $R_1$=$R_2$=H

**Scheme 1.17** Glucosylation at 5-OH position of different anthocyanidins 3-*O*-glucosides.

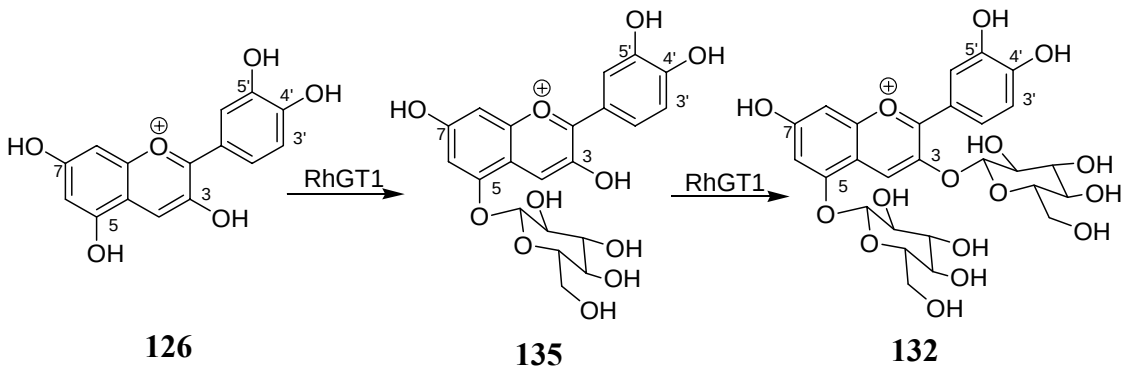


**126** **135** **132**

**Scheme 1.18** Sequential glucosylation of cyanidin (**126**) by a glucosyltransferase (RhGT1) from rose petals.

**Betalains**

Betalains, red betacyanins and yellow betaxanthins, comprise a class of chromogenic compounds which replace the anthocyanins as flower and fruit pigments in most families of the Caryophyllales (Vogt et al., 1999). Although not studied as extensively as the anthocyanin pigments, a number of studies have focused on the synthesis of betacyanins and particularly their glycosylation. Betanidin 5-O-glucosyltransferase (5-GT) was purified from cell suspension cultures of *Dorotheanthus bellidiformis* (Vogt et al., 1997), and shown to catalyze specifically the transfer of glucose to the 5-OH group of betanidin (**136**) (Scheme 1.19). The cDNA encoding 5-GT was cloned and expressed, and the highest activity of the recombinant enzyme in vitro was shown toward betanidin (**136**), with regiospecific transfer of glucose to the 5-OH position (Vogt et al., 1999). In addition, the enzyme accepted *o*-dihydroxylated flavonoids, e.g. quercetin (**102**), transferring glucose to the 4′-OH and 7-OH positions.

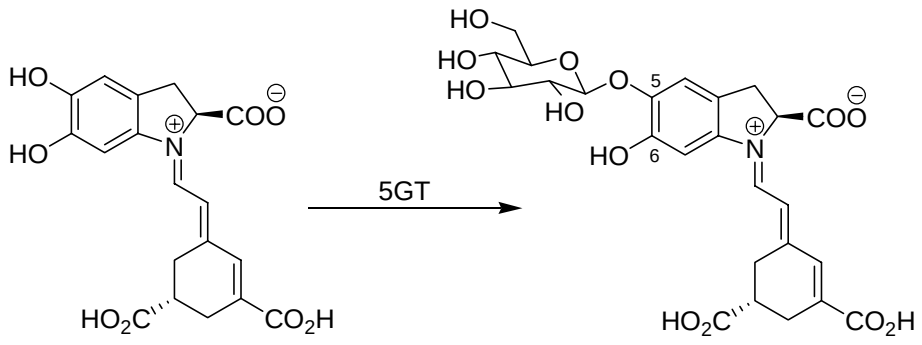


**136** **137**

**Scheme 1.19** Formation of betanin **137** catalyzed by betanidin 5-*O*-glucosyltransferase.

**Terpenoids and steroids**

In *Stevia rebaudiana*, glycosyltransferases are involved in the production of steviol glycosides, compounds that are unique in the plant world because of their intense sweetness and high concentration in leaf tissue (Richman et al., 2005). The synthesis of steviol glycosides starts with steviol (**138**). As shown in Scheme 1.20, the C-13 alcohol is glucosylated first, yielding steviolmonoside (**139**), which undergoes a number of sequential glucosylation reactions yielding complex steviol glycosides (e.g., rubusoside, steviolbioside, stevioside, etc.). Recently, three GTs (UGT74G1, UGT76G1, and UGT85C2) were identified and cloned from *Stevia* leaves; and regioselective glucosylation of steviol (**138**) was confirmed through in vitro analysis of the recombinant enzymes (Richman et al., 2005). Among them, UGT85C2 was reported to catalyze the formation of steviolmonoside (**139**) from steviol (**138**) (Scheme 1.20).

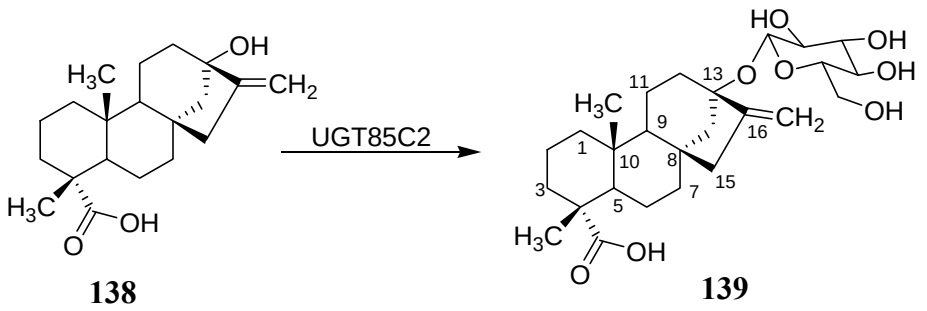


**138** **139**

**Scheme 1.20** Formation of steviolmonoside (**139**) catalyzed by *Stevia rebaudiana* glucosyltransferase, UGT85C2.

Steroidal glycoalkaloids are a family of nitrogenous secondary metabolites produced in solanaceous plants (Moehs et al., 1997). Addition of glycosyl residues to the aglycon, steroidal alkaloids (Fig. 1.10), has been proposed to occur in a sequential manner, initiated by UDP-glucose and UDP-galactose glycosyltransferases. For example, the enzyme solanidine UDP-glucose glucosyltransferase (StSGT) catalyzes the biosynthesis of solanidine 3-*O*-glucoside (also known as γ-chaconine, **143**) from UDP-glucose and solanidine (**140**) (Scheme 1.21). Moehs et al. (1997) reported the isolation of a cDNA clone encoding StSGT from wound-induced potato (*Solanum tuberosum*). The recombinant StSGT from yeast could glucosylate solanidine (**140**) at a slower rate than the other two aglycons, solasodine (**141**) and tomatidine (**142**). The enzyme showed the highest substrate specificity towards the substrate, tomatidine (**142**). Recently, Kohara et al. (2005) showed that the glucosyltransferase StSGT also glucosylated steroidal sapogenins such as diosgenin (**144**), nuatigenin (**145**), and tigogenin (**146**), in addition to its reported substrates, solanidine (**140**), solasodine (**141**) and tomatidine (**142**) (Moehs et al., 1997). Another cDNA encoding glucosyltransferase (SaGT4A) from *S. aculeatissimum* has been reported that catalyzed the 3-*O*-glucosylation of steroidal sapogenins, such as diosgenin (**144**), nuatigenin (**145**), and tigogenin (**146**) forming saponins (Fig. 1.11 and Scheme 1.22) (Kohara et

al., 2005). Similar to StSGT, the enzyme SaGT4A also glucosylated steroidal alkaloids, solanidine (**140**), solasodine (**141**) and tomatidine (**142**).

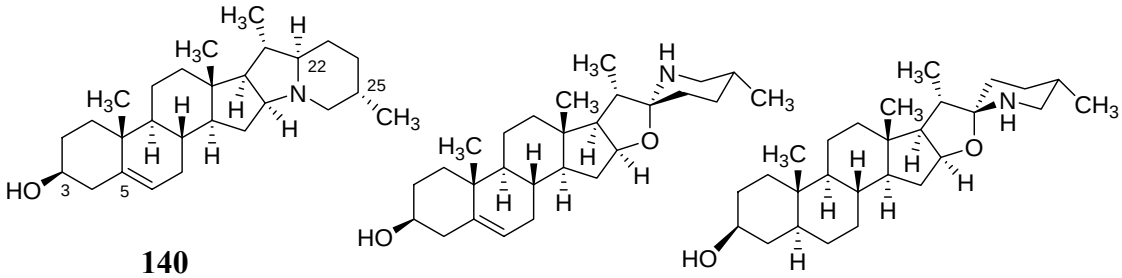

**140** **141** **142**

**Figure 1.10** Chemical structures of steroidal alkaloids: solanidine (**140**), solasodine (**141**) and tomatidine (**142**).

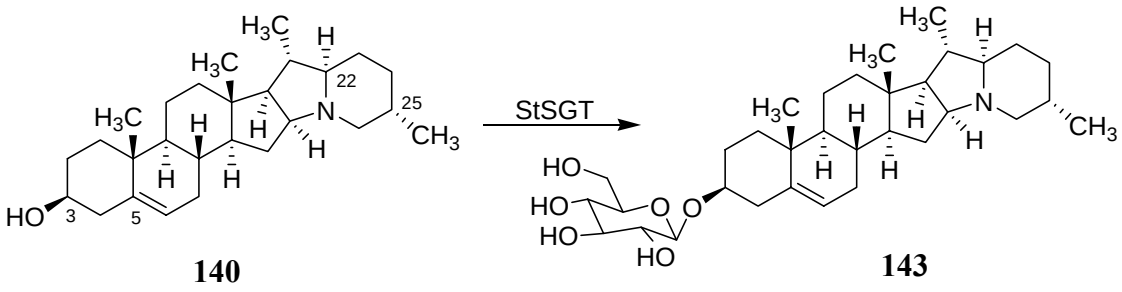


**140** **143**

**Scheme 1.21** Formation of solanidine 3-*O*-glucoside (**143**) catalyzed by solanidine UDP-glucose glucosyltransferase (StSGT).

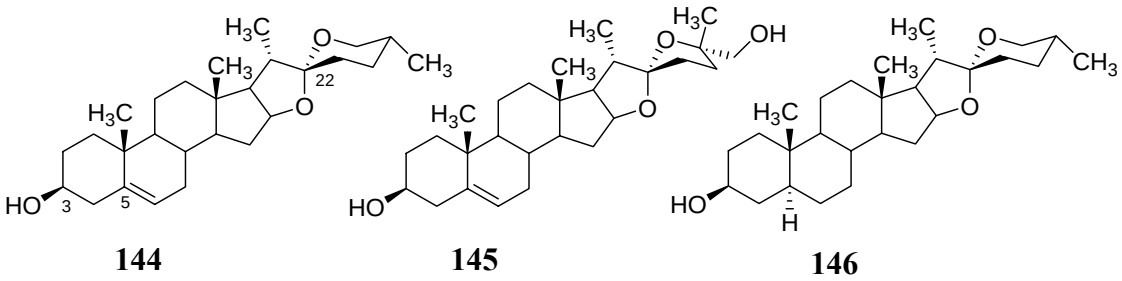

**144** **145** **146**

**Figure 1.11** Chemical structures of steroidal sapogenins: diosgenin (**144**), nuatigenin (**145**) and tigogenin (**146**).

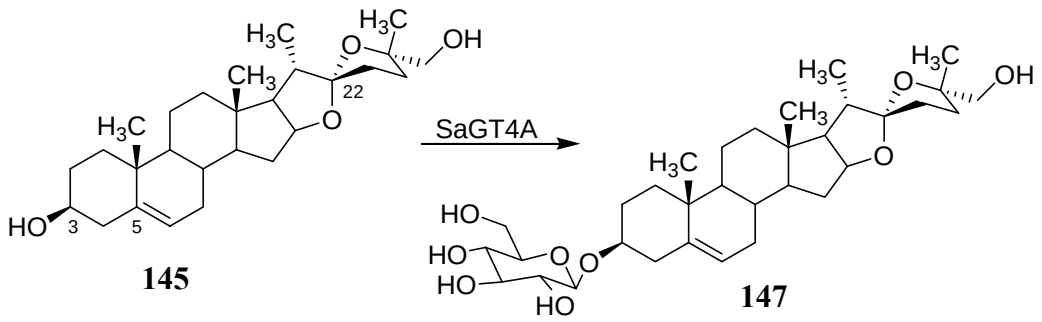


**Scheme 1.22** Formation of nuatigenin 3-*O*-glucoside (**147**) catalyzed by the glucosyltransferase, SaGT4A.

**Glucosinolates and cyanogenic glucosides**

Glucosinolates **152** are a class of secondary metabolites with important roles in plant defense and human nutrition produced mainly by Brassicaceae. Biosynthesis of glucosinolates **152** involves the oxidation of the amino group of amino acid **148**, followed by oxidation/decarboxylation to aldoxime **149** which is subsequently converted to thiohydroximate **150** in several steps. The thiohydroximate **150** intermediate is then glucosylated on the sulfur by UDP-glucose:thiohydroximate *S*-glucosyltransferase (*S*-GT) to give desulfoglucosinolate **151**. The final step is the exchange of the hydroxyl on the nitrogen with a sulfate group by a sulfotransferase to give a glucosinolate anion **152** (Scheme 1.23) (Halkier and Gershenzon, 2006). A thiohydroxymate *S*-glucosyltransferase (*S*-GT) that catalyzed the formation of desulfobenzylglucosinolate (**151**, R=Ph) was partially purified from leaves of *Tropaeolum majus* L. and its substrate specificities were determined using a number of acceptor substrates, thiohydroximates (Matsuo and Underhill, 1971). Except acetothiohydroximate, all of the thiohydroximate homologues (e.g. propiothiohydroximate, butyrothiohydroximate, isobutyrothiohydroximate, 4-methylthiobutyrothiohydroximate, and benzothiohydroximate) were active as glucose acceptors. The authors found similar glucosyltransferase activity in the cell-free extracts of other glucosinolate containing plants such as *Sinapis alba* L., *Nasturtium*

*officinale* R. Br. and *Armoracia lapathifolia* Gilib. The *S*-GT enzyme from *Brassica napus* L. seedlings was purified to near homogeneity and specific activities were determined using phenylacetothiohydroximate, 3-phenylpropanothiohydroximate, and 2-(3-indolyl)acetothiohydroximate as glucose acceptors (Reed et al., 1993). The enzyme showed similar substrate specificities towards these acceptors. *S*-GT enzymes were also reported from florets of *B. oleracea* ssp. *botrytis* (cauliflower) and *A. thaliana* inflorescences (GrootWassink et al., 1994; Guo and Poulton, 1994). The first gene encoding a thiohydroxymate *S*-glucosyltransferase (*S*-GT) was cloned from *B. napus* and the activity of the recombinant enzyme partially characterized in vitro (Marillia et al., 2001). Grubb et al. (2004) also reported a gene encoding thiohydroxymate *S*-glucosyltransferase (UGT74B1) from *Arabidopsis* that catalyzed the synthesis of desulfobenzylglucosinolate (**151**, R=Ph) from phenylacetothiohydroximate (**150**, R=Ph) and UDP-glucose in vitro (Scheme 1.23). The role of UGT74B1 was also analyzed in plant using a T-DNA insertional mutant. In the mutant, significantly decreased levels of glucosinolates were observed together with chlorosis along the leaf veins, suggested to be caused by toxicity from the build up of thiohydroximates.

Mandelonitrile was used as substrate to purify a glucosyltransferase (HMNGT) from *Sorghum bicolor*, and its sequence used to clone a gene whose recombinant product was assayed in vitro for activity against a range of acceptors (Jones et al., 1999; Hansen et al., 2003). The recombinant enzyme showed a broad substrate specificity including the conversion of *p*-hydroxymandelonitrile (**153**) to yield the cyanogenic glucoside, dhurrin (**154**) (Scheme 1.24).

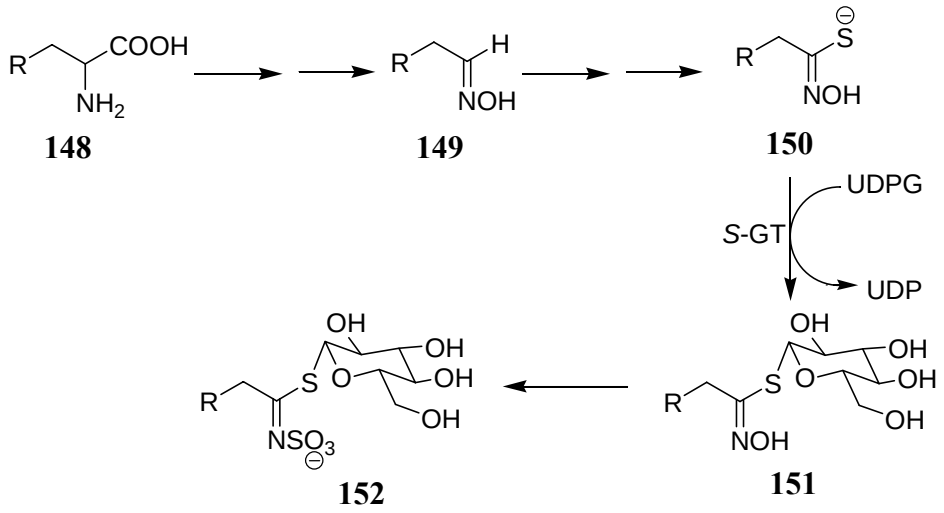


**Scheme 1.23** Partial pathway for the biosynthesis of glucosinolates **152** and glucosylation of thiohydroximates (**150**) to desulfoglucosinolate (**151**) catalyzed by thiohydroximate *S*-glucosyltransferase (*S*-GT) (Halkier and Gershenzon, 2006).

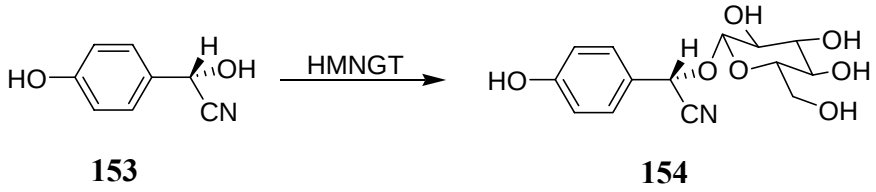


**Scheme 1.24** Formation of cyanogenic glucoside, dhurrin (**154**) catalyzed by *p*-hydroxymandelonitrile *O*-glucosyltransferase (HMNGT).

### *1.6.1.2 Detoxification of secondary metabolites*

Plants need to detoxify or regulate the bioactivity of a diverse set of low-molecular-weight compounds (Jones and Vogt, 2001). These chemicals are either produced as endogenous defense or signaling molecules or they are imposed on plants from exogenous sources. Plants are known to have a wide range of glucosyltransferases to detoxify endogenous or exogenous toxic secondary metabolites produced by themselves or by other organisms. Endogenous aglycones originate from biosynthetic as well as degradative or turnover metabolism (Bak et al., 1999; Walter et al., 2000). For example, some phytoanticipins are detoxified to non-toxic glucosides and stored in

vacuoles of plant cells. Upon invasion by pathogens or herbivores, these non-toxic glucosides are then hydrolyzed to active phytoanticipins by glycosidases and act as a plant defense mechanism (Osbourn, 1996). Plants also utilize glucosyltransferases to detoxify exogenous secondary metabolites produced by other organisms such as phytotoxins and allelochemicals. For the glucosylation, where functional groups such as –OH, -NH, -SH or –COOH are not present in the aglycones, they may be introduced by oxidation, most typically catalyzed by mono-oxygenases, or may be produced by hydrolysis or reduction of the molecule (Cole and Edwards, 2000). It has been known that glucosylations in plants usually take place in the cytosol and then the glucosylated products are transported either into the vacuole or into the apoplast (Sandermann et al., 1997).

During the last two decades, a significant number of reports on detoxification of secondary metabolites such as mycotoxins, phytotoxins, and allelochemicals where glucosyltransferases play important roles has been reported. The results of these detoxifications and the related glucosyltransferases that have been isolated and characterized from different plant sources are discussed in the following sections.

**Fungal secondary metabolites**

Cultivated plants are potential hosts for pathogenic fungi during crop growth and are colonized by saprophytic fungi after the harvest. Some field and storage fungi are producers of a variety of secondary metabolites, some of which are known as mycotoxins- fungal metabolites that affect human and animal health (Gilbert, 1995). Mycotoxins can be toxic, mutagenic, carcinogenic, immunosuppressive or interfere with hormonal functions. Many secondary metabolites of plant pathogenic fungi, termed phytotoxins, are involved in pathogenesis (Graniti, 1991). Some secondary metabolites can be regarded as both mycotoxins and phytotoxins.

**Mycotoxins**

4-Deoxynivalenol (**155**), produced by *Fusarium* species such as *F. graminearum* and *F. culmorum*, is an important mycotoxin that causes inhibition of protein synthesis in eukaryotes and is also phytotoxic, causing chlorosis, necrosis and wilting in planta (Lemmens et al., 2005). *Fusarium* species are causative agents of Fusarium head blight (FHB) of wheat and ear rot of maize (Sewald et al., 1992). Results of several studies suggested that the *in vitro* resistance of wheat cultivars toward 4-deoxynivalenol (**155**) correlates with FHB resistance in the field (Mesterhazy, 2003). Miller and Arnison (1986) found that cell suspension cultures of the FHB-resistant wheat cv. Frontana converted more $^{14}$C-labeled **155** into uncharacterized products than cell cultures derived from the susceptible wheat cv. Casavant. When they incubated $^{14}$C-labeled **155** with cell suspension cultures of wheat, three metabolites of $^{14}$C-labeled **155** were detected. One of these metabolites was proposed to be a glucoside of **155** based on the molecular weight. Later Fujita et al. (1990) also found three metabolites of **155** in sweet potato root tissues in a similar experiment with radiolabeled material, but the structures of the glucosylated metabolites were not elucidated. Later on, the isolation and structure elucidation of this glucosylated compound was first reported by Sewald et al. (1992). They also detected three metabolites of **155** when $^{14}$C-labeled **155** was incubated with cell suspension cultures of maize. The main metabolite was isolated from the cultures and the structure was elucidated as 3-β-D-glucopyranosyl-4-deoxynivalenol (**156**) by using different 1D and 2D NMR techniques (Scheme 1.25).

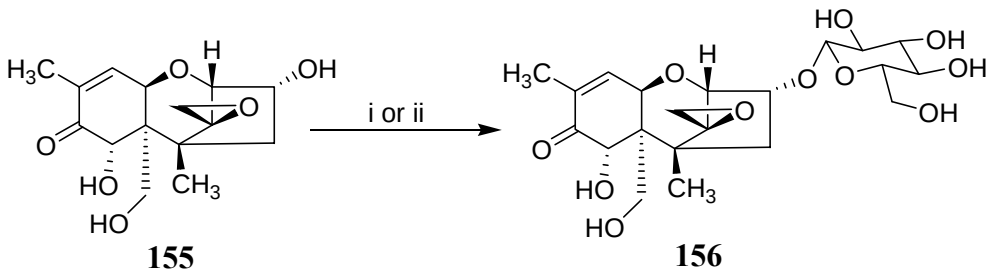


**Scheme 1.25** Glucosylation of 4-deoxynivalenol (**155**): (i) in cell suspension cultures of maize (Sewald et al., 1992); (ii) *Arabidopsis* DOGT1 glucosyltransferases expressed in yeast cells (Poppenberger et al., 2003).

Poppenberger et al. (2003) reported the isolation and characterization of a gene from *A. thaliana* encoding a UDP-glucosyltransferase that is able to glucosylate 4-deoxynivalenol (**155**) (Scheme 1.25). The enzyme, assigned as DOGT1 (previously assigned as UGT73C5), can catalyze the transfer of glucose from UDP-glucose to the hydroxyl group at carbon 3 of **155** (Scheme 1.25). They found that the expression of this glucosyltransferase was developmentally regulated and induced by **155**, as well as salicylic acid, ethylene and jasmonic acid. They also showed that, compared with **155**, 3-β-D-glucopyranosyl-4-deoxynivalenol (**156**) had a strongly reduced ability to inhibit protein synthesis by a wheat germ extract in vitro (Poppenberger et al., 2003). This result indicated that glucosylation of 4-deoxynivalenol (**155**) represents a detoxification process. The transgenic *A. thaliana* constitutively expressing DOGT1 displayed resistance against 4-deoxynivalenol (**155**) (Poppenberger et al., 2003). Compared with wild type, germination occurred earlier, roots were formed, cotyledons did not bleach, and true leaves appeared in the transgenic *A. thaliana*. The glucosyltransferase DOGT1 was also found to detoxify the acetylated derivative 15-acetyl-4-deoxynivalenol (**157**), whereas no protective activity was observed against the structurally similar nivalenol (**158**) (Poppenberger et al., 2003) (Fig. 1.12). Recently, Lemmens et al. (2005) examined ninety-six double haploid lines of wheat from a cross between CM-82036 (highly resistant to FHB) and Remus (susceptible) for 4-deoxynivalenol (**155**)

resistance. They found that in resistant wheat lines, the applied compound **155** was also converted to the glucoside **156** as the detoxification product. From their observations, it was suggested that resistance to **155** is important in the FHB resistance complex of wheat and hypothesized that the resistant genes either encode a deoxynivalenol-glucosyltransferase or regulate the expression of such an enzyme.

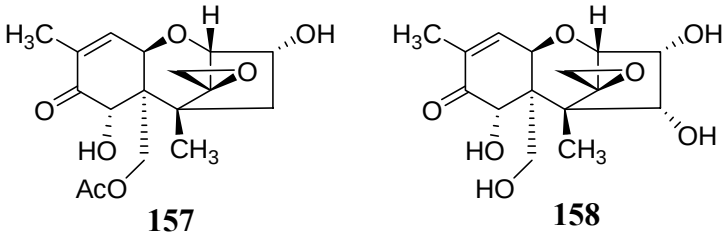


**Figure 1.12** Structure of 15-acetyl-4-deoxynivalenol (**157**) and nivalenol (**158**).

The mycotoxin zearalenone (**159**) is a secondary metabolite with estrogenic activity produced also by a series of *Fusarium* strains, especially *Fusarium graminearum* and *F. culmorum* on cereal grains in the field and in storage (Bennett and Shotwell, 1979). Zearalenone (**159**) contaminated feed has been implicated in numerous cases of fertility disturbances in farm animals, especially pigs (Kuiper-Goodman et al., 1987). Engelhardt et al. (1988) reported the transformation of **159** in cell suspension cultures of *Zea mays*. In this study, $^{14}$C-labeled **159** was incubated with cell suspension cultures of maize and monitored the disappearance of the toxin. Three metabolites were isolated from the cultures which were identified as α-zearalenol (**160**), β-zearalenol (**161**) and zearalenone-4-β-D-glucopyranoside (**162**) by co-chromatography with authentic samples and by mass spectrometry (Scheme 1.26). Although the structure elucidation of **162** was only performed by LC-MS and specific hydrolysis with β-glucosidase, it was later confirmed by the comparison of $^{1}$H NMR data of the isolated compound with that of the synthetic compound (Zill et al., 1990). Zearalenone-4-β-D-glucopyranoside (**162**) was also detected as a product of

zearalenone (**159**) metabolism in wheat cells (Schneweis et al., 2002). It has been found that attachment of the glucose moiety to zearalenone (**159**) prevented the interaction of the mycotoxin with the human estrogen receptor in vitro (Poppenberger et al., 2006). Though plants can inactivate zearalenone (**159**) as glucosylated zearalenone **162**, this glucoside can be easily hydrolyzed to free zearalenone (**159**) during digestion and implicated in the development of mycotoxicosis (Schneweis et al., 2002).

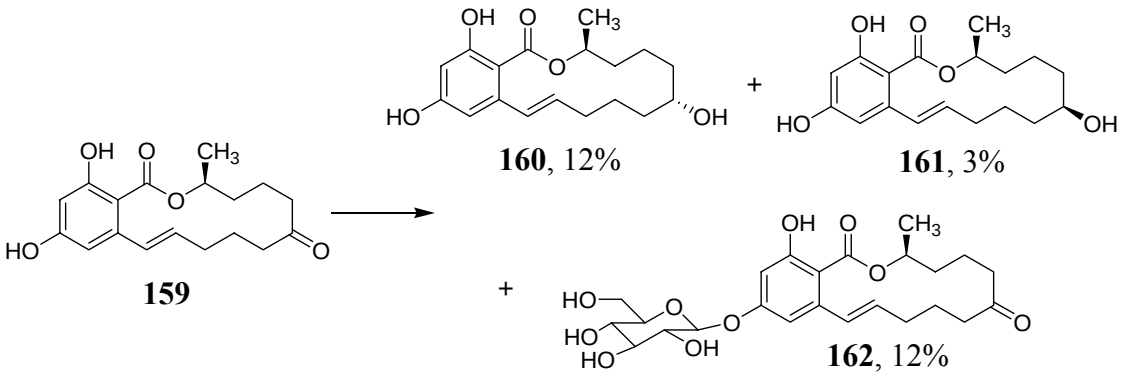


**Scheme 1.26** Biotransformation of zearalenone (**159**) in cell suspension cultures of maize (Engelhardt et al., 1988).

Poppenberger et al. (2006) recently reported that two similar *UGT73C* genes of *A. thaliana* encoded glucosyltransferases that glucosylate zearalenone (**159**) to zearalenone-4-β-D-glucopyranoside (**162**) in yeast (*Saccharomyces cerevisiae*) (Scheme 1.27). Comparison of chemically synthesized **162** and the yeast product by HPLC-MS/MS indicated that **159** was converted to this glucoside by the *Arabidopsis* UGT73C5 and UGT73C6 glucosyltransferases. The other four highly similar glucosyltransferases encoded by the *UGT73C* cluster did not make this conversion. These results were not consistent with the hypothesis that sequence similarity indicates similar substrate specificities for glucosyltransferases (Poppenberger et al., 2006).

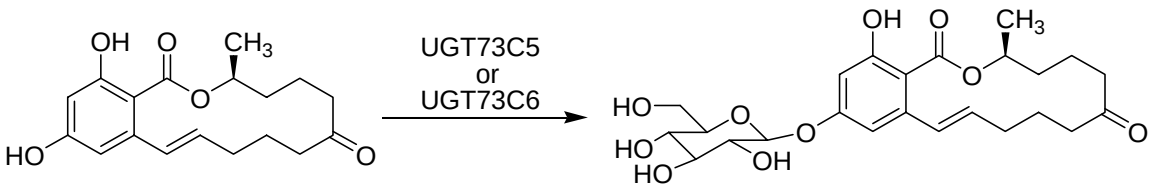


**159** **162**

**Scheme 1.27** Glucosylation of zearalenone (**159**) by two *Arabidopsis* UGT73C glucosyltransferases expressed in *Saccharomyces cerevisiae* (Poppenberger et al., 2006).

**Phytotoxins**

Maculosin (**163**) is a host-specific phytotoxin produced by the fungal pathogen, *Alternaria alternata*, on a weedy plant, spotted knapweed (*Centaurea maculosa*) (Park et al., 1994). The toxin **163** is a dioxopiperazine of cyclo(L-Pro-L-Tyr). Although a number of dioxopiperazines were reported from *A. alternata*, only maculosin (**163**) was found to cause chlorotic spots developing into black necrotic lesions on the leaves of knapweed (Stierle et al., 1988; Park et al., 1994). The metabolism of **163** in leaves of spotted knapweed was investigated by Park et al. (1994) using $^{14}$C-labeled **163**. It was reported that **163** was converted to three metabolites which were more polar than **163**. The major metabolite was isolated and characterized as maculosin β-*O*-D-glucoside (**164**) (Scheme 1.28). The glucoside **164** did not induce any symptoms on the leaves of spotted knapweed in contrast to maculosin (**163**). These results indicated that the metabolism of **163** in spotted knapweed was a detoxification process. The other two metabolites of **163** were not characterized although one of them was proposed to be a methyl ester of dipeptides (L-Pro-L-Tyr-COOH or L-Tyr-L-Pro-COOH), resulting from hydrolysis followed by methylation of the dioxopiperazine moiety of maculosin (**163**), on the basis of its chemical properties.

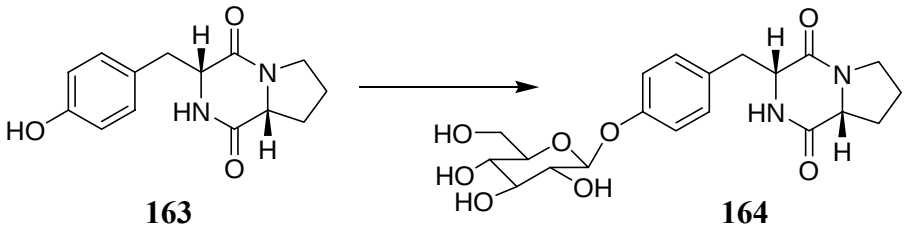


**Scheme 1.28** Biotransformation of maculosin (**163**) in leaves of spotted knapweed (*Centaurea maculosa*) (Park et al., 1994).

Fomannoxin (**165**) is a phytotoxic secondary metabolite produced by the pathogenic root and butt rot fungus *Heterobasidion annosum* during the infection process (Hirotani et al., 1977; Heslin et al., 1983). Sonnenbichler et al. (1989) reported that **165** had strong inhibitory effect on the growth of various organisms such as antagonistic fungi, bacteria and plant cells, and on the protein biosynthesis in protoplasts of *Picea abies* and *Nicotiana tabacum*. The biotransformation of **165** was investigated in *Pinus sylvestris* cultures (conifer cell cultures); **165** was completely metabolized in five days to fomannoxin alcohol (**166**) and fomannoxin carboxylic acid-β-D-glucoside (**167**) (Scheme 1.29) (Zweimüller et al., 1997). The authors reported that the reduction of fomannoxin (**165**) to the corresponding alcohol **166** started immediately, then the alcohol concentration decreased together with a continuous increase of the glucoside **167** both in the culture supernatant and in the cells. The chemical structures of both metabolites (**166** and **167**) were determined spectroscopically (IR, MS, NMR) and confirmed by chemical synthesis. Fomannoxin (**165**) showed phytotoxic and growth inhibition effects on callus of *P. sylvestris*, with necrotization. In contrast to **165**, both **166** and **167** did not show any toxic effect which indicated that these metabolic products were detoxification products.

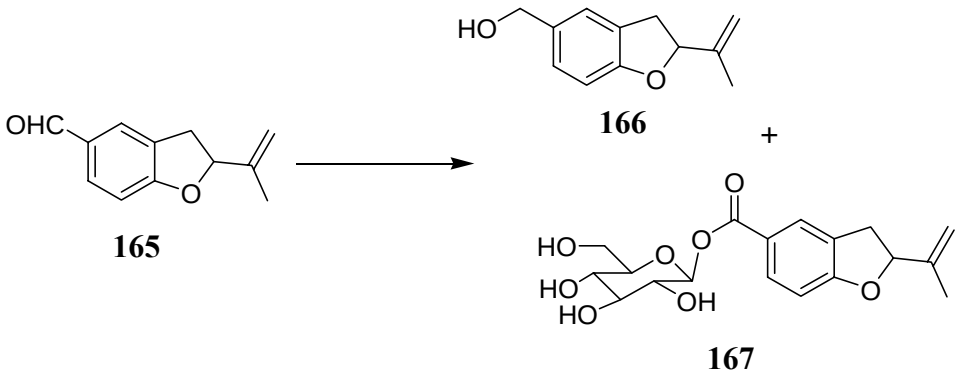


**Scheme 1.29** Biotransformation of fomannoxin (**165**) in conifer (*Pinus sylvestris*) cell cultures (Zweimüller et al., 1997).

*Acremonium sp.* is an endophytic fungus of the European yew, *Taxus baccata*. The fungus is a producer of an extremely bioactive peptide, leucinostatin A (**168**) which is phytotoxic, broadly antifungal, and has toxicity against certain cancer cell lines (Strobel et al., 1997; Fukushima et al., 1983). Using $^{14}$C-leucinostatin A (**168**) in aseptic *Taxus* tissues, Strobel and Hess (1997) showed that **168** was metabolized to a unique product, leucinostatin A β di-*O*-glucoside (**169**) (Scheme 1.30), which has a lower bioactivity against plants, fungi and cancer cell lines than leucinostatin A (**168**). Acetone powder extracts from various plants were also shown to have UDP-glucose:leucinostatin A glucosyltransferase that could catalyze the production of leucinostatin A β di-*O*-glucoside (**169**) from leucinostatin A (**168**). Higher levels of enzymatic activity were generally associated with those plants that are relatively resistant to the phytotoxic effects of leucinostatin A (**168**), including all yew species tested (Strobel and Hess, 1997).

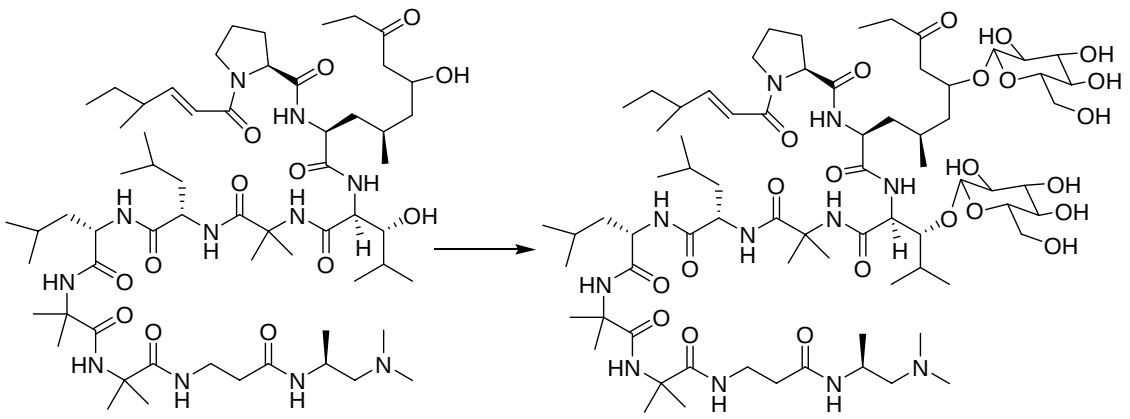

**168** **169**

**Scheme 1.30** Glucosylation of leucinostatin A in European yew (*Taxus baccata*) (Strobel and Hess, 1997).

Destruxin B (**4**) is a host-selective phytotoxin produced both in vitro and in plants by the fungal pathogen *Alternaria brassicae*, which causes blackspot disease in crucifers (Pedras et al., 2001). The toxin **4** is a cyclic depsipeptide that causes tissue damage similar to that observed in plants naturally infected with *A. brassicae* (Agarwal et al., 1994). Pedras et al. (2001) reported that white mustard (*Sinapis alba* cultivar Ochre, resistant to black spot) was able to metabolize $^{14}$C-labeled destruxin B (**4**) to a less toxic compound, hydroxydestruxin B (**170**) (Scheme 1.31). This transformation occurred substantially faster than in any of the susceptible *Brassica* species (*B. napus* cultivar Westar and *B. juncea* cultivar Cutlass). They also reported that the $^{14}$C-labeled **170** was further metabolized to β-D-glucosyl hydroxydestruxin B (**171**) and that this glucosylation of **170** in resistant species occurred at a slower rate than that of susceptible species. The chemical structures of both metabolites (**170** and **171**) were elucidated from their spectroscopic data (NMR, HR-MS, IR) and confirmed by chemical synthesis. Bioassays using leaves and cell suspension cultures to determine the phytotoxicity of **170** and **171** indicated that the hydroxylated compound **170** was less phytotoxic than destruxin B (**4**) and that the glucosylated compound **171** had no

toxic effect on either leaves or cell suspension cultures. Wild crucifers such as *Camelina sativa*, *Capsella bursa-pastoris*, and *Eruca sativa* are also reported to detoxify destruxin B (**4**) by hydroxylation followed by glucosylation as shown in Scheme 1.31 (Pedras et al., 2003c).

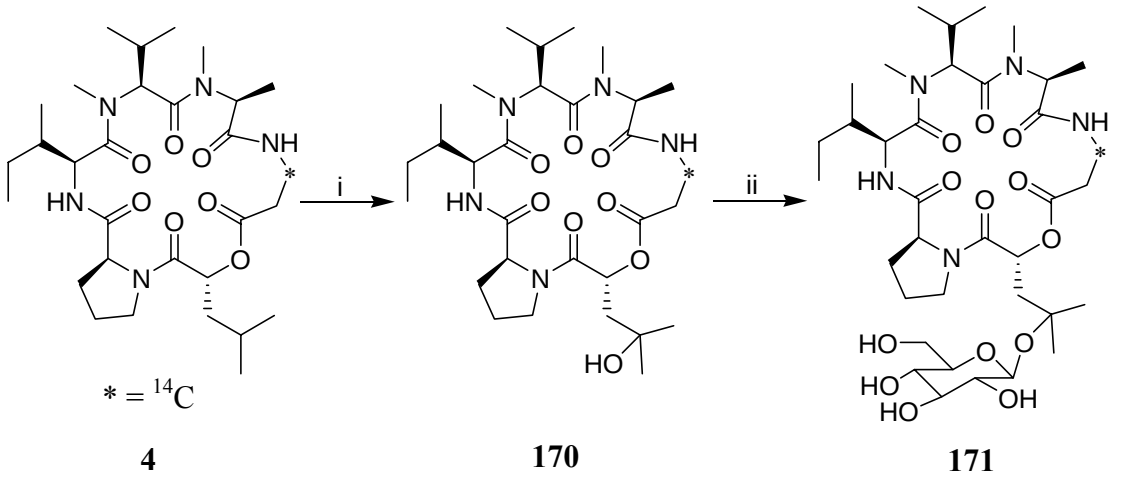


**Scheme 1.31** Biotransformation of destruxin B (**4**) by crucifers: (i) hydroxylation; (ii) glucosylation (Pedras et al., 2001).

Thaxtomin A (**172**) is a bacterial secondary metabolite produced by *Streptomyces scabies* which is a causal organism of common scab disease in potato (King et al., 2000). Thaxtomin (**172**) is known to be a phytotoxin which causes typical symptoms of the common scab disease (King et al., 1992). Acuna et al. (2001) reported that scab-resistant potato tubers were able to metabolize **172** to thaxtomin A-β-di-*O*-glucoside (**173**) (Scheme 1.32), which was six-fold less phytotoxic to potato tuber tissue, thus avoiding cell collapse and necrosis. Using mini tubers of scab-resistant and -susceptible individuals treated with $^{14}$C-labeled **172**, they showed that resistant plants were able to produce a higher amount of a radioactive metabolite, with $R_f$ similar to that of thaxtomin A-β-di-*O*-glucoside (**173**), than susceptible ones. They have also evaluated the thaxtomin A glucosyltransferase activity in crude enzyme extracts of scab-resistant and –susceptible plants and found almost twice as much enzyme-specific

activity in resistant than in susceptible individuals. Their results suggested that glucosylation of thaxtomin A (**172**) was a detoxification mechanism of thaxtomin A (**172**) in potato plants, and it was related to scab resistance and susceptibility in potato plants.

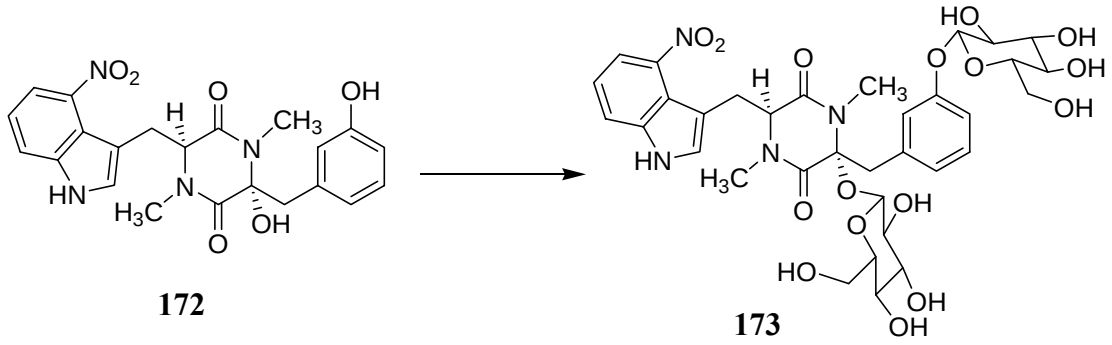

**172** **173**

**Scheme 1.32** Glucosylation of thaxtomin A (**172**) in potato tubers (Acuna et al., 2001).

## Plant secondary metabolites

### Allelochemicals

Environmental concerns about the use of herbicides and other pesticides have inspired the search for alternative weed and pest control strategies. Interdisciplinary investigations by biologists, biochemists, and chemists are now stimulated by the interest to make environmental friendly agrochemicals from natural sources. For example, the natural phenomenon of allelopathy offers a potential new methodology to supplement conventional weed control programs. Allelopathy is the chemical inhibition of one plant species by another and it represents a form of chemical warfare between neighboring plants competing for limited light, water, and nutrient resources (Inderjit and Duke, 2003; Weston and Duke, 2003). One of the more intensively studied classes of allelochemicals is benzoxazinoids and their benzoxazolinone derivatives. For example, the genes encoding all of the enzymes required for the biosynthesis of the benzoxazinoid, 2,4-dihydroxy-7-methoxy-2*H*-1,4-benzoxazin-3(4*H*)-one (**175**) have

been identified in maize and they represent the first known example of a plant secondary metabolic pathway organized as a gene cluster (Frey et al., 1997) (Scheme 1.33).

Benzoxazinoids such as 2,4-dihydroxy-2*H*-1,4-benzoxazin-3(4*H*)-one (**174**) and 2,4-dihydroxy-7-methoxy-2*H*-1,4-benzoxazin-3(4*H*)-one (**175**) are abundant secondary metabolites of Poaceae, including the major agricultural crops maize, wheat and rye (Sicker et al., 2000). While benzoxazinoid **174** is found to be predominant in rye, **175** is the main benzoxazinoid in maize and wheat. Benzoxazinoids **174** and **175** not only play an important role as allelochemicals but also act as defense compounds against microbial pathogens and insect herbivores (Sicker et al., 2000). Benzoxazinoids **174** and **175** are known to have strong phytotoxicity. Therefore, the plants that produce benzoxazinoids usually add a glucose moiety at the 2-position of **174** and **175** (Scheme 1.33) in order to reduce their toxicity and store the glucosides in the vacuole as inactive compounds (von Rad et al., 2001). When the plant tissue is damaged by pathogen infection or herbivore attack, plants produce benzoxazinoids by hydrolyzing the glucosides using glucosidases. For example, it has been reported that the enzymatic release of toxic benzoxazinoid **175** occurred in maize within 30 min after wounding is completed (von Rad et al., 2001).

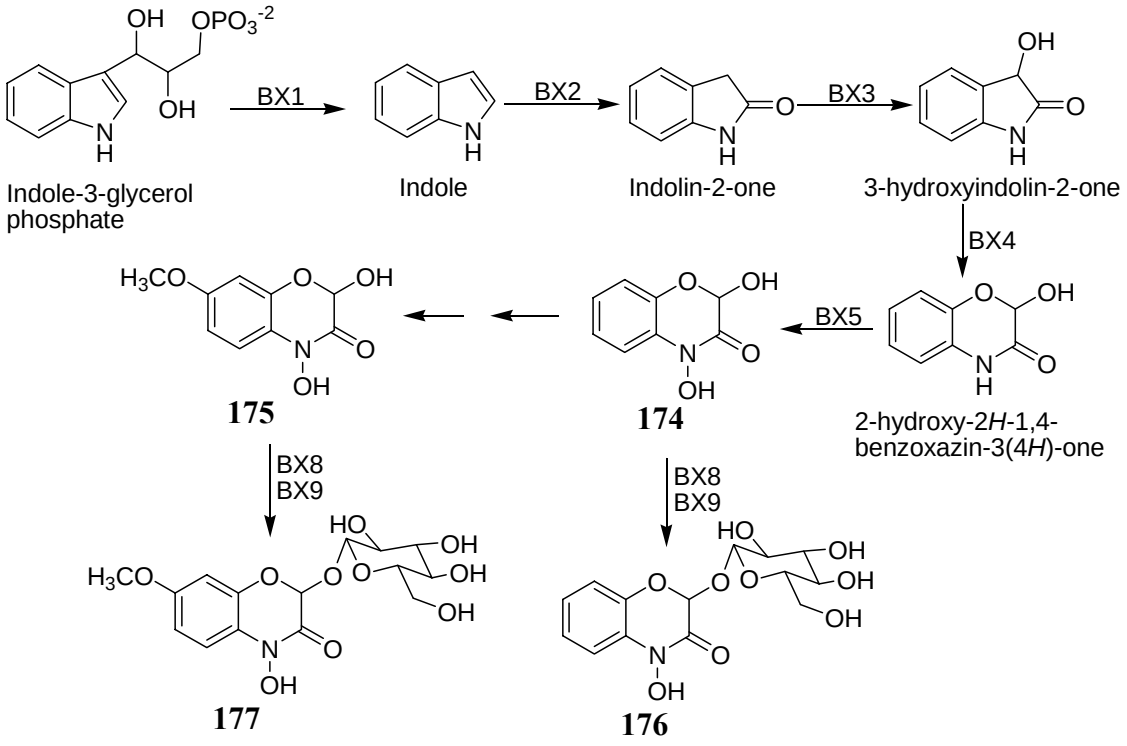


**Scheme 1.33** Biosynthesis of benzoxazinoids (**174**, **175**) and their glucosides (**176**, **177**) in maize (Frey et al., 1997; von Rad et al., 2001).

The presence of the benzoxazinoid glucosides **176** and **177** in maize and wheat was first established in 1959 (Wahlroos and Virtanen, 1959). Bailey and Larson (1989) latter reported that two glucosyltransferases are involved in the biosynthesis of **176** and **177** in maize seedlings. They have shown with the partially purified enzymes that **175** was a substrate for both transferases with similar $K_m$ value whereas **174** was a better substrate for one glucosyltransferase than the other. Two glucosyltransferases capable of transferring glucose at the 2-position of **174** and **175** were also partially purified from rye, wheat and a wild barley species (*Hordeum lechleri*) (Leighton et al., 1994; Sue et al., 2000). von Rad et al. (2001) reported the isolation and characterization of two maize glucosyltransferases, BX8 and BX9, via functional cloning (Scheme 1.33). Although BX8 and BX9 displayed 89% similarity to each other at the amino acid sequence, they had no close relationship to any other known glucosyltransferases. The

glucosyltransferase BX8 accepted benzoxazinoids **174** and **175** equally well as substrates, whereas the enzyme BX9 converted **175** more actively to the respective glucoside **177** than it did **174**. von Rad et al. (2001) also showed that the presence of benzoxazinoids **174** and **175** reduced the growth of wild-type *Arabidopsis* at concentrations that had proven to be effective in natural plant communities (Sicker et al., 2000) whereas transgenic plants expressing *Bx8* and *Bx9* had no toxicity effect of **174** and **175**. These results indicated both the allelopathic capacity of **174** and **175** and the potency of two glucosyltransferases (BX8 and BX9) in reducing the phytotoxicity of these chemicals to a level that is tolerable for the plant.

In nature, not only benzoxazinoids **174** and **175** but also their decomposition products such as benzoxazolin-2(3*H*)-one (**178**) and 6-methoxy benzoxazolin-2(3*H*)-one (**184**) act as allelochemicals. It has been known that benzoxazolin-2(3*H*)-one (**178**) results from a two-step degradation of the glucoside **176** (Scheme 1.34) (Sicker et al., 2004). These compounds are secondary metabolites in several species of Acanthaceae, Poaceae, Ranunculaceae and Scrophulariaceae families (Sicker et al., 2004). Once released to the environment, benzoxazolinones **178** and **184** cause dose-dependent growth inhibitions in dicotyledonous and to a smaller extent, in monocotyledonous species. However, a number of plant species exhibit tolerance to benzoxazolinones and are able to detoxify them to less phytotoxic glucoside and glucoside carbamate derivatives (Scheme 1.35) (Sicker et al., 2004).

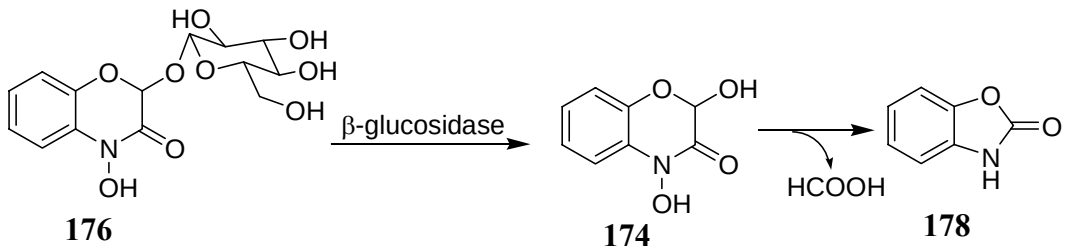


**176** **174** **178**

**Scheme 1.34** Formation of benzoxazolin-2(3*H*)-one (**178**) from enzymatic and chemical degradation of 2-β-D-glucopyranosyloxy-4-hydroxy-2*H*-1,4-benzoxazin-3(4*H*)-one (**176**) (Sicker et al., 2004).

As shown in Scheme 1.35, two major pathways leading to the formation of benzoxazolinone metabolites exhibiting reduced phytotoxicity have been identified in plants. Earlier, when oat roots were analyzed after incubation of benzoxazolinone **178** with seedlings, two new products were detected in the extracts, which were characterized as 6-hydroxybenzoxazolin-2(3*H*)-one (**179**) and its glucoside, 6-*O*-β-D-glucopyranosyloxybenzoxazolin-2(3*H*)-one (**180**) (Wieland et al., 1998) (Scheme 1.35). It was reported that the glucoside **180** was formed via the intermediate **179**, which was subsequently *O*-glucosylated. Later a third product, representing the second route of metabolism, was found that increased with incubation time. It was slightly less polar than **179** with an UV spectrum very similar to benzoxazolin-2(3*H*)-one (**178**). Subsequently, the third product was isolated from oat roots and characterized as 3-β-D-glucopyranosylbenzoxazolin-2(3*H*)-one (**181**) which undergoes spontaneous isomerization to form 1-(2-hydroxyphenylamino)-1-deoxy-β-glucopyranoside 1,2-carbamate (**182**) (Scheme 1.35). The structures of glucoside **181** and its isomeric carbamate **182** were determined from their spectroscopic data and confirmed by chemical synthesis (Wieland et al., 1998, Sicker et al., 2001). Sicker et al. (2001) reported an additional compound as detoxification product of **178** in corn roots, which was characterized as 1-(2-hydroxyphenylamino)-1-deoxy-β-D-gentiobioside 1,2-carbamate (**183**) from its spectroscopic data and chemical analysis. It was proposed that compound **183** was formed from further glucosylation of **182** in corn roots (Scheme

1.36). The phytotoxicity of benzoxazolin-2(3*H*)-one (**178**) and of the metabolites **179**, **180**, and **182** was investigated using the cress test (Schulz and Wieland, 1999). Only the carbamate **182** had no inhibitory influence on radicle growth up to 1 mM, the *O*-glucoside **180** was still slightly toxic, but **179** was more toxic than the original compound **178**.

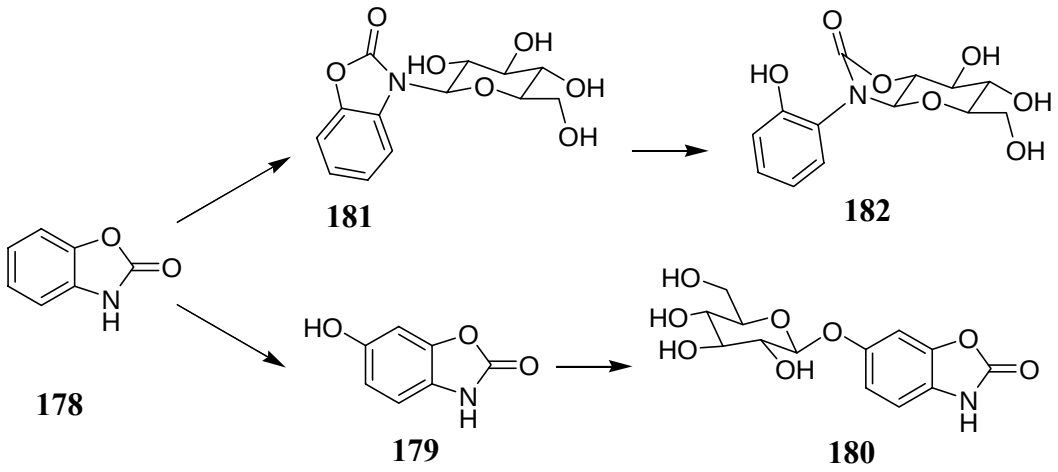


**Scheme 1.35** Common detoxification pathways (*O*- and *N*-glucosylation) of benzoxazolin-2(3*H*)-one (**178**) in plants (Sicker et al., 2004).

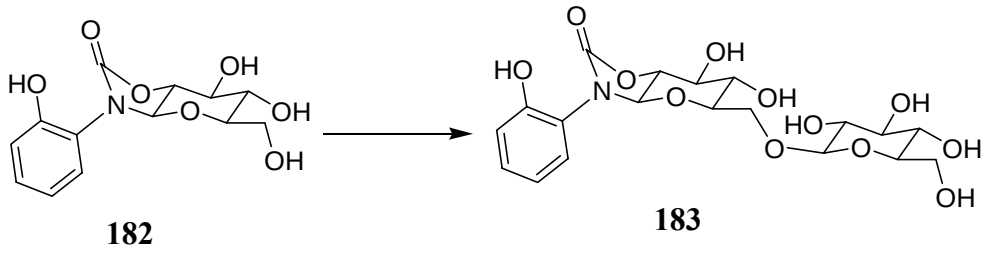


**Scheme 1.36** Formation of gentiobioside carbamate **183** by glucosylation of glucoside carbamate **182** in corn roots (Sicker et al., 2001).

Schulz and Wieland (1999) investigated the ability to metabolize **178** by a number of weeds associated with rye and wheat and compared the metabolism with species of other associations. They found that all tested species were able to metabolize benzoxazolin-2(3*H*)-one (**178**) to **179** and its glucoside **180**. Except three species, the second way of metabolism of **178** resulting in *N*-glucoside **181** was also possible with

all tested species. The detoxification of benzoxazolin-2(3*H*)-one (**178**) in *Arabidopsis* was also investigated (Baerson et al., 2005) and it was found that detoxification occurred predominantly through *O*-glucosylation of the intermediate **179**.

Recently, Hofmann et al. (2006) investigated the detoxification of 6-methoxybenzoxazolin-2(3*H*)-one (**184**) in *Zea mays*. When maize seedlings were incubated with **184** for 24 h, a large amount of glucoside **180** was found in the methanolic extract of maize roots along with a trace amount of new metabolite **185**. When the incubation time was increased up to 48 h, the metabolite **185** was accumulated in higher amount. Subsequently, the metabolite **185** was isolated, purified and characterized as 1-(2-hydroxy-4-methoxyphenylamino)-1-deoxy-β-glucopyranoside 1,2-carbamate (**185**) from its spectroscopic data (Scheme 1.37). Therefore, similar to detoxification of benzoxazolin-2(3*H*)-one (**178**), the detoxification of its methoxy derivative **184** occurred in two pathways: (i) demethylation of **184** followed by *O*-glucosylation to the corresponding glucoside **180** and (ii) direct *N*-glucosylation of **184** followed by isomerization to yield **185**.

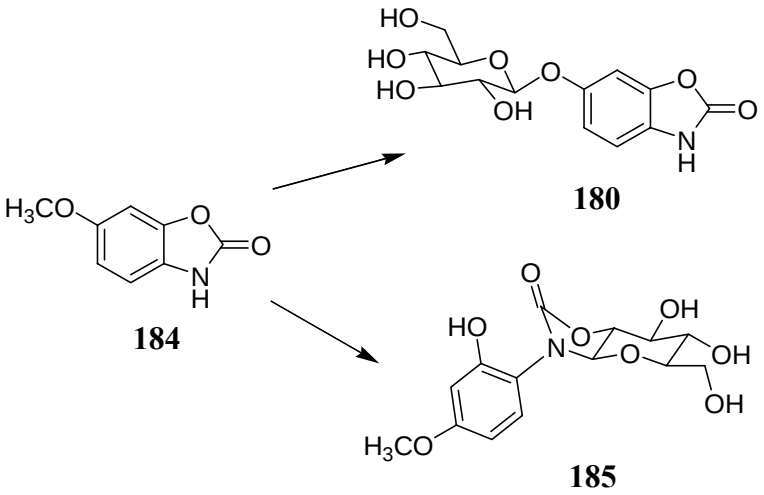


**Scheme 1.37** Detoxification of 6-methoxybenzoxazolin-2(3*H*)-one (**184**) in *Zea mays* (Hofmann et al., 2006).

Hydroquinone (**186**) is a simple phenol that is strongly phytotoxic to leafy spurge (*Euphorbia esula*) and is biosynthesized by small everlasting (*Antennaria microphylla*) (Manners and Galitz, 1986). This phytotoxin participates in the allelopathic interaction between small everlasting and leafy spurge. Hogan and Manners (1990) reported the biotransformation of hydroquinone (**186**) to its nonphytotoxic monoglucoside, arbutin (**187**), in callus and suspension cultures of small everlasting and leafy spurge (Scheme 1.38). Small everlasting was able to detoxify **186** more efficiently than leafy spurge. Differences in the ability of the two species to detoxify hydroquinone were proposed to be a prominent factor in the observed dominance of small everlasting over leafy spurge. UDPG-dependent glucosyltransferase activities were reported in cell-free extracts of small everlasting callus as well as in cell-free extracts of leafy spurge. However, the specific activity of the enzyme preparation from small everlasting callus was six-fold greater than in preparation obtained from leafy spurge (Hogan and Manners, 1991).

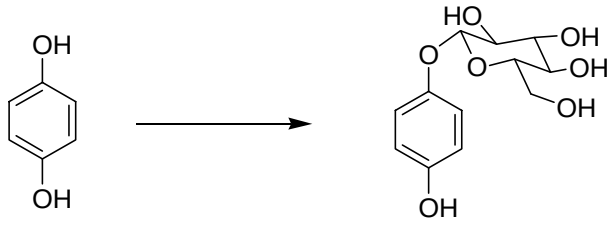


**186** **187**

**Scheme 1.38** Detoxification of hydroquinone (**186**) in everlasting (*Antennaria microphylla*) and leafy spurge (*Euphorbia esula*) (Hogan and Manners, 1990).

### 1.6.2 Microbial glucosyltransferases

Glycosyltransferases play important roles in the biosynthesis of secondary metabolites in microbes, particularly in bacteria. Bacterial glycosyltransferases and their corresponding carbohydrate donating substrates contribute significantly to the diversity of pharmaceutically important metabolites (Thorson et al., 2001; Coutinho et al., 2003a). Secondary metabolites from bacteria containing a carbohydrate moiety and their role in biologically active natural products have been extensively reviewed (Weymouth-Wilson, 1997; Thorson et al., 2001). Although glycosylated secondary metabolites are widespread in bacteria, monoglucosylated (i.e., glucose containing compounds) compounds are less common. One of the extensively studied bacterial glucosyltransferases is the enzyme that transfers a D-glucose to the phenolic hydroxyl of 4-OH-Phegly of a heptapeptide scafold during the biosynthesis of vancomycin (**188**) family (Fig. 1.13) (Mulichak et al., 2001). There are three glycosyltransferase genes in tandem in the chloroeremomycin (**189**) biosynthetic cluster corresponding to GtfA, GtfB and GtfC, respectively. Among these three enzymes, GtfB is responsible for transferring the glucose moiety from a UDP-glucose donor to the vancomycin aglycone acceptor. As shown in Fig. 1.13, two other enzymes, GtfA and GtfC, are responsible for transferring the corresponding carbohydrate moiety indicated by arrows. The X-ray crystal structures of the glucosyltransferase GtfB and two glycosyltransferases GtfA and GtfD have been reported by Mulichak et al. (2001, 2003 and 2004). All these structures contain two Rossmann folds, each built with a central sheet of several β-strands flanked on either side by α-helices. Results from the co-crystallization of these enzymes with their substrates indicated that residues in the *N*-terminal half of the protein were responsible for acceptor biding, whereas those in the C-terminal half were involved mainly in donor interactions.

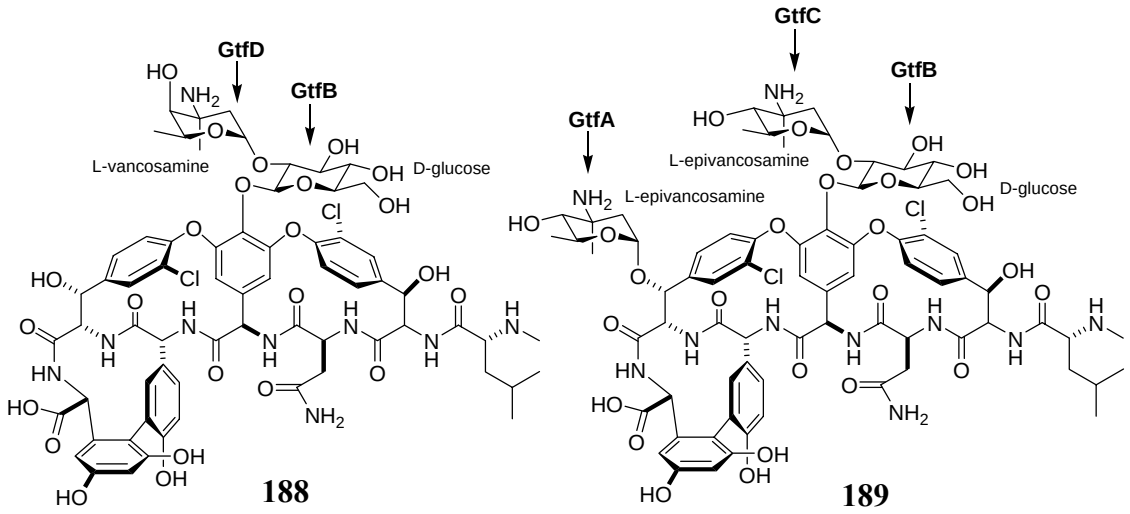


**Figure 1.13** Structure and glycosylation pattern of vancomycin (**188**) and chloroeremomycin (**189**); the enzymes reponsible for the glycosyl transfer are shown above the indicated carbohydrate (Mulichak et al., 2001).

Monoglucosylated secondary metabolites have been reported from a number of fungi. However, the glucosyltransferases involved in the biosynthesis of these metabolites have not been described. Therefore, the microbes that have been used for the biotransformation of biologically active secondary metabolites where glucosyltransferases appear to play an important role are discussed below.

The biotransformation of the mycotoxin zearalenone (**159**) has been studied with a number of nonmycotoxigenic fungi (Kamimura, 1986). Among them, *Rhizopus* sp. was the only fungus which produced zearalenone 4-β-D-glucopyranoside (**162**) from zearalenone (**159**) in addition to α- and β-zearalenol **160** and **161** (Scheme 1.26). This was a similar biotransformation pathway that was also observed in cell suspension cultures of maize (Engelhardt et al., 1988). The flavonoids psiadiarabin (**190**) and its 6-demethoxy analogue **191** were reported to be metabolized by the fungus *Cunninghamella elegans* NRRL 1392 to yield two glucosylated compounds **192** and

**193** (Ibrahim et al., 1997). As shown in Scheme 1.39, the glucosylation position was found to be at C-3′, which was determined by spectroscopic data.

Microbial biotransformation of thaxtomin A (**172**) and thaxtomin B (**194**), the two major phytotoxins associated with the common scab of potato disease, were investigated by King et al. (2000) using the bacterium, *Bacillus mycoides*, in oatmeal broth. It was reported that *B. mycoides* could *O*-glucosylate both thaxtomin A and B (**172** and **194**) to yield glucosides **195** and **196** respectively. Glucosides **195** and **196** were less toxic to potato tubers than the phytotoxins **172** and **194**.

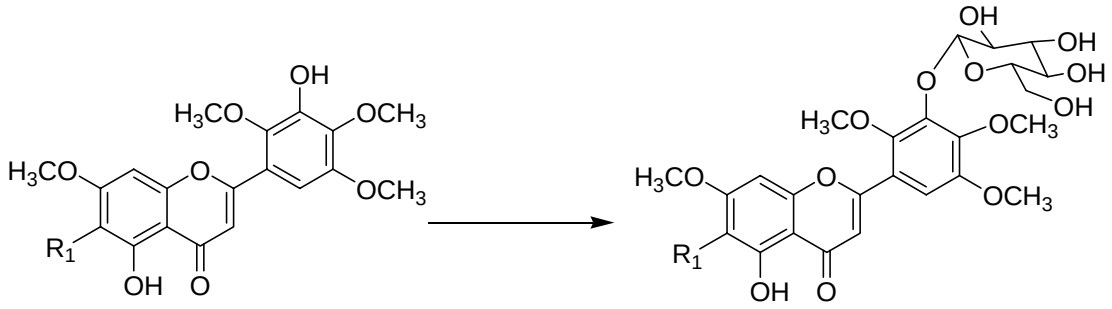

**190** $R_1$=$OCH_3$
**191** $R_1$=H

**192** $R_1$=$OCH_3$
**193** $R_1$=H

**Scheme 1.39** Biotransformation of psiadiarabin (**190**) and its 6-demethoxy analogue **191** by the fungus *Cunninghamella elegans* NRRL 1392 (Ibrahim et al., 1997).

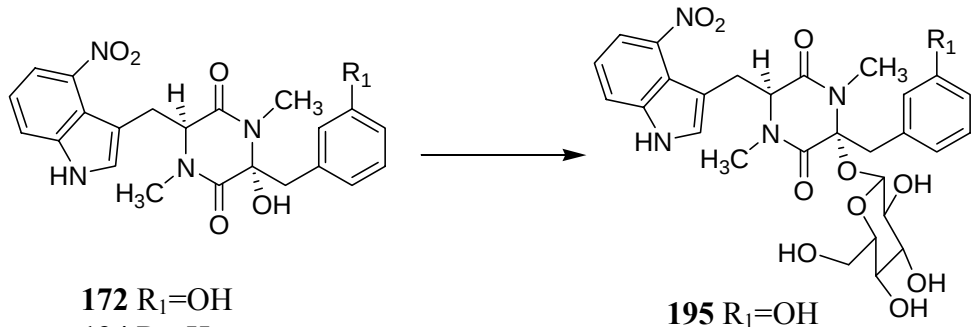

**172** $R_1$=OH
**194** $R_1$=H

**195** $R_1$=OH
**196** $R_1$=H

**Scheme 1.40** Biotransformation of thaxtomin A (**172**) and thaxtomin B (**194**) by *Bacillus mycoides* (King et al., 2000).

## 1.7 Conclusions

From the results described in the previous section, it is concluded that a single glucosyltransferase can accept multiple substrates and that multiple glucosyltransferases within a single plant species can recognize the same substrate. However, some glucosyltransferases display a high degree of substrate specificity and regioselectivity towards a particular substrate. Despite the progress in the isolation and gene cloning of plant glucosyltransferases, catalytic mechanisms and complete structural information about these glucosyltransferases have not been reported. This information is fundamental to understand the substrate selectivity, regiospecificity and to design inhibitors of glucosyltransferases. While a plausible system based on sequence and 3D structure comparisons has been proposed for 65 UGT families (Coutinho et al., 2003b; Hu and Walker, 2002; Ünligil and Rini, 2000), for which different folds, active sites and mechanisms were discussed, efforts to obtain suitable crystal structures of Family 1 glucosyltransferases (GT1) have not been reported. To date, only two GT1 from plants (Shao et al., 2005; Offen et al., 2006) and one GT1 from bacteria (Mulichak et al., 2001) have been crystallized and their three-dimensional structures have been solved. A catalytic mechanism for UDP-glucose dependent betanidin 5-*O*-glucosyltransferase from *Dorotheanthus bellidiformis* was proposed on the basis of results obtained from site-directed mutagenesis and protein 3D-homology modeling using a homologous bacterial glucosyltransferase template (Hans et al., 2004). However, because of a limited sequence homology to the bacterial template, this model of the glucosyltransferase may have a high probability of uncertainty. Although Family 1 glucosyltransferases of plant and bacteria have been investigated, fungal glucosyltransferases of Family 1 have not been reported to date. It will thus be interesting to investigate glucosyltransferases of *S. sclerotiorum* that are responsible for detoxification of phytoalexins. It is expected that additional structural

information of these glucosyltransferases will be a discovery that may lead to a better understanding of fungal enzyme evolution, as well as catalytic enzyme mechanisms. No doubt that this understanding will help to design inhibitors of phytoalexin detoxification that may be applicable to the selective control of the stem rot fungus *S. sclerotiorum*.

# Chapter 2: RESULTS

## 2.1 Synthesis and antifungal activity of phytoalexins and analogues

Phytoalexins are important antimicrobial secondary metabolites produced by plants in response to biological, physical, or chemical stress. However, isolation of such compounds from plants is very difficult and time consuming because of their extremely low quantity in plants. To study the biological activity and biotransformation of phytoalexins by phytopathogenic fungi, relatively large amounts of phytoalexins are required. Sufficient quantities for such studies are obtainable through synthesis. Among 38 reported cruciferous phytoalexins, synthetic methods are known for 31 (Pedras et al., 2003a, Pedras et al., 2006a, 2006b). Thus, the phytoalexins used in my research project were synthesized following known procedures. Before probing the biotransformation pathways of cruciferous phytoalexins in *S. sclerotiorum*, it was necessary to determine their bioactivity. The minimal inhibitory concentrations of phytoalexins and analogues were determined using antifungal assays (Pedras and Ahiahonu, 2002).

### 2.1.1 Synthesis

There are several methods reported for the synthesis of particular phytoalexins (Pedras et al., 2003a). For example, three methods are known for the synthesis of brassinin (**9**) using different starting materials. In my research project, the synthetic methods were chosen according to the yields reported in the literature. Therefore, the

synthesis of brassinin (**9**), cyclobrassinin (**18**) (Takasugi et al., 1988), 1-methoxybrassinin (**11**) (Pedras and Zaharia, 2000), brassilexin (**24**), sinalexin (**25**) (Pedras and Zaharia, 2001), camalexin (**31**) (Ayer et al., 1992), brassicanal A (**34**) (Pedras and Okanga, 1999), spirobrassinin (**27**) (Monde et al., 1994) and 1-methoxyspirobrassinin (**28**) (Kutschy et al., 2002) were carried out as shown in Schemes 2.1 to 2.9 and reported in the experimental section. The spectroscopic data were consistent with the structures of the products and identical to the reported data. 1-Methylbrassilexin (**215**), an analogue of brassilexin (**24**), and 1-methylspirobrassinin (**216**), an analogue of spirobrassinin (**27**), were synthesized from their parent compounds following treatment with NaH and MeI as shown in Scheme 2.10 and 2.11 (Pedras and Hossain, 2006).

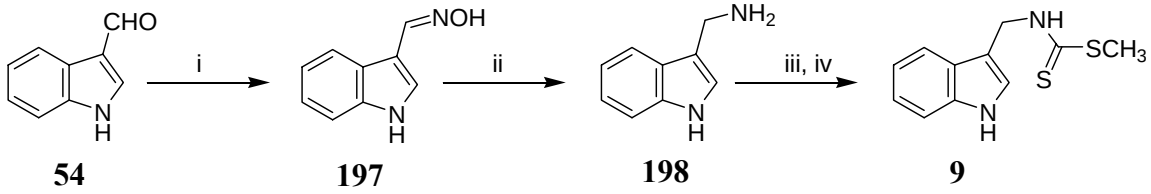


**54** **197** **198** **9**

**Scheme 2.1** Synthesis of brassinin (**9**). Reagents and conditions: (i) $NH_2OH.HCl$, $Na_2CO_3$, 91%; (ii) Devarda's alloy, NaOH, MeOH, 72%; (iii) $Et_3N$, pyridine, $CS_2$, 0 °C; (iv) MeI, 5 °C, 80% (Takasugi et al., 1988).

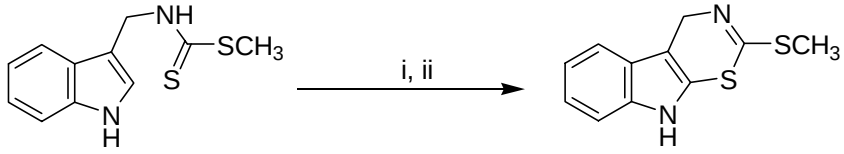


**9** **18**

**Scheme 2.2** Synthesis of cyclobrassinin (**18**). Reagents and conditions: (i) Pyridinium bromide perbromide, THF; (ii) DBU, 58% (Takasugi et al., 1988).

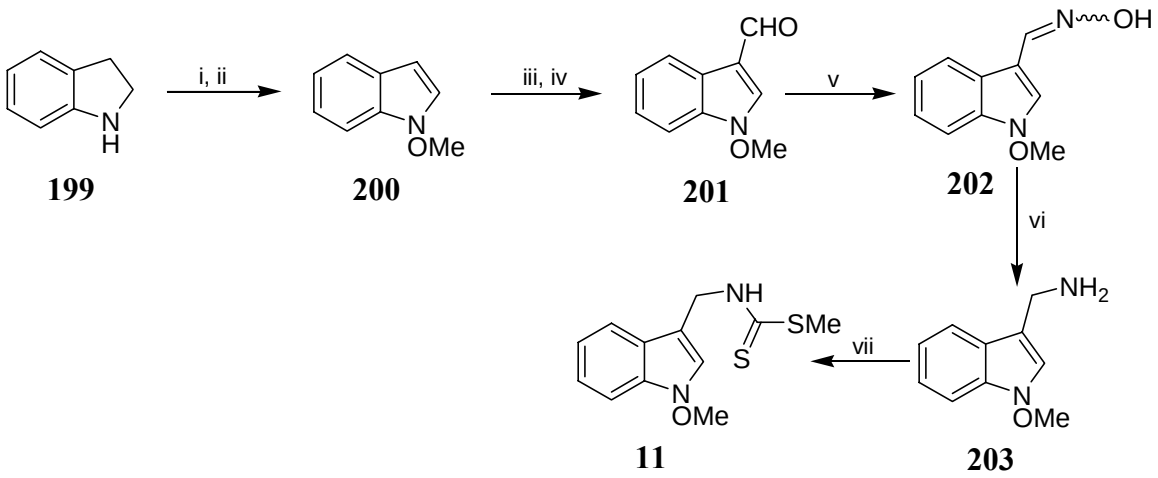


**Scheme 2.3** Synthesis of 1-methoxybrassinin (**11**). Reagents and conditions: (i) $Na_2WO_4.2H_2O$, 30% $H_2O_2$; (ii) $Me_2SO_4$, $K_2CO_3$, 56%; (iii) $POCl_3$, DMF; (iv) NaOH, 86%; (v) $NH_2OH.HCl$, $Na_2CO_3$, $EtOH/H_2O$, 99%; (vi) $NaBH_3(CN)$, $TiCl_3$, $NH_4OAc$, MeOH; (vii) Py, $Et_3N$, $CS_2$, $CH_3I$, 65% (Pedras and Zaharia, 2000).

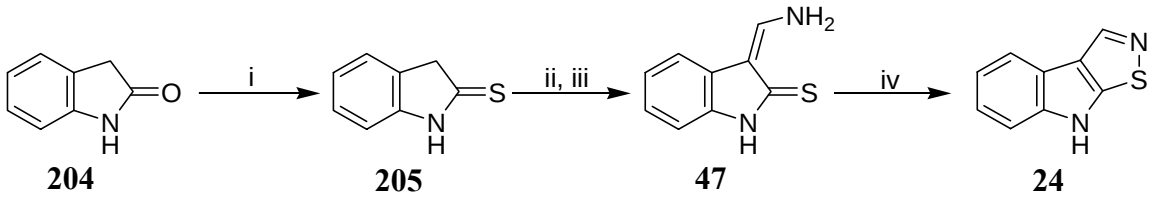


**Scheme 2.4** Synthesis of brassilexin (**24**). Reagents and conditions: (i) $P_4S_{10}$, $NaHCO_3$, THF, 86%; (ii) $POCl_3$, DMF; (iii) $NH_4OH$; (iv) $I_2$, Pyridine, 22% (Pedras and Zaharia, 2001).

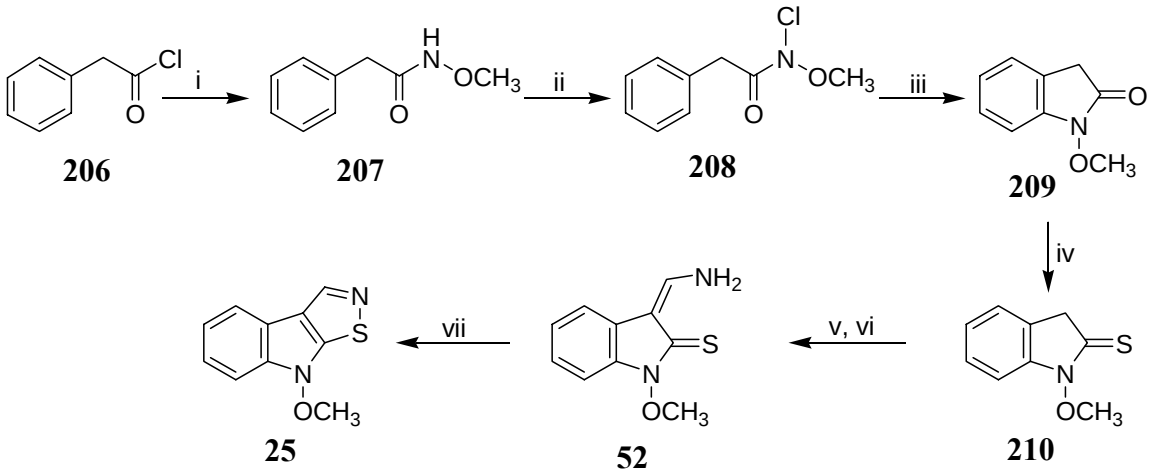


**Scheme 2.5** Synthesis of sinalexin (**25**). Reagents and conditions: (i) $NH_2OCH_3.HCl$, $Na_2CO_3$, benzene, $H_2O$, 85%; (ii) $(CH_3)_3COCl$, $CH_2Cl_2$, 96%; (iii) $Ag_2CO_3$, TFA, 69%; (iv) $P_4S_{10}$, $NaHCO_3$, THF, 86%; (v) $POCl_3$, DMF; (vi) $NH_4OH$; (vii) $I_2$, Pyridine 36% (Pedras and Zaharia, 2001).

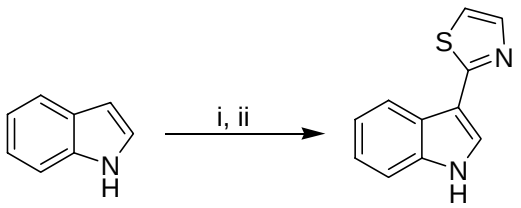


**Scheme 2.6** Synthesis of camalexin (**31**). Reagents and conditions: (i) Mg, $CH_3I$, $Et_2O$; (ii) benzene, 2-bromothiazole, 90 °C, 57% (Ayer et al., 1992).

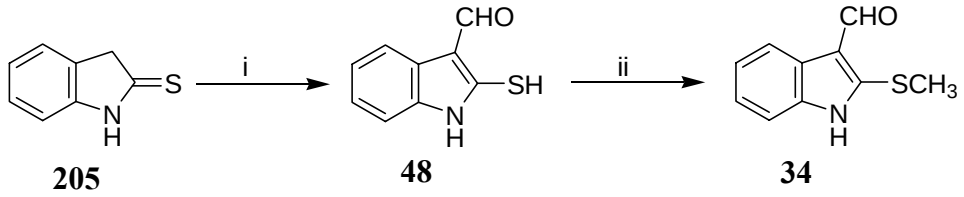


**Scheme 2.7** Synthesis of brassicanal A (**34**). Reagents and conditions: (i) NaH, HCOOEt, 99%; (ii) $CH_2N_2$, ether, 54% (Pedras and Okanga, 1999).

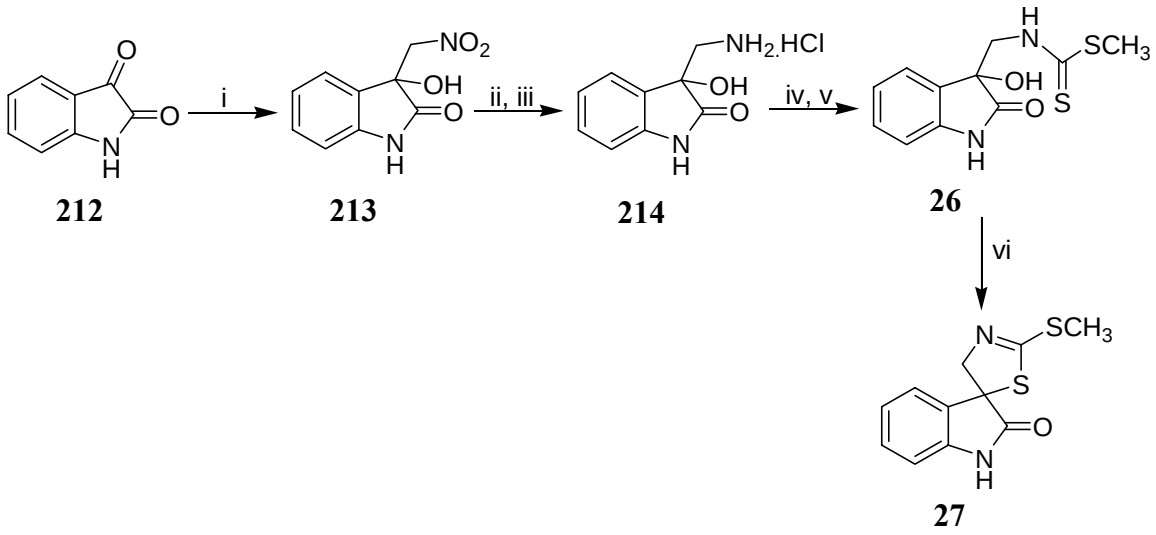


**Scheme 2.8** Synthesis of (±)-spirobrassinin (**27**). Reagents and conditions: (i) $CH_3NO_2$; (ii) $H_2$, Pd/C, MeOH/AcOH; (iii) HCl, 57%; (iv) Py, $Et_3N$, $CS_2$; (v) $CH_3I$, 75%; (vi) $SOCl_2$, Py, 82% (Monde et al., 1994).

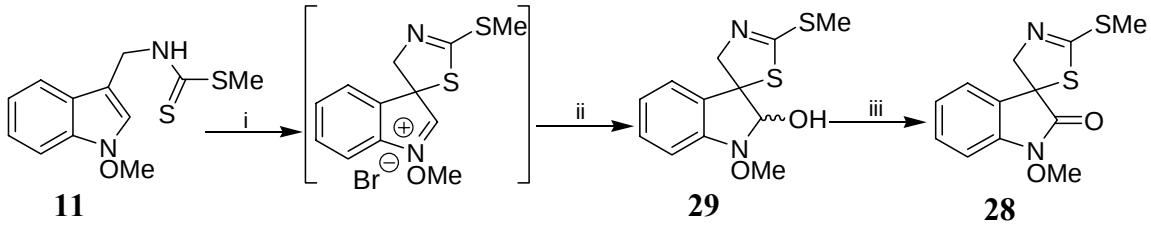


**Scheme 2.9** Synthesis of (±)-1-methoxyspirobrassinin (**28**). Reagents and conditions: (i) dioxane, $Br_2$; (ii) $Et_3N$, $H_2O$, 86%; (iii) $CrO_3$, AcOH, 30% (Kutschy et al., 2002).

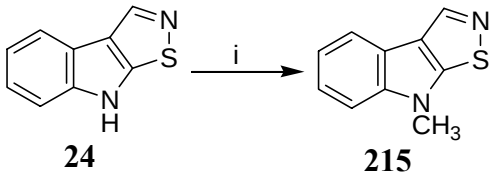


**Scheme 2.10** Synthesis of 1-methylbrassilexin (**215**). Reagents: (i) NaH, MeI (Pedras and Hossain, 2006).

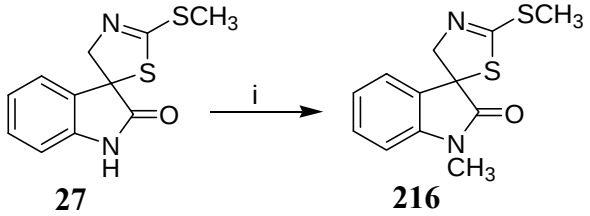


**Scheme 2.11** Synthesis of (±)-1-methylspirobrassinin (**216**). Reagents: (i) NaH, MeI (Pedras and Hossain, 2006).

In order to obtain (*R*)- and (*S*)-spirobrassinin (**27**), enantioresolution of racemic **27** was achieved by derivatization with (*S*)-(-)-1-phenylethyl isocyanate (**217**), chromatographic separation of diastereomeric amides (**218**, **219**) and their cleavage with $CH_3ONa$ (Suchy et al., 2001) (Scheme 2.12). Racemic spirobrassinin (**27**) was allowed to react with **217** with the addition of triethylamine for reaction acceleration to produce urea derivatives (**218**, **219**). The diastereomeric pairs of amides **218** and **219** were separated by simple silica gel chromatography. Removal of the chiral auxiliary by treatment with sodium methoxide afforded (*R*)- and (*S*)-spirobrassinins (**27**). The

enantiopurity of (*R*)- and (*S*)-spirobrassinin (**27**) was measured by $^1$H NMR using (*R*)-2,2,2-trifluoro-1-(9-anthryl)ethanol (TFAE) as chiral solvating agent as described in section 2.2.10.

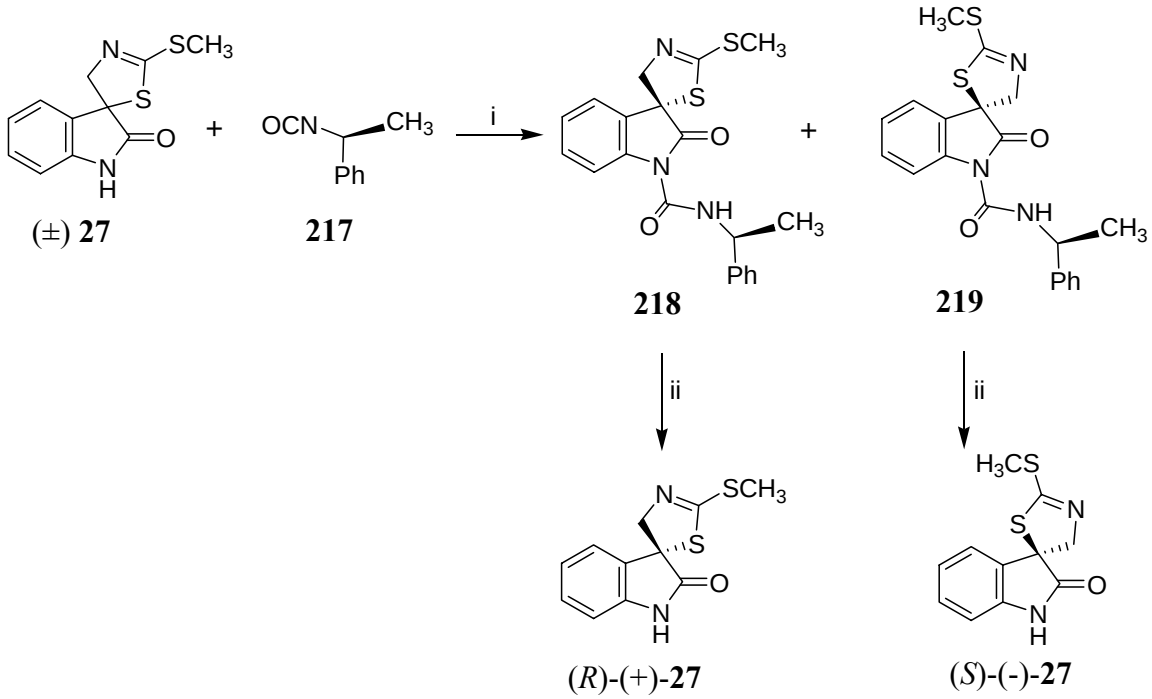


**Scheme 2.12** Enantioresolution of (±)-spirobrassinin (**27**). Reagents: (i) $Et_3N$, acetone; (ii) $CH_3ONa$, $CH_3OH$ (Suchy et al., 2001).

## 2.1.2 Antifungal activity

There are several types of bioassays useful for the determination of antifungal activity, namely the fungal spore germination assay on agar or TLC plates (Pedras, 1998; Pedras and Sorenson, 1998), fungal radial growth assay using minimal media or PDA media (Pedras and Ahiahonu, 2002; Pedras and Montaut, 2003), and filter paper disc assay (Lazarevic et al., 2001). For simplicity and to obtain reproducible results and because *S. sclerotiorum* does not form spores in vitro, fungal radial growth assays performed on minimal media (Pedras and Ahiahonu, 2002) were selected to determine the antifungal activity of phytoalexins and analogues against *S. sclerotirum*.

The antifungal activity of brassinin (**9**), cyclobrassinin (**18**), 1-methoxybrassinin (**11**), brassilexin (**24**), 1-methylbrassilexin (**215**), sinalexin (**25**), brassicanal A (**34**), spirobrassinin (**27**), 1-methoxyspirobrassinin (**28**), 1-methylspyrobrassinin (**216**), and camalexin (**31**) against *S. sclerotiorum* were investigated using the mycelial radial growth bioassay reported in the experimental section. Solutions of each compound in DMSO (50 mM) were used to prepare assay solutions in minimal media (0.5, 0.3, 0.1, 0.05, and 0.02 mM) by serial dilution; control solutions contained 1% DMSO in minimal media. Sterile tissue culture plates (12-well, 23mm diameter) containing test solutions and control solution (1 ml per well) were inoculated with mycelium plugs (4mm cut from 3-day-old PDA plates of *S. sclerotiorum*, clone # 33) placed upside down on the center of each plate and incubated under constant light for 3 days. All bioassay experiments were carried out in triplicate, at least two times.

After incubation for three days, the mycelium of control plates incubated with *S. sclerotiorum* covered full plate surfaces. As shown in Table 2.1, brassilexin (**24**) caused complete growth inhibition at 0.05 mM while sinalexin (**25**) caused complete inhibition at 0.1 mM and 1-methylbrassilexin (**215**) at 0.3 mM. Camalexin (**31**) also caused 100% inhibition in the fungal growth at 0.1 mM. Brassinin (**9**) and 1-methoxybrassinin (**11**) displayed similar antifungal activity against *S. sclerotiorum* causing complete inhibition at 0.3 mM. Due to lower solubility of cyclobrassinin (**18**) in aqueous solutions, the minimum inhibitory concentration of **18** could not be determined. Brassicanal A (**34**), spirobrassinin (**27**), 1-methoxyspirobrassinin (**28**), and 1-methylspyrobrassinin (**216**) did not cause complete inhibition even at the highest concentration. Among all the cruciferous phytoalexins that were tested against *S. sclerotiorum*, brassilexin (**24**) showed the strongest antifungal activity against *S. sclerotiorum*.

**Table 2.1** Percentage of growth inhibition[a] of *Sclerotinia sclerotiorum* incubated with phytoalexins (**9**, **11**, **18**, **24**, **25**, **27**, **28**, **31**, **34**) and derivatives (**215**, **216**) (48 h, constant light).

| Compound assayed against *S. sclerotiorum* | Concentration (mM) | Inhibition ± SD (%)[a] |
|---|---|---|
| Brassinin (**9**) | 0.50 | 100 ± 0 |
| | 0.30 | 100 ± 0 |
| | 0.10 | 42 ± 5 |
| 1-Methoxybrassinin (**11**) | 0.50 | 100 ± 0 |
| | 0.30 | 100 ± 0 |
| | 0.10 | 56 ± 6 |
| Cyclobrassinin (**18**) | 0.50 | Not soluble |
| | 0.30 | Not soluble |
| | 0.10 | <10 |
| Brassilexin (**24**) | 0.10 | 100 ± 0 |
| | 0.05 | 100 ± 0 |
| | 0.02 | 76 ± 5 |
| Sinalexin (**25**) | 0.10 | 100 ± 0 |
| | 0.05 | 80 ± 4 |
| | 0.02 | 60 ± 6 |
| Spirobrassinin (**27**) | 0.50 | 58 ± 3 |
| | 0.30 | 38 ± 8 |
| | 0.10 | 23 ± 5 |
| 1-Methoxyspirobrassinin (**28**) | 0.50 | 24 ± 4 |
| | 0.30 | 10 ± 4 |
| | 0.10 | No inhibition |
| Camalexin (**31**) | 0.30 | 100 ± 0 |
| | 0.10 | 100 ± 0 |
| | 0.05 | 81 ± 6 |
| Brassicanal A (**34**) | 0.50 | 42 ± 5 |
| | 0.30 | 17 ± 4 |
| | 0.10 | No inhibition |
| 1-Methylbrassilexin (**215**) | 0.30 | 100 ± 0 |
| | 0.10 | 43 ± 3 |
| | 0.05 | 24 ± 6 |
| 1-Methylspirobrassinin (**216**) | 0.50 | 49 ± 2 |
| | 0.30 | 36 ± 7 |
| | 0.10 | 20 ± 7 |

[a] The percentage of inhibition was calculated using the formula: % inhibition = 100 – [(growth on amended/growth in control) × 100].

## 2.2 Metabolism of phytoalexins and analogues in *Sclerotinia sclerotiorum*

A possible strategy for controlling the stem rot fungus is the inhibition of the enzymes involved in the detoxification of phytoalexins (Pedras and Khan, 1996; Pedras and Hossain, 2006). However, before such inhibitors can be rationally designed, it is important to determine whether the stem rot fungus metabolizes and detoxifies phytoalexins. Ultimately, a correlation between the bioactivity of the phytoalexins and of their biotransformation products will allow an understanding of the detoxification mechanisms utilized by the stem rot fungus to overcome the plant's defenses. Previous results demonstrated that *S. sclerotiorum* can effectively detoxify brassinin (**9**), camalexin (**31**) and 6-methoxycamalexin (**243**) to their glucosylated derivatives (Schemes 1.4, 1.7 and 1.8) (Pedras et al., 2004c; Pedras and Ahiahonu, 2002). In continuation of these investigations of phytoalexin detoxification reactions occurring in *S. sclerotiorum*, the metabolism of the phytoalexins 1-methoxybrassinin (**11**), cyclobrassinin (**18**), brassilexin (**24**), sinalexin (**25**), brassicanal A (**34**), spirobrassinins **27** and **28**, as well as methyl derivatives **215** and **216** were investigated. So, in this section the detoxification pathways and the characterization of various new metabolites as well as the chemistry involved in these processes will be described.

### 2.2.1 1-Methoxybrassinin (11)

The concentration of 1-methoxybrassinin (**11**) used in the biotransformation experiment was based on results of antifungal bioassays. The concentration that was moderately toxic to fungal growth was selected for biotransformation studies. Subsequently, fungal cultures of *S. sclerotiorum* were initiated by inoculating sclerotia of *S. sclerotiorum* in minimal media. After 6 days of incubation, 1-methoxybrassinin (**11**) dissolved in $CH_3CN$ was administered to fungal cultures and to uninoculated media (final concentration in media 0.1 mM). Control cultures of the fungus were

grown separately. Cultures were incubated and samples were withdrawn at different time intervals, extracted with ethyl acetate and the extracts were analyzed by HPLC. Comparison of the HPLC chromatograms of extracts of fungal cultures containing 1-methoxybrassinin (**11**) and control cultures indicated that 1-methoxybrassinin (**11**) was completely metabolized to a major product (HPLC $t_R$ = 9.2 min) in ca. 12 h. To establish the structure of this product, larger scale cultures of *S. sclerotiorum* were incubated with 1-methoxybrassinin (**11**) for 12 h, were extracted, and the extract was fractionated by reverse phase silica gel chromatography. Each fraction was analyzed by HPLC. The fraction containing the biotransformation product, substantially more polar than 1-methoxybrassinin, was further separated by prep. TLC. The structure of this polar metabolite (**220**) was determined by analyses of its spectroscopic data as follows. Comparison of its $^1$H NMR spectrum, obtained in $CD_3CN$, with that of 1-methoxybrassinin (**11**) indicated the presence of an additional substituent either at C-4 or C-7, since only three protons were displayed in the benzene nucleus. The new metabolite (**220**) contained the intact methylene protons ($\delta_H$ 5.00), $SCH_3$ ($\delta_H$ 2.59), and *N*-methoxy groups ($\delta_H$ 4.14). Additional proton signals at $\delta_H$ 5.14 (d, $J$ = 8 Hz, 1H) and several multiplets at $\delta_H$ 3.42–3.84 suggested the presence of a carbohydrate moiety. As well, the molecular formula of $C_{18}H_{25}N_2O_7S_2$ obtained by HRMS-ESI and the $^{13}$C NMR spectral data corroborated the presence of a carbohydrate residue. The identity of the monosaccharide unit was established through homonuclear $^1$H-$^1$H decoupling experiments (upon addition of $D_2O$). The coupling constants ($J$ = 7-9 Hz) indicated axial-axial proton couplings in a pyranose ring, thus allowing the assignment of a β-glucopyranose substituent. In addition, as summarized in Fig. 2.1, NOE difference experiments (enhancement of the H-6 signal at $\delta_H$ 7.02 upon irradiation of H-1′ at $\delta_H$ 5.14 and vice-versa; enhancement of both $CH_2$ and H-5 at $\delta_H$ 5.00 and 7.06, respectively, upon irradiation of H-4 at $\delta_H$ 7.33; enhancement of H-2 at $\delta_H$ 7.41 upon irradiation of $CH_3$-(O)) and HMBC (correlation between H-1′ and C-7 at $\delta_C$ 144.0)

spectral data confirmed that the β-glucopyranose unit was located at C-7 and not at C-4. Thus, the structure of this metabolic product was assigned as 7-oxy-(*O*-β-D-glucopyranosyl)-1-methoxybrassinin (**220**) (Scheme 2.13).

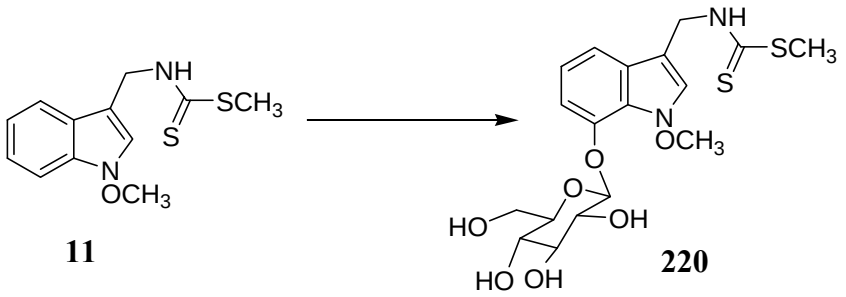


**Scheme 2.13** Biotransformation of 1-methoxybrassinin (**11**) in *Sclerotinia sclerotiorum* (Pedras et al., 2004c).

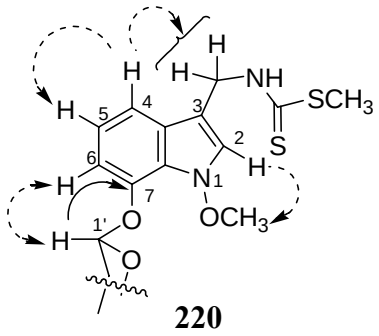


**Figure 2.1** Selected NOE (dashed lines) and HMBC (solid line) correlations for 7-oxy-(*O*-β-D-glucopyranosyl)-1-methoxybrassinin (**220**).

## 2.2.2 Cyclobrassinin (18)

Similar to 1-methoxybrassinin (**11**), antifungal bioassays were performed to determine the minimum inhibitory concentration of cyclobrassinin before carrying out the biotransformation experiment. Due to the lower solubility of cyclobrassinin (**18**) in aqueous solutions, the minimum inhibitory concentration could not be determined; a slight inhibitory effect was observed at 0.5 mM. Subsequently, liquid cultures of *S. sclerotiorum* were initiated by inoculating minimal media with sclerotia of *S. sclerotiorum.* Cyclobrassinin (**18**) dissolved in $CH_3CN$ was administered to 6-day-old

fungal cultures (final concentration 0.1 mM) and to uninoculated minimal medium. Cultures were incubated, samples were withdrawn at different time intervals and extracted with EtOAc. Cyclobrassinin (**18**) was found to be stable in uninoculated medium for at least 8 days. HPLC analysis of EtOAc extracts of fungal cultures incubated with cyclobrassinin (**18**) indicated it to be completely metabolized to a major product (HPLC $t_R$ = 8.6 min) in *ca*. 12 h. To establish the structure of this metabolic product, larger scale cultures of *S. sclerotiorum* incubated with cyclobrassinin (**18**) for 8 h, were filtered, extracted, and the organic extract fractionated by column chromatography followed by prep. TLC to yield a major metabolite (**221**) with HPLC $t_R$ = 8.6 min and also a minor metabolite (**34**) with HPLC $t_R$ = 10.2 min. The structure of the major metabolite (**221**) was determined by analyses of standard spectroscopic methods including $^1$H and $^{13}$C NMR spectroscopy, 2D-NMR and HRMS. Comparison of the $^1$H NMR spectrum of the major metabolite (**221**) with that of cyclobrassinin (**18**) indicated the presence of the intact cyclobrassinin (**18**) tricyclic system, as well as the intact $SCH_3$ group of the side-chain. In addition, several multiplets at $\delta_H$ 3.63–4.09 suggested the presence of a carbohydrate moiety. The molecular formula of **221** ($C_{17}H_{20}N_2O_5S_2$) determined by HRMS-FAB also corroborated the presence of a carbohydrate residue. As described above for metabolite **220**, the identity of the carbohydrate moiety was determined to be a β-glucopyranosyl substituent. HMBC spectral data confirmed that the β-glucopyranose unit was located at *N*-1 (correlations of the anomeric proton H-1 with C-2 and C-7a of indole) and thus the structure of **221** was assigned as 1-β-D-glucopyranosylcyclobrassinin (**221**) (Scheme 2.14). The structure of the minor metabolic product of cyclobrassinin (**18**) was established to be brassicanal A (**34**) by comparison with a synthetic sample (Pedras and Khan, 1996).

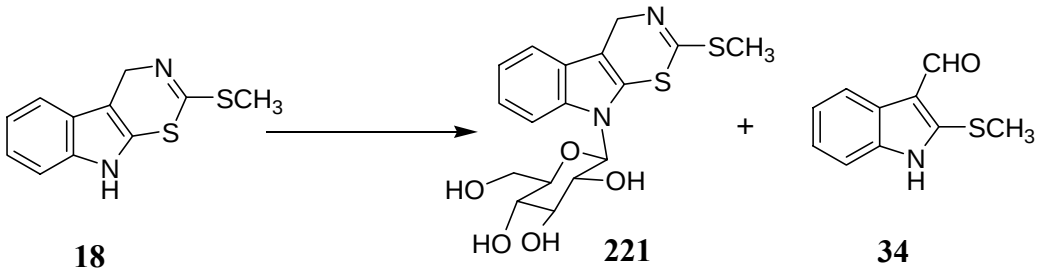


**Scheme 2.14** Biotransformation of cyclobrassinin (**18**) in *Sclerotinia sclerotiorum* (Pedras et al., 2004c).

## 2.2.3 Brassilexin (24)

### *2.2.3.1 Biotransformation*

Similar to 1-methoxybrassinin (**11**) and cyclobrassinin (**18**), antifungal bioassays were performed to determine the minimum inhibitory concentration of brassilexin (**24**) before carrying out the biotransformation experiment. Subsequently, brassilexin (**24**, final concentration 0.1 mM) was administered to fungal cultures grown in minimal media by inoculating sclerotia of *S. sclerotiorum*. The cultures were incubated and analyzed over a period of several days. The stability of brassilexin (**24**) was determined by adding brassilexin in minimal media and analyzing the media over a period of several days. Brassilexin (**24**) was stable in minimal media for at least 8 days. HPLC chromatograms of extracts of fungal cultures incubated with brassilexin (**24**) indicated that **24** was completely metabolized in *ca.* 48 h (Fig. 2.2). The metabolites were found to be an unknown compound with $t_R$ = 4.5 min (**222**), the known phytoalexin brassicanal A (**34**), and 3-(amino)methylenindoline-2-thione (**47**), resulting from reduction of the isothiazole ring of brassilexin (**24**) (Pedras and Suchy, 2005) (Scheme 2.15). Enamine **47** was detected in culture immediately after adding brassilexin (**24**), while brassicanal A (**34**) was detected after 6 h of incubation and the unknown metabolite (**222**) was detected after 12 h. To determine the sequence of the

biotransformation steps, enamine **47** was synthesized and administered to cultures of *S. sclerotiorum*. Culture samples were withdrawn at different times, these were extracted and the extracts were analyzed by HPLC; the chromatograms indicated that enamine **47** was completely metabolized to brassicanal A (**34**) in *ca.* 12 h. Subsequently, to isolate the unknown metabolite with $t_R$ = 4.5 min (**222**), larger scale cultures of *S. sclerotiorum* were incubated with brassilexin (**24**). After 24 h, the extracts obtained from these cultures were fractionated by reverse phase silica gel chromatography, and each fraction was analyzed by HPLC. The fractions containing the unknown metabolite (**222**) were combined and further separated by preparative TLC to yield chromatographically homogeneous material. The $^1$H NMR spectrum, obtained in $CD_3OD$, indicated the presence of the intact brassilexin (**24**) tricyclic system plus a doublet at $\delta_H$ 5.75 ($J$ = 9 Hz, 1H) and several multiplets at $\delta_H$ 3.49–3.96, suggesting the presence of a carbohydrate moiety. Both the molecular formula ($C_{15}H_{16}N_2O_5S$ obtained by HRMS-ESI) and the $^{13}$C NMR spectral data corroborated the presence of a carbohydrate residue. The identity of the carbohydrate moiety was assigned as β-glucopyranosyl residue from $^1$H–$^1$H homonuclear decoupling experiments (axial-axial couplings, $J$ = 7–9 Hz, between the various protons). The β-glucopyranosyl unit was established to be located at *N*-1 from analysis of the HMBC data (correlations of the anomeric proton H-1′ with C-2 and C-7a of the indole moiety). Furthermore, the structure of this new metabolic product of brassilexin (**24**) was confirmed to be 1-β-D-glucopyranosylbrassilexin (**222**) by synthesis, as described below. Hence, the biotransformation of brassilexin (**24**) in *S. sclerotiorum* proceeded *via* two different pathways (Scheme 2.15): (i) glucosylation of brassilexin at N-1, and (ii) reductive ring opening of the isothiazole moiety. Although the yield of glucoside **222** was lower than that of brassicanal A (**34**) (Table 2.4), since **222** was further metabolized at a faster rate than brassicanal A (**34**) (48 h *vs.* 7 d), it becomes apparent that glucosylation represents the main metabolic pathway (Pedras and Hossain, 2006).

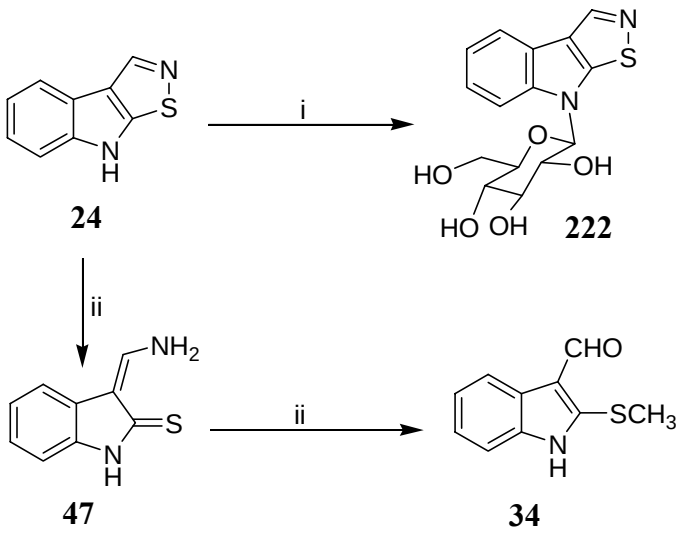


**Scheme 2.15** Biotransformation of brassilexin (**24**) in *Sclerotinia sclerotiorum*: (i) main pathway, (ii) minor pathway (Pedras and Hossain, 2006).

### *2.2.3.2 Chemical synthesis of 1-β-D-glucopyranosylbrassilexin (222)*

The chemical synthesis of 1-β-D-glucopyranosylbrassilexin (**222**) was carried out to confirm the absolute stereochemistry of the biotransformation product of brassilexin (**24**) and to obtain sufficient amounts for bioassays. *N*-Glucosylation of indolyl-containing molecules has been reported for a number of substrates (Ohkubo et al., 1997; Gallant et al., 1993) including the syntheses of *N*-glucosylated brassinin (**9**), brassenins A and B, cyclobrassinin (**18**) and related compounds (Humenik, et al., 2005a; Humenik, et al., 2005b; Humenik, et al., 2004; Kutschy, et al., 2004). However, the indoline-indole methodology (Preobrazhenskaya and Korbukh, 1988) or the various carbohydrate donors used in those preparations were not readily applicable to brassilexin (**24**). On the other hand, the reaction of 6-nitroindole with 2,3,4,6-tetra-*O*-acetyl-α-D-glucopyranosyl bromide (**223**) in the presence of silver oxide, reported to yield a mixture of *O*-acetylated 1,2-*O*-[1-(6-nitroindol-1-yl)ethylidene]-α-D-glucose and 1,2-*O*-[1-(6-nitroindol-3-yl)ethylidene]-α-D-glucose, appeared promising (Sokolova, et al., 1980). Although in that synthesis no *N*-glucosylated product was

observed, because brassilexin (**24**) had the C-2 and C-3 positions of the indole moiety blocked and no electron withdrawing groups were present, it was expected to be substantially more reactive than 6-nitroindole. Thus, an approach similar to that used for 6-nitroindole was chosen to synthesize 1-β-D-glucopyranosylbrassilexin (**222**). Subsequently, coupling of brassilexin (**24**) with 1-bromo-2,3,4,6-tetra-*O*-acetyl-α-D-glucopyranose (**223**) in the presence of silver oxide yielded a mixture of D-glucopyranosylbrassilexins **224** and **225** in a 1 : 1 ratio (Scheme 2.16). Finally, deacetylation of **224** yielded 1-β-D-glucopyranosylbrassilexin (**222**, 12% yield) (Pedras and Hossain, 2006). Synthetic 1-β-D-glucopyranosylbrassilexin (**222**) was identical in all respects to the sample isolated from fungal cultures of *S. sclerotiorum* and was used to carry out all bioassays. It is likely that the yield of **224** could be improved by using other protecting groups in **223**, to prevent the neighboring group assistance effect depicted in Scheme 2.16 (Nukada et al., 1998). The absolute stereochemistry of the stereogenic center C-1′ of compound **225** was established using NOESY data. The NOESY spectrum of **225** showed a correlation between the methyl group at C-1′ and the H-5″ of the glucosyl residue (Scheme 2.16). This correlation suggested that the new stereocenter C-1′ had the *S* configuration, which was consistent with that reported for tryptophan *N*-glucoside (Schnabel, et al., 2004). Furthermore, contrary to 1-β-D-glucopyranosylbrassilexin (**222**), the H-H coupling constants obtained for H-1″, H-2″ and H-3″ (see experimental data) suggest that the glucosyl moiety of **225** is not in a chair conformation.

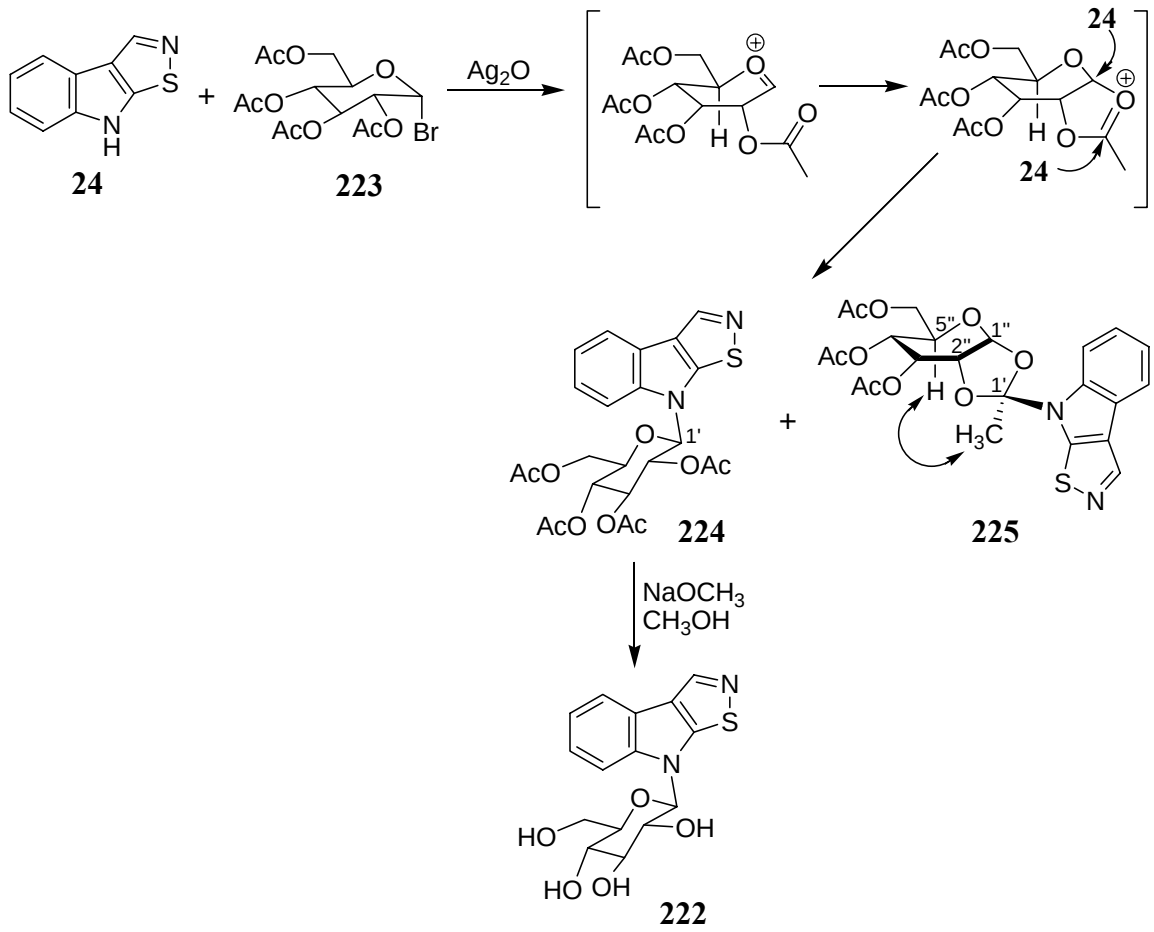


**Scheme 2.16** Synthesis of 1-β-D-glucopyranosylbrassilexin (**222**) and selected NOE of compound **225** (Pedras and Hossain, 2006).

## 2.2.4 Sinalexin (25)

Similar to the above phytoalexins, after determining the minmum inhibitory concentration of sinalexin (**25**) by antifungal bioassys, a time course experiment was conducted with sinalexin (**25**) using fungal cultures of *S. sclerotiorum*. The fungal cultures were grown in minimal media by inoculating sclerotia of *S. sclerotiorum*. Sinalexin (**25**, final concentration 0.1 mM) was added to fungal cultures and to uninoculated media (to determine the stability of sinalexin in minimal media), the cultures were incubated, and samples were collected at different time intervals and extracted with ethyl acetate. The HPLC analysis of EtOAc extracts of uninoculated

media incubated with **25** suggested that sinalexin (**25**) was stable in media for at least 8 days whereas the HPLC analysis of the broth extracts of cultures incubated with sinalexin (**25**) indicated it to be completely metabolized to two products with $t_R$ = 4.9 and 12.0 min, in *ca.* 48 h (Fig. 2.2). To obtain sufficient quantities of each product for both chemical characterization and bioassay, larger scale mycelial cultures incubated with **25** were extracted, the extract was fractionated by reverse phase silica gel chromatography and each fraction was analyzed by HPLC. The fractions containing new metabolites were combined and further separated by reverse phase preparative TLC. The molecular formula of the less polar metabolite (**226**, $t_R$ = 12.0 min) (obtained by HRMS-EI) indicated the presence of an additional oxygen atom relative to that of sinalexin (**25**) ($C_{10}H_8N_2O_2S$ *vs.* $C_{10}H_8N_2OS$) and the $^1$H NMR spectrum indicated the presence of a substituted sinalexin, since only four protons were displayed in the aromatic region. Three of the signals were assigned to the spin system in the benzene ring and a singlet at $\delta_H$ 8.63 was assigned to the isothiazole ring. These spectroscopic data suggested that the less polar metabolite (**226**) contained an OH group located either at C-5 or C-6. That the OH group was attached to C-6 rather than C-5 was finally deduced from NOE experiments, as follows. Irradiation of the *N*-methoxy group at $\delta_H$ 4.14 caused an enhancement of the signal due to H-7 ($\delta_H$ 6.98) and *vice versa*. That is, assignment of the resonance of H-7 demonstrated that the HO group was located at H-6 and thus **226** was the structure of the less polar metabolite. The molecular formula of the more polar metabolite (**227**, $t_R$ = 4.9 min, $C_{16}H_{18}N_2O_7$) obtained by HRMS-ESI indicated the presence of a hexose unit, which was corroborated by NMR data. The identity of the hexose unit was determined as β-D-glucopyranose from homonuclear ($^1$H) decoupling experiments and X-ray crystallography (Fig 2.3). To establish the sequence of biotransformation steps of sinalexin (**25**), compound **226** was administered to cultures of *S. sclerotiorum*, samples were withdrawn at different times, and these were extracted and analyzed by HPLC. As expected, compound **226** was completely

metabolized to **227** in *ca.* 12 h. This result indicated that sinalexin (**25**) was metabolized to 6-oxy-(*O*-β-D-glucopyranosyl)sinalexin (**227**) *via* 6-hydroxysinalexin (**226**) (Scheme 2.17) (Pedras and Hossain, 2006).

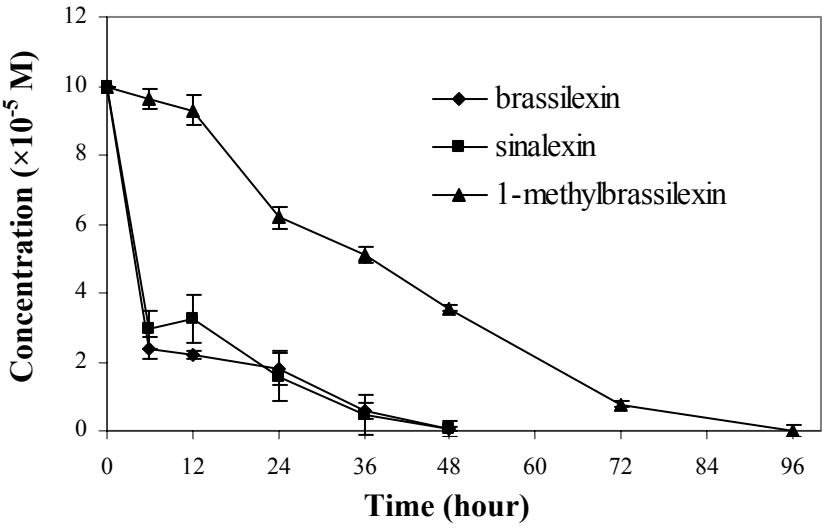


**Figure 2.2** Progress curves of the metabolism of brassilexin (**24**), sinalexin (**25**) and 1-methylbrassilexin (**215**) in *Sclerotinia sclerotiorum*. Cultures were extracted and extracts were analyzed by HPLC; concentrations were determined using calibration curves; each point is an average of experiments conducted in triplicate ± standard deviation (Pedras and Hossain, 2006).

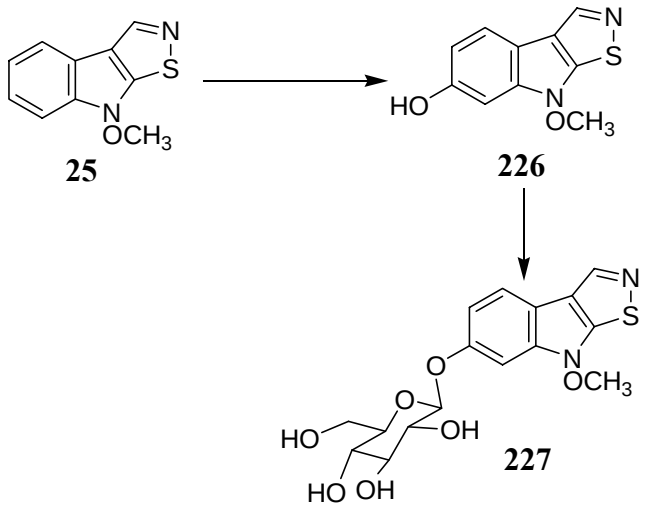


**Scheme 2.17** Biotransformation of sinalexin (**25**) in *Sclerotinia sclerotiorum* (Pedras and Hossain, 2006).

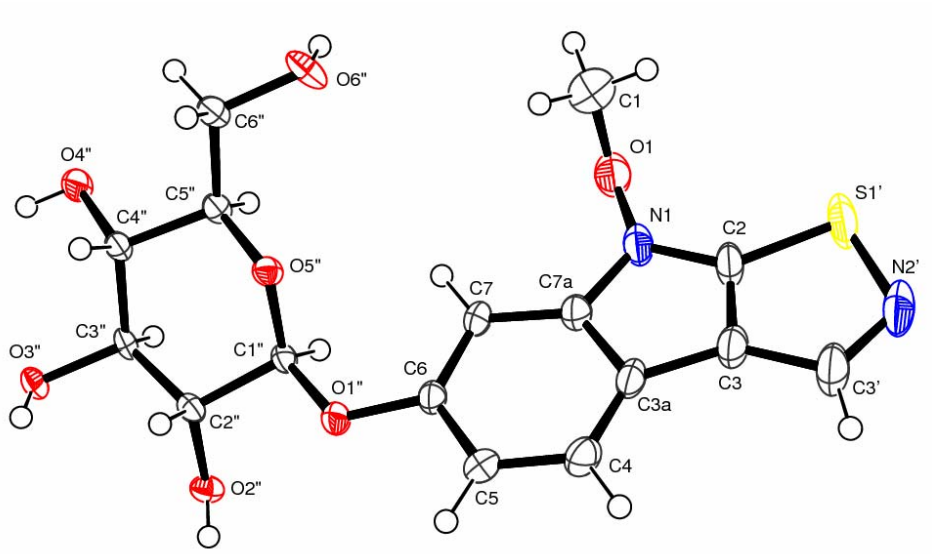


**Figure 2.3** X-ray structure of 6-oxy-(*O*-β-D-glucopyranosyl)sinalexin (**227**): general ORTEP-3 view with non-H atom displacement ellipsoids drawn at the 50% probability level. The H atoms are drawn as small spheres of arbitrary size (Pedras and Hossain, 2006).

### 2.2.5 1-Methylbrassilexin (215)

To probe the substrate specificity of the enzyme(s) involved in the metabolism of brassilexin (**24**) and sinalexin (**25**), 1-methylbrassilexin (**215**) was synthesized and incubated (final concentration 0.1 mM) with cultures of *S. sclerotiorum* as described for brassilexin (**24**). Culture samples were withdrawn at different time intervals and analyzed by HPLC. HPLC chromatograms of extracts of fungal cultures containing 1-methylbrassilexin (**215**) suggested that the rate of metabolism of **215** was slower than the transformation rates of brassilexin (**24**) and sinalexin (**25**) (Fig. 2.2).While the naturally-occurring **24** and **25** were completely metabolized in about two days, 1-methylbrassilexin (**215**) was completely metabolized to an unknown polar compound (**228**, $t_R$ = 4.4 min) in about four days. To establish the structure of this polar metabolite (**228**), larger scale cultures of *S. sclerotiorum* incubated with 1-methylbrassilexin (**215**) were extracted and the extracts were fractionated by reverse phase silica gel column chromatography. Fractions containing the new metabolite were further separated by

preparative TLC to yield a chromatographically homogeneous solid material. The $^{1}H$ NMR spectrum of this compound [**228**, $(CD_3)_2CO$)] showed five aromatic hydrogens, suggesting the presence of an intact brassilexin moiety, and a methylene group ($\delta_H$: 6.13, d, $J$ = 11.5 Hz, 1H; 5.90, d, $J$ = 11.5 Hz) instead of the (*N*)Me group. The $^{13}C$ NMR spectrum of **228** confirmed the absence of the (*N*)Me group and the presence of the methylene at $\delta_C$ 73.4, which indicated that the (*N*)Me group had been oxidized to (*N*)$CH_2O$–R. Additional signals at $\delta_H$ 4.39 (d, $J$ = 8 Hz, 1H) and several multiplets at $\delta_H$ 3.85–3.50 suggested the presence of a carbohydrate moiety. The molecular formula of $C_{16}H_{18}N_2O_6S$ (obtained by HRMS-ESI) and $^{13}C$ NMR spectral data also indicated the presence of a carbohydrate residue. The identity of the carbohydrate moiety was assigned as a β-glucopyranosyl residue from $^{1}H$-$^{1}H$ homonuclear decoupling experiments (axial-axial couplings, $J$ = 7–9 Hz). HMBC spectral data showed correlations of (*N*)$CH_2O$ protons with C-2 and C-7a of indole and also with the anomeric carbon (C-1′) as shown in Scheme 2.18, suggesting that the β-glucopyranose unit was attached to the oxygen atom of the (*N*)$CH_2O$ group. From this reasoning the structure of the biotransformation product of 1-methylbrassilexin (**215**) was assigned as 1-methyl-(oxy-*O*-β-D-glucopyranosyl)brassilexin (**228**) (Scheme 2.18) (Pedras and Hossain, 2006).

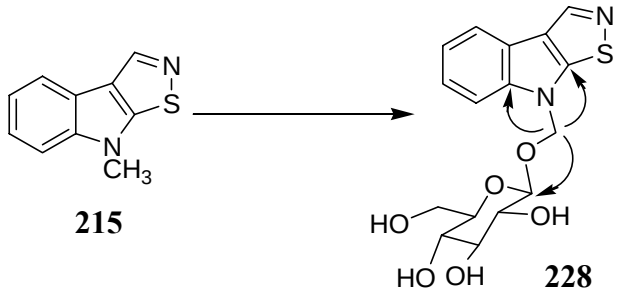


**Scheme 2.18** Biotransformation of 1-methylbrassilexin (18) in Sclerotinia s*clerotiorum* and selected HMBC correlations of **228** (Pedras and Hossain, 2006).

### 2.2.6 Brassicanal A (34)

Brassicanal A (**34**, final concentration 0.1 mM) was incubated with fungal cultures of *S. sclerotiorum* (grown in minimal media by inoculating sclerotia), samples were collected and analyzed by HPLC over a period of several days to determine the best time to isolate potential metabolic products. Comparison of the HPLC chromatograms of extracts of fungal cultures containing brassicanal A (**34**) and control cultures indicated that brassicanal A (**34**) was completely metabolized to 3-(hydroxymethyl)indole-2-methylsulfoxide (**230**) *via* brassicanal A sulfoxide (**229**) (Scheme 2.19) in *ca.* 7 d (Fig. 2.4). After isolation of metabolites **229** and **230** their structures were deduced from comparison of their spectroscopic data to those of brassicanal A as described below and finally confirmed by synthesis. The $^{1}$H NMR spectrum of each compound showed the four hydrogens characteristic of a 2,3-disubstituted indole nucleus. In addition, the sulfoxide **229** showed the aldehyde hydrogen, as well as the signal for the Me group, which was shifted downfield in both the $^{1}$H (2.68 ppm in **34** vs 3.08 ppm in **229**) and the $^{13}$C (16.9 ppm in **34** vs 42.2 ppm in **229**) NMR spectra. These changes in the chemical shifts suggested that the S-Me group present in brassicanal A (**34**) had been oxidized to the corresponding Me-S=O by the fungus. EIMS of **229** (molecular ion peak at 207) also confirmed that the addition of oxygen had occurred. Further corroboration of the structure was confirmed by synthesis as described in the experimental section (Pedras and Khan, 1996). In addition to the indolyl hydrogens, compound **230** showed a Me-S=O group, a methylene group (doublets at 4.88 and 4.81 ppm), and the absent of aldehyde hydrogen. EIMS of **230** (molecular ion peak at 209) confirmed that the aldehyde group of brassicanal A (**34**) had been reduced to the corresponding alcohol. The structure of **230** was also confirmed by synthesis (Pedras and Khan, 1996). To ascertain the sequence of the biotransformation steps, compound **229** was separately incubated with cultures of *S.*

*sclerotiorum*, and extracts of the fungal cultures collected at different times were analyzed by HPLC. These experiments confirmed that the aldehyde group of brassicanal A (**34**) was enzymatically reduced to alcohol **230** (Scheme 2.19) (Pedras and Hossain, 2006).

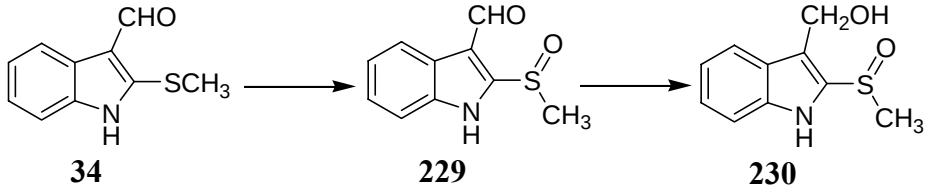


**34** **229** **230**

**Scheme 2.19** Biotransformation of the phytoalexin brassicanal A (**34**) in *Sclerotinia sclerotiorum* (Pedras and Hossain, 2006).

### 2.2.7 (±)-Spirobrassinin (27)

Similar to other phytoalexins, after determining the minmum inhibitory concentration of (±)-spirobrassinin (**27**) by antifungal bioassys, the biotransformation of this phytoalexin was studied by carrying out a time course experiment. Spirobrassinin (**27**, 0.1 mM) was added to fungal cultures of *S. sclerotiorum*, cultures were incubated and analyzed by HPLC over a period of several days. From these analyses, it was found that compared to the transformation of other phytoalexins such as 1-methoxybrassinin (**11**), cyclobrassinin (**18**), brassilexin (**24**) and sinalexin (**25**), the biotransformation of the phytoalexin (±)-spirobrassinin (**27**) in *S. sclerotiorum* was a much slower process. Spirobrassinin (**27**) was detected in cultures up to nine days after incubation with *S. sclerotiorum* (Fig. 2.4); a single biotransformation product (**231**, HPLC $t_R$ = 5.1 min) substantially more polar than spirobrassinin was detected. Similar to the experiments described above, to establish the structure of this metabolic product, larger scale cultures of *S. sclerotiorum* were incubated with (±)-spirobrassinin (**27**) for seven days, then filtered, extracted, and the broth extract fractionated by column

chromatography followed by preparative TLC to yield a new metabolite (**231**). Standard spectroscopic analyses ($^1$H and $^{13}$C NMR, HMQC, HMBC, and HRMS-EI) indicated the molecular formula $C_{10}H_8N_2O_2S$. Comparison of the $^1$H NMR spectra of spirobrassinin (**27**) and that of the new metabolite (**231**) revealed the presence of an NH signal at $\delta_H$ 6.40 and the absence of the $SCH_3$ signal in the latter. A downfield shift for the C-2′ carbon ($\delta_H$ 163.2 in **27** to 171.9 in **231**) in the $^{13}$C NMR spectrum suggested the presence of a carbonyl group (NHC=OSR). Hence, on the basis of these spectral data, the structure of the new metabolite **231** was assigned as a spirothiazolidinone attached to C-3 of the oxoindole ring (Scheme 2.20, **231**, $[\alpha]_D$ = −35). The enantiomeric excess (ee) of untransformed spirobrassinin (**27**) recovered from cultures after a seven day incubation period was determined to be 14% by $^1$H NMR spectroscopy (integration of the SMe resonances) using the chiral solvating agent (*R*)-2,2,2-trifluoro-1-(9-anthryl)ethanol (TFAE, Table 2.2) as described in section 2.2.10 (Pedras et al., 2004d). However, the enantiomeric excess of metabolite **231** could not be determined (the diastereotopic methylene protons were not sufficiently resolved in the presence of the chiral solvating agent TFAE) (Pedras and Hossain, 2006).

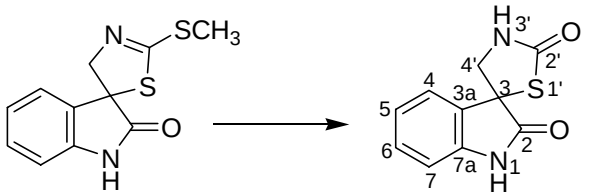


**27** **231**

**Scheme 2.20** Biotransformation of (±)-spirobrassinin (**27**) in *Sclerotinia sclerotiorum* (Pedras and Hossain, 2006).

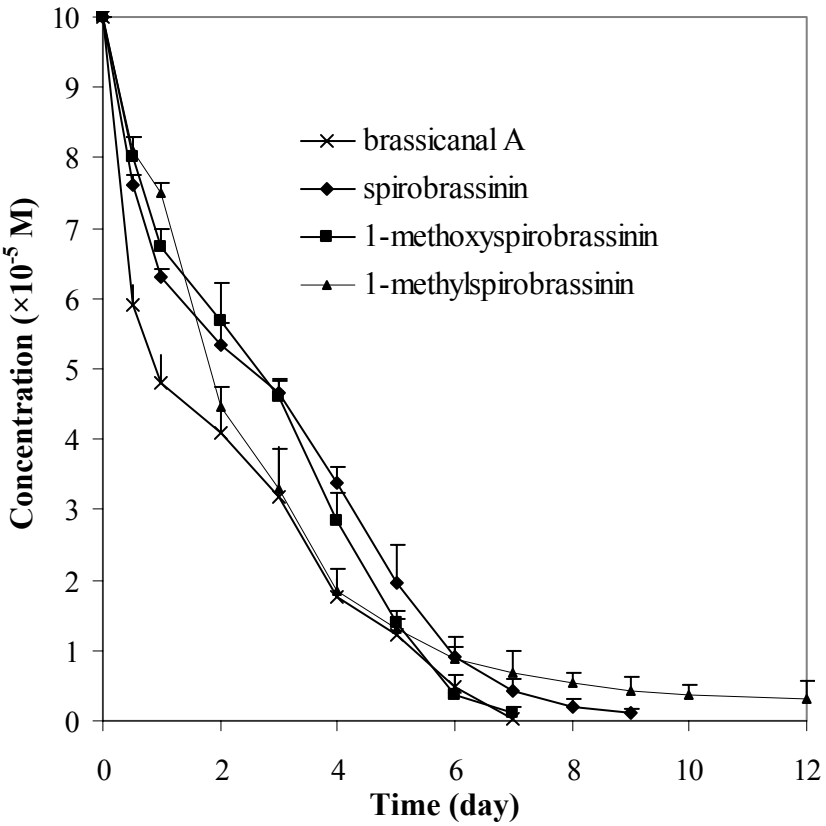


**Figure 2.4** Progress curves of the metabolism of brassicanal A (**34**), (±)-spirobrassinin (**27**), 1-methoxyspirobrassinin (**28**) and 1-methylspirobrassinin (**216**) in *Sclerotinia sclerotiorum*. Cultures were extracted and the extracts were analyzed by HPLC; concentrations were determined using calibration curves; each point is an average of experiments conducted in triplicate ± standard deviation (Pedras and Hossain, 2006).

### 2.2.8 (±)-1-Methoxyspirobrassinin (28)

Similar to other phytoalexins, the metabolism of (±)-1-methoxyspirobrassinin (**28**) by *S. sclerotiorum* was investigated in liquid cultures. Initially, an experiment was carried out to determine the time required for complete metabolism of (±)-1-methoxyspirobrassinin (**28**), as well as the best time for isolation of potential metabolic products of **28**. Fungal cultures and control medium were incubated with (±)-1-methoxyspirobrassinin (**28**) up to two weeks; samples were withdrawn at different times and analyzed by HPLC. 1-Methoxyspirobrassinin (**28**) was found to be stable in

control over the period of analysis. Comparison of the HPLC chromatograms of extracts of fungal cultures containing 1-methoxyspirobrassinin (**28**) and control cultures indicated that 1-methoxyspirobrassinin (**28**) was completely metabolized to two products with $t_R$ = 7.5 and 11.5 min in *ca.* 10 days (Fig. 2.4). The structure of each product was determined from comparison of their spectroscopic data and those of 1-methoxyspirobrassinin (**28**). The $^1$H NMR spectra of both compounds (**232** and **233**) showed four aromatic hydrogens, characteristic of a 2-oxoindole nucleus and two additional hydrogens (H-4′) with geminal coupling. In addition, both compounds showed a signal for an exchangeable hydrogen and the absence of the $SCH_3$ signal. The $^{13}$C NMR spectrum of the compound with $t_R$ = 7.5 min (**232**) displayed a downfield shift attributable to C-2′ ($\delta_C$ 163.2 in **28** to 171.4 in **232**), suggesting the presence of a carbonyl group [NH(S)C=O], whereas the compound with the $t_R$ = 11.5 min (**233**) showed a substantially higher chemical shift for C-2′ ($\delta_C$ 163.2 in **28** to 198.3 in **233**), suggesting the presence of a thiocarbonyl group [NH(S)C=S]. These data were consistent with the molecular formula of each compound determined by HRMSEI (**232**, $C_{11}H_{10}N_2O_3S$, and **233**, $C_{11}H_{10}N_2O_2S_2$). That is, the $SCH_3$ group of 1-methoxyspirobrassinin (**28**) had been transformed to a carbonyl group in **232** and to a thiocarbonyl group in **233**. On the basis of these results, the structure of the major metabolite ($t_R$ = 7.5 min) was established as the spirothiazolidinone **232** and the structure of the minor metabolite ($t_R$ = 11.5 min) was established as the spirothiazolidinethione **233** (Scheme 2.21) (Pedras and Hossain, 2006). As established for spirobrassinin (**27**), the ee of 1-methoxyspirobrassinin (**28**) isolated after incubation for seven days (33% ee) and of metabolites **232** (11% ee) and **233** (30% ee) were determined by $^1$H NMR spectroscopy using the chiral solvating agent TFAE (Table 2.2) as described in section 2.2.10 (Pedras et al., 2004d).

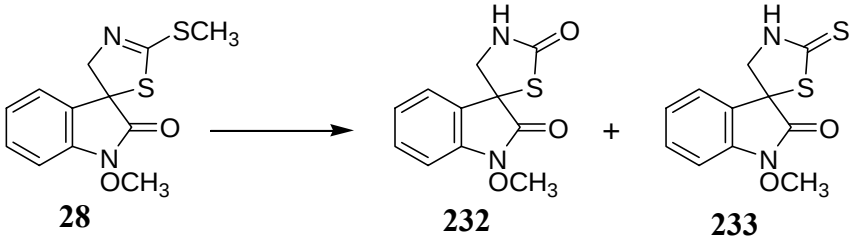


**Scheme 2.21** Biotransformation of 1-methoxyspirobrassinin (**28**) in *Sclerotinia sclerotiorum* (Pedras and Hossain, 2006).

**Table 2.2** Enantiomeric excess (ee) and optical rotation of spirobrassinins **27**, **28**, **216**, and metabolites **231**, **232**, **233**, and **234** (Pedras and Hossain, 2006).

| **Compounds; amount recovered from cultures after incubation for 7 d** | **ee (%)[a]** | **Optical rotation $[\alpha]_D$** |
|---|---|---|
| Spirobrassinin (**27**); 20% | 14[b] | -15 (*c* 0.34, MeOH) |
| 1-Methoxyspirobrassinin (**28**); 20% | 33[d] | +11(*c* 0.21, MeOH) |
| 1-Methylspirobrassinin (**216**); 16% | 26[e] | +7 (*c* 0.25, MeOH) |
| Spirooxathiazolidinone (**231**); 22% | nd[c] | -35 (*c* 0.33, MeOH) |
| Spirooxathiazolidinone (**232**); 16% | 11[d] | -7 (*c* 0.34, MeOH) |
| Spirooxathiazolidinethione (**233**); 7% | 30[d] | -31 (*c* 0.10, MeOH) |
| Spirooxathiazolidinone (**234**); 16% | 33[e] | -5 (*c* 0.20, MeOH) |

[a] Enantiomeric excess {ee=([*R*−*S*]/[*R*+*S*])×100}was determined using chiral solvating reagent (*R*)-2,2,2-trifluoro-1-(9-anthryl)ethanol (TFAE) by $^1$H NMR. [b] Determined by integration of the $^1$H NMR signals of SC*H*$_3$. [c] nd = not determined as $^1$H NMR signals were not resolved. [d] Determined by integration of the $^1$H NMR signals of OC*H*$_3$. [e]Determined by integration of the $^1$H NMR signals of NC*H*$_3$.

## 2.2.9 (±)-1-Methylspirobrassinin (216)

To probe the detoxification pathway of spirobrassinins **27** and **28** in *S. sclerotiorum*, (±)-1-methylspirobrassinin (**216**), a synthetic analogue of spirobrassinin (**27**), was incubated with fungal cultures of *S. sclerotiorum* and cultures were analyzed by HPLC over a period of several days. Similar to the biotransformation of

spirobrassinins **27** and **28**, it was found that the biotransformation of (±)-1-methylspirobrassinin (**216**) by *S. sclerotiorum* was a very slow process. Compound **216** was completely metabolized only after incubation for 12 days (Fig. 2.4). The metabolism of this compound by the fungus *S. sclerotiorum* led to the detection of three metabolites with $t_R$ = 6.6, 11.1 and 13.2 min (**234**, **235**, and **27**, respectively, Scheme 2.22). Subsequently, to isolate these metabolites, larger scale cultures were incubated with 1-methoxyspirobrassinin (**216**) for 7 days; cultures were filtered and extracted with EtOAc. The EtOAc extract was subjected to reverse phase FCC followed by preparative TLC to yield the metabolites **234**, **235**, and **27**. The structure of each metabolite was determined from comparison of its spectroscopic data and those of 1-methylspirobrassinin (**216**). The $^1$H NMR spectrum of the most polar compound ($t_R$ = 6.6 min, **234**) showed the four aromatic hydrogens characteristic of a 2-oxoindole nucleus and two additional hydrogens (H-4′) showing geminal coupling. In addition, compound **234** showed a proton resonance attributable to the NH and the absence of the proton resonance due to $SCH_3$. The $^{13}$C NMR of **234** showed a downfield shift for the C-2′ carbon ($\delta_C$ 163.2 in **216** to 171.9 in **234**) which suggested the presence of a carbonyl group, *i.e.* transformation of the N=C($SCH_3$)S group to the NH–C=O(S) group. These assumptions were consistent with the molecular formula obtained by HRMS-EI ($C_{11}H_{10}N_2O_2S$,). Thus, on the basis of these results the structure of this metabolite was assigned as the spirothiazolidinone **234** (Scheme 2.22). The compound of intermediate polarity ($t_R$ = 11.1 min, **235**), relative to 1-methylspirobrassinin (**216**) ($C_{12}H_{12}N_2OS_2$) contained an additional oxygen atom ($C_{12}H_{12}N_2O_2S_2$), as determined by HRMSEI. Comparison of the $^1$H NMR spectrum of the parent compound **216** with that of **235** indicated the presence of signals attributable to $NCH_2OH$ ($\delta_H$ 5.21 and 5.35) and the absence of the $NCH_3$ signal. This reasoning was corroborated by the $^{13}$C NMR spectrum [downfield shift for the (N)*C*$H_2$OH carbon $\delta_C$ 26.7 in **216** to 64.7 in **235**]. That is, the *N*–$CH_3$ group was oxidized enzymatically to the *N*–$CH_2$–OH group.

Therefore, the structure of this metabolite was assigned as 1-hydroxymethylspirobrassinin (**235**, Scheme 2.22). The third metabolite was established as spirobrassinin (**27**) based on its spectroscopic data and comparison with an authentic sample. To establish the sequence of biotransformation steps, compound **235** was administered to cultures of *S. sclerotiorum*. As expected, spirobrassinin (**27**) was detected in the HPLC chromatogram of the broth extract of these cultures, demonstrating it to be a metabolite of **235** resulting from enzymatic oxidation followed by decarboxylation of **235** (Scheme 2.22) (Pedras and Hossain, 2006). As described for 1-methoxyspirobrassinin (**28**), the ee values of untransformed 1-methylspirobrassinin (**216**) and metabolite **234** were determined using the chiral solvating agent TFAE (Table 2.2) as described in section 2.2.10 (Pedras et al., 2004d).

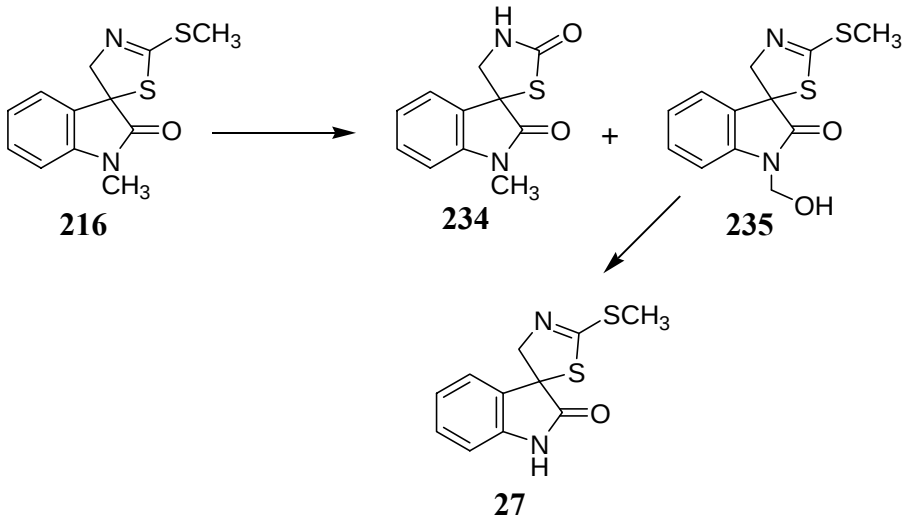


**Scheme 2.22** Biotransformation of 1-methylspirobrassinin (**216**) in *Sclerotinia sclerotiorum* (Pedras and Hossain, 2006).

### 2.2.10 Determination of the enantiomeric excess of spirobrassinins 27, 28, 216, and metabolites 232, 233, and 234

As shown in Table 2.2, the optical rotation values of untransformed spirbrassinins **27**, **28**, **216**, and metabolites **232**, **233**, and **234** recovered from cultures after a seven day incubation period suggested that some of these compounds were optically active. Thus, it was of interest to determine the enantiomeric excess of these compounds. Because chiral HPLC did not give baseline resolution of racemic spirobrassinin (**27**), and the specific optical rotation values of small amounts of sample were not sufficiently accurate to determine the enantiomeric excess, NMR methods were sought (Pedras et al., 2004d). Chiral solvating agents (CSA) are a simple and inexpensive choice to determine enantiomeric excess using NMR spectroscopy. CSA have been used for more than three decades to analyze mixtures of enantiomers and measure the enantiomeric composition of samples of chiral compounds of unknown enantiomeric excess using $^1$H NMR (Wenzel, 2000; Parker, 1991; Pirkle and Hoover, 1982). Subsequently, this section describes a simple and inexpensive method for enantiomeric discrimination of the phytoalexins spirobrassinin (**27**), 1-methoxyspirobrassinin (**28**) and synthetic analog 1-methylspirobrassinin (**216**) and their metabolites **232**, **233**, and **234** using the chiral solvating agent (*R*)-2,2,2-trifluoro-1-(9-anthryl)ethanol (TFAE) in $C_6D_6$ (Pedras et al., 2004d).

Initially, the $^1$H NMR spectra of (±)-spirobrassinin (**27**) was obtained in $CDCl_3$ containing increasing amounts of TFAE. Enantiodifferentiation with peak baseline resolution was observed for the signals corresponding to protons of the (S)$CH_3$ group when the concentration of TFAE was four times that of **27**. Close inspection of the $^1$H NMR spectra showed several additional resonances related to spirobrassinin, suggesting modifications in its structure. Eventually it was discovered that spirobrassinin (**27**) decomposed slowly (<5% in 24h) on standing in $CDCl_3$ to yield a

mixture of undetermined compounds. Next, additional deuterated solvents in which spirobrassinin was stable were tested. Although spirobrassinin (**27**) appeared stable in both $CD_3OD$ and $CD_3CN$, these solvents did not allow sufficient chiral discrimination of both spirobrassinin enantiomers. Finally, chiral discrimination of spirobrassinins **27**, **28**, and **216** was achieved in $C_6D_6$ containing 6 equiv of (*R*)-TFAE and $D_2O$ (to exchange OH of TFAE). By comparing the spectra of racemic spirobrassinins (**27**, **28**, **216**) in the free state and in the presence of the chiral solvating agent (CSA), it was established that (*R*)-TFAE induced non-equivalence in the $–SCH_3$ protons of the two enantiomers of each spirobrassinins (**27**, **28**, **216**). Significant chemical-shift non-equivalence ($\Delta\delta_H^{RS}$) for $–SCH_3$ resonance in the diastereoisomeric complexes was observed in $C_6D_6$ (Fig. 2.5-2.7). Higher values of $\Delta\delta_H$ were found near 1:6 stoichiometry of spirobrassinins: CSA. The chemical-shift non-equivalence $\Delta\delta_H$ between two enantiomers for $–SCH_3$ protons are listed in Table 2.3. The observed shift non-equivalence of the $–SCH_3$ resonance is sufficient not only to determine the enantiomeric purity of enantiomerically enriched samples of spirobrassinins (**27**, **28**, **216**) but also for assignment of the absolute configuration. For example, naturally occurring samples of spirobrassinin (**27**) isolated from rutabaga ($[\alpha]_D$ -53; *c* 0.30 g/100 ml in $CHCl_3$) (Pedras et al., 2004b), and cauliflower ($[\alpha]_D$ -109; *c* 0.35 g/100 ml in $CD_2Cl_2$) (Pedras et al., 2006b) were determined to have the *S* configuration (Fig. 2.5D) upon comparison with an authentic sample of (*S*)-spirobrassinin (**27**) synthesized and resolved as shown in Scheme 2.8 and 2.12 respectively (Fig 2.5C). The enantiomeric excess of resolved synthetic and naturally occurring spirobrassinin (**27**) samples could be accurately measured by integration of the areas of the $^1H$ NMR peaks corresponding to the $(S)CH_3$ group of each enantiomer ($\delta_H$ 2.14 for *R* and 2.10 for *S*). Partial chemical shift non-equivalence was observed for the $CH_2$ group. The enantiomers of 1-methoxyspirobrassinin (**28**) and 1-methylspirobrassinin (**216**) could also be discriminated, and the percentage of each enantiomer could be measured accurately by

integration of areas of the $^1$H NMR peaks corresponding to the (S)$CH_3$ group of each one (**28**, $\delta_H$ 2.13 and 2.10; **216**, $\delta_H$ 2.16 and 2.13), as shown in Figs. 2.6 and 2.7, respectively. Partial chemical shift non-equivalence was also observed for the additional methyl groups in the case of **28** and **216**. The enantiomeric excess of spirooxathiazolidinone **232**, and **234** (metabolites of **28** and **216** respectively) and spirooxathiazolidinethione **233** (metabolite of **28**) could also be determined using the same procedure. Significant chemical-shift non-equivalence ($\Delta\delta_H^{RS}$) for –$OCH_3$ resonance in case of **232** and **233** and for –$NCH_3$ resonance in case of **234** in the diastereoisomeric complexes was observed in $C_6D_6$ with 6 equiv of *R*-TFAE (Table 2.3). However, enantiomeric excess of **231** (metabolite of **27**) could not be determined using the same procedure as the peaks corresponding to the $CH_2$ group were not resolved sufficiently (Pedras et al., 2004d).

**Table 2.3** Chemical shift non-equivalence observed between two enantiomers of each spirobrassinins **27**, **28**, **216** and metabolites **232**, **233**, **234** treated with 6-equiv of *R*-TFAE in $C_6D_6$ and $D_2O$ (*ca.* 20 μl) (Pedras et al., 2004d)

| **Compounds** | **$\Delta\ \delta_H$ (ppm)** |
|---|---|
| Spirobrassinin (**27**) | 0.038[a] |
| 1-Methoxyspirobrassinin (**28**) | 0.027[a] |
| 1-Methylspirobrassinin (**216**) | 0.038[a] |
| Spirooxathiazolidinone (**232**) | 0.018[b] |
| Spirooxathiazolidinethione (**233**) | 0.021[b] |
| Spirooxathiazolidinone (**234**) | 0.043[c] |

[a] $^1$H NMR peaks corresponding to –$SCH_3$ group; [b] $^1$H NMR peaks corresponding to –$OCH_3$ group; [c] $^1$H NMR peaks corresponding to –$NCH_3$ group.

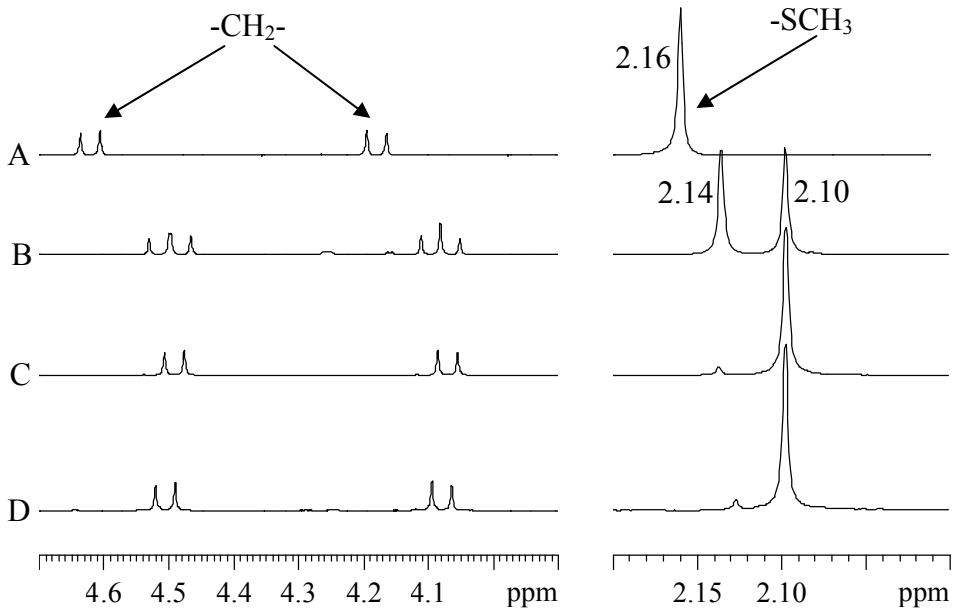


**Figure 2.5** $^{1}$H NMR spectra of spirobrassinin (**27**): A – racemic mixture (1.8 mg) in $C_6D_6$ (500 μl); B – racemic mixture containing six equivalents of (*R*)-TFAE in $C_6D_6$ and $D_2O$ (*ca.* 20 μl); C – synthetic *S* enantiomer containing six equivalents of TFAE in $C_6D_6$ and $D_2O$ (*ca.* 20 μl); naturally occurring from cauliflower containing six equivalents of TFAE in $C_6D_6$ and $D_2O$ (*ca.* 20 μl) (Pedras et al., 2004d).

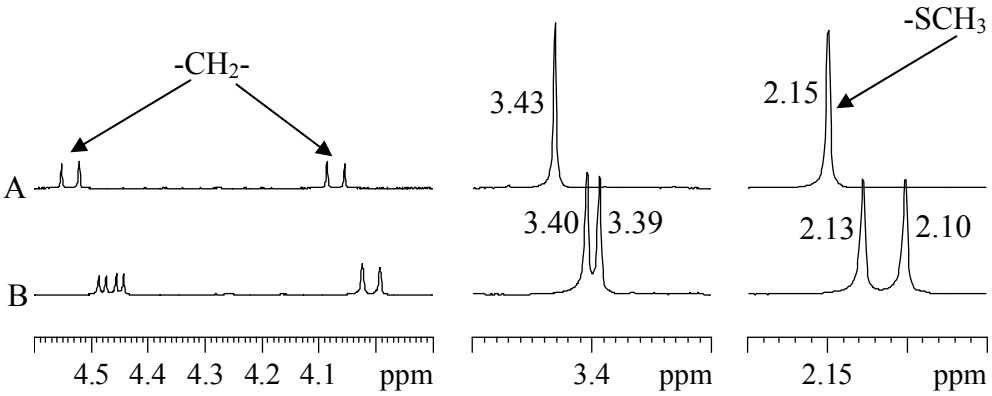


**Figure 2.6** $^{1}$H NMR spectra of 1-methoxyspirobrassinin (**28**): A – racemic mixture (1.5 mg) in $C_6D_6$ (500 μl); B – racemic mixture containing six equivalents of (*R*)-TFAE in $C_6D_6$ and $D_2O$ (*ca.* 20 μl) (Pedras et al., 2004d).

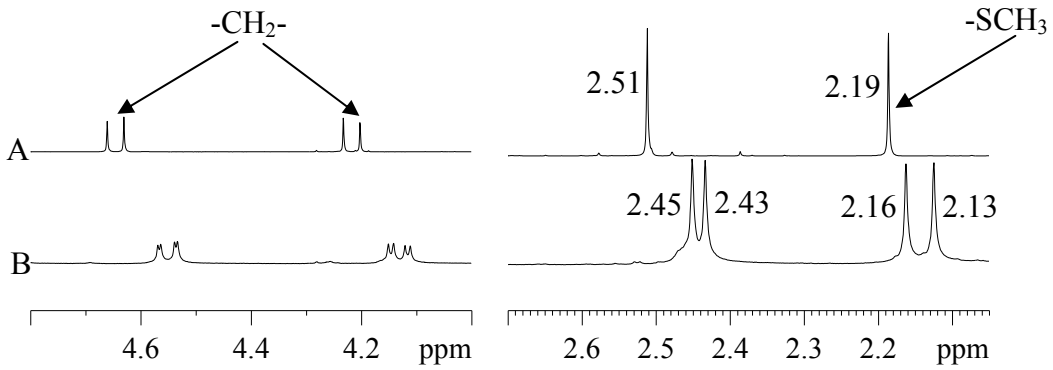


**Figure 2.7** $^{1}$H NMR spectra of 1-methylspirobrassinin (**216**): A – racemic mixture (1.4 mg) in $C_6D_6$ (500 μl); B – racemic mixture containing six equivalents of (*R*)-TFAE in $C_6D_6$ and $D_2O$ (*ca.* 20 μl) (Pedras et al., 2004d).

### 2.2.11 Summary

The results of these biotransformations suggested that *S. sclerotiorum* produces various enzymes that can detoxify cruciferous phytoalexins via different pathways. The metabolism and detoxification of strongly antifungal phytoalexins in *S. sclerotiorum* were fast and led to glucosylated products whereas the metabolism of weakly antifungal phytoalexins were very slow and yielded non-glucosylated compounds (Pedras and Hossain 2006). These results of biotransformations are summarized below in Table 2.4.

**Table 2.4** Products of metabolism of phytoalexins **11**, **18**, **24**, **25**, **27**, **28** and **34** and their analogues **215**, and **216** (0.1 mM) in cultures of *Sclerotinia sclerotiorum* (Pedras et al., 2004c; Pedras and Hossain, 2006).

| **Compound added to cultures** | **Incubation time** | **Products of metabolism (%)[a]** | **Recovered starting material (%)[a]** |
|---|---|---|---|
| 1-Methoxybrassinin (**11**) | 12 h | **220** (15%) | 5 |
| Cyclobrassinin (**18**) | 12 h | **34** (6%); **221** (36%) | 10 |
| Brassilexin (**24**) | 24 h | **34** (18%); **222** (7%) | 10 |
| Sinalexin (**25**) | 30 h | **226** (2%); **227** (15%) | 8 |
| Spirobrassinin (**27**) | 7 d | **231** (22%) | 20 |
| 1-Methoxyspirobrassinin (**28**) | 7 d | **232** (16%); **233** (17%) | 20 |
| Brassicanal A (**34**) | 6 d | **229** (15%); **230** (13%) | 28 |
| 3-(Amino)methylenindoline-2-thione (**47**) | 6 h | **34** (10%) | None |
| 1-Methylbrassilexin (**215**) | 4 d | **228** (7%) | 10 |
| 1-Methylspirobrassinin (**216**) | 7 d | **27** (7%) **234** (16%); **235** (5%) | 16 |
| 7-Oxy-(*O*-β-D-glucopyranosyl)-1-methoxybrassinin (**220**) | 24 h | Complete transformation to undetermined products | None |
| 1-β-D-Glucopyranosylbrassilexin (**222**) | 48 h | Complete transformation to undetermined products | None |
| 1-β-D-Glucopyranosylcyclobrassinin (**221**) | 24 h | Complete transformation to undetermined products | None |
| 6-Oxy-(*O*-β-D-glucopyranosyl)sinalexin (**227**) | 48 h | Complete transformation to undetermined products | None |

[a] Percentage yields (molar) of products represent HPLC-determined yields.

## 2.3 Design and synthesis of potential brassinin detoxification inhibitors

Previous work (Pedras and Ahiahonu, 2002; Pedras et al., 2004c) and the results described in the above section suggested that *S. sclerotiorum* has acquired or evolved efficient glucosyltransferase(s) that can disarm some of the most active plant chemical defenses (Pedras and Hossain 2006). By considering the antifungal activity of phytoalexins against *S. sclerotiorum* and their role as the plant chemical defenses, it can be suggested that glucosylation reactions could be reasonable metabolic targets to control the stem rot fungus. For example, application of potential phytoalexin detoxification inhibitors to infected plants might prevent the pathogen from metabolizing these phytoalexins. A concentration increase of strongly antifungal phytoalexins is expected to slow down if not stop growth of *S. sclerotiorum*. However, among the phytoalexins that were studied, the detoxification of brassinin (**9**) appeared to be one of the most important reactions to inhibit. Brassinin (**9**) is known to be a biosynthetic precursor of cyclobrassinin (**18**), brassilexin (**24**), brassicanal A (**34**), spirobrassinin (**27**), and dioxibrassinin (**26**) (Pedras et al., 2003a). Therefore, selective inhibition of brassinin detoxification might allow plants to accumulate brassinin (**9**) and other phytoalexins that would be expected to slow down if not stop the growth of *S. sclerotiorum*. As depicted in Scheme 1.4, the detoxification of brassinin (**9**) in *S. sclerotiorum* involves glucosylation at the *N*-1 position of the indole ring and this glucosylation reaction requires an inducible brassinin glucosyltransferase (BGT) (Pedras et al., 2004c). Furthermore, it was reported that 6-fluorocamalexin (**75**) could slow down substantially the rate of metabolism of brassinin (**9**) both in fungal cultures and in cell-free extracts of *S. sclerotiorum*. Thus, based on these results two groups of potential brassinin detoxification inhibitors were designed: (i) one group was based on the structure of brassinin (Fig. 2.8) and (ii) another group was based on the structure of

camalexin (**31**) (Fig. 2.9). Since BGT appeared to be selective, it was anticipated that replacing the indole nitrogen with other heteroatoms, e.g. oxygen and sulfur, in compounds **236** and **237** respectively, or changing the position of side chain of brassinin (**9**) from C-3 to C-2, e.g. compounds **240** and **241**, could inhibit the glucosyltransferase involved in the metabolism of brassinin. It was found that blocking the *N*-1 position of the indole ring in brassinin (**9**) with a methoxy group would lead to oxidation at C-7 followed by glucosylation (Scheme 2.13). Hence, compounds **238** and **239** were designed by replacing C-7 or C-7a carbons in brassinin with nitrogen in order to stop the possible oxidation of **238** and **239** at C-7. In addition, compounds **242** and **243** were designed by replacing the dithiocarbamate side chain with an ester or an amide to reduce the overall antifungal activity. Since 6-fluorocamalexin (**75**) could slow down the rate of metabolism of brassinin it was anticipated that compounds **244**, **245**, **246**, **247**, **248**, **249**, and **250** could slow down the rate of metabolism of brassinin as well (Fig 2.9). It was also thought that replacing the thiazole ring in camalexin with a phenyl group would reduce the antifungal activity of potential inhibitors, thus 3-phenylindoles **245**, **246**, **247** were designed. However, because biotransformation of 3-phenylindole (**245**) yielded the *N*-1 glucosylated compound, 3-phenylbenzofuran (**248**) was designed by replacing nitrogen of indole ring with oxygen. In addition, 2-phenylindole (**249**) and thiabendazole (**250**) were designed by changing the position of the aromatic side chain from C-3 to C-2.

Among all these potential inhibitors (Figs. 2.8 and 2.9), syntheses of **240**, **242**, **244**, and **245** were known (Pedras et al., 2006a; Elsner et al., 2006; Pedras and Liu, 2004; Rodriguez et al., 2000) and compounds **249**, and **250** were commercially available. The remaining compounds **236**, **237**, **238**, **239**, **241**, **246**, and **247** were synthesized for the first time as described below.

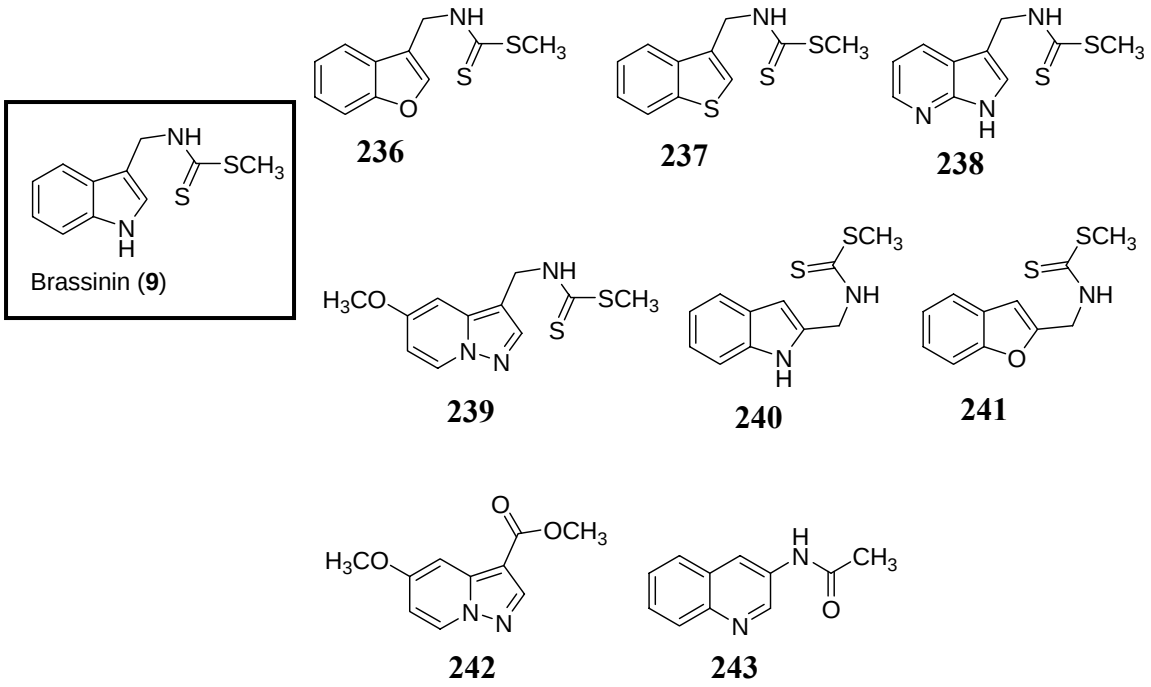


**Figure 2.8** Potential brassinin detoxification inhibitors with structures based on brassinin (**9**).

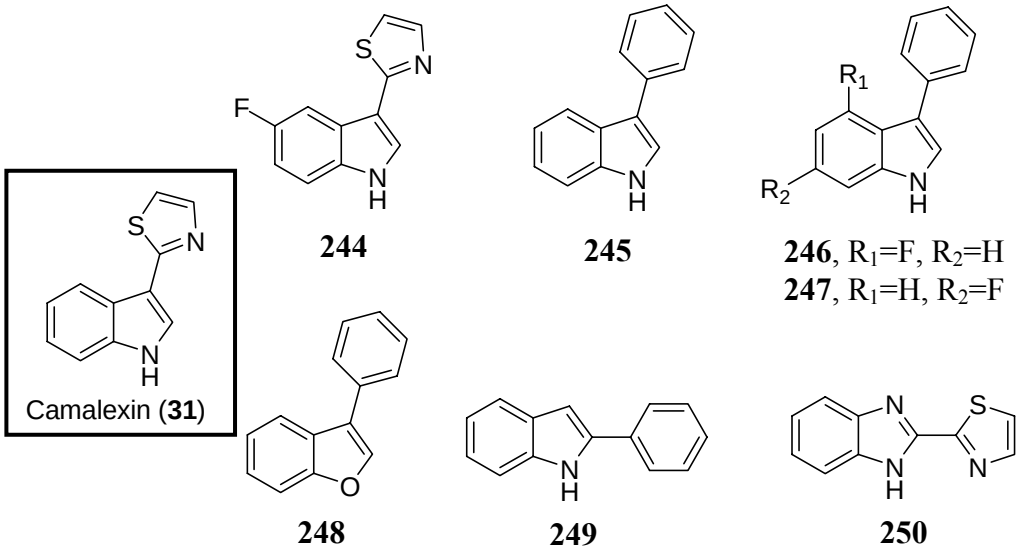


**Figure 2.9** Potential brassinin detoxification inhibitors with structures based on camalexin (**31**).

### 2.3.1 Synthesis of methyl (indol-2-yl)methyldithiocarbamate (240), fluorocamalexins (75, 244) and 3-(*N*-acetylamino)quinoline (243)

Methyl (indol-2-yl)methyldithiocarbamate or isobrassinin (**240**) was synthesized as shown in Scheme 2.23 (Pedras et al., 2006a), starting from indole-2-carboxylic acid (**251**) in 6-steps. Similar to the synthesis of camalexin (**31**), 5-fluorocamalexin (**244**) and 6-fluorocamalexin (**75**) were also synthesized from 5-fluoro- and 6-fluoroindoles (**257**, **258**), respectively, upon treatment with a Grignard reagent followed by reaction with 2-bromothiazole as shown in Scheme 2.24 (Pedras and Liu, 2004; Pedras and Ahiahonu, 2002). 3-(*N*-acetylamino)quinoline (**243**) was synthesized by acetylation of 3-aminoquinoline using acetic anhydride and pyridine.

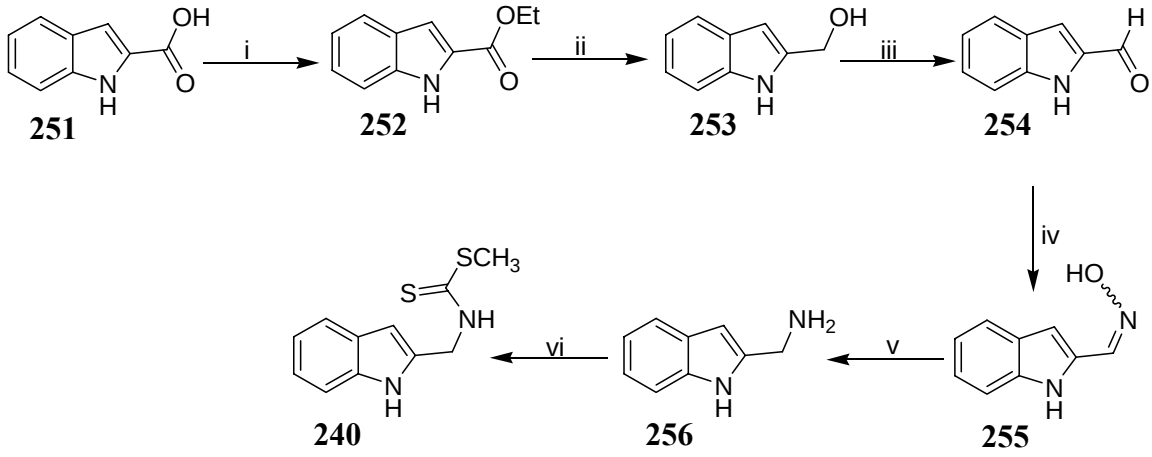


**Scheme 2.23** Synthesis of methyl (indol-2-yl)methyldithiocarbamate (240). Reagents: (i) EtOH, $H_2SO_4$, 115 °C, 85%; (ii) $LiAlH_4$, THF, 0 °C; (iii) $MnO_2$, $CH_2Cl_2$, 81%; (iv) $NH_2OH.HCl$, $Na_2CO_3$, $EtOH/H_2O$, 99%; (v) $NaBH_4$, $NiCl_2.6H_2O$, MeOH; (vi) Py, $Et_3N$, $CS_2$, $CH_3I$, 43% (Pedras et al., 2006a).

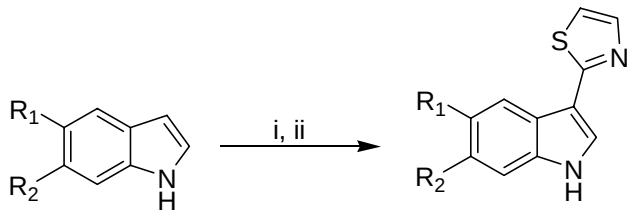


**257**, $R_1$ = F, $R_2$ = H
**258**, $R_1$ = H, $R_2$ = F

**244**, $R_1$ = F, $R_2$ = H
**75**, $R_1$ = H, $R_2$ = F

**Scheme 2.24** Synthesis of 6-fluorocamalexin (**75**) and 5-fluorocamalexin (**244**). Reagents and conditions: (i) Mg, $CH_3I$, $Et_2O$; (ii) benzene, 2-bromothiazole, 90 °C, 57% (Pedras and Liu, 2004; Pedras and Ahiahonu, 2002).

### 2.3.2 Synthesis of methyl (benzofuran-3-yl)methyldithiocarbamate (236)

Methyl (benzofuran-3-yl)methyldithiocarbamate (**236**) was prepared from benzofuran-3-carboxaldehyde (**263**) as shown in Scheme 2.25. Benzofuran-3-carboxaldehyde (**263**) was obtained upon oxidation of 3-methylbenzofuran (**262**) (Zaidlewicz et al., 2001) which was obtained from *o*-hydroxyacetophenone (**259**) (Nielek and Lesiak, 1982). Oxidation of 3-methylbenzofuran (**262**) with selenium dioxide afforded a mixture of aldehyde **263**, and alcohol **264** in an 11:1 ratio. The resulting aldehyde **263** was allowed to react with hydroxylamine hydrochloride to give a mixture of (*E*)- and (*Z*)- oximes (**265**), which after reduction with sodium cyanoborohydride in the presence of $TiCl_3$ yielded 3-benzofuranylmethylamine (**266**). Reaction of amine **266** with carbon disulfide in the presence of pyridine and triethylamine gave a dithiocarbamate salt, which was subsequently methylated with iodomethane to give methyl (benzofuran-3-yl)methyldithiocarbamate (**236**) in 22% overall yield in a 7-step process (Scheme 2.25).

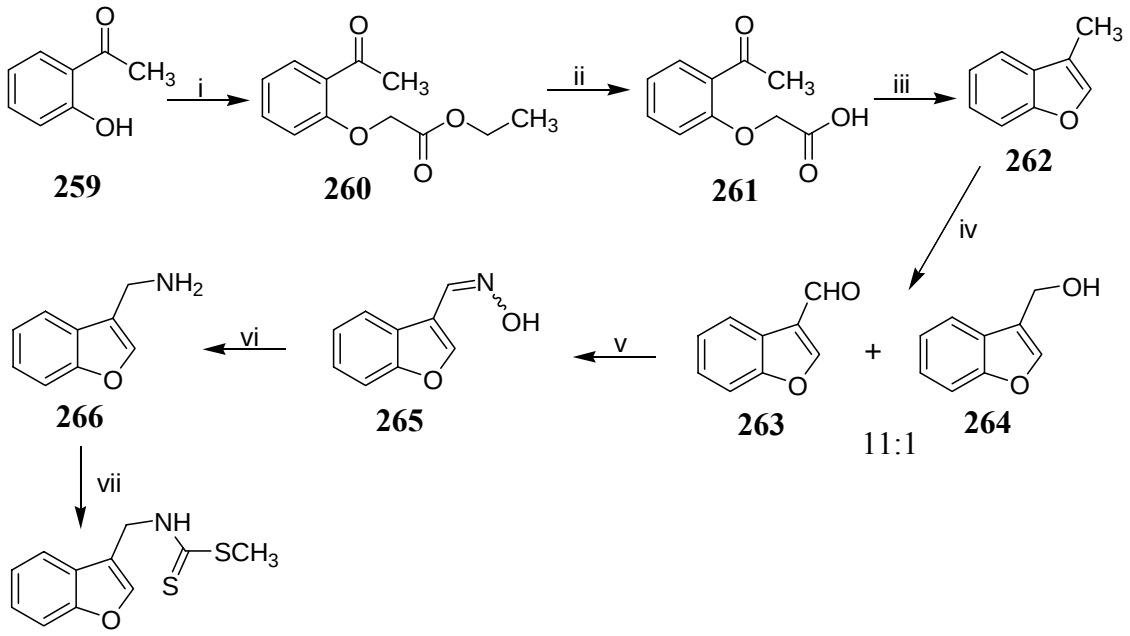


**Scheme 2.25** Synthesis of methyl (benzofuran-3-yl)methyldithiocarbamate (**236**). Reagents and conditions: (i) $ClCH_2CO_2Et$, $K_2CO_3$, acetone, 65 °C, 92%; (ii) $Na_2CO_3$, $H_2O$, 100 °C, 92%; (iii) NaOAc, $Ac_2O$, 160 °C, 65%; (iv) $SeO_2$, 1,4-dioxane, 105 °C, 96%; (v) $NH_2OH.HCl$, $Na_2CO_3$, $EtOH/H_2O$, 84%; (vi) $Na(CN)BH_3$, $NH_4OAc$, $TiCl_3$, MeOH; (vii) Py, $Et_3N$, $CS_2$, $CH_3I$, 48%.

## 2.3.3 Synthesis of methyl (benzofuran-2-yl)methyldithiocarbamate (241)

Similar to dithiocarbamate **236**, methyl (benzofuran-2-yl)methyldithiocarbamate (**241**) was synthesized from benzofuran-2-carboxaldehyde (**268**) which was obtained by Vilsmeier formylation (Jones and Stanforth, 1997; Suu et al., 1962) of benzofuran (**267**) using $POCl_3$ (6 eq.) and DMF (Scheme 2.26). Reaction of the carboxaldehyde **268** with hydroxylamine hydrochloride afforded oxime **269**, which was reduced to the corresponding amine **270** using $Na(CN)BH_3$ and $TiCl_3$. The amine **270** was converted to dithiocarbamate **241** after treatment with carbon disulfide and iodomethane in 40% overall yield (Scheme 2.26).

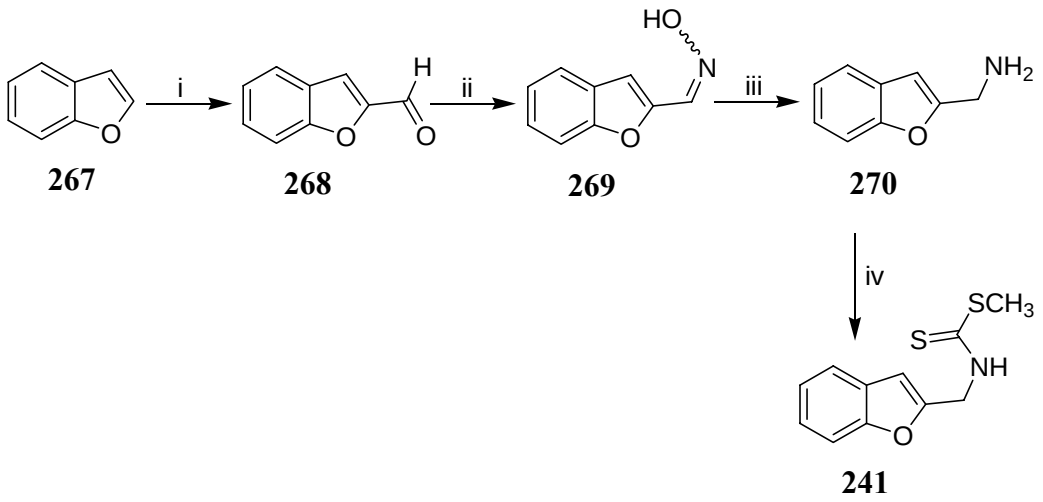


**Scheme 2.26** Synthesis of methyl (benzofuran-2-yl)methyldithiocarbamate (**241**). Reagents and conditions: (i) $POCl_3$, DMF, 95 °C, 78%; (ii) $NH_2OH.HCl$, $Na_2CO_3$, $EtOH/H_2O$, 93%; (iii) $Na(CN)BH_3$, $NH_4OAc$, $TiCl_3$, MeOH; (iv) Py, $Et_3N$, $CS_2$, $CH_3I$, 56%.

### 2.3.4 Synthesis of methyl (thianaphthen-3-yl)methyldithiocarbamate (237)

Dithiocarbamate **237** was synthesized from 3-bromothianaphthene (**271**) as shown in Scheme 2.27. The 3-bromothainaphthene (**271**) was converted to thianaphthene-3-carboxaldehyde (**272**) after lithiation of **271** with *t*-butyllithium followed by reaction with dimethylformamide. The resultant aldehyde **272** was converted to a mixture of (*E*)- and (*Z*)- oximes (**273**) upon reaction with hydroxylamine hydrochloride. Finally, the dithiocarbamate **237** was obtained upon reduction of oximes **273** with sodium cyanoborohydride, $TiCl_3$ and $NH_4OAc$, followed by standard treatment with carbon disulfide and iodomethane in 48% overall yield (based on 3-bromothianaphthene (**271**), Scheme 2.27).

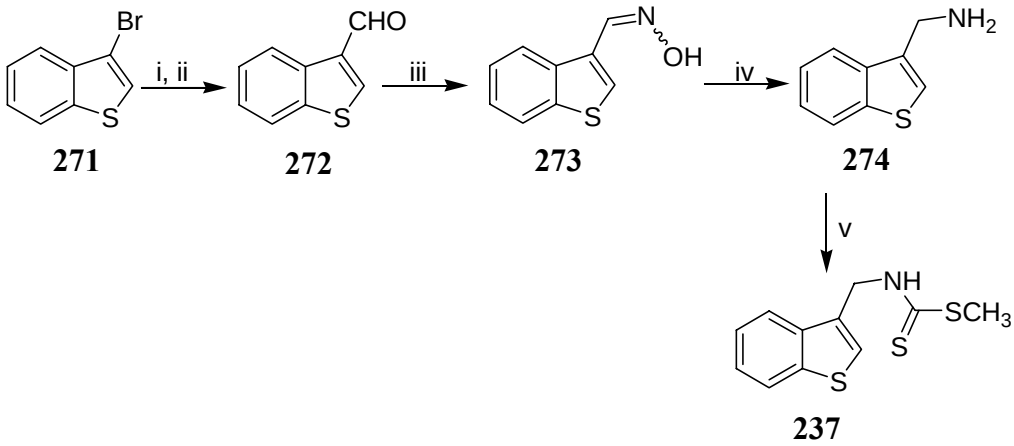


**Scheme 2.27** Synthesis of methyl (thianaphthen-3-yl)methyldithiocarbamate (**237**). Reagents and conditions: (i) *t*-BuLi, $Et_2O$, -78 °C; (ii) DMF, 73%; (iii) $NH_2OH.HCl$, $Na_2CO_3$, $EtOH/H_2O$, 93%; (iv) $Na(CN)BH_3$, $NH_4OAc$, $TiCl_3$, MeOH; (v) Py, $Et_3N$, $CS_2$, $CH_3I$, 71%.

### 2.3.5 Synthesis of methyl (7-azaindole-3-yl)methyldithiocarbamate (238)

Methyl (7-azaindol-3-yl)methyldithiocarbamate (**238**) was synthesized starting from commercially available 7-azaindole (**275**) as shown in Scheme 2.28. The azaindole (**275**) was first converted to 7-azaindole-3-carboxaldehyde (**276**) by Vilsmeier formylation which was allowed to react with hydroxylamine hydrochloride to give a mixture of (*E*)- and (*Z*)-oximes (**277**). The oximes **277** were reduced to the corresponding amine **278** using Zn/HCl, which upon treatment with carbon disulfide in the presence of pyridine and triethylamine followed by iodomethane afforded methyl (7-azaindol-3-yl)methyldithiocarbamate (**238**) in 12% overall yield, based on 7-azaindole (**275**).

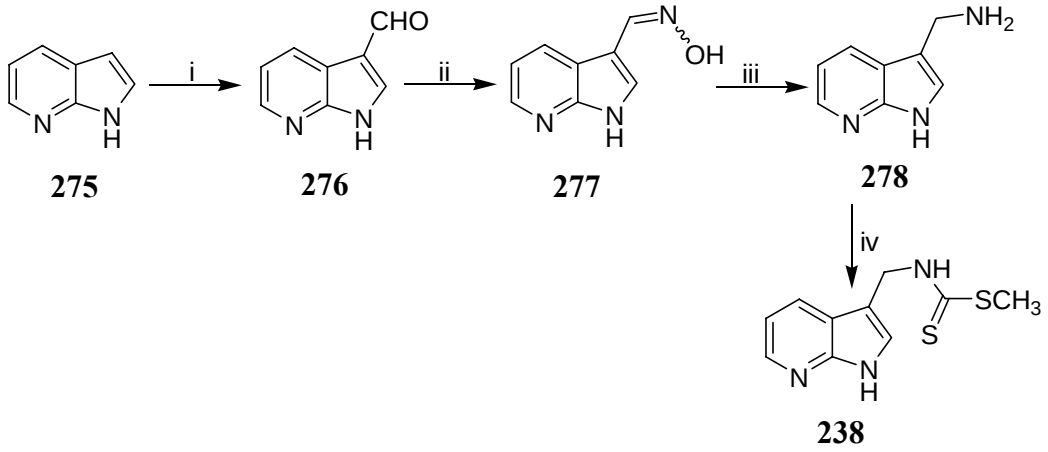


**Scheme 2.28** Synthesis of methyl (7-azaindol-3-yl)methyldithiocarbamate (**238**). Reagents and conditions: (i) $POCl_3$, DMF, 105 °C, 47%; (ii) $NH_2OH.HCl$, $Na_2CO_3$, $EtOH/H_2O$, 94%; (iii) Zn, HCl, 35%; (iv) Py, $Et_3N$, $CS_2$, $CH_3I$, 83%.

### 2.3.6 Synthesis of methyl (5-methoxypyrazolo[1,5-a]pyridin-3-yl)methyldithiocarbamate (239)

Dithiocarbamate **239** was synthesized from methyl 5-methoxypyrazolo[1,5-a]pyridine-3-carboxylate (**242**) (Scheme 2.30), which was obtained as previously reported (Elsner et al., 2006) in a 4-step process shown in Scheme 2.29. Elsner et al. recently reported the synthesis of *N*-aminopyridinium salt **283** by taking advantage of a highly efficient synthesis of *O*-(2,4-dinitrophenyl)hydroxylamine (**282**) (Legault and Charette, 2003). 1,3-Dipolar cycloaddition of **283** with methylpropiolate under oxidative conditions furnished methyl 5-methoxypyrazolo[1,5-a]pyridine-3-carboxylate (**242**) in good yield (Scheme 2.29). Reduction of the resultant ester **242** with $LiAlH_4$, followed by oxidation with $MnO_2$ afforded the corresponding aldehyde **285**. The aldehyde **285** was allowed to react with hydroxylamine hydrochloride to yield the corresponding oximes **286**, which after reduction with Zn/HCl followed by reaction with $CS_2$ and iodomethane afforded methyl (5-methoxypyrazolo[1,5-a]pyridin-3-yl)methyldithiocarbamate (**239**) in 10% overall yield based on **279**.

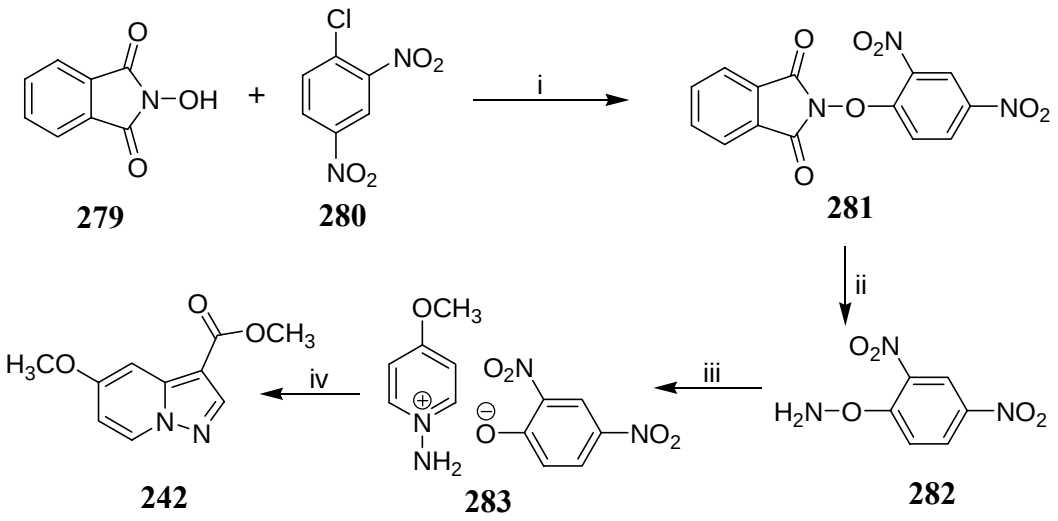

**Scheme 2.29** Synthesis of methyl 5-methoxypyrazolo[1,5-a]pyridine-3-carboxylate (**242**). Reagents and conditions: (i) $Et_3N$, acetone, 92%; (ii) $NH_2NH_2.xH_2O$, $CH_2Cl_2$, MeOH, 0 °C, 87% (Legault and Charette, 2003); (iii) 4-methoxypyridine, MeCN, 45 °C, 96%; (iv) methyl propiolate, $K_2CO_3$, air-$O_2$, DMF, 40% (Elsner et al., 2006).

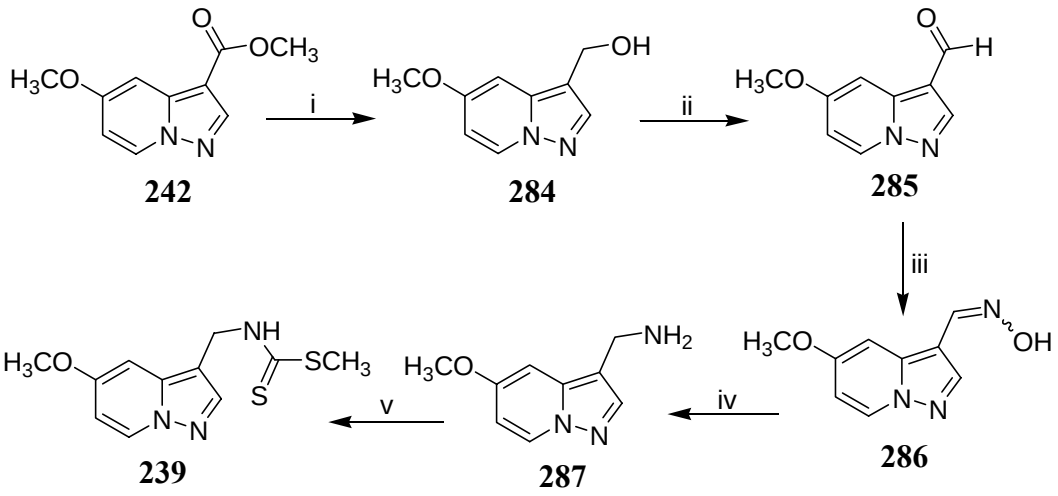

**Scheme 2.30** Synthesis of methyl (5-methoxypyrazolo[1,5-a]pyridin-3-yl)methyldithiocarbamate (**239**). Reagents and conditions: (i) $LiAlH_4$, THF, 0 °C; (ii) $MnO_2$, $CH_2Cl_2$, 65%; (iii) $NH_2OH.HCl$, $Na_2CO_3$, EtOH/$H_2O$, 91%; (iv) Zn, HCl; (v) Py, $Et_3N$, $CS_2$, $CH_3I$, 49%.

## 2.3.7 Synthesis of 3-phenylindoles (245, 246, 247)

3-Phenylindoles **245**, **246**, **247** were synthesized by means of the Fischer indole reaction, starting from the phenylhydrazones (**291**, **292**) of the phenylacetaldehyde (**290**) in the presence of $ZnCl_2$ (Rodriguez et al., 2000). Reaction of phenylhydrazines **288** and **289** with phenylacetaldehyde (**290**) at 100 ºC afforded phenylhydrazones **291** and **292** respectively, which on treatment with $ZnCl_2$ in ethanol afforded 3-phenylindole (**245**) and a mixture of 4-fluoro- and 6-fluoro-3-phenylindoles (**246**, **247**), respectively (Scheme 2.31).

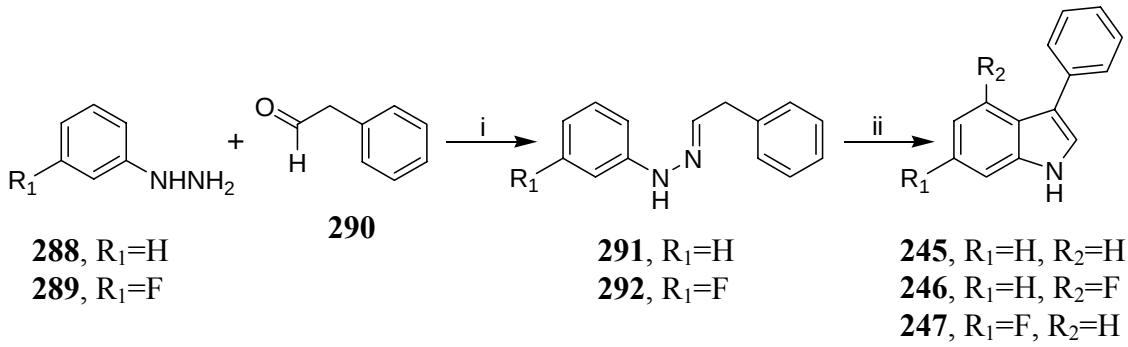


**288**, $R_1$=H
**289**, $R_1$=F

**290**

**291**, $R_1$=H
**292**, $R_1$=F

**245**, $R_1$=H, $R_2$=H
**246**, $R_1$=H, $R_2$=F
**247**, $R_1$=F, $R_2$=H

**Scheme 2.31** Synthesis of 3-phenylindoles (**245, 246, 247**). Reagents and conditions: (i) 100 ºC, 1 h (ii) $ZnCl_2$, EtOH, 100 ºC (Rodriguez et al., 2000).

## 2.3.8 Synthesis of 3-phenylbenzofuran (248)

Roshchin et al. reported (Roshchin et al., 1998) the synthesis of substituted 2-methylbenzofurans from 2-allylphenols via Pd(II)-catalyzed oxidative cylization using $Cu(OAc)_2$-LiCl as a reoxidant and DMF-$H_2O$ as a solvent. A similar method was applied to synthesize 3-phenylbenzofuran (**248**) from *o*-(1-phenylvinyl)phenol (**294**) as shown in Scheme 2.32. Compound **294** was obtained from commercially available 2′-hydroxyacetophenone (**259**), upon reaction with a Grignard reagent prepared from bromobenzene and magnesium followed by elimination of $H_2O$ by iodine (Brady and Giang, 1985). The resultant *o*-(1-phenylvinyl)phenol (**294**) was converted to 3-

phenylbenzofuran (**248**), albeit in a rather poor yield (10%), after Pd(II)-catalyzed oxidative cyclization of **294** using $Cu(OAc)_2$-LiCl and DMF-$H_2O$ system as shown in Scheme 2.32.

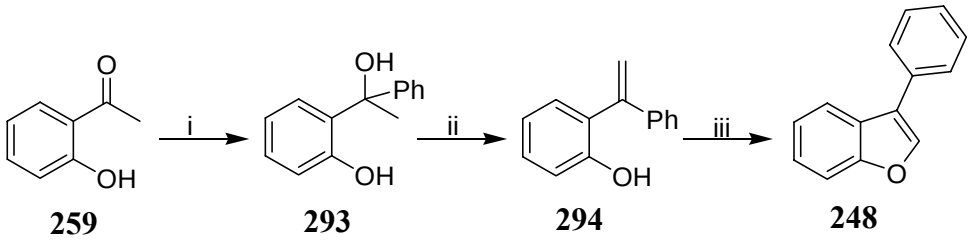


**Scheme 2.32** Synthesis of 3-phenylbenzofuran (**248**). Reagents and conditions: (i) Ph-Br, Mg, THF, 80 ºC, 82%; (ii) $I_2$, benzene, 90 ºC, 93%; (Brady and Giang, 1985) (iii) $Cu(OAc)_2.H_2O$, LiCl, $PdCl_2$, DMF/$H_2O$, 100 ºC, 10%.

## 2.4 Antifungal activity of potential brassinin detoxification inhibitors against *Sclerotinia sclerotiorum*

The antifungal activity of potential brassinin detoxification inhibitors was determined using mycelial growth antifungal assay, as described in the experimental section. The percentage of growth inhibition of *S. sclerotiorum* due to each potential inhibitor **236**, **237**, **238**, **239**, **240**, **241**, **242**, **243**, **244**, **245**, **246**, **247**, **248**, **249**, and **250** is summarized in Table 2.5. As shown in Table 2.1 and 2.5, dithiocarbamates **236**, **237**, **238**, and **239** showed lower antifungal activity against *S. sclerotiorum* than the naturally occurring dithiocarbamate brassinin (**9**). Dithiocarbamates **240** and **241** showed similar antifungal activity against *S. sclerotiorum* as brassinin (**9**). Similar to brassinin (**9**), dithiocarbamates **240** and **241** caused complete inhibition at 0.3 mM. By contrast, dithiocarbamates **236**, **237**, and **238** did not show inhibition even at the highest concentration (0.5 mM). However, at 0.5 mM, dithiocarbamates **237**, **238**, and **236** caused 89%, 65% and 45% growth inhibition of *S. sclerotiorum,* respectively. The antifungal activity of dithiocarbamate **239** could not be determined as compound **239** (at 0.1 mM) was not soluble in aqueous media. The ester containing pyrazolo[1,5-

a]pyridine nucleus, **242**, displayed very little antifungal activity (*ca.* 20% inhibition) and the amide containing quinoline nucleus, **243**, displayed no antifungal activity. 5-Fluorocamalexin (**244**) was found to be less antifungal against *S. sclerotiorum* than naturally occurring camalexin (**31**). For example, camalexin (**31**) caused complete inhibition at 0.3 and 0.1 mM whereas 5-fluorocamalexin (**244**) caused 85% and 70% inhibition respectively at the similar concentrations. The antifungal activity of 3-phenylbenzofuran (**248**) and 5-fluorocamalexin (**244**) were similar. Among all the potential brassinin detoxification inhibitors, 3-phenylindoles **245**, **246**, and **247** were found to be the most antifungal against *S. sclerotiorum*, even stronger than the commercial fungicide thiabendazole (**250**). While 3-phenylindoles completely inhibited fungal growth at 0.08 mM concentration, thiabendazole (**250**) caused about 90% growth inhibition at 0.5 mM concentration. Due to the lower solubility of 2-phenylindole (**249**) in aqueous solution, the antifungal activity of **249** could not be determined.

**Table 2.5** Percentage of growth inhibition[a] of *Sclerotinia sclerotiorum* incubated with potential brassinin detoxification inhibitors (**236**, **237**, **238**, **239**, **240**, **241**, **242**, **243**, **244**, **245**, **246**, **247**, **248**, **249**, and **250**) (48 h, constant light).

| **Compound assayed against *S. sclerotiorum*** | **Concentration (mM)** | **Inhibition ± SD (%)[a]** |
|---|---|---|
| Brassinin (**9**) | 0.50 | 100 ± 0 |
| | 0.30 | 100 ± 0 |
| | 0.10 | 37 ± 8 |
| Camalexin (**31**) | 0.30 | 100 ± 0 |
| | 0.10 | 100 ± 0 |
| | 0.05 | 81 ± 6 |
| Methyl (benzofuran-3-yl)methyldithiocarbamate (**236**) | 0.50 | 45 ± 6 |
| | 0.30 | 23 ± 4 |
| | 0.10 | No inhibition |
| Methyl (thianaphthen-3-yl)methyldithiocarbamate (**237**) | 0.50 | 89 ± 4 |
| | 0.30 | 63 ± 3 |
| | 0.10 | 10 ± 5 |

| *Compound assayed against* **S. sclerotiorum** | *Concentration (mM)* | *Inhibition ± SD (%)*[a] |
|---|---|---|
| Methyl (7-azaindol-3-yl)methyldithiocarbamate (**238**) | 0.50 | 65 ± 5 |
| | 0.30 | 28 ± 4 |
| | 0.10 | No inhibition |
| Methyl (5-methoxypyrazolo[1,5-a]pyridin-3-yl)methyldithiocarbamate (**239**) | 0.10 | Not soluble |
| Methyl (indol-2-yl)methyldithiocarbamate (**240**) | 0.50 | 100 ± 0 |
| | 0.30 | 100 ± 0 |
| | 0.10 | 48 ± 2 |
| Methyl (benzofuran-2-yl)methyldithiocarbamate (**241**) | 0.50 | 100 ± 0 |
| | 0.30 | 100 ± 0 |
| | 0.10 | 32 ± 8 |
| Methyl-5-methoxypyrazolo[1,5-a]pyridine-3-carboxylate (**242**) | 0.50 | 20 ± 3 |
| | 0.30 | No inhibition |
| | 0.10 | No inhibition |
| 3-(*N*-acetylamino)quinoline (**243**) | 0.50 | No inhibition |
| | 0.30 | No inhibition |
| | 0.10 | No inhibition |
| 5-Fluorocamalexin (**244**) | 0.30 | 85 ± 3 |
| | 0.10 | 70 ± 4 |
| | 0.05 | 61 ± 2 |
| 3-Phenylindole (**245**) | 0.08 | 100 ± 0 |
| | 0.05 | 93 ± 1 |
| | 0.01 | 78 ± 4 |
| 4-Fluoro-3-phenylindole (**246**) | 0.08 | 100 ± 0 |
| | 0.05 | 100 ± 0 |
| | 0.01 | 47 ± 3 |
| 6-Fluoro-3-phenylindole (**247**) | 0.08 | 93 ± 1 |
| | 0.05 | 87 ± 6 |
| | 0.01 | 65 ± 5 |
| 3-Phenylbenzofuran (**248**) | 0.50 | 80 ± 1 |
| | 0.30 | 64 ± 3 |
| | 0.10 | 32 ± 5 |
| 2-Phenylindole (**249**) | 0.10 | Not soluble |
| Thiabendazole (**250**) | 0.50 | 93 ± 0 |
| | 0.30 | 93 ± 0 |
| | 0.10 | 86 ± 1 |

[a] The percentage of inhibition was calculated using the formula: % inhibition = 100 – [(growth on amended/growth in control) × 100].

## 2.5 Metabolism of potential inhibitors of brassinin detoxification in *Sclerotinia sclerotiorum*

Before determining the inhibitory activity of designed compounds towards brassinin detoxification, it was important to investigate the metabolism of these potential inhibitors (**236**, **237**, **238**, **239**, **240**, **241**, **242**, **243**, **244**, **245**, **246**, **247**, **248**, **249**, and **250**) in fungal cultures of *S. sclerotiorum*. Time course experiments were conducted with each of the designed compounds. To be a good candidate to inhibit the brassinin detoxification, the inhibitor must not be metabolized by the fungus or if it is metabolized the metabolism has to be much slower than that of brassinin (**9**). The results of the time course experiments suggested that all of the designed compounds were metabolized in fungal cultures within 12 to 48 hours to undetermined products. However, in order to design more active inhibitors of brassinin detoxification, the metabolic products of selected compounds were isolated and their chemical structures were elucidated. In this section, the metabolism of methyl (indol-2-yl)methyldithiocarbamate (**240**), methyl (thianaphthen-3-yl)methyldithiocarbamate (**237**), and 3-phenylindole (**245**) in *S. sclerotiorum* will be discussed.

### 2.5.1 Methyl (indol-2-yl)methyldithiocarbamate (240)

Dithiocarbamate **240** was administered to fungal cultures of *S. sclerotiorum*, the cultures were incubated and analyzed over a period of several days to determine the best time to isolate potential metabolic products. HPLC analysis of the broth extracts of fungal cultures indicated that dithicarbamate **240** was completely metabolized in *ca*. 48 h to a major product with HPLC $t_R$ = 9.4 min. To establish the structure of this metabolite (**295**), larger scale cultures of *S. sclerotiorum* were incubated with dithiocarbamate **240**, were extracted, and the extract was fractionated by reverse phase silica gel chromatography. The fractions containing the metabolite with $t_R$ = 9.4 min (**295**) were combined and further separated by prep. TLC. The structure of this

metabolite (**295**) was determined by analyses of spectroscopic data as follows. The HRMS-ESI spectral data indicated a molecular formula of $C_{17}H_{22}N_2O_6S_2$. The FTIR spectral data displayed a broad absorption band at ca. 3300 $cm^{-1}$ indicative of the presence of hydroxyl groups. The $^1H$ NMR spectrum showed two broad singlets at $\delta_H$ 9.58 and 9.25 ($D_2O$ exchangeable), and resonances for an indole system with substitutions at C-2 and C-3 ($\delta_H$ 7.65, d, *J* = 8 Hz, 1H, 7.37, d, *J* = 8 Hz, 1H, 7.17, dd, *J* = 8, 8 Hz, 1H, 7.08, dd, *J* = 8, 8 Hz, 1H), signals for an intact side chain ($\delta_H$ 5.34, dd, *J* = 14.5, 6.5 Hz, 1H, 4.84, dd, *J* = 14.5, 6.5 Hz, 1H, 2.62, $SCH_3$), and resonances for a hexose unit. As in the biotransformation of phytoalexins, the identity of the hexose unit was determined to be β-D-glucopyranose from homonuclear ($^1H$-$^1H$) decoupling experiments. The HMBC correlations of the anomeric proton with C-2 and C-7a of indole suggested that the β-D-glucopyranose unit was located at *N*-1 position of indole ring. A downfield shift for the C-3 carbon ($\delta_C$ 102.5 in **240** to 125.7 in **295**) in the $^{13}C$ NMR spectrum suggested that a hydroxyl group was also attached to the C-3 carbon of the indole ring. Thus the structure of this metabolic product was assigned as methyl (1-β-D-glucopyranosyl-3-hydroxylindol-2-yl)methyldithiocarbamate (**295**) (Scheme 2.33).

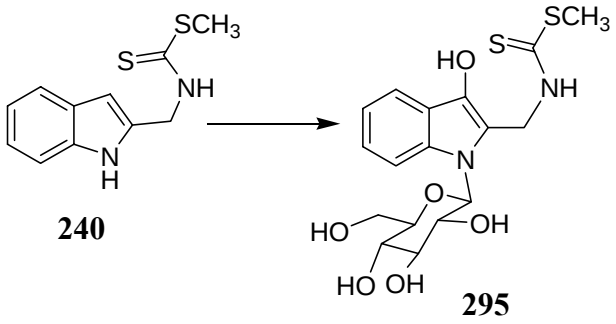


**Scheme 2.33** Biotransformation of methyl (indol-2-yl)methyldithiocarbamate (**240**) in *Sclerotinia sclerotiorum*.

### 2.5.2 Methyl (thianaphthen-3-yl)methyldithiocarbamate (237)

Dithiocarbamate **237** was administered to cultures of *S. sclerotiorum* and culture samples were withdrawn and analyzed over a period of time. The HPLC chromatograms of EtOAc extracts of fungal cultures indicated that dithiocarbamate **237** was completely metabolized in *ca*. 6 h to two main products with $t_R$ = 9.6 and 11.0 min. While the less polar metabolite (**296**, $t_R$ = 11.0 min) was detected in culture after 6 hours, the more polar metabolite (**297**, $t_R$ = 9.6 min) was detected after 12 hours and increased up to 48 hours. Subsequently, larger scale cultures of *S. sclerotiorum* were incubated with the dithiocarbamate **237** for 6 hours to isolate the metabolite with $t_R$ = 11.0 min (**296**) and for 48 hours to isolate the metabolite with $t_R$ = 9.6 min (**297**). After isolation and purification, the structure of each compound was determined by standard spectroscopic methods, including $^1$H and $^{13}$C NMR spectroscopy, HMQC, HMBC, and HRMS-ESI. The molecular formula of the less polar metabolite (**296**, $t_R$ = 11.0 min) (obtained by HRMS-ESI) indicated the presence of an additional oxygen atom relative to that of dithiocarbamate **237** ($C_{11}H_{11}NOS_3$ vs. $C_{11}H_{11}NS_3$). The $^1$H NMR spectrum of **296**, obtained in $CD_3OD$, indicated the presence of five aromatic hydrogens characteristic of a 3-substituted thianaphthene ring system, two additional hydrogens (H-1′, AB quartet) and a singlet for a $–SCH_3$ group. These spectroscopic data suggested that the additional oxygen atom of metabolite **296** was attached to a sulfur atom as a sulfoxide either at the thainaphthene ring or at the dithiocarbamate group. That the sulfoxide group was present in the thianaphthene ring rather than in the dithiocarbamate group was suggested by the up field chemical shift for H-2 hydrogen ($\delta_H$ 7.54 in **237** to 7.01 in **296**) in the $^1$H NMR. Hence, on the basis of these spectral data, the structure of the less polar metabolite of methyl (thianaphthen-3-yl)methyldithiocarbamate (**237**) was assigned as methyl (thianaphthen-3-yl-1-*S*-

oxide)methyldithiocarbamate (**296**) (Scheme 2.34). Furthermore, the structure of this metabolite **296** was confirmed by synthesis, as described below.

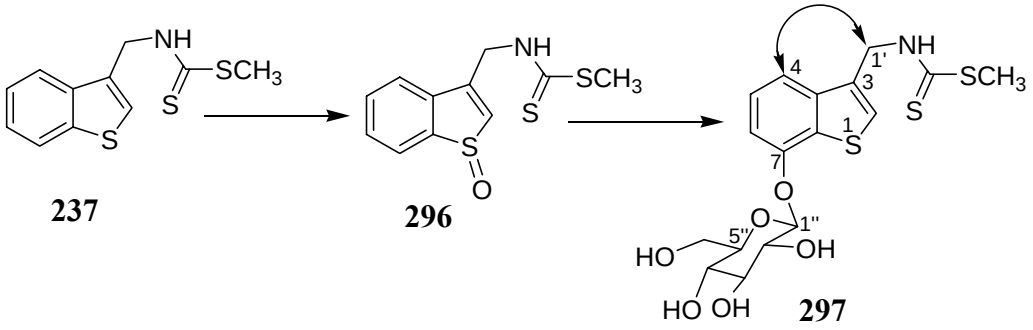


**Scheme 2.34** Biotransformation of methyl (thianaphthen-3-yl)methyldithiocarbamate (**237**) in *Sclerotinia sclerotiorum* and selected NOE of compound **297**.

The molecular formula of the polar metabolite (**297**, $t_R$ = 9.6 min, $C_{17}H_{21}NO_6S_3$) obtained by HRMS-ESI indicated the presence of a hexose unit, which was corroborated by NMR data. The identity of the hexose unit was determined as β-D-glucopyranose from homonuclear ($^1$H-$^1$H) decoupling experiments. In addition, the $^1$H NMR spectrum suggested that the β-D-glucopyranose unit was located either at C-4 or C-7. That the β-D-glucopyranose unit was attached to C-7 rather than C-4 was finally deduced from NOE experiments (upon addition of pyridine-$d_5$ to separate the signals due to H-1″ and H-1′), as follows. Irradiation of H-1′ at $\delta_H$ 5.15 caused an enhancement of the signal due to H-4 ($\delta_H$ 7.53) and vice-versa (Scheme 2.34). Hence, on the basis of these spectral data, the structure of the polar metabolite of dithiocarbamate **237** was assigned as methyl (7-oxy-*O*-β-D-glucopyranosylthianaphthen-3-yl)methyldithiocarbamate (**297**) (Scheme 2.34). To establish the sequence of biotransformation steps of dithiocarbamate **237**, compound **296** was administered to cultures of *S. sclerotiorum*, culture samples were withdrawn at different times and analyzed by HPLC. Interestingly, it was found that compound **296**

was metabolized to **297** at a much slower rate than other dithiocarbamates (e.g. brassinin (**9**) was metabolized completely in ca. 12 h whereas **296** was metabolized in ca. 3 d). This result indicated that dithiocarbamate **237** was metabolized to methyl (7-oxy-*O*-β-D-glucopyranosylthianaphthen-3-yl)methyldithiocarbamate (**297**) via methyl (thianaphthen-3-yl-1-*S*-oxide)methyldithiocarbamate (**296**) (Scheme 2.34).

To confirm the structure of the biotransformation product of methyl (thianaphthen-3-yl)methyldithiocarbamate (**237**) and to obtain sufficient amounts for bioassay and biotransformation the chemical synthesis of methyl (thianaphthen-3-yl-1-*S*-oxide)methyldithiocarbamate (**296**) was carried out. Thus, amine **274** was oxidized to the corresponding sulfoxide **298** using $H_2O_2$ in TFA-$CH_2Cl_2$ (1:2), which upon treatment with carbon disulfide in the presence of pyridine and triethylamine followed by iodomethane afforded multiple undetermined products; one of these products was identified as methyl (thianaphthen-3-yl-1-*S*-oxide)methyldithiocarbamate (**296**) (overall yield 5%, based on **274**) (Scheme 2.35).

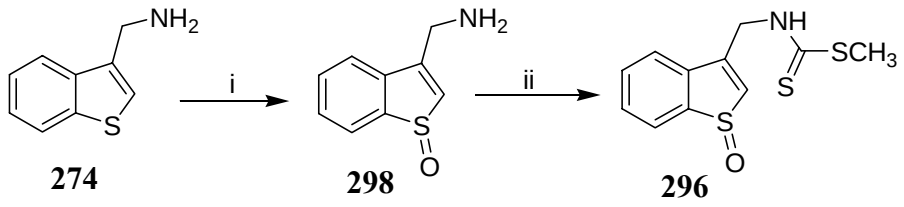


**Scheme 2.35** Chemical synthesis of methyl (thianaphthen-3-yl-1-*S*-oxide)methyldithiocarbamate (**296**). Reagents: (i) $H_2O_2$, TFA/$CH_2Cl_2$ (1:2); (ii) Py, $Et_3N$, $CS_2$, $CH_3I$, 5%.

### 2.5.3 Metabolism of 3-phenylindole (245)

Similar to the metabolism of dithiocarbamates **240** and **237**, HPLC analysis of the EtOAc extracts of fungal cultures incubated with 3-phenylindole (**245**) indicated it to be completely metabolized to an unknown compound (HPLC $t_R$ = 10.9 min) in about 24 h. As described in the above examples, to establish the structure of this metabolic

product, larger scale cultures of *S. sclerotiorum* incubated with 3-phenylindole (**245**) for 24 h, were filtered, extracted, and the EtOAc extract fractionated by reverse phase column chromatography followed by prep. TLC to yield the unknown metabolite (**299**). The structure of this metabolite **299** was determined by analyses of standard spectroscopic methods including $^{1}H$ and $^{13}C$ NMR spectroscopy, a variety of 2D-NMR techniques and HRMS. Comparison of its $^{1}H$ NMR spectrum with that of 3-phenylindole (**245**) indicated the presence of an intact 3-phenylindole. In addition, several multiplets at $\delta_H$ 3.51–3.98 suggested the presence of a carbohydrate moiety. The molecular formula of **299** ($C_{20}H_{21}NO_5$) determined by $^{13}C$ NMR and HRMS-ESI spectral data also corroborated the presence of a carbohydrate residue. As described above for metabolites **295** and **297**, the identity of the carbohydrate moiety was determined to be a β-glucopyranose substituent. HMBC spectral data confirmed that the β-glucopyranose unit was located at *N*-1 (correlations of the anomeric proton H-1 with C-2 and C-7a of indole) and thus the structure of **299** was assigned as 1-β-D-glucopyranosyl-3-phenylindole (**299**) (Scheme 2.36).

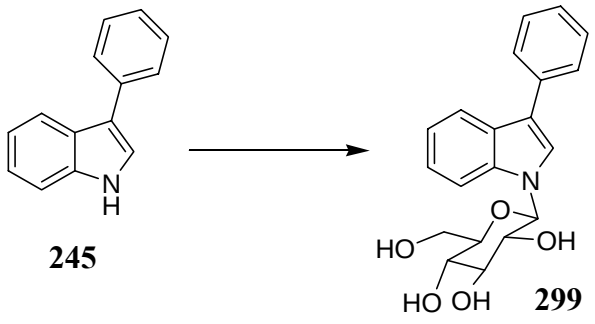


**Scheme 2.36** Biotransformation of 3-phenylindole (**245**) in *Sclerotinia sclerotiorum*.

### 2.5.4 Summary

Results of the biotransformations of potential inhibitors of brassinin detoxification suggested that *S. sclerotiorum* utilizes oxidases and/or glucosyltransferases to metabolize potential inhibitors, as in the case of strongly antifungal phytoalexins. The antifungal activity of the biotransformed products of these potential inhibitors indicated that all these transformations were detoxification processes.

## 2.6 Co-metabolism of brassinin, camalexins and potential brassinin detoxification inhibitors in *Sclerotinia sclerotiorum*

Since brassinin (**9**) was shown to be detoxified to 1-β-D-glucopyranosylbrassinin (**66**) in fungal cultures of *S. sclerotiorum*, it was important to screen the potential inhibitors to determine their effect on the rate of brassinin (**9**) transformation. In a typical experiment, brassinin and the potential inhibitor were co-incubated in mycelial cultures of *S. sclerotiorum*, samples were withdrawn at different time intervals, extracted with ethyl acetate, and the ethyl acetate extracts were analyzed by HPLC. To obtain consistent results, all cultures used in the screening experiments were inoculated with mycelial plugs. Inoculation using sclerotia resulted different amounts of mycelia in different flasks due to the size variation of sclerotia. The concentration of brassinin (**9**) and potential inhibitors to be used in the screening experiments were determined on the basis of the antifungal bioassay results (reported in sections 2.1.2 and 2.4). Concentrations that were moderately toxic or non-toxic to fungal growth were selected for screening experiments. That is, brassinin was added at 0.05 mM concentration while potential inhibitors were added at two different concentrations (0.05 and 0.1 mM).

Initial experiments were conducted to determine the rate of metabolism of brassinin in mycelial cultures of *S. sclerotiorum* at two different concentrations (0.05 and 0.1 mM). Mycelial plugs of 4-day-old mycelial plates (6 mm diameter, 3 pieces per 50 ml) of *S. sclerotiorum* were inoculated in minimal media for four days; brassinin dissolved in DMSO was then added to fungal cultures (Final concentration 0.05 and 0.1 mM). Samples were withdrawn immediately after addition of brassinin (**9**) and at 2, 5, 8, 12 and 24 h. It was found that brassinin at 0.05 mM concentration was almost completely metabolized in fungal cultures of *S. sclerotiorum* in 8 h whereas at 0.1 mM concentration the complete metabolism of brassinin (**9**) to glucoside **66** occurred in 12 h (Figure 2.10). In both cases (0.05 and 0.1 mM) the highest amount of the biotransformation product glucoside **66** was obtained after 12 h of incubation (Figure 2.10).

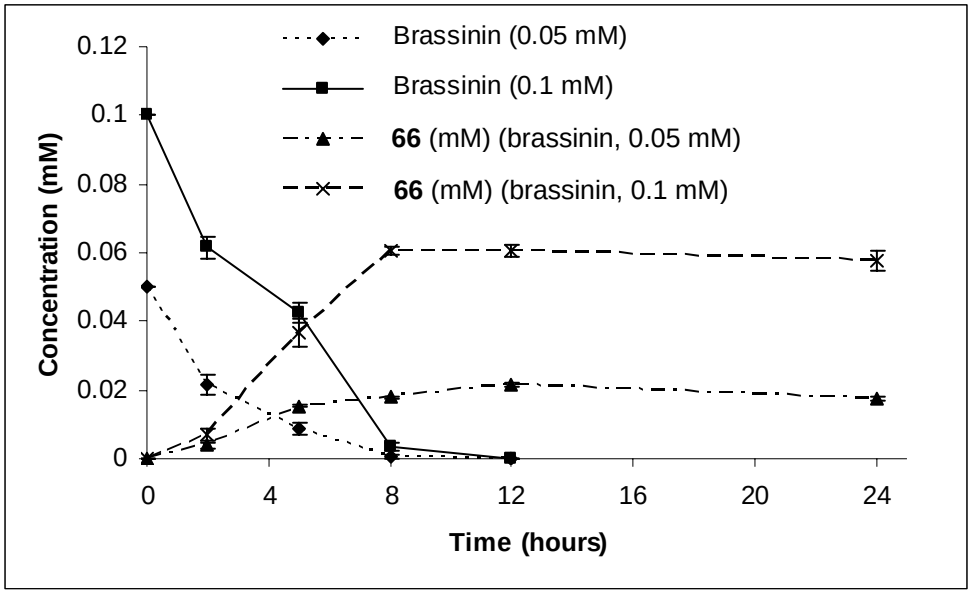


**Figure 2.10** Curves for transformation of brassinin (**9**, 0.05 and 0.1 mM) to 1-β-D-glucopyranosylbrassinin (**66**) in culture of *Sclerotinia sclerotiorum*.

After establishing the rate of metabolism of brassinin at different concentrations in cultures of *S. sclerotiorum*, each potential inhibitor was screened to find out the inhibitory activity. First, three pieces of mycelial plugs (4-day old, 6 mm) were inoculated in 50 ml of minimal media for 4 days; potential inhibitors were added at two different concentrations (0.05 and 0.1 mM) and cultures were incubated for 10 min (to allow absorption/transport of compounds into cells) before adding brassinin (**9**, 0.05 mM). Control cultures of *S. sclerotiorum* containing only brassinin (**9**, 0.05 and 0.1 mM) or each potential inhibitor (0.1 mM) were incubated separately. The stability of brassinin and all potential inhibitors was determined by incubation in uninoculated minimal media under similar conditions. Samples were withdrawn from cultures immediately after addition of brassinin and at different time intervals and extracted with ethyl acetate. The organic extract was analyzed using HPLC (brassinin $t_R = 18.8 \pm 0.5$ min) to determine the concentration of brassinin (**9**) remaining in cultures at different times. Brassinin (**9**) and all other potential inhibitors were found to be stable in minimal media for at least 8 days. The rate of disappearance of brassinin (**9**) in the presence of the potential inhibitor was compared with that in the controls (fungal cultures containing only brassinin at 0.05 and 0.1 mM, Figure 2.10). Several of the potential inhibitors were able to affect the rate of metabolism of brassinin (**9**). For example, in the first set of compounds (that were designed based on structure of brassinin (**9**), Figure 2.8), methyl (benzofuran-3-yl)methyldithiocarbamate (**236**), methyl (indol-2-yl)methyldithiocarbamate (**240**), and methyl (benzofuran-2-yl)methyldithiocarbamate (**241**) (Figure 2.11) slowed down the rate of metabolism of brassinin (**9**). In the second set of compounds (that were designed based on the structure of camalexin (**31**), Figure 2.9), 3-phenylindoles (**245**, **247**) and 5-fluorocamalexin (**244**) (Figure 2.11) were able to slow down the rate of metabolism of brassinin (**9**). The remaining compounds (**237**, **238**, **239**, **242**, **243**, **249**, and **250**) did not show a detectable effect on the rate of brassinin metabolism. The compounds that

did not affect the rate of metabolism of brassinin (**9**) in cultures of *S. sclerotiorum* are shown in Figure 2.12.

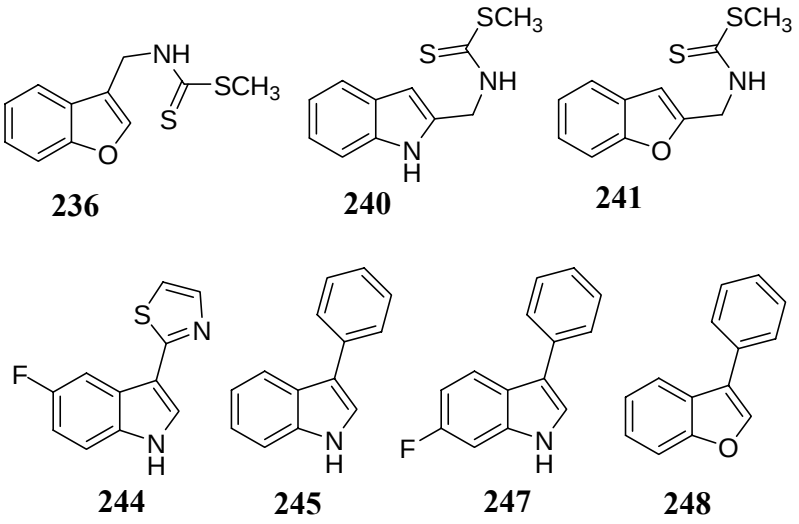


**Figure 2.11** Chemical structure of compounds that slowed down the rate of metabolism of brassinin (**9**) in mycelial cultures of *Sclerotinia sclerotiorum*.

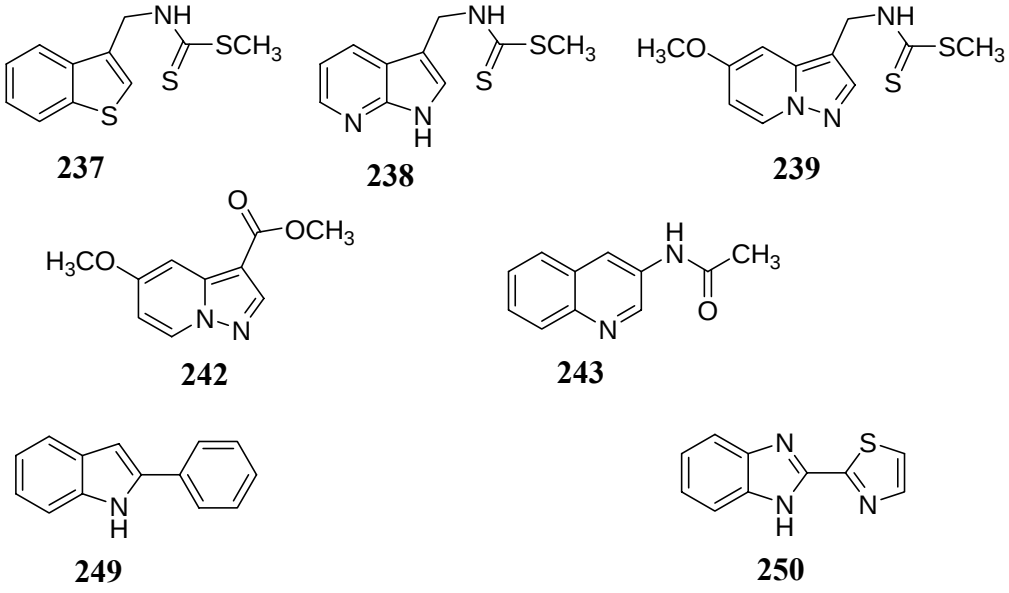


**Figure 2.12** Chemical structure of compounds that did not affect the rate of metabolism of brassinin (**9**) in mycelial cultures of *Sclerotinia sclerotiorum*.

The effects of dithiocarbamates **236**, **240**, and **241** on rate of metabolism of brassinin (**9**) in mycelial cultures of *S. sclerotiorum* are shown in Figs. 2.13-2.15. As shown in Fig. 2.13, complete metabolism of brassinin (**9**, 0.05 mM) took place in *ca.* 16 h in the presence of methyl (benzofuran-3-yl)methyldithiocarbamate (**236**, 0.1 mM) whereas in the absence of compound **236**, brassinin (**9**) was completely metabolized in 8 h at 0.05 mM concentration and in 12 h at 0.1 mM concentration. In the presence of **236** at 0.05 mM concentration, brassinin was also found to be metabolized in 12 h but at a much slower rate (Fig. 2.13). This can be rationalized as dithiocarbamate **236** was itself metabolized to an undetermined *O*-glucosylated compound (detected by LC-MS) in the cultures of *S. sclerotiorum* in *ca*. 12 h. It was found that brassinin (**9**) was completely metabolized in the cultures only after the complete metabolism of dithiocarbamate **236**. A similar effect was observed when brassinin (**9**) was co-incubated with methyl (benzofuran-2-yl)methyldithiocarbamate (**241**). As shown in Fig. 2.14, the detoxification of brassinin (**9**) in *S. sclerotiorum* took place in 12 h in the presence of **241** (0.05 mM) but at a slower rate than that of control cultures (fungal cultures containing only brassinin). Upon doubling the concentration of **241** (0.1 mM) the detoxification of brassinin (**9**) was found to be complete in 24 h (Fig. 2.14). Similar to dithiocarbamate **236**, compound **241** was also completely metabolized in the cultures of *S. sclerotiorum* to undetermined *O*-glucosylated compounds (detected by LC-MS) in 12 h and brassinin (**9**) was completely metabolized in the cultures only after the complete metabolism of **241**. The rate of metabolism of brassinin (**9**) in cultures when brassinin (**9**, 0.05 mM) was co-incubated with methyl (indol-2-yl)methyldithiocarbamate (**240**) at 0.05 mM was not affected but a significant effect was observed when **9** was co-incubated with 0.1 mM of **240** (Fig. 2.15). Brassinin (**9**, 0.05 mM) was found to be completely metabolized in *ca*. 16 h in the presence of 0.1 mM of **240**.

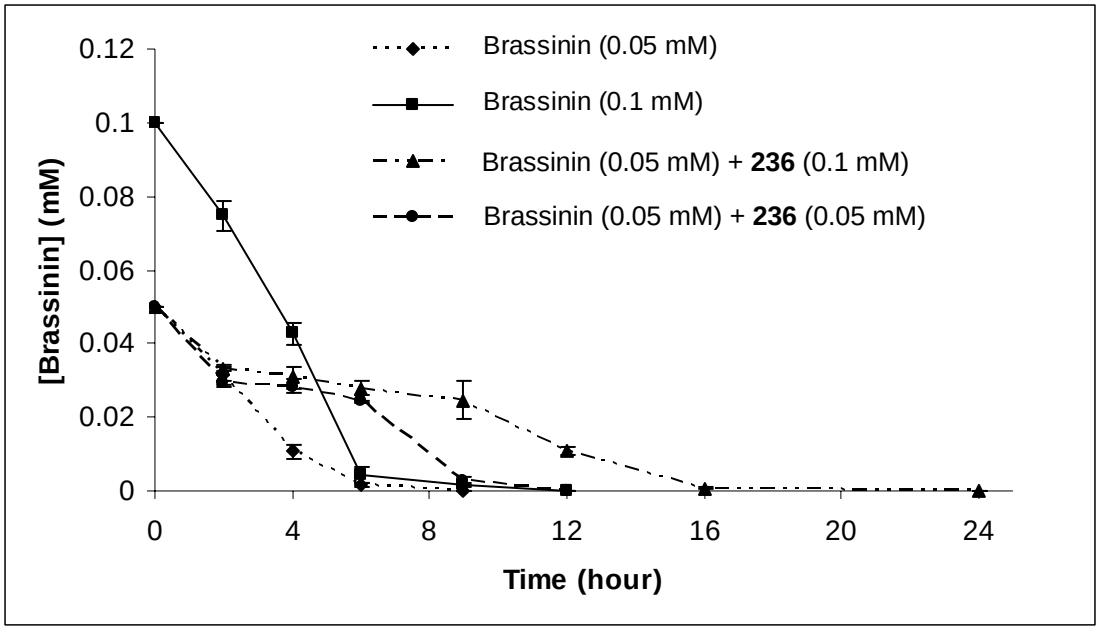


**Figure 2.13** Transformation of brassinin (**9**, 0.05 mM) in the presence of methyl (benzofuran-3-yl)methyldithiocarbamate (**236**, 0.05 and 0.1 mM) in cultures of *Sclerotinia sclerotiorum*.

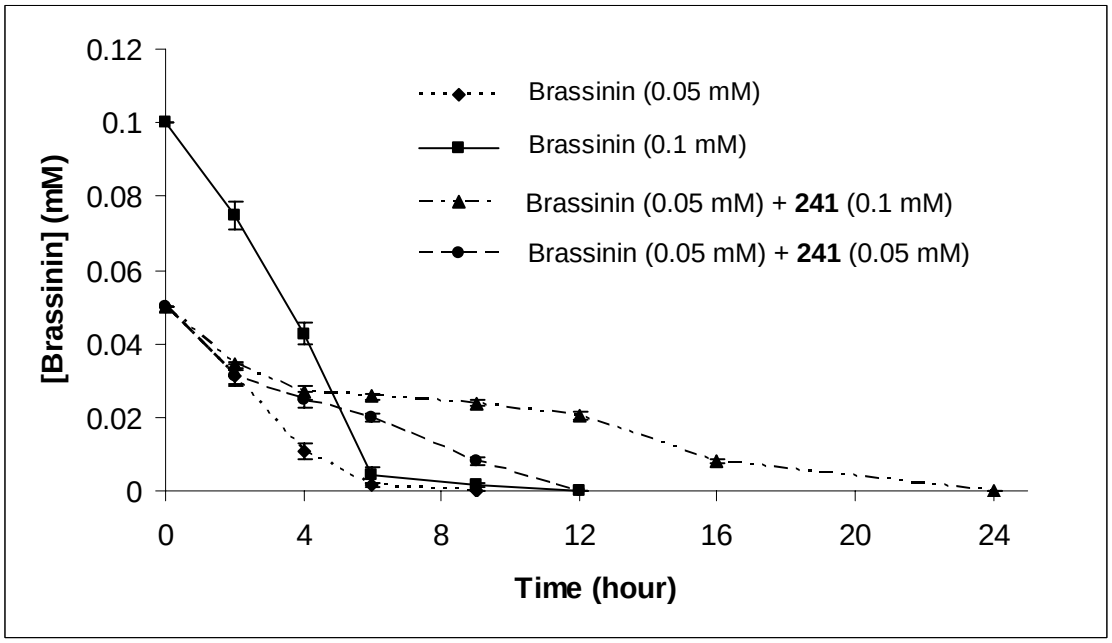


**Figure 2.14** Transformation of brassinin (**9**, 0.05 mM) in the presence of methyl (benzofuran-2-yl)methyldithiocarbamate (**241**, 0.05 and 0.1 mM) in cultures of *Sclerotinia sclerotiorum*.

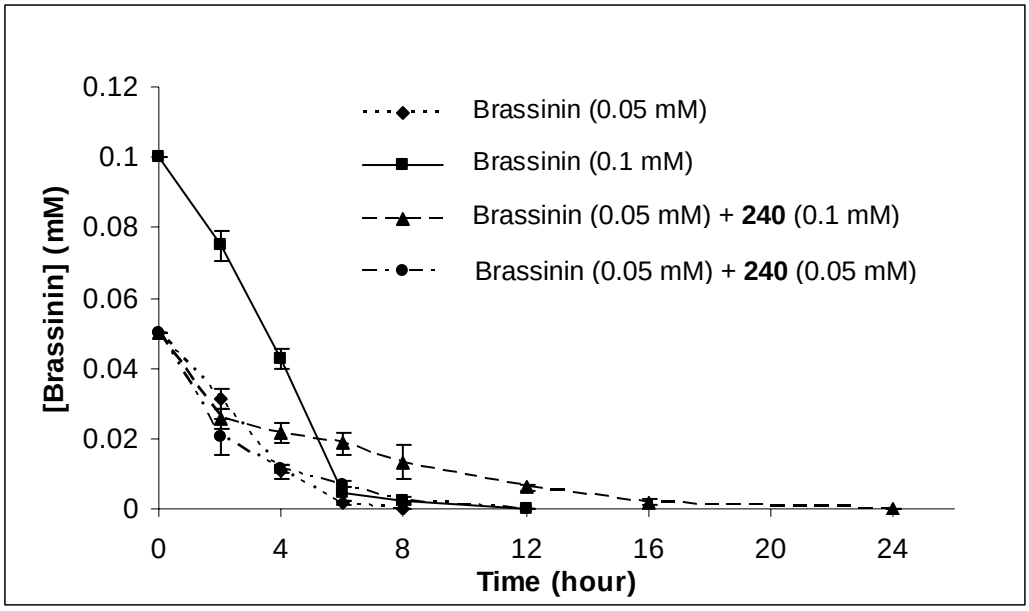


**Figure 2.15** Transformation of brassinin (**9**, 0.05 mM) in the presence of methyl (indol-2-yl)methyldithiocarbamate (**240**, 0.05 and 0.1 mM) in cultures of *Sclerotinia sclerotiorum*.

Since 6-fluorocamalexin (**75**) can slow down the rate of metabolism of brassinin (**9**) in mycelial cultures of *S. sclerotiorum* (Pedras et al., 2004c), the phytoalexin camalexin (**31**) and its derivative 5-fluorocamalexin (**244**) were screened in cultures to determine their inhibitory activity on brassinin detoxification. When camalexin (**31**, 0.1 mM) was co-incubated with brassinin (**9**, 0.05 mM), brassinin was completely metabolized in about 24 h. On the other hand, 5-fluorocamalexin (**244**) had a stronger effect on the brassinin metabolism than camalexin (**31**). For example, 0.05 mM of 5-fluorocamalexin (**244**) slowed down the brassinin metabolism to 24 h and 0.1 mM of 5-fluorocamalexin (**244**) slowed down to 48 h. The strongest effect was observed when brassinin (**9**) was co-incubated either with 3-phenylindole (**245**) or with 6-fluoro-3-phenylindole (**247**). As shown in Figs. 2.16 and 2.17, both 3-phenylindoles (**245**, **247**) were able to slow down the rate of metabolism of brassinin. As long as 3-phenylindoles (**245**, **247**) were present in the cultures, brassinin (**9**) was not metabolized. It was found that both **245**, and **247** were completely metabolized in

cultures of *S. sclerotiorum* to **299** and to an undetermined compound, respectively, in about 24 h. However, in the presence of 3-phenylindole (**245**, 0.05 mM) or 6-fluoro-3-phenylindole (**247**, 0.05 mM), brassinin (**9**, 0.05 mM) was completely metabolized in about 24 h and upon doubling the concentration of **245**, or **247** (0.1 mM) complete metabolism of brassinin occurred in 72 h.

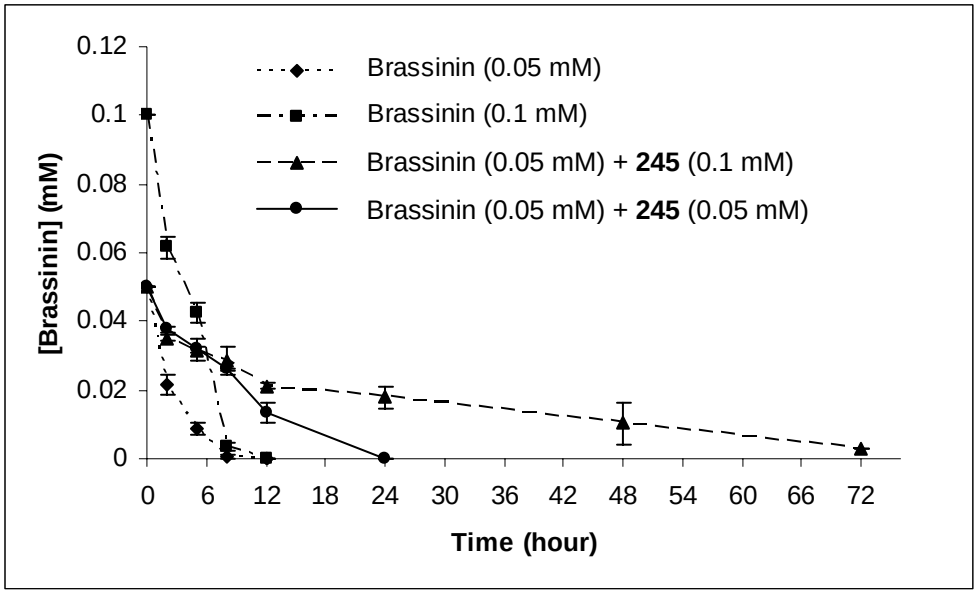


**Figure 2.16** Transformation of brassinin (**9**, 0.05 mM) in the presence of 3-phenylindole (**245**, 0.05 and 0.1 mM) in cultures of *Sclerotinia sclerotiorum*.

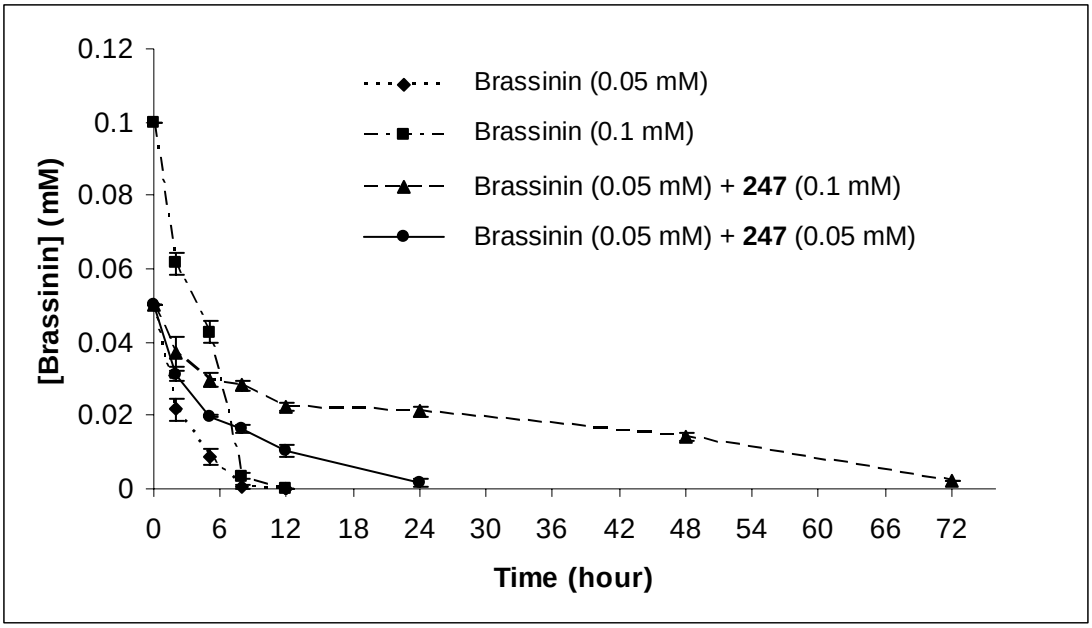


**Figure 2.17** Transformation of brassinin (**9**, 0.05 mM) in the presence of 6-fluoro-3-phenylindole (**247**, 0.05 and 0.1 mM) in cultures of *Sclerotinia sclerotiorum*.

## 2.7 Screening of potential brassinin detoxification inhibitors using crude cell-free extracts

Brassinin (**9**) is detoxified to non toxic 1-β-D-glucopyranosylbrassinin (**66**) by the stem rot fungus *S. sclerotiorum* through enzymatic glucosylation. This transformation of brassinin (**9**) to glucoside **66** suggested the involvement of a putative brassinin glucosyltransferase (BGT) in the detoxification process (Pedras et al., 2004c). Isolation and purification of BGT has not been reported to date. However, considering the importance of brassinin (**9**) in plant chemical defenses, one of my research goals was to design inhibitors of BGT and to screen them using cell-free extracts containing BGT. Results obtained from the initial screening of potential inhibitors of brassinin detoxification using fungal cultures (Section 2.6) indicated that compounds **236**, **240**, **241**, **244**, **245**, and **247** slowed down the rate of metabolism of brassinin (**9**). To determine whether the decrease in the rate of brassinin metabolism was due to growth

inhibition of *S. sclerotiorum* (because of toxicity of added compounds) or due to inhibition of BGT responsible for brassinin detoxification, screening using cell-free extracts was undertaken. Therefore, all the potential inhibitors (Fig. 2.8 and 2.9) were screened using cell-free extracts in order to find out their inhibitory activity against BGT. Pedras' group (Pedras et al., 2004c) reported a method to prepare crude cell-free extracts from mycelia of *S. sclerotiorum* for glucosylation of brassinin (**9**). It was also reported that the brassinin glucosyltransferase (BGT) was an inducible enzyme. That is, BGT activity was detected in crude cell-free extracts only when *S. sclerotiorum* was grown in the presence of compounds related to brassinin (**9**) such as camalexin (**31**), methyl tryptamine dithiocarbamate, methyl-1-methyltryptamine dithiocarbamate or spirobrassinin (**27**). BGT activity was also found to be UDPG dependent. Without UDPG no BGT activity was detected in cell-free extracts prepared from induced mycelia of *S. sclerotiorum*.

Cell-free extracts were prepared by modifying the published procedure (Pedras et al., 2004c) as follows. Cultures of *S. sclerotiorum* were grown in PDB media for 7 days after which camalexin (final concentration, $5 \times 10^{-5}$ M) in DMSO was added to induce the production of BGT. After an additional 24 h, the mycelia were collected by filtration and stored at -20 ºC. Frozen mycelial cells were homogenized in ice cold Tris HCl (50 mM) buffer pH 8.0 (containing 5% glycerol, 2 mM dithiothreitol, 2 mM PMSF, and 0.01% triton X-100) at 4 ºC using a mortar and pestle. The cell-free homogenate was obtained by centrifuging the mixture at 22,000 rpm for 40 min and used to assay the enzymatic activity. The Bradford protein assay was used to quantify proteins in cell-free extracts using bovine serum albumin standard curves. The specific activity of cell-free extracts was defined as the amount (nmol) of 1-β-D-glucopyranosylbrassinin (**66**) product formed per min per mg of protein.

BGT activity was determined using brassinin (**9**) as a substrate and UDPG as a glucose donor. The 0.5 ml standard assay mixture contained 0.5 ml of cell free extract as enzyme source, 3 µl of 50 mM UDPG (final concentration 0.3 mM) solution in water, and 3 µl of 50 mM brassinin (final concentration 0.3 mM) in DMSO. After incubation of the assay mixture for 1 hour at 25 ºC, solvent extraction and HPLC analysis were used for the detection and quantification of the reaction product. In subsequent experiments the enzyme assays were carried out with different concentrations of brassinin (**9**) to determine the ideal concentration for inhibition assays. As shown in Fig. 2.18, the $V_{max}$ (concentration for saturated activity) of BGT was obtained at 0.3 mM of brassinin (**9**). Therefore, in a typical enzyme inhibition assay, 0.3 mM of brassinin (**9**) and UDPG were used as substrate and glucose donor respectively and the potential inhibitor was used at two concentrations, 0.3 and 0.6 mM.

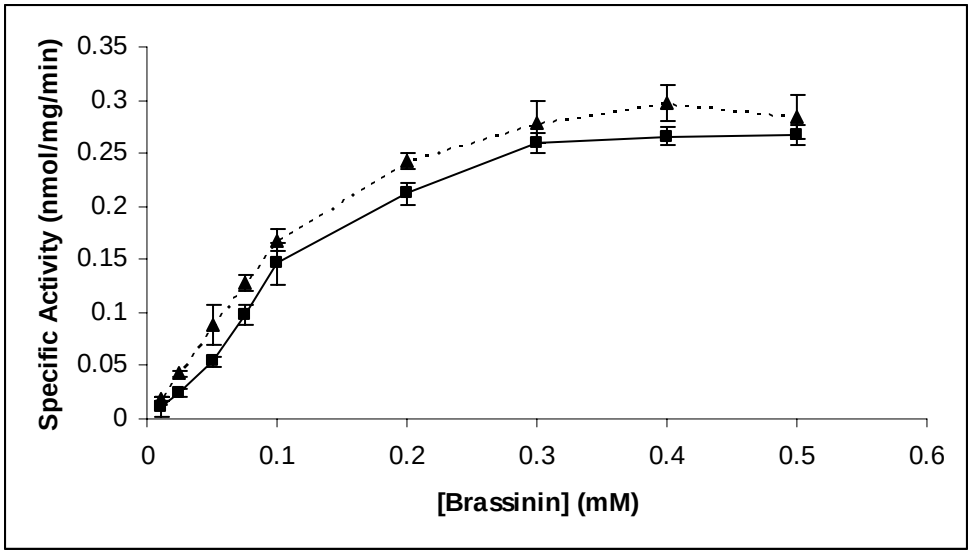


**Figure 2.18** Specific activity of brassinin glucosyltransferase (BGT) in crude cell-free extracts of *Sclerotinia Sclerotiorum* at different brassinin (**9**) concentrations (two independent experiments conducted in triplicate).

Camalexins (**31**, **75**, **244**), dithiocarbamates **236**, **237**, **238**, **239**, **240**, and **241**, 3-phenylindoles (**245**, **246**, **247**), ester **242**, amide **243**, 3-phenylbenzofuran (**248**), and 2-phenylindole (**249**) were tested as potential inhibitors of BGT as follows. First, the stability of each compound was tested under identical reaction conditions in the assay buffer. All compounds were found to be stable within 1.5 h of incubation in the assay mixture. Each potential inhibitor (final concentration 0.3 and 0.6 mM) dissolved in DMSO was added to a vial containing 2.0 ml of cell-free extracts and UDPG (final concentration 0.3 mM, dissolved in water) and the mixture was incubated at room temperature for 30 min. After that, brassinin (**9**, 0.3 mM) was added in each vial and the mixture was immediately divided into four samples in separate vials (0.5 ml each). Three samples were incubated for additional 60 min and the remaining sample was extracted immediately with ethyl acetate. After 60 min of incubation the three samples were extracted separately with ethyl acetate and the extracts were analyzed by HPLC for the detection and quantification of the reaction product 1-β-D-glucopyranosylbrassinin (**66**) to determine the enzyme specific activity (Table 2.6). Control experiments containing only brassinin (**9**, 0.3 mM) were performed similarly. The relative activity (Table 2.6) of BGT was determined by comparing the specific activity of BGT in presence of the potential inhibitor with that in control samples. The calculated relative activity suggested that the BGT activity was inhibited by the presence of some compounds. As shown in Table 2.6, the inhibition effect was much higher with 3-phenylindole (**245**) and 6-fluoro-3-phenylindole (**247**) (about 80% inhibition) and moderate (about 60% inhibition) with dithiocarbamates **236**, **240**, and **241**, 4-fluoro-3-phenylindole (**246**), 3-phenylbenzofuran (**248**), and 2-phenylindole (**249**). Camalexins (**31**, **75**, **244**) showed about 40% inhibition and methyl (7-azaindol-3-yl)methyldithiocarbamate (**238**) showed about 30% inhibition of BGT activity in cell-free extracts while very low inhibition was observed with methyl (thianaphthen-3-yl)methyldithiocarbamate (**237**) (about 20% inhibition) and almost no inhibitory

activity was observed with **239**, **242**, and **243**. Although 3-phenylindole (**245**) appears to be a strong inhibitor among all other potential inhibitors, it undergoes enzymatic transformation (with specific activity, 0.03 nmol/mg/min) slowly to 1-β-D-glucopyranosyl-3-phenylindole (**299**) in cell-free extracts. Therefore, in order to determine the type of inhibition of BGT with 3-phenylindole (**245**), the kinetics of enzyme inhibition using cell-free extracts was obtained from multiple curves of brassinin (**9**) transformation (Fig. 2.19). Each of the curves was obtained by calculating enzyme specific activities for a constant concentration of 3-phenylindole (**245**) with different concentrations of brassinin (**9**). As shown in Fig. 2.19, the pattern of the multiple curves of brassinin transformation suggested that the inhibition of BGT activity due to 3-phenylindole (**245**) is noncompetitive inhibition.

**Table 2.6** Effect of compounds on brassinin glucosyltransferase (BGT) in cell-free extracts of mycelia of *Sclerotinia sclerotiorum*.

| **Substrate + Inhibitor** | **Specific activity [a] ($\times 10^{-1}$ nmol/mg/ min) ± SD** | | **Relative activity % (brassinin = 100)** | |
|---|---|---|---|---|
| Brassinin (**9**) | 1.50 ± 0.01 | | 100 | |
| Brassinin (**9**) + camalexin (**31**) | 0.95 ± 0.02 (1 : 1) | 0.84 ± 0.03 (1 : 2) | 63 (1 : 1) | 56 (1 : 2) |
| Brassinin (**9**) + 6-fluorocamalexin (**75**) | 0.97 ± 0.01 (1 : 1) | 1.00 ± 0.02 (1 : 2) | 66 (1 : 1) | 63 (1 : 2) |
| Brassinin (**9**) + methyl (benzofuran-3-yl)methyldithiocarbamate (**236**) | 0.75 ± 0.02 (1 : 1) | 0.55 ± 0.03 (1 : 2) | 50 (1 : 1) | 37 (1 : 2) |
| Brassinin (**9**) + methyl (thianaphthen-3-yl)methyldithiocarbamate (**237**) | 1.22 ± 0.06 (1 : 1) | 1.12 ± 0.04 (1 : 2) | 81 (1 : 1) | 75 (1 : 2) |
| Brassinin (**9**) + methyl (7-azaindol-3-yl)methyldithiocarbamate (**238**) | 1.02 ± 0.03 (1 : 1) | 0.75 ± 0.07 (1 : 2) | 68 (1 : 1) | 50 (1 : 2) |

| *Substrate + Inhibitor* | *Specific activity [a] (× $10^{-1}$ nmol/mg/ min) ± SD* | | *Relative activity % (brassinin = 100)* | |
|---|---|---|---|---|
| Brassinin (**9**) + methyl (5-methoxypyrazolo[1,5-a]pyridin-3-yl)methyldithiocarbamate (**239**) | 1.47 ± 0.05 (1 : 1) | 1.48 ± 0.05 (1 : 2) | 98 (1 : 1) | 99 (1 : 2) |
| Brassinin (**9**) + methyl (indol-2-yl)methyldithiocarbamate (**240**) | 0.63 ± 0.06 (1 : 1) | 0.41 ± 0.05 (1 : 2) | 42 (1 : 1) | 27 (1 : 2) |
| Brassinin (**9**) + methyl (benzofuran-2-yl)methyldithiocarbamate (**241**) | 0.64 ± 0.01 (1 : 1) | 0.43 ± 0.03 (1 : 2) | 43 (1 : 1) | 29 (1 : 2) |
| Brassinin (**9**) + methyl-5-methoxypyrazolo[1,5-a]pyridine-3-carboxylate (**242**) | 1.51 ± 0.03 (1 : 1) | 1.49 ± 0.08 (1 : 2) | 100 (1 : 1) | 100 (1 : 2) |
| Brassinin (**9**) + 3-(*N*-acetylamino)quinoline (**243**) | 1.58 ± 0.06 (1 : 1) | 1.53 ± 0.02 (1 : 2) | 100 (1 : 1) | 100 (1 : 2) |
| Brassinin (**9**) + 5-fluorocamalexin (**244**) | 0.81 ± 0.06 (1 : 1) | 0.72 ± 0.05 (1 : 2) | 54 (1 : 1) | 48 (1 : 2) |
| Brassinin (**9**) + 3-phenylindole (**245**) | 0.35 ± 0.02 (1 : 1) | 0.19 ± 0.03 (1 : 2) | 23 (1 : 1) | 13 (1 : 2) |
| Brassinin (**9**) + 4-fluoro-3-phenylindole (**246**) | 0.55 ± 0.08 (1 : 1) | 0.43 ± 0.01 (1 : 2) | 37 (1 : 1) | 29 (1 : 2) |
| Brassinin (**9**) + 6-fluoro-3-phenylindole (**247**) | 0.34 ± 0.06 (1 : 1) | 0.20 ± 0.04 (1 : 2) | 23 (1 : 1) | 13 (1 : 2) |
| Brassinin (**9**) + 3-phenylbenzofuran (**248**) | 0.79 ± 0.03 (1 : 1) | 0.63 ± 0.01 (1 : 2) | 53 (1 : 1) | 42 (1 : 2) |
| Brassinin (**9**) + 2-phenylindole (**249**) | 0.59 ± 0.02 (1 : 1) | 0.59 ± 0.02 (1 : 2) | 39 (1 : 1) | 39 (1 : 2) |

[a] Results are from three triplicate data; 1:1, both brassinin and inhibitor were at 0.3 mM; 1:2, brassinin was at 0.3 mM and inhibitor was at 0.6 mM.

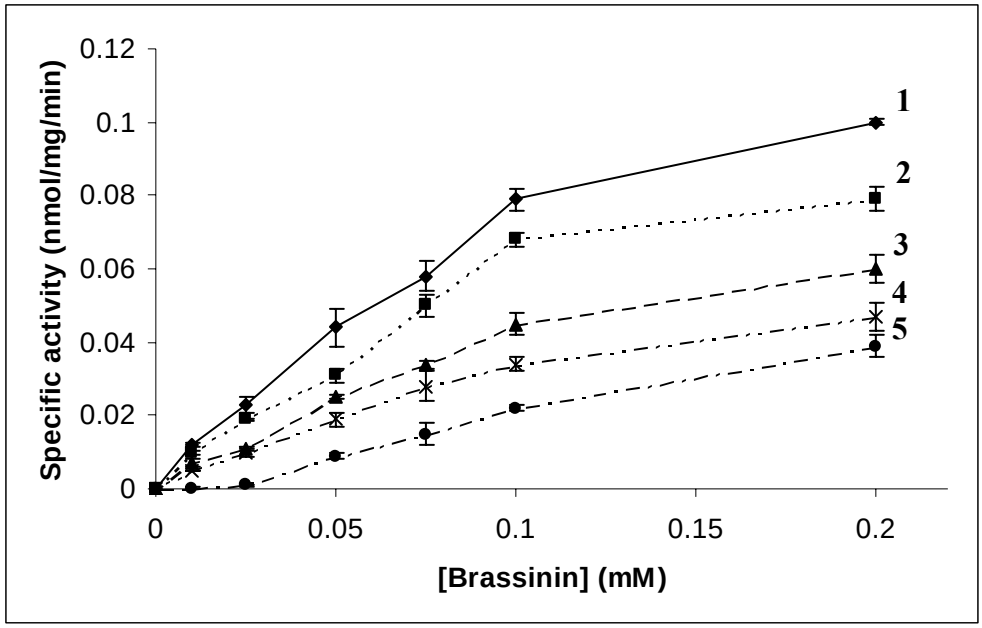


**Figure 2.19** Curves for the transformation of brassinin (**9**) at different concentrations in crude cell-free extracts of *Sclerotinia sclerotiorum*. 1. with no inhibitor; 2. with 0.01 mM 3-phenylindole (**245**); 3. with 0.05 mM 3-phenylindole (**245**); 4. with 0.1 mM 3-phenylindole (**245**); 5. with 0.2 mM 3-phenylindole (**245**).

## 2.8 Summary

A noticeable decrease in the rate of brassinin detoxification was observed in the presence of dithiocarbamates **236**, **240**, **241**, 3-phenylindoles **245**, **247** and 5-fluorocamalexin (**244**) as shown in Fig 2.13-2.17. Furthermore, these active compounds were found to be metabolized in the fungal cultures of *S. sclerotiorum*. However, as long as they were present in the cultures, brassinin (**9**) was not metabolized completely. The remaining tested compounds **237**, **238**, **239**, **242**, **243**, **248**, **249**, and **250** did not show a detectable effect on the rate of brassinin detoxification. Consistent with the results of co-metabolism, both 3-phenylindole (**245**) and 6-fluoro-3-phenylindole (**247**) showed the strongest inhibition of BGT in cell-free extracts (Figure 2.21). This result indicated that inhibition of brassinin detoxification by **245** and **247** in fungal cultures was not due to mycelial growth inhibition. Moderate inhibition of BGT in cell-free

extracts was observed with dithiocarbamates **236**, **240**, **241**, 3-phenylbenzofuran (**248**) (*ca.* 60%) and with camalexins **31**, **75**, **244** (*ca*. 40%) (Figures 2.20 and 2.21) which were also consistent with the results obtained in co-metabolism studies.

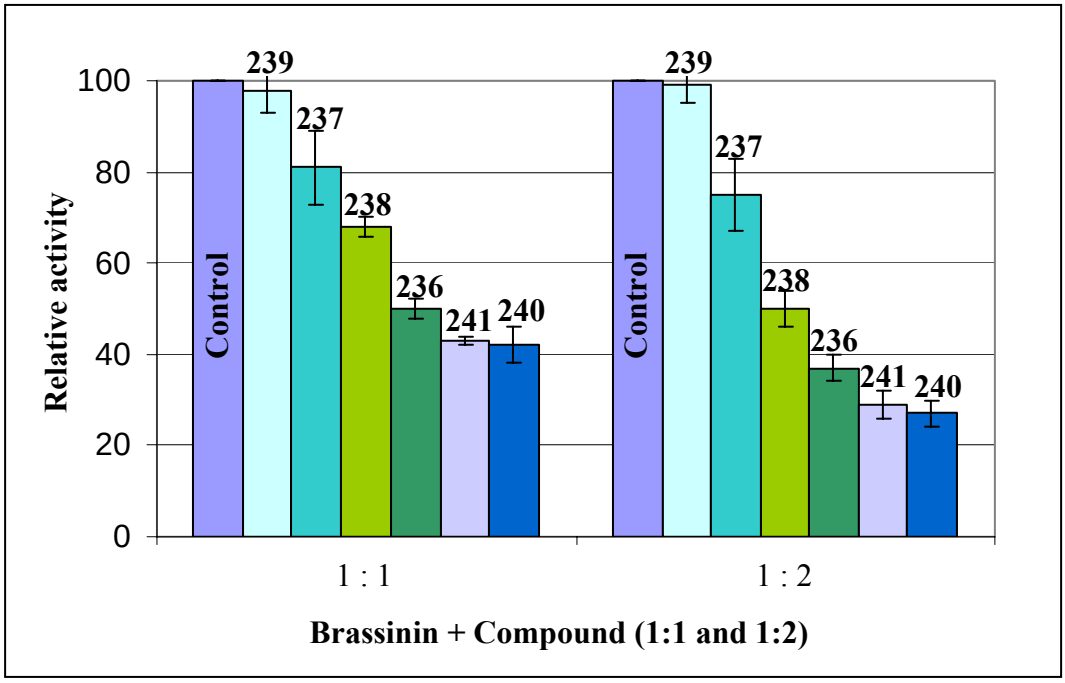


**Figure 2.20** Inhibitory effect of compounds **236**, **237**, **238**, **239**, **240**, and **241** on brassinin glucosyltransferase (BGT) in cell-free extracts of mycelia of *Sclerotinia sclerotiorum*.

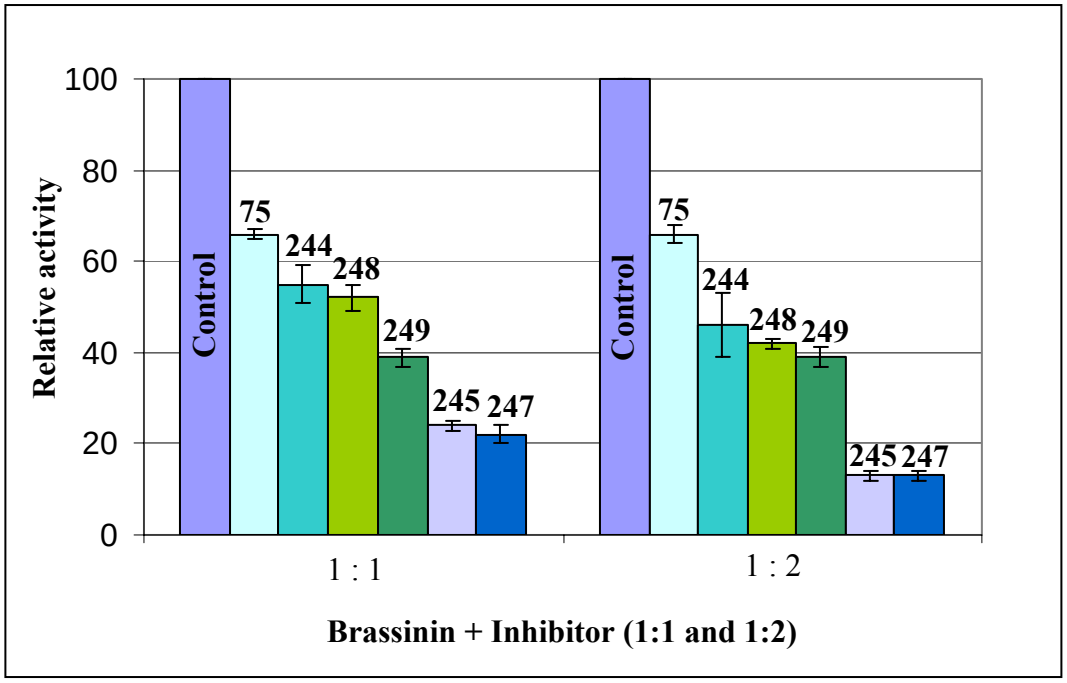


**Figure 2.21** Inhibitory effect of compounds **75**, **244**, **245**, **247**, **248**, and **249** on brassinin glucosyltransferase (BGT) in cell-free extracts of mycelia of *Sclerotinia sclerotiorum*.

# Chapter 3: DISCUSSION

## 3.1 Antifungal activity

Phytoalexins are toxic to fungi, bacteria, nematodes and plant and animal cells. However, very little is known about the mode of action of phytoalexins. Due to the diversity in chemical structures of phytoalexins, a single mode of action is unlikely. Since most of the phytoalexins are lipophilic, one of the most common chemical features is the disruption of membranes that is central to the toxicity of phytoalexins (Laks and Pruner, 1989; Arnoldi and Merlini, 1990). Like other phytoalexins, cruciferous phytoalexins show toxicity within a range of $10^{-5}$ to $10^{-4}$ M for in vitro inhibition. Except for camalexin (**31**) the mode of toxicity of cruciferous phytoalexins is not known. It was reported that camalexin (**31**), like other phytoalexins, rapidly disrupts the integrity of the inner membrane of *Pseudomonas syringae* pv. *maculicola* (Rogers et al., 1996).

The cruciferous phytoalexins brassilexin (**24**) and sinalexin (**25**) have been known to possess strong antifungal activity against some major pathogens of crucifers such as *Alternaria brassicae*, *L. maculans*, *R. solani* and *S. sclerotiorum* (Pedras and Zaharia, 2001). Consistent with the previous results, both brassilexin (**24**) and sinalexin (**25**) at 0.1 mM showed complete inhibition of mycelial growth of *S. sclerotiorum* (Table 2.1). In addition, in this investigation it was found that brassilexin inhibited *S. sclerotiorum* completely at 0.05 mM whereas sinalexin showed *ca*. 80% inhibition at the same concentration. The synthetic analogue of brassilexin (**24**), that is 1-

methylbrassilexin (**215**), was found to be less antifungal against *S. sclerotiorum* than the naturally occurring brassilexin (**24**) and sinalexin (**25**) (Table 2.1).

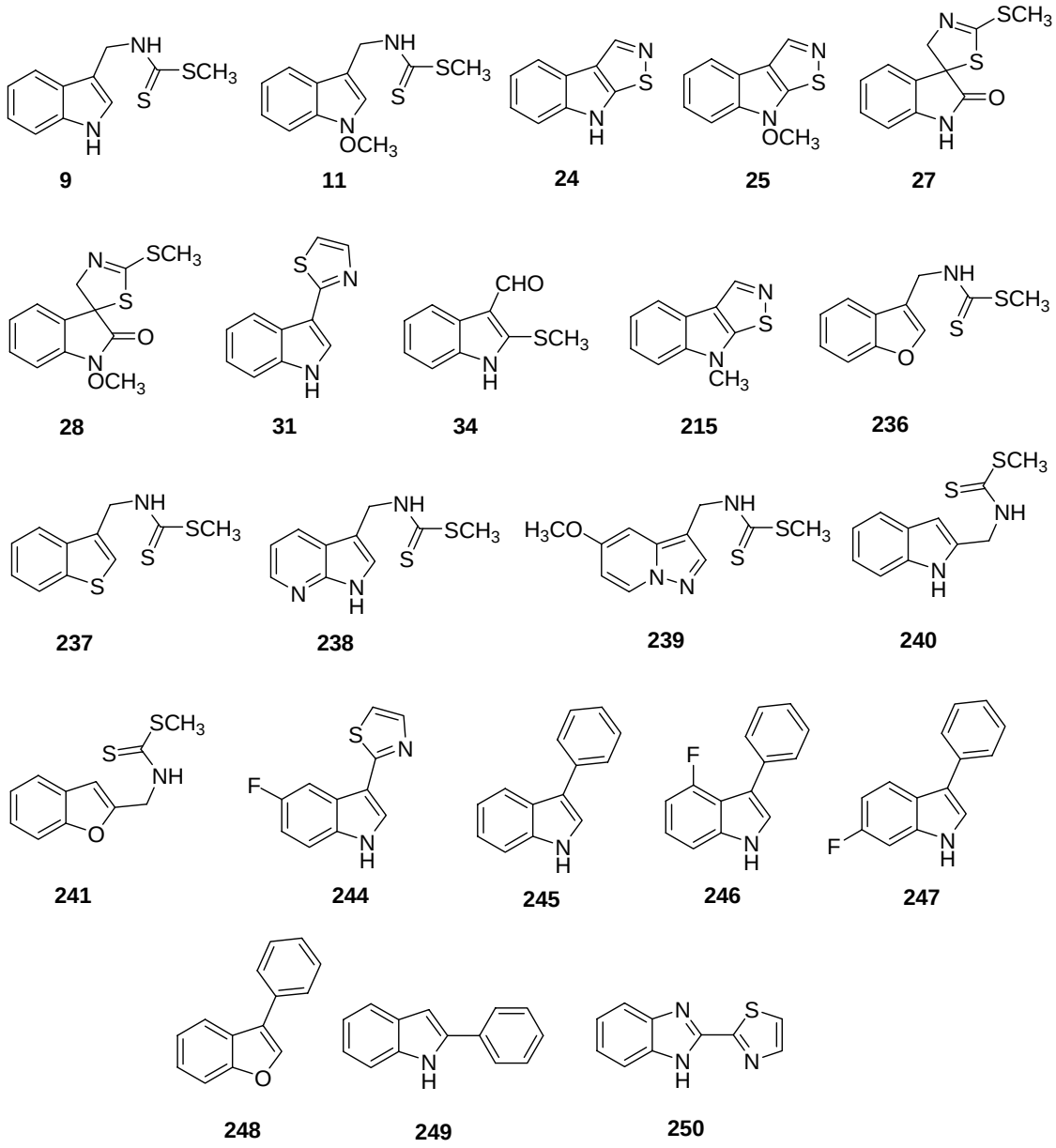


**Figure 3.1** Structure of compounds discussed in Section 3.1.

Although the mode of action of dithiocarbamate containing phytoalexins such as brassinin (**9**) and 1-methoxybrassinin (**11**) have not been reported, most likely their toxicity arises from the reaction of dithiocarbamates with the HS-containing enzymes and coenzymes of fungal cells or by complex formation of the dithiocarbamates with the metal ions of metal containing enzymes. It has long been known that dithiocarbamates containing fungicides have similar effects on fungal cells (Matolcsy et al., 1988). In this investigation, it was found that brassinin (**9**) and 1-methoxybrassinin (**11**) were highly growth inhibitory to *S. sclerotiorum* at 0.5 and 0.3 mM concentration but they showed moderate antifungal activity at 0.1 mM (Table 2.1). However, phytoalexins **9** and **11** were found to be less toxic to *S. sclerotiorum* than brassilexin (**24**), sinalexin (**25**), and camalexin (**31**).

The antifungal activity of the designed compounds **236**, **237**, **238**, **239**, **240**, and **241** containing dithiocarbamates was investigated against *S. sclerotiorum* (Table 2.5). Dithicarbamates **240** and **241** showed antifungal activity similar to the naturally occurring brassinin (**9**) and 1-methoxybrassinin (**11**), whereas dithiocarbamates **236**, **237**, and **238** showed lower antifungal activity than **9**, and **11**. The antifungal activity of dithiocarbamate **239** could not be determined as it was not soluble in aqueous solution at 0.1 mM concentration. The results of antifungal activity of all synthetic dithiocarbamates showed that dithiocarbamates in 2-substituted indole or benzofuran nuclei such as compounds **240** and **241** were more antifungal against *S. sclerotiorum* than the dithiocarbamates in 3-substituted nuclei.

Camalexin (**31**) has been known to inhibit spore germination of *L. maculans* (isolate BJ-125) (Pedras et al., 1998) and is strongly effective in inhibiting the mycelial growth of *L. maculans* at 0.5 mM in PDA agar media (Pedras et al., 2005b). Similar antifungal activity of camalexin was found against other fungi such as *R. solani* and *S. sclerotiorum* (Pedras and Liu, 2004; Pedras and Ahiahonu, 2002). Complete inhibition

of mycelial growth of *S. sclerotiorum* up to 7 days was reported with 0.5 mM camalexin (**31**). The antifungal activity of a camalexin analogue and some designed compounds, structurally similar to camalexin (**31**), were determined in the current investigation. 5-Fluorocamalexin (**244**) was found to be less antifungal against *S. sclerotiorum* compared to camalexin (**31**). The highest antifungal activity was obtained with 3-phenylindole (**245**) and its analogues **246** and **247**. Although these three compounds were expected to have lower antifungal activity compared to camalexin (**31**), they were found to have the highest antifungal activity against *S. sclerotiorum* among all tested compounds including phytoalexins. In addition, 3-phenylbenzofuran (**248**) showed lower toxicity (*ca*. 80% growth inhibition at 0.5 mM) (Table 2.5). Interestingly, commercially available fungicide thiabendazole (**250**) was not very toxic to *S. sclerotiorum*. Little growth (*ca*. 10%) of *S. sclerotiorum* was observed in the presence of thiabendazole (**250**) even at 0.5 mM concentration.

The phytoalexins brassicanal A (**34**) and spirobrassinins **27** and **28** were not very effective against *S. sclerotiorum*. Complete inhibition was not observed for these phytoalexins even at 0.5 mM.

## 3.2 Synthesis and metabolic detoxification of phytoalexins and analogues in *Sclerotinia sclerotiorum*

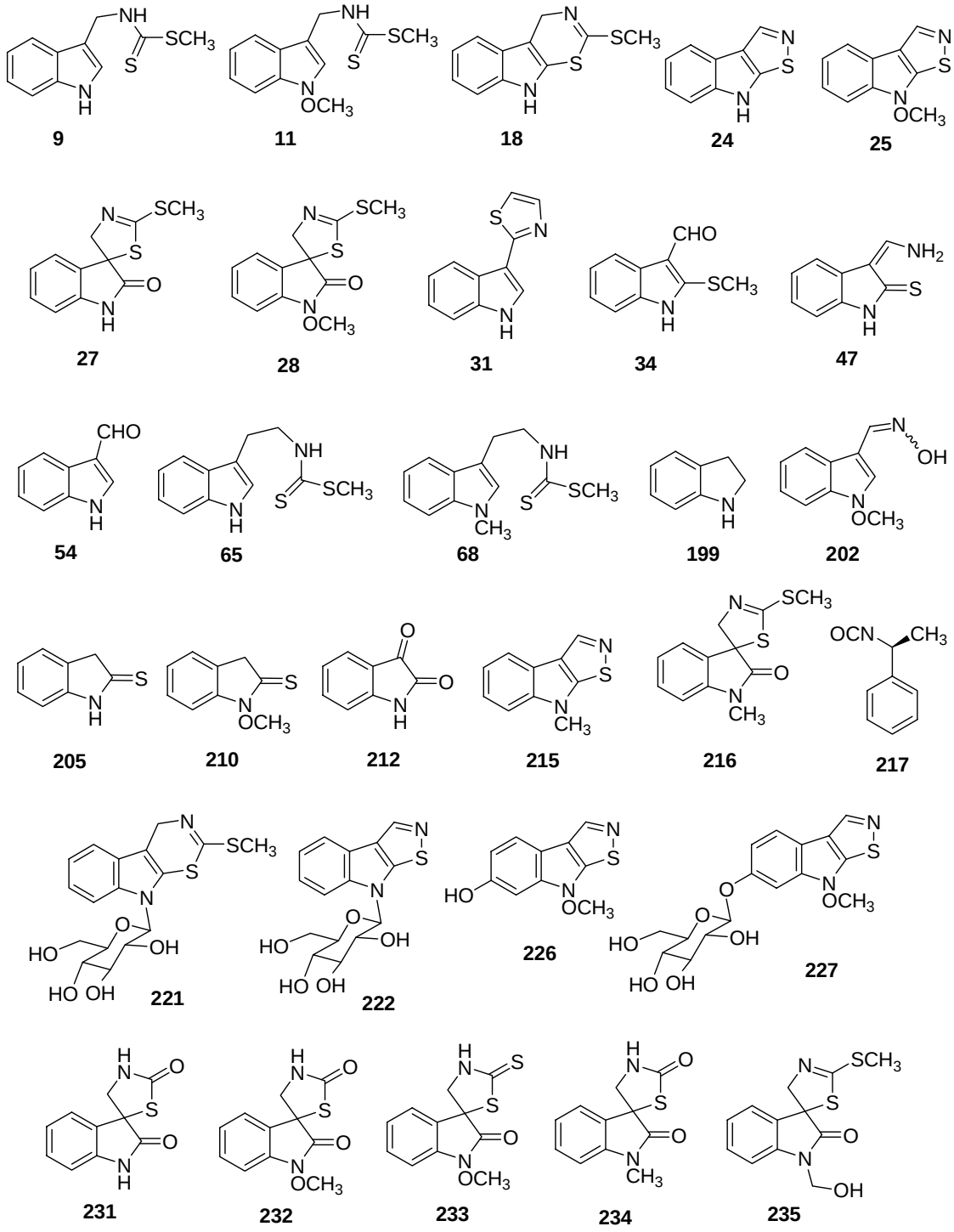


**Figure 3.2** Structure of compounds discussed in Section 3.2.

### 3.2.1 Synthesis

All the phytoalexins in this investigation were synthesized following known procedures. Brassinin (**9**) was synthesized from indole-3-carboxaldehyde (**54**) in good overall yield (52%) as shown in Scheme 2.1 (Takasugi et al. 1988). It was reported that cyclization of brassinin (**9**) using pyridinium bromide perbromide yielded cyclobrassinin (**18**) in 35% yield (Takasugi et al. 1988). This cyclization was also accomplished with NBS and triethylamine instead of pyridinium bromide perbromide and DBU in 45% yield (Mehta et al., 1995). However, the latter method was not effective (very low yield) in this investigation but with a modification (slow addition of pyridinium bromide perbromide at 0 °C) to Takasugi's method, cyclobrassinin (**18**) was obtained in higher yield (58%) (Scheme 2.2). 1-Methoxybrassinin (**11**) was synthesized from indoline (**199**) (Scheme 2.3) in seven steps in good overall yield (31%), in which the key step was the reduction of oximes **202** to the corresponding amine (Pedras and Zaharia, 2000). Brassilexin (**24**) and sinalexin (**25**) were obtained from their corresponding indoline-2-thiones **205** and **210** by formylation under Vilsmeier conditions followed by ammonia work-up (Scheme 2.4 and 2.5) (Pedras and Zaharia, 2001). A modification (2 equiv $POCl_3$, 50 °C) of this method for synthesizing brassilexin (**24**) and its analogues with improved yield was reported recently (Pedras and Jha, 2005). (±)-Spirobrassinin (**27**) was synthesized from isatin (**212**) in a 4-step process in good overall yield (35%) (Scheme 2.8) by following the procedure published by Monde (Monde et al., 1994) and it was resolved into its enantiomers through coupling with (*S*)-(-)-1-phenylethylisocyanate (**217**) followed by chromatographic separation (Scheme 2.12) (Suchy et al., 2001). The first synthesis of (±)-1-methoxyspirobrassinin (**28**) was reported by Kutschy and co-workers (Kutschy et al., 2002). Dioxane dibromide mediated spirocyclization of **11** followed by oxidation with chromium trioxide provided (±)-1-methoxyspirobrassinin (**28**) in 36% overall yield

(Scheme 2.9). The same procedure was applied to obtain (±)-1-methoxyspirobrassinin (**28**) in this project with similar yield. It is worthy to note that a more efficient synthesis of (±)-1-methoxyspirobrassinin (**28**) from 1-methoxybrassinin (**11**) was reported recently through direct oxidation of **11** with chromium trioxide (Pedras et al., 2006a) which was one step less than the previously reported work.

### 3.2.2 Metabolism

The results described in Section 2.2 demonstrated that *S. sclerotiorum* produces different enzymes to transform different phytoalexins. The metabolites resulting from the fungal transformation of phytoalexins (**11**, **18**, **24**, **25**, **27**, **28**, **34**) and analogues (**215** and **216**) did not show detectable antifungal activity against *S. sclerotiorum*. Theses results indicated that all these metabolic transformations were detoxification processes. From the results of antifungal activity of phytoalexins shown in Table 2.1 and Figure 2.1, all the phytoalexins can be divided into three classes, based on their antifungal activity: (i) high antifungal compounds; (ii) medium antifungal compounds; and (iii) low antifungal compounds.

Highly antifungal compounds, which include brassilexin (**24**), sinalexin (**25**), and camalexin (**31**), displayed complete inhibition of mycelial growth of *S. sclerotiorum* at 0.1 mM. Camalexin (**31**) is known to be detoxified by *S. sclerotiorum* to a glucosylated compound via 6-hydroxycamalexin (Pedras and Ahiahonu, 2002). The metabolic transformations of other highly antifungal phytoalexins brassilexin (**24**) and sinalexin (**25**) in *S. sclerotiorum* were studied in the current investigation and reported recently (Pedras and Hossain, 2006). The results of the metabolism of brassilexin (**24**) suggested that the main pathway of brassilexin detoxification involved glucosylation at *N*-1 to yield the corresponding *N*-glucosylated compound **224**, whereas in the case of sinalexin (**25**), in which the *N*-1 position is blocked with a methoxy group, detoxification involved oxidation to 6-hydroxysinalexin (**226**) followed by

glucosylation to 6-oxy-(*O*-β-D-glucopyranosyl)sinalexin (**227**). In addition, a minor pathway for detoxification of brassilexin (**24**) in *S. sclerotiorum* involved reductive ring opening of the isothiazole to the enamine **47**, followed by methylation and hydrolysis (or *vice versa*) to the known phytoalexin brassicanal A (**34**). The yield of metabolite **222** was lower than that of brassicanal A (**34**) (Table 2.2); however, since 1-β-D-glucopyranosylbrassilexin (**222**) was metabolized at a faster rate than brassicanal A (**34**) was metabolized (48h *vs.* 7d), the main pathway for brassilexin (**24**) detoxification appears to be glucosylation (Scheme 2.15). Compared to brassilexin (**24**) and sinalexin (**25**), detoxification of 1-methylbrassilexin (**215**), an unnatural compound, occurred at a substantially slower rate (*ca.* 2d *vs.* 4d) (Pedras and Hossain, 2006). Because oxidation of C-6 of the indole moiety was observed in the transformation of sinalexin (**25**), it was surprising to observe oxidation of 1-methylbrassilexin (**215**) at the (*N*)-$CH_3$ rather than at C-6. These differences are likely due to the substrate specificity of the enzymes involved in the transformations of the natural substrates **24** and **25**. The substrate specificity of such enzymes was previously formulated and probed using analogues of camalexin (**31**) (Pedras and Ahiahonu, 2002).

The phytoalexins brassinin (**9**) and 1-methoxybrassinin (**11**) belong to medium antifungal activity group compounds as they showed about 50% growth inhibition of *S. sclerotiorum* at 0.1 mM concentration. Although the antifungal activity of cyclobrassinin (**18**) could not be determined because of its low solubility in aqueous media, the results of metabolism of cyclobrassinin (**18**) will be discussed with the metabolism of **9** and **11**. It was reported that brassinin (**9**) and cyclobrassinin (**18**) were detoxified in *S. sclerotiorum* through direct *N*-glucosylation of indole moiety whereas 1-methoxybrassinin (**11**), in which the *N*-1 position is blocked with a methoxy group, was regioselectively oxidized at C-7 and then *O*-glucosylated (Pedras et al., 2004c). The unnatural compound methyl tryptamine dithiocarbamate (**65**) (no 1-*N*-substituents)

was also reported to be detoxified through direct *N*-glucosylation whereas the detoxification of another unnatural compound, methyl-1-methyltryptamine dithiocarbamate (**68**, *N*-1 position is blocked with a methyl group) followed the same pathway as did 1-methoxybrassinin (**11**) (Pedras et al., 2004c). Thus, it appeared that glucosylation occurred at *N*-1 of brassinin-like molecules when there was no *N*-substituent, otherwise glucosylation would occur after regioselective hydroxylation at C-7. In addition to the metabolism of cyclobrassinin (**18**) to 1-β-D-glucopyranosylcyclobrassinin (**221**), there was a minor pathway for detoxification of cyclobrassinin (**18**) in *S. sclerotiorum*. This pathway involved enzymatic oxidation of **18**, followed by hydrolysis and methylation (or *vice versa*) to the known phytoalexin brassicanal A (**34**). In previous studies, it was also reported that brassicanal A (**34**) was found to be an intermediate in the detoxification of cyclobrassinin (**18**) by another crucifer pathogen *R. solani* (Pedras and Okanga, 1999). A mechanism, similar to detoxification of **18** in *R. solani*, can also be proposed for the minor pathway of cyclobrassinin (**18**) detoxification in *S. sclerotiorum*. These detoxification mechanisms suggested that the fungal pathogens *R. solani* and *S. sclerotiorum* could metabolize the phytoalexin cyclobrassinin (**18**) by utilizing pathways that may operate in the plant (Pedras and Okanga, 1999).

The third group of phytoalexins displayed low antifungal activity against *S. sclerotiorum* and contains brassicanal A (**34**), spirobrassinin (**27**), and 1-methoxyspirobrassinin (**28**). These phytoalexins caused none or less than 25% growth inhibition of *S. sclerotiorum* at 0.1 mM concentration. The detoxification reactions of the 'low antifungal phytoalexins' brassicanal A (**34**), spirobrassinin (**27**) and 1-methoxyspirobrassinin (**28**) and an analogue **216** in *S. sclerotiorum* were slower and yielded no glucosylation products (Pedras and Hossain, 2006). The detoxification of brassicanal A (**34**) involved the oxidation of $S(CH_3)$ to the corresponding sulfoxide and

reduction of the aldehyde to the alcohol, a process similar to the detoxification of brassicanal A in *L. maculans* (Pedras and Khan, 1996). The detoxification of spirobrassinins **27**, **28**, and **216** involved the hydrolysis of the spirothiazolidine moiety to spirothiazolidinones **231**, **232**, and **234**, respectively. In addition, spirothiazolidinethione **233** was isolated as a minor metabolite of 1-methoxyspirobrassinin (**28**), and 1-hydroxymethylspirobrassinin (**235**) was isolated as a minor metabolite of 1-methylspirobrassinin (**216**). The optical rotation of metabolite **231** and the significant ee of metabolites **233** and **234** suggested that their enzymatic formation was somewhat stereoselective in *S. sclerotiorum*. Furthermore, the following suggest that two or more enzymes are involved in these processes (Table 2.3): (1) the significant ee of **28** and **216** (recovered from cultures, Table 2.3) and similarity to the ee of their biotransformation products **233** and **234**, (2) the high percentages of conversion of spirobrassinins **27**, **28** and **216** (*ca.* 80%), and (3) the similar rates of transformation of either (*R*)- or (*S*)- spirobrassinin in *S. sclerotiorum* (Pedras and Hossain, 2006). However, further studies with purified enzymes would be required to determine their potential substrate stereoselectivity.

Overall, from the above discussion it can be suggested that the plant pathogen *S. sclerotiorum* utilizes different enzymes that can detoxify selectively cruciferous phytoalexins via different pathways. The metabolism and detoxification of strongly and moderately strong antifungal phytoalexins in *S. sclerotiorum* were fast and led to glucosylated products whereas the metabolism of weakly antifungal phytoalexins was very slow and yielded non-glucosylated compounds. The enzymes involved in the biotransformation of the weakly antifungal phytoalexins brassicanal A (**34**), spirobrassinin (**27**) and 1-methoxyspirobrassinin (**28**) might be house-keeping enzymes used in general detoxification processes. By contrast, the detoxification reactions of strongly antifungal phytoalexins (camalexin (**31**), brassilexin (**24**) and sinalexin (**25**))

and of moderately strong phytoalexins (brassinin (**9**), 1-methoxybrassinin (**11**) and cyclobrassinin (**18**)) might be catalyzed by selective glucosyltransferases although selective oxidases might be required as well for **11**, **25**, and **31**. Glucosylation is less usual in microorganisms, particularly in plant pathogens, but *O*-glucosylation and, to a lesser extent, *N*-glucosylation are common detoxification mechanisms among plants (Section 1.6.1). The results of biotransformation of strongly and moderately antifungal phytoalexins suggest that *S. sclerotiorum* in its continuous adaptation and co-evolution with plants, has acquired efficient glucosyltransferases that can disarm the plant chemical defenses (Pedras et al., 2004c). Ultimately, it is anticipated that knowledge of the mechanisms of fungal detoxification can lead to the design of effective inhibitors that could prevent phytoalexin detoxification. Nonetheless, before such inhibitors can be designed, a better understanding of the enzymes and enzymatic mechanisms involved in these fungal transformations is required (Pedras and Hossain, 2006).

## 3.3 Design, synthesis, and metabolism of potential brassinin detoxification inhibitors in *Sclerotinia sclerotiorum*

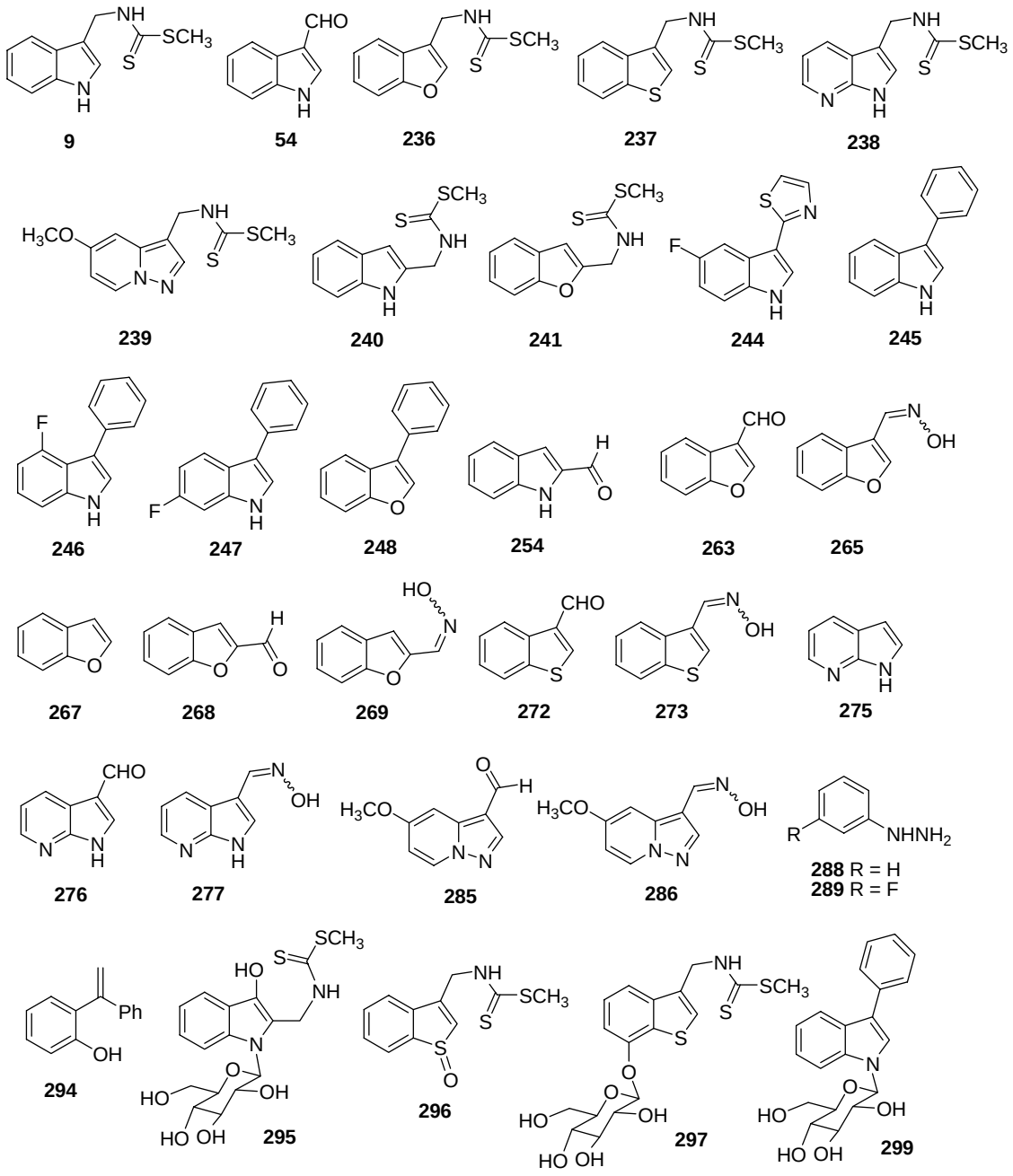


**Figure 3.3** Structure of compounds discussed in Section 3.3.

### 3.3.1 Design

As depicted in Scheme 1.4, the detoxification of brassinin (**9**) in *S. sclerotiorum* involves glucosylation at *N*-1 position of the indole ring and this glucosylation reaction requires an inducible brassinin glucosyltransferase (BGT) (Pedras et al., 2004c). Furthermore, it was reported that 6-fluorocamalexin (**75**) could slow down substantially the rate of metabolism of brassinin (**9**) both in fungal cultures and in cell-free extracts of *S. sclerotiorum*. Thus, based on these results two groups of potential brassinin detoxification inhibitors were designed: (i) one group was based on the structure of brassinin (Fig. 2.8) and (ii) another group was based on the structure of camalexin (**31**) (Fig. 2.9). Since BGT appeared to be selective, it was anticipated that replacing the nitrogen of indole with other heteroatoms, e.g. oxygen and sulfur, in compounds **236** and **237** respectively, or changing the position of side chain of brassinin (**9**) from C-3 to C-2, e.g. compounds **240** and **241**, could inhibit the glucosyltransferase involved in the metabolism of brassinin. It was found that blocking the *N*-1 position of indole ring in brassinin (**9**) with a methoxy group would lead to oxidation at C-7 followed by glucosylation (Scheme 2.13). Hence, compounds **238** and **239** were designed by replacing C-7 or C-7a carbons in brassinin with nitrogen in order to stop the possible oxidation of **238** and **239** at C-7. In addition, compounds **242** and **243** were designed by replacing the dithiocarbamate side chain with ester or amide to reduce the overall antifungal activity. Since 6-fluorocamalexin (**75**) could slow down the rate of metabolism of brassinin it was anticipated that compounds **244**, **245**, **246**, **247**, **248**, **249**, and **250** could slow down the rate of metabolism of brassinin as well (Fig 2.9). It was also thought that replacing the thiazole ring in camalexin with a phenyl group would reduce the antifungal activity of potential inhibitors, thus 3-phenylindoles **245**, **246**, **247** were designed. However, because biotransformation of 3-phenylindole (**245**) yielded the *N*-1 glucosylated compound, 3-phenylbenzofuran (**248**) was designed by

replacing nitrogen of indole ring with oxygen. In addition, 2-phenylindole (**249**) and thiabendazole (**250**) were designed by changing the position of aromatic side chain from C-3 to C-2.

### 3.3.2 Synthesis

As shown in Scheme 2.1, brassinin (**9**) was synthesized from the aldehyde **54** in a 4-step process (Takasugi et al., 1988). Similar synthetic strategy was used for synthesis of dithiocarbamates **236**, **237**, **238**, **239**, **240**, and **241**. Since aldehydes **254**, **263**, **268**, **272**, **276**, and **285** were expensive or not commercially available, their synthesis followed known procedures. Aldehydes **254**, **263**, and **272** were obtained in yields similar to those reported previously (Pedras et al., 2006a; Zaidlewicz et al., 2001) (Scheme 2.23, 2.25 and 2.27). Syntheses of aldehydes **268** and **276** were accomplished through Vilsmeier formylation of benzofuran (**267**) and 7-azaindole (**275**), respectively, in good yields as shown in Scheme 2.26 and 2.28 (Jones and Stanforth, 1997; Oh et al., 2004). It was reported that the reaction of 7-azaindole (**275**) with equimolar of $POCl_3$/DMF at 80 °C yielded 7-azaindole-3-carboxaldehyde (**276**) in 50% yield (Oh et al., 2004). Application of this procedure yielded a mixture of 1-formyl-7-azaindole (yield 8%) and **276** (yield 10%) along with recovered starting material (yield 50%). Eventually, the synthesis of aldehyde **276** was achieved in *ca.* 50% yield using 10 equivalents of $POCl_3$/DMF and refluxing the reaction mixture. Elsner et al. reported recently the synthesis of aldehyde **285** through hydrolysis and decarboxylation of ester **242**, followed by Vilsmeier formylation (Elsner et al., 2006). However, since this method did not work, selective reduction of the ester **242** with DIBALH at -78 °C was attemted to yield the corresponding alcohol **284** in a very low yield. Next, the aldehyde **285** was obtained in 65% yield after reducing the ester **242** to alcohol **284** with $LiAlH_4$, followed by oxidation with $MnO_2$.

Similar to the synthesis of brassinin (**9**), all the synthesized aldehydes **254**, **263**, **268**, **272**, **276**, and **285** were converted to their corresponding dithicarbamates **240**, **236**, **241**, **237**, **238**, and **239** in which the key step was reduction of oximes to the corresponding amines (Scheme 2.23, 2.25-2.28, and 2.30). Since $NaBH_4$ in presence of $NiCl_2$ was unable to reduce the oximes **265**, **269**, **273**, **277**, and **286**, a milder reducing agent, $Na(CN)BH_3$ in presence of $TiCl_3$ was employed for the reduction of these oximes. However, although $Na(CN)BH_3$ in presence of $TiCl_3$ was able to reduce the oximes **265**, **269**, and **273**, it did not work for **277** and **286**. Finally, reduction of **277**, and **286** to corresponding amines was achieved with Zn/HCl in good yields.

As shown in Scheme 2.31, Rodriguez et al. reported the synthesis of 3-phenylindole from phenylhydrazine (**288**) and phenylacetaldehyde (**290**) (Rodriguez et al., 2000). When this method was applied to synthesize 6-fluoro-3-phenylindole by reaction between 3-fluorophenylhydrazine (**289**) and phenylacetaldehyde (**290**), a mixture of 4-fluoro- and 6-fluoro-3-phenylindoles (**246**, **247**, 72%) was obtained in 1:1 ratio. These two compounds were separated by reverse phase ($C_{18}$) column chromatography (silica gel chromatography did not work). The synthesis of 3-phenylbenzofuran (**248**) was accomplished by following the procedure used for the synthesis of substituted 2-methylbenzofurans from 2-allylphenols (Roshchin et al., 1998). Although the reported yield for synthesis of 2-methylbenzofurans was quite good, the yield of 3-phenylbenzofuran (**248**) from *o*-(1-phenylvinyl)phenol (**294**) was rather poor.

### 3.3.3 Metabolism

The metabolites **295**, **296**, **297**, and **299** resulting from fungal transformation of potential brassinin detoxification inhibitors were not toxic to *S. sclerotiorum* which indicated that, similar to transformations of phytoalexins, these metabolic transformations were detoxification processes. The results of detoxification of methyl

(indol-2-ylmethyl)dithiocarbamate (**240**) in *S. sclerotiorum* suggested that compared to brassinin (**9**), its detoxification occurred at a substantially slower rate (*ca.* 12h *vs.* 48h). Although detoxification of brassinin (**9**) in *S. sclerotiorum* involved *N*-1 glucosylation, the detoxification of its isomer i.e. methyl (indol-2-ylmethyl)dithiocarbamate (**240**) took place at two sites, glucosylation at *N*-1 along with oxidation at C-3 (Scheme 2.33). The detoxification of methyl (thianaphthen-3-ylmethyl)dithiocarbamate (**237**) was found to be faster than that of brassinin (**9**) (6h *vs.* 12h). Although **237** was expected to have slow rate of metabolism due to replacement of the nitrogen of the indole ring in brassinin (**9**) with a sulfur atom, **237** was quickly metabolized to a sulfoxide **296** which was further metabolized slowly to methyl (7-oxy-*O*-β-glucopyranosylthianaphthen-3-yl)methyldithiocarbamate (**297**) (Scheme 2.34). Since the glucoside **297** was obtained from metabolism of **296**, it was surprising to observe the absence of the sulfoxide moiety in **297**. The metabolism of this sulfoxide **296** in *S. sclerotiorum* appears to involve enzymatic reduction of **296** to its original form i.e. **237** and then oxidation followed by *O*-glucosylation at C-7 (or *vice versa*). The detoxification of the strongest antifungal compounds (among all the tested compounds), 3-phenylindole (**245**) in *S. sclerotiorum* involved direct *N*-glucosylation of indole moiety whereas the structurally related phytoalexin, camalexin (**31**) was detoxified to 6-hydroxycamalexin followed by *O*-glucosylation to 6-oxy-(*O*-β-D-glucopyranosyl)camalexin (**73**) (Scheme 1.7 and 2.36). However, it was reported that 6-fluorocamalexin (**75**) was detoxified in *S. sclerotiorum* through direct *N*-glucosylation of the indole moiety (Pedras and Ahiahonu, 2002). Although the metabolic product of 5-fluorocamalexin (**244**) could not be isolated due to its low yield, the LC-MS data suggested that similar to 6-fluorocamalexin (**75**), the metabolism of 5-fluorocamalexin in *S. sclerotiorum* occurred through direct *N*-glucosylation of the indole moiety. It was reported that the metabolism of 5-fluorocamalexin (**244**) in *Rhizoctonia solani* occurred at the thiazole ring yielding 5-fluoroindole-3-carbonitrile as a major product (Pedras and Liu, 2004).

The metabolism of other potential inhibitors such as dithiocarbamates (**236** and **241**) and 3-phenylbenzofuran (**248**) in *S. sclerotiorum* was analyzed by LC-MS as well. The LC-MS data suggested that metabolism of **236**, **241**, and **248** were completed in about 12 to 24 h and involved oxidation at an undetermined position followed by *O*-glucosylation. Overall, the results of these metabolisms suggested that *S. sclerotiorum* employs different oxidases and/or glucosyltransferases to metabolize these designed compounds.

Recently, a number of potential inhibitors were designed to inhibit brassinin (**9**) detoxification in *Leptosphaeria maculans* by replacing the dithiocarbamate group (toxophore) of brassinin (**9**) with carbamate, dithiocarbonate, urea, thiourea, sulfamide, sulfonamide, dithiocarbazate, amide and ester functional groups and by substituting the indolyl moiety with naphthalenyl and phenyl moiety (Pedras and Jha, 2006). Their metabolic transformations were investigated in fungal cultures of *L. maculans*. It was reported that most of these compounds remained unaffected in the cultures and few of them were metabolized by the fungus. The metabolism was found to occur mainly at side chains yielding carboxaldehydes or carboxylic acids. On the contrary, all the designed compounds in the current investigation were metabolized by *S. sclerotiorum* yielding mainly *N*- or *O*-glucosylated compounds and instead of side chain transformation, metabolism occurred at the aromatic ring only. Probably, due to the ability to detoxify different natural and non-natural compounds, the fungus *S. sclerotiorum* has a wide range of host species whereas *L. maculans* has fewer host species.

## 3.4 Effect of potential inhibitors on brassinin detoxification

All the designed compounds (Fig 2.8 and 2.9) were screened for inhibition of brassinin detoxification in cultures of *S. sclerotiorum* by co-incubating compounds **236-250** with brassinin (**9**). A noticeable decrease in the rate of brassinin detoxification was observed in the presence of dithiocarbamates **236**, **240**, **241**, 3-phenylindoles **245**, **247** and 5-fluorocamalexin (**244**) as shown in Fig 2.13-2.17. Furthermore, these active compounds were found to be metabolized in the fungal cultures of *S. sclerotiorum*. However, as long as they were present in the cultures, brassinin (**9**) was not metabolized completely. The remaining tested compounds **237**, **238**, **239**, **242**, **243**, **248**, **249**, and **250** did not show a detectable effect on the rate of brassinin detoxification. These results might be explained either because the compounds do not affect BGT or are unable to reach the metabolic site inside the cell. On the other hand, it is possible that the decrease in the rate of detoxification of brassinin in the presence of **236**, **240**, **241**, **244**, **245** and **247** is due to strong inhibitory activity of the compound on mycelium growth or on BGT. These hypotheses were confirmed by co-incubating these compounds with cell-free extracts containing BGT. Therefore, further testing of all designed compounds was carried out using cell-free extracts containing BGT. Consistent with the results of co-metabolism, both 3-phenylindole (**245**) and 6-fluoro-3-phenylindole (**247**) showed the strongest inhibition of BGT in cell-free extracts. This result indicated that inhibition of brassinin detoxification by **245** and **247** in fungal cultures was not due to mycelial growth inhibition. Moderate inhibition of BGT in cell-free extracts was observed with dithiocarbamates **236**, **240**, **241**, 3-phenylbenzofuran (**248**) (*ca.* 60%) and with camalexins **31**, **75**, **244** (*ca*. 40%) which were also consistent with the results obtained in co-metabolism studies. Although 2-phenylindole (**249**) showed 60% inhibition on BGT, it did not affect the rate of brassinin detoxification in

mycelial cultures probably due to its faster metabolism (complete metabolism of **249** occurred in *ca.* 6h).

## 3.5 Overall conclusions and future work

In this thesis, it has been shown that the stem rot fungus *S. sclerotiorum* is able to circumvent phytoalexins of crucifers through metabolism and detoxification. Phytoalexins, strongly and moderately antifungal to *S. sclerotiorum*, can be detoxified to glucosylated products whereas weakly antifungal phytoalexins are detoxified to non-glucosylated pathways. Therefore the glucosylation reactions are important metabolic targets to selectively control the stem rot fungus as the inhibition of this glucosylation process may allow plants to accumulate strongly antifungal phytoalexins (Pedras and Hossain, 2006). These accumulated phytoalexins are then expected to slow if not stop the growth of *S. sclerotiorum*.

The cruciferous phytoalexin brassinin (**9**) is of great interest due to its biological activity and intermediacy in the biosynthetic pathway of other relevant phytoalexins such as cyclobrassinin (**18**), brassilexin (**24**), rutalexin (**42**), brassicanal A (**34**), and spirobrassinin (**27**) (Pedras et al., 2003a). Therefore, it is expected that the inhibition of brassinin (**9**) detoxification will allow plants to accumulate all these phytoalexins. Because brassinin (**9**) can be detoxified by *S. sclerotiorum* to an *N*-glucosylated compound (**66**) and this glucosylation reaction is catalyzed by an inducible enzyme, brassinin glucosyltransferase (BGT) (Pedras et al., 2004c), inhibitors of BGT are expected to be potential protection agents against stem rot disease of crucifer crops. It is expected that in the presence of such inhibitors, the combined effect of brassinin (**9**) and its biogenetically related phytoalexins in plants may have a deleterious effect on *S. sclerotiorum*. Thus inhibitors of BGT were designed and synthesized in this project and

their bioactivities, metabolism and screening in mycelial cultures as well as in cell-free extracts of *S. sclerotiorum* were investigated. The results of screening of designed compounds suggested that 3-phenylindoles **245**, **247** and dithiocarbamates **236**, **240**, **241** are compounds that can slow down the rate of brassinin detoxification in cultures and inhibit BGT in cell-free extracts. However, likely because these compounds are metabolized in cultures, they are not able to completely stop brassinin detoxification. Nonetheless, these lead structures (**236**, **240**, **241**, **245**, **247**) may help, in the future to design more active inhibitors of BGT. There are many examples where initial knowledge of the structural features, obtained from primary inhibitors, led to design of active inhibitors. For example, resorcinol was found to be a poor inhibitor of tyrosinase, a key enzyme in melanin biosynthesis (Kim and Uyama, 2005). Further research on derivatives of resorcinol led to inhibitors of tyrosinase. It was reported that 4-substituted resorcinols, particularly, 4-hexylresorcinol was the most effective inhibitor for use in the food industry.

In this thesis, it has been shown that potential inhibitors can be detoxified in *S. sclerotiorum* to glucosylated products by direct glucosylation or by oxidation followed by glucosylation. These results indicated that *S. sclerotiorum* has different oxidases and/or glucosyltransferases to metabolize potential inhibitors. Therefore, in order to selectively control the stem rot fungus, the inhibitors of brassinin detoxification have to be designed to inhibit not only BGT but also oxidase(s), as these enzymes appear to play an important role in metabolizing the potential inhibitors. It is expected that isolation and characterization of BGT involved in the detoxification of brassinin (**9**) will greatly facilitate the design of more effective and selective inhibitors.

## Future work

1. Purification and characterization of brassinin glucosyltransferase (BGT)
2. Testing of lead compounds using purified BGT
3. Kinetic and substrate specificity studies using purified BGT
4. Design and synthesis of more effective potential inhibitors of brassinin detoxification. Since oxidase(s) play important role in metabolizing potential inhibitors, the following compounds might be good inhibitors of brassinin detoxification:

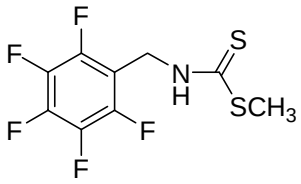


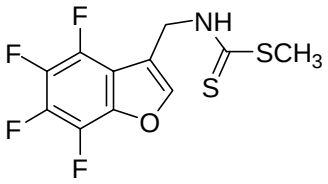


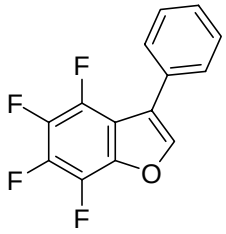

# Chapter 4: EXPERIMENTAL

## 4.1 General methods

All chemicals were purchased from Sigma-Aldrich Canada Ltd., Oakville, ON, Canada. All solvents were used as such, except for $CH_2Cl_2$ and $CHCl_3$ which were redistilled. Solvents used in syntheses were dried over the following drying agents prior to use: THF and diethyl ether over sodium/benzophenone, $CH_2Cl_2$, $CH_3CN$ and benzene over $CaH_2$ and acetone over $CaSO_4$.

Analytical thin layer chromatography (TLC) was carried out on precoated silica gel TLC aluminum sheets (Merck, 60 $F_{254}$ 5 × 2 cm × 0.2 mm). Compounds were visualized under UV light (254/366 nm) after elution with a suitable solvent system. Plates were dipped in 5% (w/v) aqueous phosphomolybdic acid solution containing 1% (w/v) ceric sulfate and 4% (v/v) $H_2SO_4$, followed by heating on a hot plate.

Preparative thin layer chromatography (PTLC) was performed on silica gel plates (Merck, 60 $F_{254}$ or reversed phase RP-8 20 × 20 cm × 0.25 mm). Flash column chromatography (FCC) was performed on silica, Merck grade 60, mesh size 230-400, 60 Å or on J. T. Baker C-18 reversed-phase silica gel, 40 μm.

High performance liquid chromatography (HPLC) analysis was carried out with a high performance liquid chromatograph equipped with quaternary pump, automatic injector, and diode array detector (wavelength range 190–600 nm), degasser, and a Hypersil octadecylsilane (ODS) column (5 μm particle size silica, 200 mm × 4.6 mm

identical diameter), equipped with an in-line filter. Mobile phase: 75% $H_2O$-25% $CH_3CN$ to 100% $CH_3CN$, for 35 min, linear gradient, and a flow rate 1.0 ml/min.

NMR spectra were obtained on Bruker Avance 500 spectrometers. For $^1H$ NMR (500 MHz), the chemical shifts (δ) are reported in parts per million (ppm) relative to TMS. The δ values were referenced to $CDCl_3$ ($CHCl_3$ at 7.27 ppm), $CD_2Cl_2$ ($CHDCl_2$ at 5.32 ppm), $CD_3CN$ ($CHD_2CN$ at 1.94 ppm), $(CD_3)_2SO$ ($CHD_2SOCD_3$ at 2.50 ppm), $(CD_3)_2CO$ ($CHD_2COCD_3$ at 2.05 ppm) and $CD_3OD$ ($CHD_2OD$ at 3.30 ppm). First-order behavior was assumed in analysis of $^1H$ NMR spectra and multiplicities are as indicated by one or more of the following s = singlet, d = doublet, t = triplet, q = quartet, m = multiplet and br = broad. Spin coupling constants (*J* values) are reported to the nearest 0.5 Hz. $^{13}C$ data were collected on the Bruker Avance 500 spectrometers at 125.8 MHz. The $^{13}C$ chemical shift (δ values) were referenced to $CDCl_3$ (77.2 ppm), $CD_2Cl_2$ (54.0 ppm), $CD_3CN$ (118.7 ppm), $(CD_3)_2SO$ (39.5 ppm), $(CD_3)_2CO$ (29.9 ppm) and $CD_3OD$ (49.2 ppm). The multiplicities of $^{13}C$ signals refer to the number of attached protons: s = C, d = CH, t = $CH_2$, q = $CH_3$) and were determined based upon HMQC experiments. In some cases it was determined based on chemical shift and consistency within a series of similar structures, as well as the relative intensity of each signal.

Fourier transform infrared (FTIR) spectra were recorded on Bio-Rad FTS-40 spectrometers. Spectra were measured by the diffuse reflectance method on samples dispersed in KBr.

Specific rotations, $[\alpha]_D$ were determined at ambient temperature on a Rudolph DigiPol DP781 polarimeter using a 1 ml, 10 cm path length cell; the units are $10^{-1}$ deg $cm^2$ $g^{-1}$ and the concentrations (*c*) are reported in g/100mL. UV spectra were recorded on Varian-Cary spectrophotometer in MeOH or $CH_3CN$. Mass spectra (MS) were

obtained on a VG 70 SE mass spectrometer using a solid probe or on a Q Star XL, Applied Biosystems.

The Bradford protein assay was used to quantify proteins in cell-free extracts using bovine serum albumin standard curves. The optical densities (at 595 nm) were recorded on a Bio-Rad SmartSpec 3000 spectrophotometer.

## 4.2 Synthesis of phytoalexins and analogues

### 4.2.1 Brassinin (9)

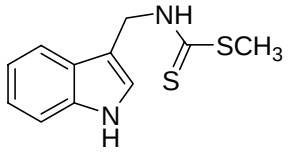


**9**

To a solution of indole-3-carboxaldehyde (**54**, 1.0 g, 6.9 mmol) in EtOH (30 ml), a solution of $NH_2OH.HCl$ (952 mg, 13.7 mmol) and $Na_2CO_3$ (803 mg, 7.6 mmol) in water (14 ml) was added. After stirring for 3 hours at 60 °C, EtOH was removed under reduced pressure and the resulting precipitate was filtered off and air dried to afford indole-3-carboxaldehyde oxime (**197**, 1.0 g) in 91% yield (Pedras et al., 1992).

The oxime (200 mg, 1.25 mmol) was dissolved in MeOH (10 ml) and an aqueous solution of NaOH (50 ml, 1M) was added. After stirring for 15 min at 0 °C, Devarda's alloy (5.8 g) was added with vigorous stirring and the reaction was allowed to stir for 20 min at rt. The reaction mixture was diluted with water (50 ml), filtered, MeOH was evaporated and the reaction mixture was extracted with $Et_2O$ (3 x 100 ml). The combined organic extracts were dried over $Na_2SO_4$ and concentrated. The residue was subjected to FCC ($CHCl_3$-MeOH-28% aq. $NH_3$, 80:20:1) to afford 3-indolylmethylamine (**198**, 136 mg) in 72% yield as colorless oil (Pedras et al., 1992).

The amine (**198**, 136 mg, 0.9 mmol) was dissolved in pyridine (1.5 ml) and $Et_3N$ (142 μL), cooled to 0˚ C and treated with $CS_2$ (85 μL, 1.4 mmol). After stirring for 1 hour at 0˚ C, $CH_3I$ (79 μL, 1.3 mmol) was added and the reaction mixture was kept at 3 ˚C for 15 hours. The reaction mixture was poured into 1.5 M $H_2SO_4$ (50 ml) and immediately extracted with $Et_2O$ (2 x 100 ml). The extracts were dried over $Na_2SO_4$ and concentrated under reduced pressure. The residue was subjected to FCC on silica gel [gradient elution, $CH_2Cl_2$-hexane (20:80, 30:70, 40:60 & 50:50)] to give brassinin (**9**) (178 mg, 52%, based on the aldehyde **54**) (Pedras et al., 1992).

Mp: 132-133 °C ($CH_2Cl_2$-hexane)

HPLC $t_R$ = 18.9 min.

$^1$H NMR (300 MHz, $CD_3CN$) δ 9.44 (br s, 1H, $D_2O$ exchangeable), 8.49 (br s, 1H, $D_2O$ exchangeable), 7.63 (d, *J* = 8 Hz, 1H), 7.42 (d, *J* = 8 Hz, 1H), 7.30 (d, *J*= 2 Hz, 1H), 7.16 (ddd, *J* = 8, 8, 1 Hz, 1H), 7.08 (ddd, *J* = 8, 8, 1 Hz, 1H), 5.03 (d, *J* = 5 Hz, 2H), 2.55 (s, 3H) and minor signals (ca. 1/10 itensity of the major peaks) due to rotamers at 4.77 (d) and 2.32 (s).

$^{13}$C NMR (300 MHz, $CD_3CN$) δ 200.7 (s), 139.4 (s), 129.7 (s), 127.8 (d), 124.8 (d), 122.3 (d), 121.6 (d), 114.5 (d), 113.5 (s), 45.2 (t), 20.12 (q).

EIMS *m/z* (% relative intensity): 236 (43), 162 (11), 130 (100), 129 (44), 102 (18).

FTIR $\nu_{max}$ 3397, 3310, 3055, 2995, 1618, 1555, 1487, 1339 $cm^{-1}$.

### 4.2.2 Cyclobrassinin (18)

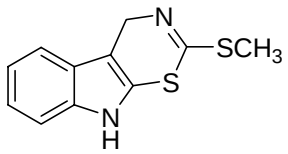


**18**

Pyridinium bromide perbromide (234 mg, 0.73 mmol) was added in small portions to a solution of brassinin (**9**) (169 mg, 0.72 mmol) in dry THF (20 ml) at room temperature. The reaction mixture was stirred at room temperature for 40 minutes, and then basified with DBU (340 μL) (Takasugi et al., 1988). After stirring for another hour at room temperature the solvent was evaporated and the residue was subjected to FCC on silica gel [gradient solvent, $CH_2Cl_2$ : hexane (10:90, 20:80, 30:70, 40:60, 50:50)] to give cyclobrassinin (**18,** 97 mg, 58%).

HPLC $t_R$ = 25.1 min.

$^1$H NMR (500 MHz, $CDCl_3$) δ 7.73 (br s, 1H, $D_2O$ exchangeable), 7.49 (d, $J$ = 7.5 Hz, 1H), 7.33 (d, $J$ = 7.5 Hz, 1H), 7.15-7.18 (m, 2H), 5.10 (s, 2H), 2.57 (s, 3H).

$^{13}$C NMR (500 MHz, $CDCl_3$) δ 152.5 (s), 137.0 (s), 125.5 (s), 122.7 (s), 122.4 (d), 120.7 (d), 117.6 (d), 111.1 (d), 104.3 (s), 49.1 (t), 15.7 (q).

EIMS *m/z* (% relative intensity): 234 ($M^+$, 30), 161 (100), 160 (23).

FTIR $\nu_{max}$ 3373, 2921, 2832, 1601, 1450, 1430, 1337, 978 $cm^{-1}$.

### 4.2.3 1-Methoxybrassinin (11)

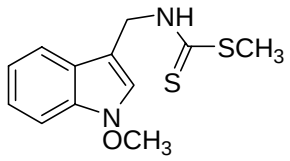


**11**

A solution of $Na_2WO_4.2H_2O$ (1.17 g, 3.5 mmol) in water was added to the solution of indoline (**199**) in MeOH (80 ml) with stirring. The mixture was cooled to -15 ºC using NaCl-ice system. During 30 minutes a solution of 30% $H_2O_2$ (17.7 ml, 173 mmol) in MeOH (20 ml) was added slowly to the reaction mixture. The stirring was continued for further 10 minutes and then solid $K_2CO_3$ (22.1 g, 160 mmol) and dimethyl sulphate (5 ml, 53 mmol) were added with vigorous stirring. The mixture was stirred for further 1.5 hour at 8-13º C, was poured into water (200 ml) and extracted with $Et_2O$ (2×150 ml). After drying ($Na_2SO_4$) and evaporation of solvent, the greenish oily residue was column chromatographed on silica gel ($CHCl_3$: hexane; 1:4) yielded 1-methoxyindole (**200**) (1.51 g, 56%) (Kawasaki et al., 1991).

To the solution of 1-methoxyindole (**200**) (333 mg, 2.3 mmol) in DMF (1.5 ml) was added distilled $POCl_3$ (252 µl, 2.7 mmol). After stirring at room temperature for 1 hour, the mixture was neutralized with 5 M NaOH, and then boiled for 5 minutes. The solution was extracted with $Et_2O$ (2 × 10 ml), the organic phase was dried over $Na_2SO_4$ and concentrated to dryness to give a residue which was purified by column chromatography on silica gel using gradient elution [$CH_2Cl_2$, $CH_2Cl_2/CH_3OH$ (100%, 99:1)] to yield 1-methoxyindole-3-carboxaldehyde (**201,** 340 mg, 86%) (Pedras and Zaharia, 2000).

The aldehyde (**201**, 140 mg, 0.8 mmol) was dissolved in EtOH (3 ml) and a solution of $NH_2OH.HCl$ (166 mg, 2.38 mmol) and $Na_2CO_3$ (126 mg, 1.19 mmol) in water (1 ml) was added. After stirring at 60 ºC for 4 hours, the reaction mixture was

diluted with water and extracted with $Et_2O$ (2 × 10 ml). The organic phase was dried over $Na_2SO_4$ and concentrated to dryness to yield 1-methoxyindole-3-carboxaldehyde oxime (**202**) (mixture of E and Z isomer) (151 mg, 99%).

$Na(CN)BH_3$ (327 mg, 5.2 mmol) and $NH_4OAc$ (439 mg, 5.7 mmol) were added to a cooled (0 ºC ) solution of 1-methoxyindole-3-carboxaldehyde oxime (**202**) (99 mg, 0.52 mmol) in MeOH (1 ml). To this mixture a neutralized solution of $TiCl_3$ 30% wt in 2N HCl (2.1 ml, 4.1 mmol) was added. After stirring for 15 min at 0 ºC, the reaction mixture was diluted with 1% aqueous $NH_4OH$ (40 ml), basified with 5N NaOH and extracted with EtOAc (2 × 40 ml). The organic phase was dried over $Na_2SO_4$ and concentrated to afford crude 1-methoxyindolyl-3-methylamine (**203**).

To the cooled (0 ºC) solution of crude amine (**203**) in pyridine (0.5 ml), $Et_3N$ (105 µl) and $CS_2$ (93 µl, 1.55 mmol) were added. After 1 hour of stirring at 0 ºC, $CH_3I$ (96 µl, 1.57 mmol) was added and the reaction was left at 5 ºC for 16 hours. The reaction mixture was poured into 1.5 M $H_2SO_4$ (10 ml) and extracted with $Et_2O$ (2 × 15 ml). The organic phase was dried over $Na_2SO_4$ and concentrated and the residue was subjected to FCC on silica gel ($CH_2Cl_2$/hexane, 40:60 & 50:50) to afford 1-methoxybrassinin (**11,** 90 mg, 31% overall yield from indoline **199**) (Pedras and Zaharia, 2000).

HPLC $t_R$ = 24.2

$^1$H-NMR (500 MHz, $CD_3CN$) δ 8.29 (br, s, $D_2O$ exchangeable, 1H), 7.68 (d, *J* = 8 Hz, 1H), 7.49-7.43 (m, 2H), 7.28 (dd, *J* = 7, 7 Hz, 1H), 7.14 (dd, *J* = 7, 7 Hz, 1H), 5.04 (d, *J* = 5 Hz, 2H), 4.09 (s, 3H), 2.59 (s, 3H).

HREIMS *m/z* measured 266.0547 (266.0548 calcd. for $C_{12}H_{14}N_2OS_2$).

EIMS *m/z* (% relative intensity): 266 ($M^+$, 8), 235 (100), 160 (99), 145 (21), 129 (48), 128 (23), 102 (21), 90 (33).

FTIR $\nu_{max}$ 3325, 2938, 1494, 1451, 1352, 1304, 1076, 920 $cm^{-1}$.

### 4.2.4 Brassilexin (24)

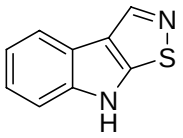

**24**

A mixture of 2-oxindole (**204**) (500 mg, 3.8 mmol), $P_4S_{10}$ (1 g, 2.3 mmol, and $NaHCO_3$ (631 mg, 7.5 mmol) in THF (25 ml) was stirred for 4 hours at room temperature. THF was removed under reduced pressure and ice cold water was added to the residue. The ppt was filtered off, washed with ice cold water and air dried to yield indoline-2-thione (**205**, 484 mg, 86%) (Kamila and Biehl, 2004).

The thione **205** (460 mg, 3.1 mmol) was dissolved in dry DMF (6 ml), cooled to 0 ˚C and then distilled $POCl_3$ (600 μL, 6.5 mmol) was added slowly. After stirring at room temperature for 2 hours, the reaction mixture was cooled to 0 ˚C, basified carefully with 28% $NH_4OH$ (100 ml) and extracted with $CH_2Cl_2$ (3 x 100 ml). The extracts were dried over $Na_2SO_4$ and concentrated under reduced pressure. The residue was dissolved in pyridine (5 ml) and then $I_2$ (680 mg, 2.7 mmol) was added to it. After stirring for 1.5 hours at room temperature, the reaction mixture was acidified with 1.5 M $H_2SO_4$ (30 ml) and extracted with $CH_2Cl_2$ (3 × 30 ml). The extracts were dried over $Na_2SO_4$ and concentrated under reduced pressure. The crude product was subjected to FCC on silica gel (EtOAc-hexane, 20:80) to give brassilexin (**24**, 120 mg, 19% yield from the oxindole **204**) (Pedras and Jha, 2005).

HPLC $t_R$ = 12.2

$^{1}$H NMR (500 MHz, $CD_3CN$) δ 9.85 (br s, 1H, $D_2O$ exchangeable), 8.70 (s, 1H), 7.91 (d, *J* = 8 Hz, 1H), 7.56 (d, *J* = 8 Hz, 1H), 7.33 (dd, *J* = 8, 8 Hz, 1H), 7.22 (dd, *J* = 8, 8 Hz, 1H).

$^{13}$C NMR (500 MHz, $CD_3CN$) δ 159.5 (s), 147.8 (d), 144.6 (s), 127.7 (s), 124.1 (d), 120.9 (d), 120.4 (s), 120.2 (d), 112.4 (d).

### 4.2.5 1-Methylbrassilexin (215)

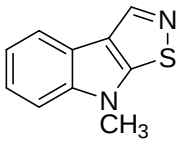


**215**

Sodium hydride (60% suspension in mineral oil, 35 mg, 1.46 mmol) was added to a solution of brassilexin (**24**) (51 mg, 0.29 mmol) in THF (3 ml) at 0 ºC under an argon atmosphere. After 15 minutes of stirring at 0 ºC, methyl iodide (27 µl, 0.44 mmol) was added, and stirring was continued at 0 ºC for 1 more hour. Ice cold water was added to quench the reaction, the reaction mixture was extracted with $CH_2Cl_2$ (2 × 10 ml) and the combined extracts were dried and concentrated. The crude reaction mixture was subjected to column chromatography on silica gel ($CH_2Cl_2$/hexane, 80:20) to yield 1-methylbrassilexin (**215**, 52 mg, 94%) (Pedras and Hossain, 2006)

Mp: 68-69 ºC ($CH_2Cl_2$-hexane)

HPLC $t_R$ = 16.9 min.

$^{1}$H NMR (500 MHz, $CD_3CN$) δ 8.71 (s, 1H), 7.93 (d, *J* = 8 Hz, 1H), 7.48 (d, *J* = 8 Hz, 1H), 7.40 (dd, *J* = 7.5, 8 Hz, 1H), 7.27 (dd, *J* = 7.5, 7.5 Hz, 1H), 3.88 (s, 3H).

$^{13}C$ NMR (125.8 MHz, $CD_3CN$): δ 162.2 (s), 148.4 (d), 145.2 (s), 125.9 (s), 124.0 (d), 120.8 (d), 120.4 (d), 120.4 (s), 110.3 (d), 33.2 (q).

HRMS-EI *m/z*: measured 188.04082 ($[M]^+$, calcd. 188.040773 for $C_{10}H_8N_2S$).

MS-EI *m/z* (% relative intensity): 188 ($[M]^+$, 100), 155 (15), 146 (11).

FTIR $\nu_{max}$: 1490, 1464, 1319, 1261, 912, 743 $cm^{-1}$.

### 4.2.6 Sinalexin (25)

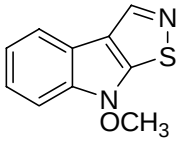


**25**

2-Phenylacetylchloride (**206**) (428 μl, 3.23 mmol) was added to a vigorously stirred solution of methoxylamine hydrochloride (297 mg, 3.56 mmol) and sodium carbonate (686 mg, 6.47 mmol) in a mixture of benzene (6 ml) and water (6 ml) with cooling at 0 ºC. The reaction mixture was stirred for ca. 4 hours at room temperature, and extracted with EtOAc (3 × 20 ml). The combined extracts were washed with brine, dried over $Na_2SO_4$, filtered and concentrated under reduced pressure. The residue was subjected to column chromatography on silica gel (EtOAc/hexane 3:2) to afford N-methoxy-2-phenylacetamide (**207**, 452 mg, 85%).

To a solution of N-methoxy-2-phenylacetamide (**207**) (399 mg, 2.42 mmol) in $CH_2Cl_2$ (10 ml) was added slowly t-butyl hypochlorite (339 mg, 3.12mmol) at 0 ºC. The reaction mixture was stirred at 0 °C in dark for about 20 minutes, solvent was evaporated under reduced pressure, and the residue was subjected to FCC on silica gel

(EtOAc/hexane 1:5) to afford *N*-chloro-*N*-methoxy-2-phenylacetamide ( **208**, 458 mg, 95%) as a yellow oil (Kawase et al., 1989).

The *N*-chloro-*N*-methoxy-2-phenylacetamide (**208**) (400 mg, 2 mmol) was dissolved in TFA (0.6 ml) and was added to a solution of silver carbonate (654 mg, 4 mmol) in TFA (4 ml) at 0 °C with stirring. The stirring was continued for 30 minutes to complete the reaction and then the solvent was removed under reduced pressure. The residue was basified with 5% $Na_2CO_3$ with cooling at 0º C, the precipitated salts were filtered off, and the filter cake was washed with $CH_2Cl_2$. The aqueous solution was extracted with $CH_2Cl_2$ (3 × 15 ml). The combined $CH_2Cl_2$ solution was washed with brine, dried over $Na_2SO_4$, and concentrated under reduced pressure. The residue was purified by column chromatography on silica gel, eluting with EtOAc/hexane (2:5) to yield 1-methoxy-2-oxindole (**209**, 225 mg, 69%).

To a solution of 1-methoxy-2-oxindole (**209**) (150 mg, 0.92 mmol) and $P_4S_{10}$ (245 mg, 0.55 mmol) in THF (3.5 ml) was added sodium bicarbonate in small portions at room temperature. The reaction mixture was stirred at room temperature for about 15 hours, the THF was removed and water was added to the residue. The suspension was then extracted with $CH_2Cl_2$ (3 × 30 ml). The combined extracts were dried over $Na_2SO_4$, concentrated under reduced pressure and the residue was crystallized from EtOH/water mixture to yield 1-methoxyindoline-2-thione (**210**) (142 mg, 86%).

The thione **210** (58 mg, 0.32 mmol) dissolved in dry DMF (1 ml) was first treated with $POCl_3$ (90 μL, 0.98 mmol) (3 h at 40° C), and then the reaction mixture was cooled to 0° C, basified with aqueous $NH_3$ (pH > 11), and extracted with $CH_2Cl_2$ (3 × 15 ml). The combined $CH_2Cl_2$ extracts were dried and concentrated under reduced pressure. The reaction residue was dissolved in pyridine (1 ml) and $I_2$ (85 mg) (1.5 hour at room temperature). The mixture was then acidified with 1.5 M $H_2SO_4$ (15 ml) and extracted with $CH_2Cl_2$ (3×15 ml). After evaporation of $CH_2Cl_2$ the residue was purified

by column chromatography on silica gel, eluting with ether/hexane (1:9) to give sinalexin (**25**, 24 mg, 36%) (Pedras and Jha, 2005).

HPLC $t_R$ = 20.1 min

$^1$H NMR (500 MHz, $CD_3CN$) δ 8.72 (s, 1H), 7.94 (d, *J* = 8 Hz, 1H), 7.58 (d, *J* = 8 Hz, 1H), 7.44 (m, 1H), 7.31 (m, 1H), 4.16 (s, 3H).

$^{13}$C NMR (125.8 MHz, $CD_3CN$): δ 156.2 (s), 148.5 (d), 141.7 (s), 124.8 (d), 124.3 (s), 122.0 (d), 120.8 (d), 117.5 (s), 109.7 (d), 64.7 (q).

### 4.2.7 Brassicanal A (34)

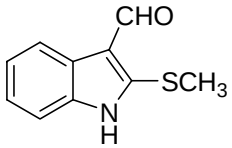


**34**

NaH (60%, 514 mg, 21.4 mmol, washed with hexane) was added to a solution of indoline-2-thione (**205**) (159 mg, 1.1 mmol) in HCOOEt (4 ml, 40 mmol), and the reaction mixture was stirred at room temperature. After 3 hours, the reaction mixture was diluted with water, the mixture was acidified with 2.5 M HCl, and the precipitate formed was filtered off and washed with water. The precipitate was dried to yield 2-mercaptoindole-3-carboxaldehyde (**48**) in 99% yield.

To a solution of 2-mercaptoindole-3-carboxaldehyde (**48**) (178 mg, 1 mmol) in $Et_2O$ (7 ml) a solution of diazomethane (5 ml) in $Et_2O$ was added. After stirring the reaction mixture at room temperature for 2 hours, the solvent was removed and the residue was subjected to FCC on silica gel ($CH_2Cl_2$-MeOH, 99:1) to afford brassicanal A (**34**, 54% yield from **205**) (Pedras and Okanga, 1999).

HPLC $t_R$ = 10.8 min

$^1$H NMR (500 MHz, $CD_3CN$) δ 10.16 (s, 1H), 8.07 (d, *J* = 7.5 Hz, 1H), 7.47 (d, *J* = 7 Hz, 1H), 7.26-7.24 (m, 2H), 2.67 (s, 3H).

$^{13}$C NMR (125.8 MHz, $CD_3CN$): δ 184.7 (d), 146.6 (s), 137.9 (s), 127.2 (s), 124.4 (d), 123.6 (d), 120.5 (d), 116.8 (s), 112.2 (d), 16.9 (q).

HRMS-EI *m/z*: measured 191.0402 ($[M]^+$, calcd. 191.0405 for $C_{10}H_9NOS$).

MS-EI *m/z* (% relative intensity): 191 ($[M]^+$, 100), 176 (23), 158 (55), 148 (13).

## 4.2.8 Spirobrassinin (27)

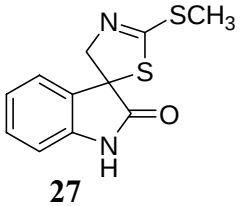


**27**

### *4.2.8.1 Synthesis*

Isatin (**212**) (1.0 g, 6.8 mmol) was suspended in a solution of nitromethane (1.6 g, 27.2 mmol) and EtOH (2 ml). After cooling to 0 ºC, $Et_3N$ (150 µl) was added and the mixture was kept at -10 °C for 24 hours. The resulting precipitate was filtered, washed with cold $CHCl_3$ and air dried to yield (3-hydroxy-2-oxindol-3-yl)nitromethane (**213**, 1.3 g). The (3-hydroxy-2-oxindol-3-yl)nitromethane (**213**) (1.30 g, 6.24 mmol) was dissolved in a mixture of MeOH (20 ml) and glacial acetic acid (700 µl) and 10% Pd/C (130 mg) was added. The reduction was performed at atmospheric pressure of $H_2$. Reaction mixture was stirred for 20 hours, filtered, acidified with conc. HCl and the solvent was removed under reduced pressure. The residue was crystallized form glacial acetic acid. The crystals were washed with $Et_2O$ and dried to yield (3-hydroxy-2-oxindol-3-yl)methylammonium chloride (**214**, 758 mg, 57%).

To a solution of (3-hydroxy-2-oxindol-3-yl)methylammonium chloride (**214**) (400 mg, 1.86 mmol) in pyridine (2 ml) was added $Et_3N$ (395 µl, 2.79 mmol) and $CS_2$ (174 µl, 2.8 mmol) at 0 ºC. After 2 hours of stirring at 0 ºC, $CH_3I$ (153 µl, 2.42 mmol) was added and the mixture was stirred at room temperature for 4 hours. The mixture was acidified with 1.5 M $H_2SO_4$ (30 ml), extracted with EtOAc (2 × 50 ml), dried over $Na_2SO_4$, and concentrated under reduced pressure. The residue was subjected to column chromatography on silica gel [gradient elution, acetone/hexane (10:90, 20:80, 30:70, 40:60)] to afford dioxibrassinin (**26**) (373 mg, 75%).

The dioxibrassinin (**26**) (79 mg, 0.29 mmol) was dissolved in pyridine (0.8 ml) and $SOCl_2$ (63 mg, 39 µl, 0.53 mmol) was added in portions with continuous stirring. After one hour stirring at room temperature, the reaction mixture was acidified with 5% HCl (10 ml), extracted with EtOAc (2 × 20 ml), the extracts were dried over $Na_2SO_4$ and concentrated. The residue was subjected to column chromatography on silica gel ($CH_2Cl_2$-MeOH, 99:1)]. Finally, pure spirobrassinin (**27**, 61 mg, 82%) was obtained after crystallization from acetone-hexane mixture (Monde et al., 1994).

HPLC $t_R$ = 12.8

$^1$H NMR (500 MHz, $CD_3CN$): δ 8.59 (br, s, 1H), 7.35 (d, *J* = 7.5 Hz, 1H), 7.28 (ddd, *J* = 7.5, 7.5, 1 Hz, 1H), 7.08 (ddd, *J* = 7.5, 7.5, 1 Hz, 1H), 6.93 (d, *J* = 7.5 Hz, 1H), 4.56 (d, *J* = 15.5 Hz, 1H), 4.44 (d, *J* = 15.5 Hz, 1H), 2.60 (s, 3H).

$^{13}$C NMR (125.8 MHz, $CD_3CN$): δ 177.5 (s), 163.2 (s), 141.1 (s), 130.9 (s), 130.1 (d), 124.6 (d), 123.4 (d), 110.5 (d), 75.0 (t), 64.8 (s) 15.3 (q).

### *4.2.8.2 Enantioresolution*

**Synthesis of diastereomeric amides**

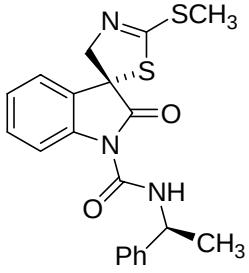

(+)-**218**

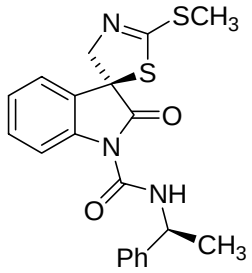

(+)-**219**

(*S*)-(-)-1-Phenylethyl isocyanate (**217**, 50 mg, 48 μL, 0.34 mmol) and $Et_3N$ (32 mg, 43 μL, 0.31 mmol) were added to a solution of (±)-spirobrassinin (**27**, 60 mg, 0.24 mmol) in dry acetone (1.5 ml) were added. After stirring for 48 hours at room temperature, the reaction mixture was concentrated and the residue was submitted to column chromatography ($CH_2Cl_2$). The first fraction gave (+)-**218** (34 mg, 36%) and the second fraction afforded (+)-**219**, contaminated with (+)-**218**. Repeated chromatography of the second fraction afforded pure (+)-**219** (19 mg, 20%) (Suchy et al., 2001).

**(+)-*N*1-[(1*S*)-1-Phenylethyl]-1-[(*R*)-spirobrassinin]carboxamide [(+)-218]**

$[\alpha]^{23}_D$ = +64 (*c* 2.54, $CH_2Cl_2$)

$^1$H NMR (500 MHz, $CDCl_3$): δ 8.81 (br d, *J* = 7 Hz, 1H, NH), 8.23 (d, *J* = 8 Hz, 1H), 7.37 (m, 6H), 7.29 (m, 1H), 7.24 (dd, *J* = 7.5, 7.5 Hz, 1H), 5.13 (quintet, *J* = 7 Hz, 1H), 4.72 (d, *J* = 15 Hz, 1H), 4.52 (d, *J* = 15 Hz, 1H), 2.72 (s, 3H), 1.60 (d, *J* = 7 Hz, 3H).

$^{13}$C NMR (125.8 MHz, $CDCl_3$): 179.2 (s), 164.0 (s), 150.6 (s), 143.0 (s), 139.1 (s), 130.2 (d), 128.7 (d), 128.3 (s), 127.4 (d), 126.1 (d), 125.6 (d), 123.7 (d), 116.7 (d), 75.5 (t), 65.5 (s), 50.0 (d), 22.7 (q), 15.7 (q).

HRMS-EI *m/z*: measured 397.0916 ($[M]^+$, calcd. 397.0919 for $C_{20}H_{19}N_3O_2S_2$).

MS-EI *m/z* (% relative intensity): 397 ($[M]^+$, 8), 250 (100), 249 (23), 202 (17), 177 (27), 145 (21), 132 (13), 105 (34).

**(+)-*N*1-[(1*S*)-1-Phenylethyl]-1-[(*S*)-spirobrassinin]carboxamide [(+)-219]**

$[\alpha]^{25}_D$ = +19 (*c* 2.97, $CH_2Cl_2$)

$^1$H NMR (500 MHz, $CDCl_3$) δ 8.79 (br d, *J* = 7 Hz, 1H, NH), 8.24 (d, *J* = 8 Hz, 1H), 7.37 (m, 6H), 7.29 (m, 1H), 7.24 (dd, *J* = 7.5, 7.5 Hz, 1H), 5.13 (quintet, *J* = 7 Hz, 1H), 4.76 (d, *J* = 15 Hz, 1H), 4.56 (d, *J* = 15 Hz, 1H), 2.74 (s, 3H), 1.60 (d, *J*= 7 Hz, 3H).

$^{13}$C NMR (125.8 MHz, $CDCl_3$): 179.2 (s), 164.1 (s), 150.6 (s), 142.9 (s), 139.3 (s), 130.2 (d), 128.9 (d), 128.4 (s), 127.4 (d), 126.1 (d), 125.6 (d), 123.7 (d), 116.6 (d), 75.5 (t), 65.5 (s), 50.2 (d), 22.7 (q), 15.7 (q).

HRMS-EI *m/z*: measured 397.0908 ($[M]^+$, calcd. 397.0919 for $C_{20}H_{19}N_3O_2S_2$).

MS-EI *m/z* (% relative intensity): 397 ($[M]^+$, 9), 250 (100), 249 (27), 202 (18), 177 (31), 148 (20), 144 (19), 132 (13), 105 (34).

**Synthesis of enantiomers of spirobrassinin [(*R*)-(+)-27, (*S*)-(-)-27]**

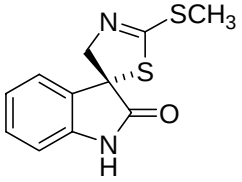


(*R*)-(+)-**27**

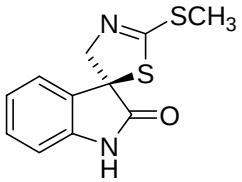


(*S*)-(-)-**27**

To a stirred solution of (+)-**218** or (+)-**219** (65 mg, 0.16 mmol) in dry $CH_3OH$ (4 ml) was added a solution of $CH_3ONa$ (89 mg, 1.7 mmol) in dry $CH_3OH$ (2 ml) within 5 min at -10 °C. After being stirred at the same temperature for 40 min, the reaction mixture was diluted with water (1 ml) and neutralized with 1 N HCl. After removal of $CH_3OH$, the product was extracted with EtOAc, and the extract was dried

over $Na_2SO_4$ and was concentrated in vacuo. Purification of the residue by flash chromatography ($CH_2Cl_2/CH_3OH$ 99:1) afforded (*R*)-(+)-**27** [15 mg, 37% from (+)-**218**] and (*S*)-(-)-**27** [12 mg, 30% from (+)-**219**] (Suchy et al., 2001).

**(*R*)-(+)-Spirobrassinin [(*R*)-(+)-27]:** $[\alpha]^{24}_D$ +83 (*c* 0.38, $CH_2Cl_2$), $^1$H NMR, UV and HPLC retention time identical with those of synthetic (±)-spirobrassinin.

**(*S*)-(-)-Spirobrassinin [(*S*)-(-)-27]:** $[\alpha]^{24}_D$ -84 (*c* 0.36, $CH_2Cl_2$); $^1$H NMR, UV and HPLC retention time were identical with those of synthetic (±)-spirobrassinin.

### 4.2.9 1-Methylspirobrassinin (216)

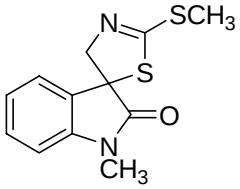


**216**

Sodium hydride (60% suspension in mineral oil, 30.6 mg, 1.28 mmol) was added to a solution of spirobrassinin **(27)** (127 mg, 0.51 mmol) in THF (10 mL) at 0º C under argon atmosphere. The reaction mixture was allowed to stir for 10 minutes, methyl iodide (49 µl, 0.77 mmol) was added and stirring at room temperature was continued for 4 hours. Ice cold water was added to quench the reaction, the reaction mixture was extracted with EtOAc (3×30 ml) and the combined extracts were dried and concentrated. The crude reaction mixture was subjected to column chromatography on silica gel ($CH_2Cl_2/CH_3OH$, 99:1) to yield 1-methylspirobrassinin (**216**) (125 mg, 93%) (Pedras and Hossain, 2006).

HPLC $t_R$ = 15.9 min.

$^{1}$H NMR (500 MHz, $CD_3CN$): δ 7.38-7.36 (m, 2H), 7.12 (ddd, *J* = 7.5, 7.5, 1 Hz, 1H), 6.95 (d, *J* = 7.5 Hz, 1H), 4.53 (d, *J* = 15.5 Hz, 1H), 4.44 (d, *J* = 15.5 Hz, 1H), 3.17 (s, 3H).

$^{13}$C NMR (125.8 MHz, $CD_3CN$): δ 176.0 (s), 163.2 (s), 143.5 (s), 130.5 (s), 130.1 (d), 124.1 (d), 123.6 (d), 109.2 (d), 75.0 (t), 64.5 (s), 26.7 (q), 15.3 (q).

HRMS-EI *m/z*: measured 264.0389 ($[M]^+$, calcd. 264.0389 for $C_{12}H_{12}N_2OS_2$).

MS-EI *m/z* (% relative intensity): 264 ($[M]^+$, 67), 217 (82), 191 (100), 159 (22), 158 (21), 130 (41), 87 (41), 71 (32).

FTIR $\nu_{max}$ (KBr): 2934, 2855, 1737, 1620, 1581, 1465, 1086, 945, 743 $cm^{-1}$.

### 4.2.10 1-Methoxyspirobrassinin (28)

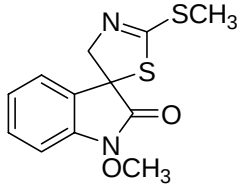


**28**

To a stirred solution of 1-methoxybrassinin (**11**) (62.5 mg, 0.24 mmol) in a mixture of dioxane/water (95:5, 5.4 ml) was added a freshly prepared solution of dioxane dibromide (DDB, 2.2 ml, 0.25 mmol; the stock solution was obtained by dissolving of 26.7 μl of bromine in 4 ml of dioxane). The reaction mixture was stirred for 10 minutes at room temperature, then $Et_3N$ (35 μl, 0.25 mmol) was added. The mixture was poured into water (30 ml), extracted with diethyl ether (2 × 30 ml), and the extracts were dried over $Na_2SO_4$. The residue obtained after evaporation of the solvent was subjected to flash column chromatography on silica gel (EtOAc/hexane, 1:5) to obtain 1-methoxyspirobrassinol (**29**, 67 mg) in 86% yield. To a stirred solution of 1-methoxyspirobrassinol (**29**) (57 mg, 0.2 mmol) in 98% acetic acid (4.8 ml) was added

$CrO_3$ (22 mg, 0.22 mmol). After stirring for 1 hour at room temperature, the reaction mixture was poured into water and extracted with diethyl ether. The extracts were dried over $Na_2SO_4$ and concentrated. The residue was subjected to PTLC on silica gel ($CH_2Cl_2$/MeOH, 98/2) to afford 1-methoxyspirobrassinin (**28**, 17 mg, 30%) (Kutschy et al., 2002).

HPLC $t_R$ = 16.9 min

$^1$H NMR (500 MHz, $CD_3CN$) δ 7.44-7.39 (m, 2H), 7.17 (dd, *J* = 7.5, 7.5 Hz, 1H), 7.06 (d, *J* = 7.5 Hz, 1H), 4.59 (d, *J* = 15.5 Hz, 1H), 4.46 (d, *J* = 15.5 Hz, 1H), 3.99 (s, 3H), 2.61 (s, 3H).

$^{13}$C NMR (125.8 MHz, $CD_3CN$): δ 171.0 (s), 163.2 (s), 140.0 (s), 130.3 (d), 126.9 (s), 124.6 (d), 124.3 (d), 108.2 (d), 74.6 (t), 72.6 (s), 63.9 (q), 15.3 (q).

HRMS-EI *m/z*: measured 280.0336 ($[M]^+$, calcd. 280.0339 for $C_{12}H_{12}N_2O_2S_2$).

MS-EI *m/z* (% relative intensity): 280 ($[M]^+$, 100), 252 (9), 249 (13), 234 (15), 221 (25), 176 (52), 148 (50), 87 (37).

FTIR $\nu_{max}$ (KBr): 2925, 2854, 1737, 1618, 1584, 1465, 1086, 945, 747 $cm^{-1}$.

### 4.2.11 Camalexin (31)

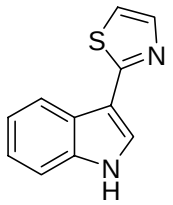

**31**

Methyl iodide (295 μL, 4.75 mmol) was added slowly by injection at room temperature under argon atmosphere to magnesium turning (77 mg, 3.2 mmol) in dry ether (15 ml). After all magnesium had reacted, the ether was distilled off and dry benzene (7 ml) was added. A solution of indole (**211**) (200 mg, 1.7 mmol) in benzene (1 ml) was added to the solution of methyl magnesium iodide in benzene and stirred for 15 minutes after which 2-bromothiazole was added. After refluxing at 90 ºC for 24 h, the reaction mixture was poured into 20 ml of saturated $NH_4Cl$ solution and was extracted with EtOAc (2 × 20 ml). The EtOAc extract was dried over $Na_2SO_4$, concentrated under reduced pressure and the residue was chromatographed first with normal phase column using silica gel (EtOAc/hexane, 20/80) and then with reverse phase column using $C_{18}$ ($H_2O/CH_3CN$, 60/40) to yield camalexin (**31**, 191 mg, 60%) as an off white solid (Ayer et al., 1992).

$^1$H NMR (500 MHz, $CD_3CN$): δ 9.79 (br, s, $D_2O$ exchangeable, 1H), 8.24 (dd, *J* = 9, 2.5 Hz, 1H) 7.91 (d, *J* = 3 Hz, 1H), 7.77 (d, *J* = 3.5 Hz, 1H), 7.52 (dd, *J* = 9, 2.5 Hz, 1H), 7.33 (d, *J* = 3.5 Hz, 1H), 7.35 (m, 2H).

$^{13}$C NMR (125.8 MHz, $CD_3CN$): δ 166.1 (s), 145.5 (d), 140.0 (s), 128.9 (d), 127.5 (s), 125.6 (d), 124.1 (d), 123.5 (d), 118.9 (d), 115.0 (d), 114.3 (s).

HRMS-EI *m/z*: measured 200.0408 ($[M]^+$, calcd. 200.0408 for $C_{11}H_8N_2S$).

MS-EI *m/z* (% relative intensity): 200 ($[M]^+$, 100), 142 (20), 56 (18).

### 4.2.12 5-Fluorocamalexin (244)

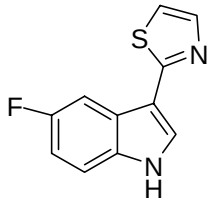


**244**

This compound was prepared as described above for camalexin (**31**) using 5-fluoroindole (**257**) (100 mg, 0.74 mmol), $Et_2O$ (10 ml), magnesium turning (31 mg, 1.3 mmol), $CH_3I$ (120 µl, 1.9 mmol), 2-bromothiazole (80 µl, 0.89 mmol) and benzene (6 ml) yielding 5-fluorocamalexin (**244**, 70 mg, 57% based on recovered starting material) after purification by normal (silica gel, EtOAC/hexane, 20/80) and reverse phase ($C_{18}$, $CH_3CN/H_2O$, 35/65) column chromatography as an off white solid (Pedras and Liu, 2004).

$^1$H NMR (500 MHz, $CDCl_3$): δ 7.99 (s, 1H), 7.81 (dd, $J$ = 9, 2.5 Hz, 1H), 7.80 (d, $J$ = 3.5 Hz, 1H), 7.45 (dd, $J$ = 9, 4.5 Hz, 1H), 7.44 (d, $J$ = 3.5 Hz, 1H), 7.02 (ddd, $J$ = 9, 9, 2.5 Hz, 1H).

$^{13}$C NMR (125.8 MHz, $CDCl_3$): δ 164.4 (s), 159.0 (d, $^1J_{C\text{-}F}$ = 235 Hz), 142.0 (s), 134.0 (s), 127.5 (s), 125.2 (d, $^3J_{C\text{-}F}$ = 10 Hz), 116.1 (s), 113.1 (d, $^3J_{C\text{-}F}$ = 10 Hz), 111.3 (d, $^4J_{C\text{-}F}$ = 5 Hz), 111.0 (d, $^2J_{C\text{-}F}$ = 26 Hz), 104.9 (d, $^2J_{C\text{-}F}$ = 25 Hz).

HRMS-EI *m/z*: measured 218.0312 ($[M]^+$, calcd. 218.0314 for $C_{11}H_7N_2FS$).

MS-EI *m/z* (% relative intensity): 218 ($[M]^+$, 100), 58 (20).

### 4.2.13 6-Fluorocamalexin (75)

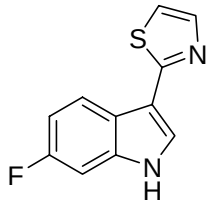

**75**

This compound was prepared as described above for camalexin (**31**) using 6-fluoroindole (**258**) (100 mg, 0.74 mmol), $Et_2O$ (10 ml), magnesium turning (31 mg, 1.3 mmol), $CH_3I$ (120 µl, 1.9 mmol), 2-bromothiazole (80 µl, 0.89 mmol) and benzene (6 ml) yielding 6-fluorocamalexin (**75**, 75 mg, 60%, based on recovered starting material) after purification by normal (silica gel, EtOAC/hexane, 20/80) and reverse phase ($C_{18}$, $CH_3CN/H_2O$, 35/65) column chromatography as an off white solid (Pedras and Ahiahonu, 2002).

$^1$H NMR (500 MHz, $CD_3CN$): δ 9.75 (br, s, $D_2O$ exchangeable, 1H), 8.25 (dd, $J$ = 9, 5.5 Hz, 1H) 7.90 (s, 1H), 7.77 (d, $J$ = 3.5 Hz, 1H), 7.34 (d, $J$ = 3.5 Hz, 1H), 7.23 (dd, $J$ = 10, 2.5 Hz, 1H), 7.04 (ddd, $J$ = 10, 9, 2.5 Hz, 1H).

HRMS-EI *m/z*: measured 218.0313 ($[M]^+$, calcd. 218.0314 for $C_{11}H_7N_2FS$).

MS-EI *m/z* (% relative intensity): 218 ($[M]^+$, 100), 58 (20).

## 4.3 Synthesis of potential brassinin detoxification inhibitors

### 4.3.1 Methyl (indol-2-yl)methyldithiocarbamate (240)

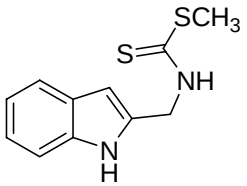


**240**

To a solution of indole-2-carboxylic acid (**251**, 1.6 g, 10 mmol) in EtOH (15 ml) was added $H_2SO_4$ (0.5 ml). The mixture was refluxed at 115 °C for 20 hours with stirring, cooled to room temperature and diluted with $CH_2Cl_2$ (30 ml). The reaction mixture was then washed with 10% $Na_2CO_3$ (2×20 ml) and water. The organic layer was dried over $Na_2SO_4$ and concentrated. The residue was subjected to FCC on silica gel (Acetone-hexane, 30/70) to afford ethyl indole-2-carboxylate (**252**, 1.6 g) in 85% yield.

The carboxylate **252** (959 mg, 5.1 mmol) was dissolved in dry THF (Ar atmosphere, 17 ml) and the solution was cooled to 0 °C with stirring. $LiAlH_4$ (230 mg, 6.1 mmol) was then added in small portions during 10 minutes and stirring was continued for further 1 hour at 0 °C. Reaction was quenched with 5 N NaOH (1 ml) and the precipitate was filtered off through a celite pad. The celite pad was washed with THF, the filtrate was dried ($Na_2SO_4$) and concentrated under reduced pressure to yield indole-2-methanol (**253**, 790 mg). The crude alcohol **253** (774 mg, 5.3 mmol) was dissolved in $CH_2Cl_2$ (20 ml), $MnO_2$ was added and the mixture was stirred for 18 h at room temperature. $MnO_2$ was filtered off, the filter cake was washed with acetone and the filtrate was concentrated under reduced pressure to yield indole-2-carboxaldehyde (**254**, 620 mg, 81%) as a brown solid (Meyer and Kruse, 1984).

To a solution of indole-2-carboxaldehyde (**254**, 550 mg, 3.8 mmol) in EtOH (10 ml), a solution of $NH_2OH.HCl$ (792 mg, 11.4 mmol) and $Na_2CO_3$ (645 mg, 6.1 mmol) in water (5 ml) was added. After refluxing for 1 hour at 95 °C, EtOH was removed under reduced pressure, water (5 ml) was added and the resulting precipitate was filtered off and air dried to afford indole-2-carboxaldehyde oxime (**255**, 601 mg) in 99% yield.

The oxime (215 mg, 1.3 mmol) and $NiCl_2.6H_2O$ (319 mg, 1.3 mmol) were dissolved in MeOH (20 ml). $NaBH_4$ (320 mg, 8.5 mmol) was added and the mixture was stirred for 5 min. at room temperature. The black precipitate was filtered off, filtrate was concentrated (*ca*. 25%) and then poured into 30 ml of 1% aqueous $NH_4OH$. The mixture was extracted with EtOAc (2×30 ml), the combined organic extracts were dried over $Na_2SO_4$ and concentrated. The residue was dissolved in pyridine (0.5 ml) and $Et_3N$ (208 µl, 1.5 mmol), cooled to 0˚ C and treated with $CS_2$ (180 µl, 3 mmol). After stirring for 1 hour at 0 ˚C, $CH_3I$ (140 µl, 2.3 mmol) was added and the reaction mixture was kept at 3 ˚C for 15 hours. The reaction mixture was poured into 1.5 M cold $H_2SO_4$ (15 ml) and immediately extracted with $Et_2O$ (2 x 15 ml). The extracts were dried over $Na_2SO_4$ and concentrated under reduced pressure. The residue was subjected to FCC on silica gel [gradient solvent, $CH_2Cl_2$-hexane (30:70, 40:60 & 50:50)] to give methyl (indol-2-yl)methyldithiocarbamate (**240**) (138 mg, 43% from oxime **255**) (Pedras et al., 2006a).

Mp = 83-84 ˚C

HPLC $t_R$ = 21.3 min

$^1$H NMR (500 MHz, $CDCl_3$): δ 8.94 (br, s, $D_2O$ exchangeable, 1H), 7.59 (d, *J* = 8 Hz, 1H), 7.36 (d, *J* = 8 Hz, 2H, 1H $D_2O$ exchangeable), 7.21 (dd, *J* = 8, 8 Hz, 1H), 7.12 (dd, *J* = 8, 8 Hz, 1H), 6.43 (s, 1H), 5.09 (d, *J* = 5.5 Hz, 2H), 2.69 (s, 3H)..

$^{13}$C NMR (125.8 MHz, $CDCl_3$): δ 201.6 (s), 136.6 (s), 134.8 (s), 127.9 (s), 122.9 (d), 120.9 (d), 120.4 (d), 111.6 (d), 102.5 (d), 44.2 (t), 18.9 (q).

HRMS-EI *m/z*: measured 236.0445 ($[M]^+$, calcd. 236.0442 for $C_{11}H_{12}N_2S_2$).

MS-EI *m/z* (% relative intensity): 236 ($[M]^+$, 20), 188 (21), 163 (13), 130 (100).

FTIR $\nu_{max}$ (KBr): 3387, 3312, 2917, 1499, 1294, 1067, 919, 749 $cm^{-1}$.

## 4.3.2 Methyl (benzofuran-3-yl)methyldithiocarbamate (236)

### *4.3.2.1 Synthesis of ethyl (2-acetylphenoxy)acetate (260)*

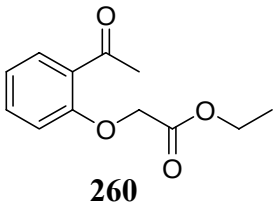

**260**

To a solution of 2′-hydroxyacetophenone (1.1 g, 8.0 mmol) in acetone (7 ml) were added anhydrous $K_2CO_3$ (1.2 g, 8.8 mmol) and ethyl chloroacetate (1.3 ml, 12 mmol). The mixture was refluxed at 65 ˚C for 56 hours. The formed precipitate was filtered off and washed with acetone. The filtrate was concentrated and the residue was subjected to FCC on silica gel ($CH_2Cl_2$, 100%) to afford ethyl (2-acetylphenoxy)acetate (**260**, 1.67 g, 92%) (Nielek and Lesiak, 1982).

$^1$H NMR (500 MHz, $CDCl_3$): δ 7.76 (dd, *J* = 7.5, 1.5 Hz,1H), 7.44 (ddd, *J* = 7.5, 7.5, 1.5 Hz, 1H), 7.05 (dd, *J* = 7.5, 7.5 Hz, 1H), 6.83 (d, *J* = 7.5 Hz, 1H), 4.73 (s, 2H), 4.28 (q, *J* = 7 Hz, 2H), 2.72 (s, 3H), 1.31 (t, *J* = 7 Hz, 3H).

$^{13}$C NMR (125.8 MHz, $CDCl_3$): δ 200.1 (s), 168.5 (s), 157.3 (s), 133.9 (d), 131.1 (d), 129.3 (s), 122.1 (d), 112.6 (d), 65.9 (t), 61.9 (t), 32.4 (q), 14.5 (q).

HRMS-EI *m/z*: measured 222.0888 ($[M]^+$, calcd. 222.0892 for $C_{12}H_{14}O_4$).

MS-EI *m/z* (% relative intensity): 222 ([M]$^+$, 31), 207 (29), 151 (63), 149 (100), 121 (68), 105 (34), 91 (34).

FTIR $\nu_{max}$ (KBr): 3107, 3073, 2978, 2929, 1757, 1668, 1597, 1488, 1410, 1302, 1214, 1167, 1082, 968, 761 cm$^{-1}$.

### *4.3.2.2 Synthesis of 2-acetylphenoxyacetic acid (261)*

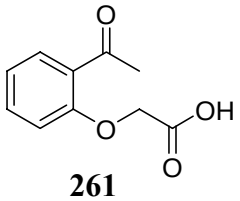


**261**

To a vigorously stirred solution of $Na_2CO_3$ (847 mg, 8.0 mmol) in water (12 ml), ethyl (2-acetylphenoxy)acetate (**260**, 1.36 g, 6.1 mmol) was added and the mixture was refluxed at 100 ˚C. After 1 hour refluxing, the reaction mixture was cooled to 0 ˚C and was acidified with concentrated HCl. The ppt was filtered off, washed with ice cold water and crystallized from hot water to yield 2-acetylphenoxyacetic acid (**261**, 1.1 g, 92 %) (Nielek and Lesiak, 1982).

Mp = 114-115 ˚C

$^1$H NMR (500 MHz, $CDCl_3$): δ 7.81 (dd, *J* = 8, 1.5 Hz,1H), 7.55 (ddd, *J* = 8, 8, 1.5 Hz, 1H), 7.15 (dd, *J* = 8, 8 Hz, 1H), 6.97 (d, *J* = 8 Hz, 1H), 4.79 (s, 2H), 2.70 (s, 3H).

$^{13}$C NMR (125.8 MHz, $CDCl_3$): δ 200.9 (s), 171.2 (s), 157.2 (s), 135.0 (d), 131.7 (d), 127.9 (s), 122.9 (d), 115.0 (d), 67.2 (t), 30.5 (q).

HRMS-EI *m/z*: measured 194.0581 ([M]$^+$, calcd. 194.0579 for $C_{10}H_{10}O_4$).

MS-EI *m/z* (% relative intensity): 194 ([M]$^+$, 5), 179 (8), 151 (22), 150 (14), 135 (37), 121 (100), 105 (14).

FTIR $\nu_{max}$ (KBr): 3088, 1736, 1661, 1597, 1485, 1452, 1422, 1359, 1299, 1238, 1168, 1131, 758 $cm^{-1}$.

### *4.3.2.3 Synthesis of 3-methylbenzofuran (262)*

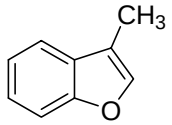


**262**

A mixture of 2-acetylphenoxyacetic acid (**261**, 1 g, 5.2 mmol), anhydrous NaOAc (1.8 g, 22.4 mmol) and $Ac_2O$ (4 ml, 36.4 mmol) was refluxed at 160 ˚C for 4 hours. After cooling to room temperature, the mixture was poured into water (20 ml) and extracted with $Et_2O$ (2×20 ml). The combined ether extracts were washed with 10% $Na_2CO_3$ solution (2×15 ml), dried over $Na_2SO_4$ and concentrated under reduced pressure. The residue was subjected to FCC on silica gel ($Et_2O$-hexane, 1:9) to afford 3-methylbenzofuran (**262**, 443 mg, 65%) (Nielek and Lesiak, 1982).

$^1$H NMR (500 MHz, $CDCl_3$): δ 7.61 (dd, $J$ = 8, 1 Hz, 1H), 7.55 (d, $J$ = 8 Hz, 1H), 7.48 (d, $J$ = 1 Hz, 1H), 7.39-7.32 (m, 2H), 2.32 (s, 3H).

$^{13}$C NMR (125.8 MHz, $CDCl_3$): δ 155.7 (s), 141.8 (d), 129.5 (s), 124.5 (d), 122.7 (d), 119.8 (d), 116.1 (s), 111.8 (d), 8.3 (q).

HRMS-EI *m/z*: measured 132.0578 ($[M]^+$, calcd. 132.0575 for $C_9H_8O$).

MS-EI *m/z* (% relative intensity): 132 ($[M]^+$, 94), 131 (100), 113 (8), 103 (11), 97 (12), 85 (13), 83 (14).

FTIR $\nu_{max}$ (KBr): 3061, 2922, 2862, 1588, 1451, 1280, 1186, 1087, 855, 788, 742 $cm^{-1}$.

### *4.3.2.4 Synthesis of benzofuran-3-carboxaldehyde (263) and benzofuran-3-methanol (264)*

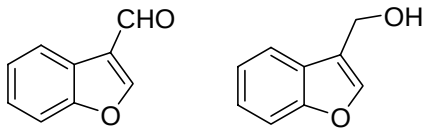


**263** **264**

$SeO_2$ (488 mg, 4.4 mmol) was added to a solution of 3-methylbenzofuran (**262**, 288 mg, 2.2 mmol) in 1,4-dioxane (3 ml) and the mixture was refluxed at 105 ˚C for 48 hours. Black precipitate was filtered off, washed with $CH_2Cl_2$ and the filtrate was concentrated under reduced pressure. The residue was subjected to FCC on silica gel eluted first with $CH_2Cl_2$-hexane, 3:7 and then with $CH_2Cl_2$, 100% to obtain benzofuran-3-carboxaldehyde (**263**, 280 mg, 88%) and benzofuran-3-methanol (**264**, 28 mg, 8%) respectively (Zaidlewicz et al., 2001).

**Benzofuran-3-carboxaldehyde (263)**

$^1$H NMR (500 MHz, $CDCl_3$): δ 10.20 (s, 1H), 8.29 (s, 1H), 8.21 (dd, *J* = 7, 1.5 Hz, 1H), 7.58 (dd, *J* = 7, 1.5 Hz, 1H), 7.45-7.39 (m, 2H).

$^{13}$C NMR (125.8 MHz, $CDCl_3$): δ 185.1 (d), 156.4 (s), 155.7 (d), 126.7 (d), 125.3 (d), 124.1 (s), 123.3 (s), 123.0 (d), 112.1 (d).

HRMS-EI *m/z*: measured 146.0361 ($[M]^+$, calcd. 146.0367 for $C_9H_6O_2$).

MS-EI *m/z* (% relative intensity): 146 ($[M]^+$, 79), 145 (100), 89 (25).

FTIR $\nu_{max}$ (KBr): 3132, 3086, 2827, 2741, 1680, 1556, 1480, 1449, 1121, 1075, 857, 785, 745 $cm^{-1}$.

**Benzofuran-3-methanol (264)**

$^1$H NMR (500 MHz, $CDCl_3$): δ 7.68 (d, 7.5 Hz, 1H), 7.62 (s, 1H), 7.51 (d, *J* = 8 Hz, 1H), 7.34 (dd, 8, 7.5 Hz, 1H), 7.29 (dd, 8, 7.5 Hz, 1H), 4.84 (s, 2H), 1.89 (s, 1H $D_2O$ exchangeable).

$^{13}$C NMR (125.8 MHz, $CDCl_3$): δ 156.02 (s), 142.7 (d), 127.1 (s), 125.0 (d), 123.2 (d), 120.8 (s), 120.3 (d), 112.0 (d), 56.1 (d).

HRMS-EI *m/z*: measured 148.0528 ($[M]^+$, calcd. 148.0524 for $C_9H_8O_2$).

MS-EI *m/z* (% relative intensity): 148 ($[M]^+$, 37), 147 (19), 132 (20), 131 (100), 103 (13), 91 (22), 77 (13).

FTIR $\nu_{max}$ (KBr): 3355, 3116, 3060, 2933, 2875, 1586, 1451, 1279, 1186, 1099, 1008, 856, 745 $cm^{-1}$.

### *4.3.2.5 Synthesis of benzofuran-3-carboxalde oxime (265)*

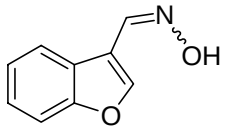


**265**

To a solution of benzofuran-3-carboxaldehyde (**263**, 285 mg, 1.95 mmol) in EtOH (24 ml) was added a solution of $NH_2OH.HCl$ (475 mg, 6.8 mmol) and $Na_2CO_3$ (371 mg, 3.5 mmol) in water (9 ml) and the mixture was refluxed for 2 hours at 95 ˚C. EtOH was removed under reduced pressure, water (10 ml) was added and the mixture was extracted with $Et_2O$ (2×20 ml). The combined organic extracts were dried over $Na_2SO_4$, concentrated under reduced pressure to leave chromatographically pure benzofuran-3-carboxaldehyde oxime (**265**, 265 mg, 84%).

### *4.3.2.6 Synthesis of benzofuran-3-methanamine (266)*

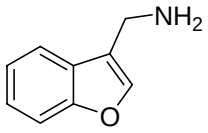

**266**

$Na(CN)BH_3$ (788 mg, 12.5 mmol) and $NH_4OAc$ (1.06 g, 13.7 mmol) were added to a cold solution (0 ˚C) of benzofuran-3-carboxaldehyde oxime (**265**, 202 mg, 1.25 mmol) in MeOH (1.5 ml). To this mixture, a neutralized (neutralization was carried out using 2 ml of 5N NaOH) solution of $TiCl_3$ (30% wt in 2N HCl, 5 ml) was added. After stirring for 20 min at 0 ˚C, the reaction mixture was diluted with 1% aqueous $NH_4OH$ (50 ml) and extracted with EtOAc (2×50 ml). The combined organic extracts were dried over $Na_2SO_4$, concentrated under reduced pressure to yield 200 mg of crude benzofuran-3-methanamine (**266**).

$^1$H NMR (500 MHz, $CD_3CN$): δ 7.69 (d, *J* = 7.5 Hz, 1H), 7.64 (s, 1H), 7.50 (d, *J* = 8 Hz, 1H), 7.33 (dd, *J* = 8, 8 Hz, 1H), 7.27 (dd, *J* = 8, 7.5 Hz, 1H), 3.94 (s, 2H).

$^{13}$C NMR (125.8 MHz, $CD_3CN$): δ 155.9 (s), 142.0 (d), 127.7 (s), 124.7 (d), 123.6 (s), 122.7 (d), 120.4 (d), 111.5 (d), 36.2 (t).

HRMS-EI *m/z*: measured 147.0683 ($[M]^+$, calcd. 147.0684 for $C_9H_9NO$).

MS-EI *m/z* (% relative intensity): 147 ($[M]^+$, 36), 146 (35), 132 (16), 131 (100), 130 (13).

FTIR $\nu_{max}$ (KBr): 3172, 3057, 2929, 2867, 1665, 1601, 1452, 1222, 1186, 1099, 856, 746 $cm^{-1}$.

### *4.3.2.7 Synthesis of methyl (benzofuran-3-yl)methyldithiocarbamate (236)*

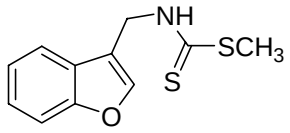


**236**

The crude amine (**266**, 200 mg, 1.4 mmol) was dissolved in pyridine (1 ml) and $Et_3N$ (390 µl, 2.8 mmol) and cooled to 0 ˚C. After adding $CS_2$ (336 µl, 5.6 mmol), the mixture was stirred for 1 hour at 0 ˚C, $CH_3I$ (262 µl, 4.2 mmol) was added and the mixture was kept at 3 ˚C for 15 hour. The reaction mixture was poured into water (15 ml) and extracted with $Et_2O$ (2×20 ml). The combined organic extracts were dried over $Na_2SO_4$ and concentrated under reduced pressure followed by addition of toluene (2×2 ml) and concentration under reduced pressure. Finally, the residue was subjected to FCC on silica gel ($CH_2Cl_2$-hexane, 3:7 and 5:5) to yield 145 mg of methyl (benzofuran-3-yl)methyldithiocarbamate (**236**) in 48% yield from the oxime (**265**).

Mp = 79-81 ˚C

HPLC $t_R$ = 24.3 min

$^1$H NMR (500 MHz, $CD_3CN$): δ 8.39 (br, s, 1H), 7.80 (s, 1H), 7.71 (d, *J* = 7.5 Hz, 1H), 7.54 (d, *J* = 7.5 Hz, 1H), 7.37 (dd, *J* = 7.5, 7.5 Hz, 1H), 7.31 (dd, *J* = 7.5, 7.5 Hz, 1H), 5.05 (d, *J* = 5 Hz, 2H), 2.59 (s, 3H).

$^{13}$C NMR (125.8 MHz, $CD_3CN$): δ 199.5 (s), 155.6 (s), 144.5 (d), 127.3 (s), 125.1 (d), 123.3 (d), 120.4 (d), 116.9 (s), 111.8 (d), 40.4 (t), 17.7 (q).

HRMS-EI *m/z*: measured 237.0275 ($[M]^+$, calcd. 237.0282 for $C_{11}H_{11}NOS_2$).

MS-EI *m/z* (% relative intensity): 237 ($[M]^+$, 10), 189 (16), 131 (100).

FTIR $\nu_{max}$ (KBr): 3339, 3232, 1498, 1451, 1379, 1322, 1305, 1185, 1101, 923, 856, 746 $cm^{-1}$.

### 4.3.3 Methyl (benzofuran-2-yl)methyldithiocarbamate (241)

#### *4.3.3.1 Synthesis of benzofuran-2-carboxaldehyde (268)*

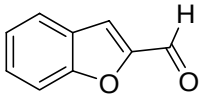

**268**

To a mixture of benzofuran (**267**, 1.02 g, 8.6 mmol) and DMF (4.0 ml, 51.8 mmol) was added $POCl_3$ (4.8 ml, 51.8 mmol) in small portions at room temperature. The mixture was refluxed at 95 ˚C for 16 hours, poured into ice cold water (50 ml) and basified with 5N NaOH (*ca.* 30 ml). The reaction mixture was extracted with $Et_2O$ (2×100 ml), the combined extracts were washed with brine and water and dried over $Na_2SO_4$. After evaporation of the solvent, the residue was subjected to FCC on silica gel ($CH_2Cl_2$-hexane, 1:1) to afford benzofuran-2-carboxaldehyde (**268**, 987 mg) in 78% yield (Jones and Stanforth, 1997; Suu et al., 1962).

$^1$H NMR (500 MHz, $CDCl_3$): δ 9.89 (s, 1H), 7.77 (d, *J* = 8 Hz, 1H), 7.62 (d, *J* = 8 Hz, 1H), 7.59 (s, 1H), 7.54 (ddd, *J* = 8, 8, 1 Hz, 1H), 7.36 (dd, *J* = 8, 8 Hz, 1H).

$^{13}$C NMR (125.8 MHz, $CDCl_3$): δ 180.1 (d), 156.7 (s), 153.2 (s), 129.5 (d), 127.1 (s), 124.6 (d), 124.0 (d), 117.8 (s), 113.1 (d).

HRMS-EI *m/z*: measured 146.0370 ($[M]^+$, calcd. 146.0368 for $C_9H_6O_2$).

MS-EI *m/z* (% relative intensity): 146 ($[M]^+$, 98), 145 (100), 118 (8), 89 (34).

FTIR $\nu_{max}$ (KBr): 3122, 3091, 2855, 1681, 1610, 1556, 1448, 1328, 1288, 1120, 948, 884, 832, 752 $cm^{-1}$.

### *4.3.3.2 Synthesis of benzofuran-2-carboxaldehyde oxime (269)*

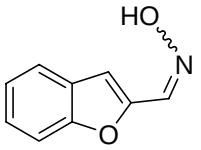


**269**

To a solution of benzofuran-2-carboxaldehyde (**268**, 843 mg, 5.8 mmol) in EtOH (30 ml) was added a solution of $NH_2OH.HCl$ (1.4 g, 20.2 mmol) and $Na_2CO_3$ (1.1 g, 10.4 mmol) in water (10 ml) and the mixture was refluxed for 2 hours at 95 ˚C. EtOH was removed under reduced pressure, the precipitate formed (in water) was filtered off, washed with ice cold water and air dried to yield chromatographically pure benzofuran-2-carboxaldehyde oxime (**269**, 870 mg) in 93% yield.

### *4.3.3.3 Synthesis of benzofuran-2-methanamine (270)*

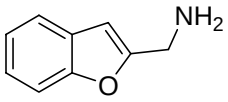


**270**

$Na(CN)BH_3$ (788 mg, 12.5 mmol) and $NH_4OAc$ (1.06 g, 13.7 mmol) were added to a cold solution (0 ˚C) of benzofuran-2-carboxaldehyde oxime (**269**, 202 mg, 1.25 mmol) in MeOH (1.5 ml). To this mixture, a neutralized (neutralization was carried out using 2 ml of 5N NaOH) solution of $TiCl_3$ (30% wt in 2N HCl, 5 ml) was added. After stirring for 30 min at 0 ˚C, the reaction mixture was basified with 5N NaOH (~3 ml), diluted with 1% aqueous $NH_4OH$ (50 ml) and extracted with EtOAc (2×50 ml). The combined organic extracts were dried over $Na_2SO_4$ and concentrated under reduced pressure to yield 244 mg of crude benzofuran-2-methanamine (**270**) as colorless oil.

$^1$H NMR (500 MHz, $CD_3CN$): δ 7.57 (d, $J$ = 7.5 Hz, 1H), 7.47 (d, $J$ = 8 Hz, 1H), 7.28-7.21 (m, 2H), 6.62 (s, 1H), 3.91 (s, 2H).

$^{13}C$ NMR (125.8 MHz, $CD_3CN$): δ 161.4 (s), 155.1 (s), 129.2 (s), 123.9 (d), 123.0 (d), 121.1 (d), 111.0 (d), 101.8 (d), 39.7 (t).

HRMS-EI *m/z*: measured 147.0682 ($[M]^+$, calcd. 147.0684 for $C_9H_9NO$).

MS-EI *m/z* (% relative intensity): 147 ($[M]^+$, 28), 146 (52), 132 (11), 131 (100), 130 (34).

FTIR $\nu_{max}$ (KBr): 3379, 3286, 3055, 2912, 2849, 1602, 1453, 1252, 1175, 945, 876, 801 $cm^{-1}$.

### *4.3.3.4 Synthesis of methyl (benzofuran-2-yl)methyldithiocarbamate (241)*

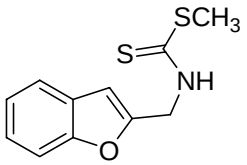


**241**

$CS_2$ (408 μl, 6.8 mmol) was added to a cold (0 ˚C) solution of crude benzofuran-2-methanamine (**270**, 244 mg, 1.7 mmol) and $Et_3N$ (463 μl, 3.3 mmol) in pyridine (1 ml). After stirring for 1 hour at 0 ˚C, $CH_3I$ (318 μl, 5.1 mmol) was added and the mixture was kept at 3 ˚C for 15 hours. The reaction mixture was poured into water (20 ml) and extracted with $Et_2O$ (2×20 ml). The combined organic extracts were dried over $Na_2SO_4$ and concentrated under reduced pressure. Toluene (2×2 ml) was added to the residue to make an azeotropic mixture with pyridine and a rotary evaporator was used to remove them. Finally, the residue was subjected to FCC on silica gel ($CH_2Cl_2$-hexane, 3:7 and 5:5) to afford methyl (benzofuran-2-yl)methyldithiocarbamate (**241**, 167 mg, 56% yield from oxime **269**) as colorless oil.

HPLC $t_R$ = 24.7 min

$^{1}$H NMR (500 MHz, $CD_3CN$): δ 8.48 (br, s, 1H), 7.60 (d, *J* = 7.5 Hz, 1H), 7.50 (d, *J* = 7.5 Hz, 1H), 7.32 (dd, *J* = 7.5, 7.5 Hz, 1H), 7.26 (dd, *J* = 7.5, 7.5 Hz, 1H), 6.77 (s, 1H), 5.05 (d, *J* = 5 Hz, 2H), 2.61 (s, 3H).

$^{13}$C NMR (125.8 MHz, $CD_3CN$): δ 200.2 (s), 155.2 (s), 153.6 (s), 128.7 (s), 124.7 (d), 123.4 (d), 121.5 (d), 111.3 (d), 105.4 (d), 43.8 (t), 17.8 (q).

HRMS-EI *m/z*: measured 237.0287 ($[M]^+$, calcd. 237.0282 for $C_{11}H_{11}NOS_2$).

MS-EI *m/z* (% relative intensity): 237 ($[M]^+$, 28), 189 (10), 132 (10), 131 (100), 77 (14).

FTIR $\nu_{max}$ (KBr): 3337, 3239, 2993, 2917, 1497, 1452, 1303, 1253, 1175, 1085, 932, 750 $cm^{-1}$.

## 4.3.4 Methyl (thianaphthen-3-yl)methyldithiocarbamate (237)

### *4.3.4.1 Synthesis of thianaphthene-3-carboxaldehyde (272)*

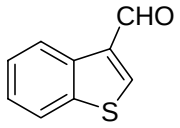


**272**

To a solution of 3-bromothianaphthene (**271**, 218 mg, 1.01 mmol) in dry $Et_2O$ (4 ml), a solution of *t*-BuLi in pentane (1.30 M, 1.57 ml, 2.02 mmol) was added drop wise at -78 ºC under argon atmosphere. After stirring the reaction mixture at -78 ºC for 30 min., dry DMF (118 μL, 1.53 mmol) was added and the mixture was stirred for 1.5 hour at room temperature. Water (10 ml) was added to quench the reaction and the mixture was extracted with $Et_2O$ (2 × 15 ml). After drying ($Na_2SO_4$) and evaporation of solvent, the residue was subjected to FCC on silica gel ($CH_2Cl_2$-hexane; 3:7) to yield thianaphthene-3-carboxaldehyde (**272**, 122 mg) in 73% yield as white solid.

$^1$H NMR (500 MHz, $CDCl_3$): δ 10.17 (s, 1H), 8.70 (d, *J* = 8 Hz, 1H), 8.34 (s, 1H), 8.90 (d, *J* = 8 Hz, 1H), 7.54 (dd, *J* = 8, 8 Hz, 1H), 7.48 (dd, *J* = 8, 8 Hz, 1H).

$^{13}$C NMR (125.8 MHz, $CD_3CN$): δ 185.7 (d), 143.4 (d), 140.9 (s), 136.9 (s), 135.6 (s), 126.6 (d), 126.5 (d), 125.2 (d), 122.8 (d).

HRMS-EI *m/z*: measured 162.0137 ($[M]^+$, calcd. 162.0139 for $C_9H_6OS$).

MS-EI *m/z* (% relative intensity): 162 ($[M]^+$, 100), 161 (99), 134 (16), 133 (22), 89 (26).

FTIR $\nu_{max}$ (KBr): 3084, 2818, 2719, 1675, 1500, 1462, 1424, 1385, 1136, 1098, 857, 758 $cm^{-1}$.

### *4.3.4.2 Synthesis of thianaphthene-3-carboxaldehyde oxime (273)*

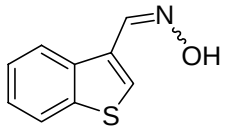


**273**

An aqueous solution (2 ml) of $NH_2OH.HCl$ (186 mg, 2.7 mmol) and $Na_2CO_3$ (170 mg, 1.6 mmol) was added to a solution of thianaphthene-3-carboxaldehyde (**272**) (219 mg, 1.34 mmol) in EtOH (6 ml). After stirring at 90º C for 2 hours, EtOH was removed, water (10 ml) was added and the mixture was extracted with $CH_2Cl_2$ (2×15 ml). The organic phase was dried over $Na_2SO_4$ and concentrated to dryness. The residue was subjected to FCC on silica gel ($CH_2Cl_2$/hexane; 3:7) to afford thianaphthene-3-carboxaldehyde oxime (mixture of E and Z isomer, 220 mg, 93%) as white solid.

### *4.3.4.3 Synthesis of thianaphthene-3-methanamine (274)*

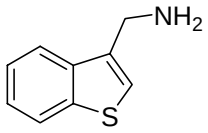


**274**

Sodium cyanoborohydride (637 mg, 10.1 mmol) and $NH_4OAc$ (856 mg, 11.1 mmol) were added to a solution of thianaphthene-3-carboxaldehyde oxime (**273**, 180 mg, 1.02 mmol) in MeOH (1.5 ml) at 0 ºC. To this mixture a neutralized (neutralization was carried out with 5N NaOH, 1.64 ml) solution of $TiCl_3$ 30% wt in 2N HCl (4.1 ml, 8.08 mmol) was added. After stirring for 10 min at 0 ºC, the reaction mixture was diluted with 1% $NH_4OH$ (40 ml) and extracted with EtOAc (2 × 50 ml). The organic phase was dried over $Na_2SO_4$ and concentrated to dryness to yield 264 mg of crude thianaphthene-3-methanamine (**274**) as colorless oil.

$^1$H NMR (500 MHz, $CD_3CN$): δ 7.93 (d, *J* = 7.5 Hz, 1H), 7.86 (d, *J* = 8 Hz, 1H), 7.44-7.37 (m, 3H), 4.07 (s, 2H).

$^{13}$C NMR (125.8 MHz, $CD_3CN$): δ 141.0 (s), 139.5 (s), 138.5 (s), 124.7 (d), 124.3 (d), 123.1 (d), 122.2 (d), 122.0 (d), 40.4 (t).

HRMS-EI *m/z*: measured 163.0457 ($[M]^+$, calcd. 163.0456 for $C_9H_9NS$).

MS-EI *m/z* (% relative intensity): 163 ($[M]^+$, 100), 162 (80), 149 (30), 147 (93), 135 (57), 134 (28), 91 (26).

FTIR $\nu_{max}$ (KBr): 3372, 3287, 3057, 2912, 2851, 1589, 1459, 1427, 1255, 825 $cm^{-1}$.

### *4.3.4.4 Synthesis of methy (thianaphthen-3-yl)methyldithiocarbamate (237)*

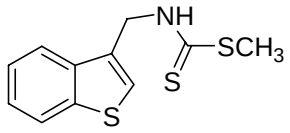


**237**

To a solution of crude thianaphthene-3-methanamine (**274**, 264 mg, 1.6 mmol) in pyridine (1 ml) were added $Et_3N$ (448 µl, 3.2 mmol) and $CS_2$ (288 µl, 4.8 mmol) at 0 ºC. After 1 hour of stirring at 0 ºC, $CH_3I$ (299 µl, 4.8 mmol) was added and the reaction mixture was kept at 3 ºC for 16 hours. The mixture was poured into cold 1.5 M $H_2SO_4$ (30 ml), extracted with $Et_2O$ (2 × 30 ml). The combined organic extracts were dried over $Na_2SO_4$ and concentrated to dryness to yield residue. Finally pure methyl (thianaphthen-3-yl)methyldithiocarbamate (**237**,184 mg, 71% yield from oxime **273**) was obtained after fractionation by FCC (silica gel, $CH_2Cl_2$/hexane, 40:60 & 50:50).

$^1$H NMR (500 MHz, $CD_3CN$): δ 8.42 (br, s, $D_2O$ exchangeable, 1H), 7.96 (d, *J* = 7.5 Hz, 1H), 7.88 (d, *J* = 7.5 Hz, 1H), 7.54 (s, 1H), 7.47-7.40 (m, 2H), 5.16 (d, *J* = 5 Hz, 2H), 2.60 (s, 3H).

$^{13}$C NMR (125.8 MHz, $CD_3CN$): δ 199.5 (s), 140.7 (s), 138.4 (s), 132.0 (s), 125.9 (d), 125.1 (d), 124.8 (d), 123.3 (d), 122.2 (d), 44.6 (t), 17.7 (q).

HRMS-EI *m/z*: measured 253.0063 ($[M]^+$, calcd. 253.0054 for $C_{11}H_{11}NS_3$).

MS-EI *m/z* (relative intensity): 253 ($[M]^+$, 15), 205 (18), 163 (18), 147 (100).

FTIR $\nu_{max}$ (KBr): 3335, 3228, 2916, 1495, 1427, 1376, 1301, 1074, 925, 757 $cm^{-1}$.

### 4.3.5 Methyl (7-azaindol-3-yl)methyldithiocarbamate (238)

#### *4.3.5.1 Synthesis of 7-azaindole-3-carboxaldehyde (276)*

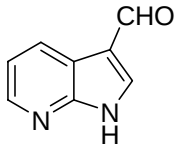


**276**

$POCl_3$ (3.2 ml, 34 mmol) was added to DMF (2.6 ml, 34 mmol) at 0 ºC and the mixture was stirred until it was solidified. To this solid mixture, 7-azaindole (**275**, 400 mg, 3.4 mmol) was added and the mixture was heated at 105 ºC for 14 hours. The reaction mixture was diluted with ice cold water (20 ml), basified with 5N NaOH (30 ml) and extracted with $CH_2Cl_2$ (3×45 ml). The combined organic extracts were washed with water and brine, dried over $Na_2SO_4$ and concentrated under reduced pressure. The resulting residue was subjected to FCC on silica gel (acetone-hexane, 1:3) to afford 7-azaindole-3-carboxaldehyde (**276**, 233 mg, 47% yield) as white solid (Oh et al., 2004).

$^1$H NMR [500 MHz, $(CD_3)_2SO$]: δ 12.69 (br, s, 1H), 9.92 (s, 1H), 8.40 (d, $J$ = 8 Hz, 1H), 8.36 (d, $J$ = 5 Hz, 1H), 7.27 (dd, $J$ = 8, 5 Hz, 1H).

$^{13}$C NMR [125.8 MHz, $(CD_3)_2SO$]: δ 186.2 (d), 150.2 (s), 145.7 (d), 139.5 (s), 130.1 (d), 119.3 (d), 117.5 (d), 117.3 (s).

HRMS-EI *m/z*: measured 146.0478 ($[M]^+$, calcd. 146.0480 for $C_8H_6N_2O$).

MS-EI *m/z* (% relative intensity): 146 ($[M]^+$, 86), 145 (100), 117 (28), 90 (17).

FTIR $\nu_{max}$ (KBr): 3109, 3082, 3025, 2893, 2813, 2736, 1657, 1590, 1464, 1282, 794 $cm^{-1}$.

### *4.3.5.2 Synthesis of 7-azaindole-3-carboxaldehyde oxime (277)*

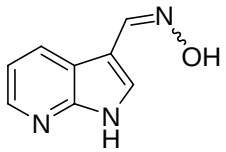

**277**

To a solution of 7-azaindole-3-carboxaldehyde (**276**, 327 mg, 2.2 mmol) in EtOH (25 ml) was added a solution of $NH_2OH.HCl$ (545 mg, 7.8 mmol) and $Na_2CO_3$ (427 mg, 4.0 mmol) in water (10 ml) and the mixture was refluxed for 2 hours at 95 ˚C. After removing EtOH under reduced pressure, the resulting precipitate was filtered off, washed with ice cold water and air dried to yield 7-azaindole-3-carboxaldehyde oxime (**277**, 341 mg) in 94% yield as white solid.

### *4.3.5.3 Synthesis of 7-azaindole-3-methanamine (278)*

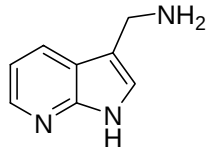

**278**

Zinc powder (1.2 g) was added in portions to a stirred solution of 7-azaindole-3-carboxaldehyde oxime (**277**, 100 mg, 0.6 mmol) in 17% HCl (20 ml) at room temperature, after which stirring was continued for a further 45 min. at room temperature. Excess 5N NaOH was added to basify the reaction mixture, the precipitate was filtered off under vacuum and the precipitate was washed with EtOAc. The filtrate was extracted with EtOAc (3×50 ml), the combined organic extracts were dried over $Na_2SO_4$ and concentrated under reduced pressure. The residue was applied for FCC on silica gel ($CHCl_3$-MeOH-$NH_4OH$, 80:20:1) to yield 7-azaindole-3-methanamine (**278**, 32 mg, 35% yield) as a colorless oil.

$^{1}$H NMR [500 MHz, $CD_3CN$]: δ 9.98 (br, s, 1H), 8.26 (dd, *J* = 4.5, 1 Hz, 1H), 8.03 (d, *J* = 8, 1 Hz, 1H), 7.29 (s, 1H), 7.07 (dd, *J* = 8, 4.5 Hz, 1H), 3.97 (s, 2H).

$^{13}$C NMR [125.8 MHz, $CD_3CN$]: δ 149.5 (s), 143.3 (d), 127.5 (d), 122.6 (s), 119.3 (s), 117.5 (d), 115.5 (d), 37.6 (t).

HRMS-EI *m/z*: measured 147.0799 ($[M]^+$, calcd. 147.0796 for $C_8H_9N_3$).

MS-EI *m/z* (% relative intensity): 147 ($[M]^+$, 100), 146 (70), 131 (72), 119 (53).

FTIR $\nu_{max}$ (KBr): 3126, 3086, 2924, 2862, 1579, 1537, 1449, 1419, 1335, 1294, 1120, 769 $cm^{-1}$.

### *4.3.5.4 Synthesis of methyl (7-azaindol-3-yl)methyldithiocarbamate (238)*

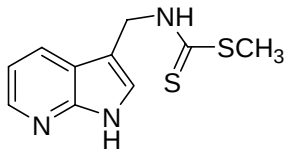


**238**

7-Azaindole-3-methanamine (**278**, 105 mg, 0.7 mmol) was dissolved in pyridine (3 ml) and $Et_3N$ (398 µl, 2.8 mmol) and cooled to 0 ˚C. After adding $CS_2$ (168 µl, 2.8 mmol), the mixture was stirred for 1 hour at 0 ˚C, $CH_3I$ (175 µl, 2.8 mmol) was added and the mixture was kept at 3 ˚C for 15 hour. The reaction mixture was poured into water (15 ml) and extracted with EtOAc (2×20 ml). The combined organic extracts were dried over $Na_2SO_4$ and concentrated under reduced pressure followed by addition of toluene (2×2 ml) and concentration under reduced pressure. Finally, the residue was subjected to FCC on silica gel ($CH_2Cl_2$-methanol, 98:2) to obtain methyl [(7-azaindol-3-yl)methyl]dithiocarbamate (**238**, 140 mg, 83%) as white solid.

Mp = 167-169 ˚C

HPLC $t_R$ = 15.3 (br) min

$^{1}$H NMR (500 MHz, $CD_3OD$): δ 8.19 (dd, *J* = 5, 1 Hz, 1H), 8.12 (dd, *J* = 8, 1 Hz, 1H), 7.44 (s, 1H), 7.11 (dd, *J* = 8, 5 Hz, 1H), 5.07 (s, 2H), 2.60 (s, 3H).

$^{13}$C NMR (125.8 MHz, $CD_3OD$): δ 198.9 (s), 148.4 (s), 142.5 (d), 128.3 (d), 125.4 (d), 120.2 (s), 115.6 (d), 110.5 (s), 42.2 (t), 16.9 (q).

HRMS-EI *m/z*: measured 237.0396 ($[M]^+$, calcd. 237.0394 for $C_{10}H_{11}N_3S_2$).

MS-EI *m/z* (% relative intensity): 237 ($[M]^+$, 23), 163 (7), 132 (9), 131 (100), 104 (9), 103 (8).

FTIR $\nu_{max}$ (KBr): 3252, 3147, 3030, 2985, 2921, 1581, 1492, 1420, 1380, 1326, 1068, 921, 764 $cm^{-1}$.

## 4.3.6 Methyl (5-methoxypyrazolo[1,5-a]pyridin-3-yl)methyldithiocarbamate (239)

### *4.3.6.1 Synthesis of 2-(2,4-dinitrophenoxy)-1H-isoindole-1,3(2H)-dione (281)*

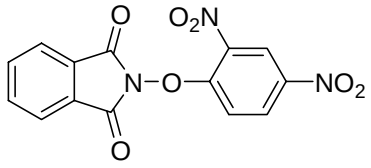


**281**

To a suspension of *N*-hydroxyphthalimide (**279,** 2 g, 12.3 mmol) in acetone (40 ml), $Et_3N$ (1.9 ml, 13.4 mmol) was added in one portion and the mixture was stirred at room temperature until all the *N*-hydroxyphthalimide was dissolved. When the solution became homogeneous mixture, 2,4-dinitrochlorobenzene (**280**, 2.5 g, 12.3 mmol) was added in one portion and the reaction was stirred at room temperature for 2 hours. The reaction mixture was poured into ice water (40 ml), the precipitate was filtered, and

washed with cold MeOH and cold hexane respectively. Finally, the solid was dried under vacuum to yield 2-(2,4-dinitrophenoxy)-1*H*-isoindole-1,3(2*H*)-dione (**281**, 3.7 g, 92% yield) as an off white solid (Legault and Charette, 2003).

Mp = 185-186 ˚C

$^{1}$H NMR (500 MHz, $CDCl_3$): δ 9.00 (d, *J* = 2.5 Hz, 1H), 8.46 (dd, *J* = 9, 2.5 Hz, 1H), 8.02-7.99 (m, 2H), 7.94-7.91 (m, 2H), 7.48 (d, *J* = 9 Hz, 1H).

$^{13}$C NMR (125.8 MHz, $CDCl_3$): δ 162.4, 156.8, 143.7, 137.8, 136.2, 129.8, 129.1, 125.1, 122.9, 116.3.

HRMS-EI *m/z*: measured 329.0282 ($[M]^+$, calcd. 329.0284 for $C_{14}H_7N_3O_7$).

MS-EI *m/z* (% relative intensity): 329 ($[M]^+$, 49), 284 (17), 283 (100), 237 (11), 197 (11), 184 (22).

FTIR $\nu_{max}$ (KBr): 3113, 3094, 1799, 1731, 1609, 1531, 1352, 1230, 1111, 1077, 970 $cm^{-1}$.

### *4.3.6.2 Synthesis of O-(2,4-dinitrophenyl)hydroxylamine (282)*

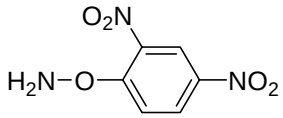


**282**

To a solution of 2-(2,4-dinitrophenoxy)-1*H*-isoindole-1,3(2*H*)-dione (**281**, 2 g, 6.1 mmol) in $CH_2Cl_2$ (40 ml), a solution of hydrazine hydrate (1 ml, 17.6 mmol) in MeOH (5.8 ml) was added in one portion at 0 ˚C. A bright yellow solution was formed rapidly and a precipitate was formed. The suspension was allowed to stand at 0 ˚C for 8 hours, cold aqueous HCl (1N, 40 ml) was added, and the reaction was shaken rapidly at 0 ˚C. The mixture was filtered over a celite pad and the celite was washed with

acetonitrile. The filtrate was poured into a separatory funnel and the organic phase was separated. The aqueous phase was extracted with $CH_2Cl_2$ (2×40 ml). The combined organic phases were dried over $Na_2SO_4$ and concentrated under reduced pressure. The residue was subjected to FCC on silica gel (EtOAc-hexane, 25:75) to afford *O*-(2,4-dinitrophenyl)hydroxylamine (**282**, 1.06 g, 87% yield) as an orange solid (Legault and Charette, 2003).

Mp = 111-112 ˚C

$^1$H NMR (500 MHz, $CDCl_3$): δ 8.82 (d, *J* = 2.5 Hz, 1H), 8.45 (dd, *J* = 9, 2.5 Hz, 1H), 8.07 (d, *J* = 9 Hz, 1H), 6.42 (br, s, 2H).

$^{13}$C NMR (125.8 MHz, $CDCl_3$): δ 160.0 (s), 141.1 (s), 136.9 (s), 129.6 (d), 122.3 (d), 116.8 (d).

HRMS-EI *m/z*: measured 199.0229 ($[M]^+$, calcd. 199.0229 for $C_6H_5N_3O_5$).

MS-EI *m/z* (% relative intensity): 199 ($[M]^+$, 7), 184 (100), 181 (39), 154 (27), 107 (24), 92 (16), 91 (31).

FTIR $\nu_{max}$ (KBr): 3324, 3261, 3118, 1605, 1516, 1340, 833, 742 cm$^{-1}$.

### *4.3.6.3 Synthesis of N-amino-(4-methoxy)pyridinium 2,4-dinitrophenolate (283)*

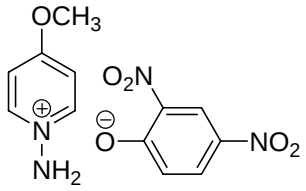


**283**

To a solution of *O*-(2,4-dinitrophenyl)hydroxylamine (**282**, 1 g, 5 mmol) in MeCN (9.7 ml) was added 4-methoxypyridine (464 µl, 4.6 mmol) at room temperature and the mixture was stirred at 45 ˚C for 24 hours. After the addition of $Et_2O$ (20 ml),

the resulting yellow-orange solid was filtered, washed with $Et_2O$ and dried under vacuum to yield *N*-amino-(4-methoxy)pyridinium 2,4-dinitrophenolate (**283**, 1.35 g, 96% yield) (Elsner et al., 2006).

Mp = 138-139 ˚C

$^1$H NMR [500 MHz, $(CD_3)_2SO$]: δ 8.66 (d, *J* = 7 Hz, 2H), 8.57 (d, *J* = 3 Hz, 1H), 7.77 (dd, *J* = 9.5, 3 Hz, 1H), 7.76 (br, s, 2H, $D_2O$ exchangeable), 7.52 (d, *J* = 7 Hz, 2H), 6.31 (d, *J* = 9.5 Hz, 1H), 4.04 (s, 3H).

$^{13}$C NMR [125.8 MHz, $(CD_3)_2SO$]: δ 171.3 (s), 169.0 (s), 144.4 (d), 137.0 (s), 128.5 (s), 128.4 (d), 127.2 (d), 125.7 (d), 114.1 (d), 58.6 (q).

HRMS-EI *m/z*: measured 184.0112 ($[M]^+$- $C_6H_8N_2O$, calcd. 184.0120 for $C_6H_4N_2O_5$).

MS-EI *m/z* (% relative intensity): 184 ($[M]^+$- $C_6H_8N_2O$, 100), 168 (11), 153 (27), 107 (26), 92 (18), 91 (33).

FTIR $\nu_{max}$ (KBr): 3198, 3095, 1535, 1507, 1256, 740 $cm^{-1}$.

### *4.3.6.4 Synthesis of methyl 5-methoxypyrazolo[1,5-a]pyridine-3-carboxylate (242)*

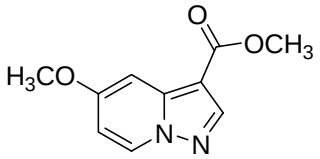


**242**

To a mixture of *N*-amino-(4-methoxy)pyridinium 2,4-dinitrophenolate (**283**, 362 mg, 1.18 mmol), $K_2CO_3$ (245 mg, 1.8 mmol) and DMF (2.5 ml), methyl propiolate (108 µl, 1.3 mmol) was added drop wise and the mixture was stirred vigorously at room temperature for 24 hours. The reaction mixture was poured into water (25 ml), extracted with $Et_2O$ (3×25 ml) and the combined organic extracts were washed two times with 50 ml of water. The organic extract was dried over $Na_2SO_4$ and concentrated

under reduced pressure. The resulting residue was applied to FCC on silica gel (EtOAc-hexane, 1:5) to yield methyl 5-methoxypyrazolo[1,5-a]pyridine-3-carboxylate (**242**, 96 mg, 40% yield) as a white solid (Elsner et al., 2006).

$^{1}$H NMR (500 MHz, $CDCl_3$): δ 8.33 (d, $J$ = 7.5 Hz, 1H), 8.28 (s, 1H), 7.42 (d, $J$ = 2.5 Hz, 1H), 6.62 (dd, $J$ = 7.5, 2.5 Hz, 1H), 3.94 (s, 3H), 3.90 (s, 3H).

$^{13}$C NMR (125.8 MHz, $CDCl_3$): δ 164.4 (s), 160.1 (s), 145.6 (d), 143.2 (s), 130.4 (d), 108.6 (d), 102.8 (s), 96.7 (d), 56.3 (q), 51.3 (q).

HRMS-EI *m/z*: measured 206.0684 ($[M]^+$, calcd. 206.0691 for $C_{10}H_{10}N_2O_3$).

MS-EI *m/z* (% relative intensity): 206 ($[M]^+$, 62), 176 (11), 175 (100), 160 (9), 148 (8).

FTIR $\nu_{max}$ (KBr): 3088, 2951, 1697, 1649, 1537, 1482, 1379, 1277, 1250, 1214, 1055 $cm^{-1}$.

### *4.3.6.5 Synthesis of 5-methoxypyrazolo[1,5-a]pyridine-3-methanol (284)*

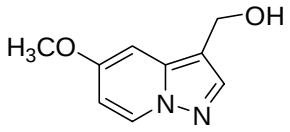


**284**

Methyl 5-methoxypyrazolo[1,5-a]pyridine-3-carboxylate (**242**, 118 mg, 0.57 mmol) was dissolved in dry THF (Ar atmosphere, 3.5 ml) and the solution was cooled to 0 °C with stirring. $LiAlH_4$ (87 mg, 2.3 mmol) was then added in small portions during 5 minutes and stirring was continued further for 2 hours at room temperature. The reaction was quenched with 5 N NaOH (0.8 ml) and the precipitate was filtered off through a celite pad. The pad was washed with THF and EtOAc, the filtrate was dried ($Na_2SO_4$) and concentrated under reduced pressure to yield 5-methoxypyrazolo[1,5-a]pyridine-3-methanol (**284**, 118 mg), that was used in the next step.

### *4.3.6.6 Synthesis of 5-methoxypyrazolo[1,5-a]pyridine-3-carboxaldehyde (285)*

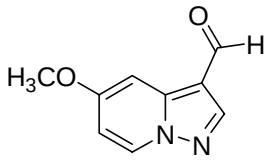

**285**

The crude 5-methoxypyrazolo[1,5-a]pyridine-3-methanol (**284**, 118 mg, 0.58 mmol) was dissolved in $CH_2Cl_2$ (6 ml), $MnO_2$ (406 mg, 4.7 mmol) was added and the mixture was stirred for 18 h at room temperature. $MnO_2$ was filtered off, the filter cake was washed with EtOAc and the filtrate was concentrated under reduced pressure. The residue was applied to FCC on silica gel (EtOAc-hexane, 2:3) to afford 5-methoxypyrazolo[1,5-a]pyridine-3- carboxaldehyde (**285**, 66 mg, 65% yield from the ester **242**) as a white solid. The $^1$H NMR data of **285** was identical with that of reported data (Elsner et al., 2006).

Mp = 92-93 ˚C

$^1$H NMR (500 MHz, $CDCl_3$): δ 9.95 (s, 1H), 8.37 (d, *J* = 7.5 Hz, 1H), 8.27 (s, 1H), 7.58 (s, 1H), 6.71 (dd, *J* = 7.5, 2 Hz, 1H), 3.95 (s, 3H).

$^{13}$C NMR (125.8 MHz, $CDCl_3$): δ 183.5 (d), 161.6 (s), 147.7 (d), 141.9 (s), 130.4 (d), 113.6 (s), 109.7 (d), 97.6 (d), 56.5 (q).

HRMS-EI *m/z*: measured 176.0582 ($[M]^+$, calcd. 176.0585 for $C_9H_8N_2O_2$).

MS-EI *m/z* (% relative intensity): 176 ($[M]^+$, 83), 175 (100), 160 (9), 131 (11), 119 (16).

FTIR $\nu_{max}$ (KBr): 3095, 1664, 1644, 1538, 1483, 1282, 1203, 1086, 1015, 831 $cm^{-1}$.

### *4.3.6.7 Synthesis of 5-methoxypyrazolo[1,5-a]pyridine-3-carboxaldehyde oxime (286)*

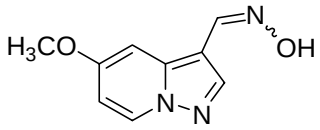

**286**

A solution of $NH_2OH.HCl$ (124.5 mg, 1.79 mmol) and $Na_2CO_3$ (97.6 mg, 0.92 mmol) in water (2.3 ml) was added to a solution of 5-methoxypyrazolo[1,5-a]pyridine-3- carboxaldehyde (**285**, 90 mg, 0.51 mmol) in EtOH (7.5 ml) and the mixture was refluxed at 95 ˚C for 3 hours. EtOH was removed under reduced pressure and water (5 ml) was added to the mixture. The resulting precipitate was filtered, washed with water and dried under vacuum to yield 5-methoxypyrazolo[1,5-a]pyridine-3-carboxaldehyde oxime (**286**, 89 mg, 91%) as a white solid.

### *4.3.6.8 Synthesis of 5-methoxypyrazolo[1,5-a]pyridine-3-methanamine (287)*

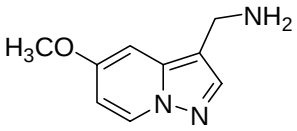

**287**

To a stirred solution of 5-methoxypyrazolo[1,5-a]pyridine-3-carboxaldehyde oxime (**286**, 120 mg, 0.63 mmol) in 17% HCl (20 ml), zinc powder (1.2 g) was added in portions at room temperature, after which the stirring was continued for a further 45 min. at room temperature. Excess 5N NaOH was added to basify the reaction mixture, the precipitate was filtered off under vacuum and the filter cake was washed with EtOAc. The filtrate was extracted with EtOAc (3×50 ml), the combined organic extracts were dried over $Na_2SO_4$ and concentrated under reduced pressure to yield

crude 5-methoxypyrazolo[1,5-a]pyridine-3-methanamine (**287**, 82 mg) as a colorless oil.

### *4.3.6.9 Synthesis of methyl (5-methoxypyrazolo[1,5-a]pyridin-3-yl)methyldithiocarbamate (239)*

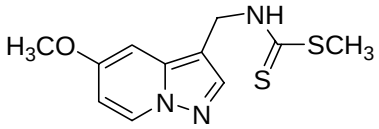


**239**

$CS_2$ (111 μl, 1.85 mmol) was added to a solution of crude amine **287** (82 mg, 0.46 mmol) and $Et_3N$ (258 μl, 1.85 mmol) in pyridine (1 ml) at 0 ˚C. After stirring the reaction mixture at 0 ˚C for an hour, $CH_3I$ (115 μl, 1.85 mmol) was added and the mixture was kept at 3 ˚C for 15 hour. The reaction mixture was poured into water (20 ml) and extracted with EtOAc (3×20 ml). The combined organic extracts were dried over $Na_2SO_4$ and concentrated under reduced pressure followed by addition of toluene (2×2 ml) and concentration. Finally, the residue was subjected to FCC on silica gel ($CH_2Cl_2$-MeOH, 99:1) to afford methyl (5-methoxypyrazolo[1,5-a]pyridin-3-yl)methyldithiocarbamate (**239**, 82 mg, 49% yield from the oxime **286**) as a white solid.

Mp = 148-149 ˚C

HPLC $t_R$ = 15.5 min

$^1$H NMR (500 MHz, $CD_3OD$): δ 8.30 (d, $J$ = 7.5 Hz, 1H), 7.88 (s, 1H), 7.14 (d, $J$ = 2 Hz, 1H), 6.57 (dd, $J$ = 7.5, 2 Hz, 1H), 5.03 (s, 2H), 3.87 (s, 3H), 2.60 (s, 3H).

$^{13}$C NMR (125.8 MHz, $CD_3OD$): δ 199.1 (s), 157.3 (s), 142.8 (d), 140.3 (s), 129.2 (d), 107.4 (d), 106.2 (s), 94.5 (d), 55.2 (q), 40.3 (t), 16.9 (q).

HRMS-ESI *m/z*: measured 266.0434 ($[M-1]^-$, calcd. 266.0427 for $C_{11}H_{12}N_3OS_2$).

MS-ESI *m/z* (% relative intensity): 266 ([M-1]$^-$, 100)

FTIR $\nu_{max}$ (KBr): 3142, 2946, 1649, 1527, 1470, 1396, 1254, 1228, 1087, 922 cm$^{-1}$.

### 4.3.7 3-Phenylindole (245)

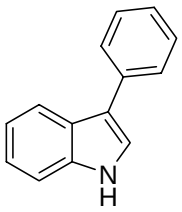

**245**

A mixture of phenyl acetaldehyde (**290**, 341 µl, 3.05 mmol) and phenyl hydrazine (**288**, 300 µl, 3.05 mmol) was stirred for 1 hour at room temperature and then for 30 minutes at 100 ºC. After that a solution of $ZnCl_2$ (1.2 g, 9.15 mmol) in EtOH (4 ml) was added, the mixture was stirred at 100 ºC for another 1 hour. After cooling, the mixture was filtered, the solvent was removed under reduced pressure and an aqueous solution of HCl (4%, 10 ml) was added. The mixture was extracted with $CH_2Cl_2$ (2×15 ml), the combined organic extracts were dried over $Na_2SO_4$ and concentrated under reduced pressure. The residue was then crystallized from hexane to give 3-phenylindole (**245**, 370 mg, 70%) as an off white solid (Rodriguez et al., 2000).

HPLC $t_R$ = 25.6 min

$^1$H NMR (500 MHz, $CD_3CN$) δ 9.48 (br, s, $D_2O$ exchangeable, 1H), 7.92 (d, *J* = 7.5 Hz, 1H), 7.72 (d, *J* = 7.5 Hz, 2H), 7.53-7.51 (m, 2H), 7.46 (dd, *J* = 7.5, 7.5 Hz, 2H), 7.29 (dd, *J* = 7.5, 7.5 Hz, 1H), 7.23 (dd, *J* = 7.5, 7.5 Hz, 1H), 7.16 (dd, *J* = 7.5, 7.5 Hz, 1H).

$^{13}$C NMR [125.8 MHz, $CD_3CN$]: δ 137.5 (s), 136.3 (s), 129.2 (d), 127.4 (d), 126.1 (d), 125.9 (s), 123.2 (d), 122.3 (d), 120.4 (d), 119.6 (d), 117.2 (s), 112.2 (d).

HRMS-EI *m/z*: measured 193.0900 ([M]$^+$, calcd. 193.0891 for $C_{14}H_{11}N$).

MS-EI *m/z* (% relative intensity): 193 ([M]$^+$, 100), 192 (12), 165 (23).

FTIR $\nu_{max}$ (KBr): 3411, 3120, 3055, 1599, 1543, 1457, 1237, 1013 cm$^{-1}$.

### 4.3.8 4-Fluoro-3-phenylindole (246) and 6-fluoro-3-phenylindole (247)

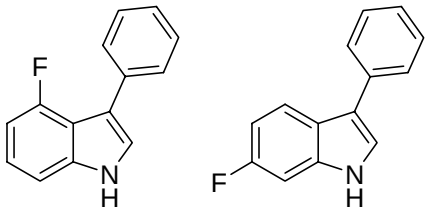


**246** **247**

To a solution of 3-fluorophenyl hydrazine hydrochloride (200 mg, 1.23 mmol) in water (5 ml), solid $Na_2CO_3$ (80 mg, 0.75 mmol) was added. When all the $Na_2CO_3$ was dissolved, the mixture was extracted with $CH_2Cl_2$ (2×10 ml), the combined organic extracts were dried over $Na_2SO_4$ and concentrated under reduced pressure. To this residue, phenyl acetaldehyde (**290**, 108 µl, 0.97 mmol) was added and the mixture was stirred for 1 hour at room temperature and then for 30 minutes at 100 ºC. After that a solution of $ZnCl_2$ (376 mg, 2.91 mmol) in EtOH (3 ml) was added and the mixture was stirred at 100 ºC for another 1 hour. After cooling, the mixture was filtered, the solvent was removed under reduced pressure and an aqueous solution of HCl (4%, 10 ml) was added. The mixture was extracted with $CH_2Cl_2$ (2×15 ml), the combined organic extracts were dried over $Na_2SO_4$ and concentrated under reduced pressure. The residue was then subjected to FCC on silica gel ($CH_2Cl_2$-hexane, 1:4) to give a mixture (150 mg, 72% yield) of 4-fluoro-3-phenylindole (**246**) and 6-fluoro-3-phenylindole (**247**) in

equal ratio. Finally, these two compounds were separated by reverse phase column chromatography using $H_2O/CH_3CN$ (55/45) as eluant.

**4-fluoro-3-phenylindole (246)**

HPLC $t_R$ = 25.8 min

$^1$H NMR (500 MHz, $CD_3CN$): δ 9.69 (br, s, $D_2O$ exchangeable, 1H), 7.64 (dd, *J* = 8, 1.5 Hz, 2H), 7.43 (dd, *J* = 7.5, 7.5 Hz, 2H), 7.41 (d, *J* = 2.5 Hz, 1H), 7.34 (d, *J* = 8 Hz, 1H), 7.31 (dd, *J* = 7, 7 Hz, 1H), 7.18-7.16 (m, 1H), 6.83 (dd, *J* = 8, 12 Hz, 1H).

$^{13}$C NMR (125.8 MHz, $CDCl_3$): δ 157.5 (d, $^1J_{C-F}$ = 248 Hz), 139.7 (d, $^3J_{C-F}$ = 12 Hz), 135.3, 129.2, 129.1, 128.6, 126.6, 123.3 (d, $^3J_{C-F}$ = 8 Hz), 122.9, 118.0 (d, $^4J_{C-F}$ = 3 Hz), 115.0 (d, $^2J_{C-F}$ = 19 Hz), 107.7 (d, $^4J_{C-F}$ = 3.5 Hz), 106.0 (d, $^2J_{C-F}$ = 21 Hz).

HRMS-EI m/z: measured 211.0834 ($M^+$, calcd. 211.0797 for $C_{14}H_{10}NF$).

MS-EI m/Z (% relative intensity): 211 ($M^+$, 100), 183 (21).

FTIR $\nu_{max}$ (KBr): 3418, 3054, 1625, 1600, 1546, 1502, 1419, 1327, 1222, 1035, 758 $cm^{-1}$.

**6-fluoro-3-phenylindole (247)**

HPLC $t_R$ = 27.4 min

$^1$H NMR (500 MHz, $CD_3CN$): δ 9.54 (br, s, $D_2O$ exchangeable, 1H), 7.87 (dd, *J* = 5, 9 Hz, 1H), 7.69 (dd, *J* = 8, 1 Hz, 2H), 7.52 (d, *J* = 2.5 Hz, 1H), 7.47 (dd, *J* = 8 Hz, 2H), 7.30 (dd, *J* = 7.5, 7.5 Hz, 1H), 7.24 (dd, *J* = 10, 2 Hz, 1H), 6.96 (ddd, *J* = 10, 9, 2.5 Hz, 1H).

$^{13}$C NMR (125.8 MHz, $CDCl_3$): δ 160.5 (d, $^1J_{C-F}$ = 239 Hz), 137.0 (d, $^3J_{C-F}$ = 12.5 Hz), 135.5, 129.2, 127.9, 126.6, 122.9, 122.2 (d, $^4J_{C-F}$ = 3.5 Hz), 121.1 (d, $^3J_{C-F}$ = 10 Hz), 118.9, 109.4 (d, $^2J_{C-F}$ = 24 Hz), 98.0 (d, $^2J_{C-F}$ = 26 Hz).

HRMS-EI m/z: measured 211.0797 ($M^+$, calcd. 211.0797 for $C_{14}H_{10}NF$).

MS-EI m/z (% relative intensity) 211 ($M^+$, 100), 183 (26).

FTIR $\nu_{max}$ (KBr): 3419, 3054, 1626, 1601, 1503, 1419, 1222, 1035, 960, 758, 733 $cm^{-1}$.

## 4.3.9 3-Phenylbenzofuran (248)

### *4.3.9.1 Synthesis of 1-phenyl-1-(2-hydroxyphenyl)ethanol (293)*

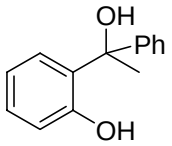


**293**

To a Grignard solution prepared from bromobenzene (1.5 ml, 14.6 mmol), magnesium (368 mg, 15.3 mmol) and THF (15 ml), a solution of 2′-hydroxyacetophenone (**259**, 1 g, 7.3 mmol) in THF (10 ml) was added with stirring. After refluxing the resulting solution at 80 ºC for 6 hours, THF was removed under reduced pressure, the residue was treated with 15% aqueous AcOH (20 ml) and extracted with benzene (2×25 ml). The combined organic extracts were washed with 5% $NaHCO_3$ (2×30 ml), dried over $Na_2SO_4$ and concentrated under reduced pressure. The residue was subjected to FCC on silica gel ($CH_2Cl_2$, 100%) to afford 1-phenyl-1-(2-hydroxyphenyl)ethanol (**293**, 1.3 g, 82%) as a white solid (Brady and Giang, 1985).

### *4.3.9.2 Synthesis of o-(1-phenylvinyl)phenol (294)*

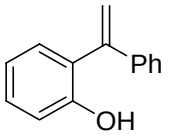


**294**

Iodine (40 mg) was added to a solution of 1-phenyl-1-(2-hydroxyphenyl)ethanol (**293**, 1.26 g, 5.9 mmol) in benzene (12 ml) and the mixture

was refluxed at 90 ºC for 8 hours. After cooling, the reaction mixture was washed with 5% aqueous sodium thiosulphate (2×10 ml), dried over $Na_2SO_4$ and concentrated under reduced pressure. The residue was subjected to FCC on silica gel ($CH_2Cl_2$-hexane, 1:1) to afford *o*-(1-phenylvinyl)phenol (**294**, 1.08 g, 93% yield) as colorless oil (Brady and Giang, 1985).

$^1$H NMR (500 MHz, $CDCl_3$): δ 7.42-7.36 (m, 5H), 7.29 (dd, *J* = 7.5 Hz, 1H), 7.18 (dd, *J* = 7.5, 1 Hz, 1H), 7.00-6.96 (m, 2H), 5.91 (s, 1H), 5.46 (s, 1H), 5.21 (s, 1H).

$^{13}$C NMR (125.8 MHz, $CDCl_3$): δ 153.5 (s), 145.7 (s), 139.9 (s), 130.8 (d), 129.9 (d), 129.1 (d), 129.0 (d), 128.0 (s), 127.4 (d) 120.9 (d), 117.1 (d), 116.3 (d).

HRMS-EI *m/z*: measured 196.0880 ($[M]^+$, calcd. 196.0888 for $C_{14}H_{12}O$).

MS-EI *m/z* (% relative intensity): 196 ($[M]^+$, 57), 195 (100), 183 (20), 181 (52).

FTIR $\nu_{max}$ (KBr): 3433, 3057, 3030, 1600, 1477, 1448, 1144, 913, 751 $cm^{-1}$.

### *4.3.9.3 Synthesis of 3-phenylbenzofuran (248)*

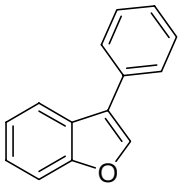

**248**

To a solution of *o*-(1-phenylvinyl)phenol (**294**, 98 mg, 0.5 mmol) in DMF (1.25 ml) were added $Cu(OAc)_2.H_2O$ (300 mg, 1.5 mmol), aqueous LiCl (10 M, 150 µl, 1.5 mmol) and aqueous $PdCl_2$ (0.1 M, 100 µl, 0.01 mmol). After refluxing at 100 ºC for 20 hours, the reaction mixture was poured into water (25 ml) and extracted with $Et_2O$ (2×25 ml). The combined organic extracts were dried over $Na_2SO_4$ and concentrated under reduced pressure. The residue was subjected to FCC on silica gel ($CH_2Cl_2$-hexane, 1:9) to afford 3-phenylbenzofuran (**248**, 8 mg, 10% yield based on recovery of

starting material) as colorless oil. The spectroscopic data of **248** was identical with that of reported data (Kashulin and Nifant'ev, 2004).

HPLC $t_R$ = 32.3 min

$^1$H NMR (500 MHz, $CDCl_3$): δ 7.88 (d, *J* = 7.5 Hz, 1H), 7.83 (s, 1H), 7.69 (d, 7.5 Hz, 2H), 7.59 (d, *J* = 7.5 Hz, 1H), 7.51 (dd, *J* = 7.5, 7.5 Hz, 2H), 7.42-7.34 (m, 3H).

$^{13}$C NMR [125.8 MHz, $CDCl_3$]: δ 156.2 (s), 141.7 (d), 132.5 (s), 129.4 (d), 127.9 (d), 127.8 (d), 126.9 (s), 124.9 (d), 123.4 (d), 122.7 (s), 120.8 (d), 112.2 (d).

HRMS-EI *m/z*: measured 194.0734 ($[M]^+$, calcd. 194.0731 for $C_{14}H_{10}O$).

MS-EI m/z (% relative intensity) 194 ($M^+$, 100), 165 (32), 139 (6).

FTIR $\nu_{max}$ (KBr): 3121, 3054, 1599, 1543, 1457, 1237, 1013 $cm^{-1}$.

## 4.4 Metabolic detoxification of phytoalexins, analogues and potential inhibitors

### 4.4.1 Preparation of minimal media

A solution of glucose (15.0 g) in 700 ml of distilled water was mixed with solution 1 (100 ml) containing 31.2 g/l $KNO_3$, 7.5 g/l $K_2HPO_4$, 7.5 g/l $KH_2PO_4$, 1.0 g/l NaCl and 2.8 g/l asparagine. Solution 3 (1 ml) containing 0.39 g/l $ZnSO_4.7H_2O$, 0.08 g/l $CuSO_4.5H_2O$, 0.41 g/l $MnSO_4.4H_2O$, 0.018 g/l $MoO_3$ (85%), 0.54 g/l ferric citrate and 0.38 g/l $Na_2B_4O_7.10H_2O$ was added to it. The mixture was diluted up to 900 ml using distilled water and autoclaved. Solution 2 (100 ml), containing 1.0 g/l $CaCl_2.7H_2O$ and 5.0 g/l $MgSO_4.7H_2O$ was prepared separately and autoclaved. After autoclaving, the two solutions were allowed to cool to room temperature before mixing them together. A sterile solution 4 (1 ml) containing 100 mg/l of thiamine was then mixed to obtain the minimal media (Pedras et al., 1997).

### 4.4.2 Preparation of fungal cultures

Sclerotia of *S. sclerotiorum* (clone # 33) were obtained from C. Lefol, AAFC, Saskatoon, Canada. The fungal isolate was grown on potato dextrose agar (PDA) plates by inoculating one piece of sclerotia per plate and the plates were incubated at 20±1 ºC in the dark. Sclerotia were collected over a 4-week period and stored at 20 ºC in the dark. Erlenmeyer flasks (250 ml) containing 100 ml of minimal media were inoculated with sclerotia of *S. sclerotiorum* and were incubated at 22±1 ºC on a shaker at 120 rpm under constant light.

### 4.4.3 Time-course experiments

Six-day-old cultures of *S. sclerotiorum* were incubated with phytoalexins or analogues or potential inhibitors at 22±2 ºC on a shaker at 120 rpm under constant light. Each compound dissolved in $CH_3CN$ (200 µl) was added to fungal cultures (final concentration $1 \times 10^{-4}$ M) and to uninoculated medium (control); $CH_3CN$ (200 µl) was added to control cultures. Samples (5 ml each) were taken from the flasks at appropriate times, frozen or immediately extracted with EtOAc (2 × 10 mL). Both, organic and water phases were concentrated, dissolved in $CH_3CN$ (0.5 mL) or $CH_3OH$ (0.5 mL) and analyzed by HPLC.

### 4.4.4 Scale up experiments: isolation of metabolites

To obtain larger amounts of extract to isolate the products of metabolism of each compound, experiments were carried out with 1-L batches, as described above for time-course studies. Only the chromatograms of the EtOAc extracts of fungal broth showed peaks not present in chromatograms of extracts of control cultures. Thus, the EtOAc extracts were fractionated by FCC on reverse phase silica gel (C-18, gradient elution: $H_2O$–$CH_3CN$, 90:10, 80:20, 70:30, 50:50, 0:100), and each fraction was analyzed by HPLC. Finally, the metabolites were isolated by preparative TLC (silica

gel, $CH_2Cl_2$–$CH_3OH$, 90:10, multiple development) and/or reverse phase preparative TLC (RP C-18 silica gel, $H_2O$-$CH_3CN$, 60:40).

## 4.4.5 Synthesis

### *4.4.5.1 1-β-D-Glucopyranosylbrassilexin (222)*

**Synthesis of 2,3,4,6-tetra-*O*-acetyl-1-β-D-glucopyranosyl brassilexin (224) and 1-[1-(3,4,6-tri-*O*-acetyl-1,2-*O*-α-D-glucopyranosyl)ethylidene]brassilexin (225)**

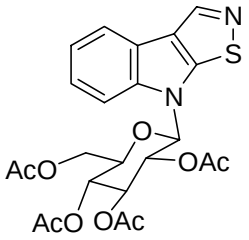


**224**

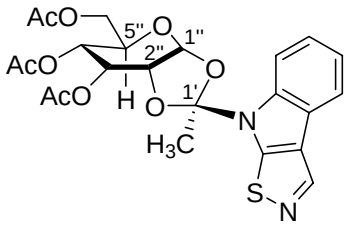


**225**

A solution of 2,3,4,6-tetra-*O*-acetyl-α-D-glucopyranosyl bromide (**223**) (142 mg, 0.35 mmol) in dry benzene (3 ml) was added dropwise during 30 min to a mixture of brassilexin (**24**) (20 mg, 0.11 mmol) and $Ag_2O$ (31 mg, 0.13 mmol) in dry benzene (3 ml) under stirring. The reaction mixture was allowed to reflux for 20 h at 90 °C, was filtered through a tight cotton plug and the insoluble material was washed with benzene. The combined filtrate and washings were concentrated, the residue was subjected to column chromatography (silica gel, EtOAc–hexane, 3 : 7), followed by preparative TLC to afford 2,3,4,6-tetra-*O*-acetyl-1-β-D-glucopyranosyl brassilexin (**224**) [6 mg, 12% based on recovered brassilexin (**24**)] and 1-[1-(3,4,6-tri-*O*-acetyl-1,2-*O*-α-D-glucopyranosyl)ethylidene]brassilexin (**225**) [6 mg, 12% based on recovered brassilexin (**24**)] (Pedras and Hossain, 2006).

**2,3,4,6-tetra-*O*-acetyl-1-β-D-glucopyranosyl brassilexin (224)**

$[\alpha]_D = -3$ (*c* 0.40, $CH_3OH$).

$^1H$ NMR (500 MHz, $CD_2Cl_2$): δ 8.71 (s, 1H), 7.90 (d, *J* = 7.5 Hz, 1H), 7.54 (d, *J* = 8 Hz, 1H), 7.41 (dd, *J* = 7.5, 8 Hz, 1H), 7.31 (dd, *J* = 7.5, 7.5 Hz, 1H), 5.90 (d, *J* = 9 Hz, 1H), 5.56 (dd, *J* = 9.5, 9.5 Hz, 1H), 5.43–5.37 (m, 2H), 4.33 (s, br, 2H), 4.18–4.16 (m, 1H), 2.17 (s, 3H), 2.12 (s, 3H), 2.02 (s, 3H), 1.52 (s, 3H).

$^{13}C$ NMR [125.8 MHz, $CD_2Cl_2$]: δ170.7 (s), 170.2 (s), 169.7 (s), 168.7 (s), 157.8 (s), 147.6 (d), 143.6 (s), 127.9 (s), 124.3 (d), 122.0 (d), 121.0 (d), 120.8 (d), 110.8 (d), 83.5 (d), 75.5 (d), 72.6 (d), 70.5 (d), 68.2 (d), 61.8 (d), 20.9 (q), 20.8 (q), 20.7 (q), 20.0 (q). HRMS-ESI *m*/*z*: measured 503.1110 ($[M - 1]^-$, calc. 503.1124 for $C_{23}H_{23}N_2O_9S$).

MS-ESI *m*/*z* (% relative intensity): 503 ($[M - 1]^-$, 100), 461 (10), 173 (6).

FTIR $\nu_{max}$ (KBr): 3059, 2945, 1752, 1503, 1473, 1444, 1370, 1222, 1102, 1039 $cm^{-1}$.

UV ($CH_3OH$) $\lambda_{max}$ (log $\varepsilon$): 222 (4.7), 244 (4.1), 264 nm (4.0).

**1-[1-(3,4,6-tri-*O*-acetyl-1,2-*O*-α-D-glucopyranosyl)ethylidene]brassilexin (225)**

$[\alpha]_D = -19$ (*c* 0.30, $CH_2Cl_2$).

$^1H$ NMR (500 MHz, $CD_2Cl_2$): δ 8.70 (s, H-3′), 7.90 (d, *J* =8 Hz, H-4), 7.82 (d, *J* = 8 Hz, H-7), 7.41 (dd, *J* = 7.5, 8 Hz, H-6), 7.33 (dd, *J* = 8, 7.5 Hz, H-5), 5.88 (d, *J* = 5 Hz, H-1″), 5.37 (underneath the solvent peak, H-3″), 4.99 (d, *J* = 9.5, Hz, H-4″), 4.35–4.26 (m, H-6a″, H-6b″, H-2″), 4.19–4.17 (m, H-5″), 2.19 (s, 3H), 2.15 (s, 3H), 2.06 (s, 3H), 2.04 (s, 3H).

$^{13}C$ NMR [125.8 MHz, $CD_2Cl_2$]: δ 170.8 (s), 170.0 (s), 169.3 (s), 158.6 (s), 147.5 (d), 142.0 (s), 126.7 (s), 126.4 (s) 124.5 (d), 122.0 (d), 120.5 (d), 113.9 (s), 113.1 (d), 98.3 (d), 73.7 (d), 69.5 (d), 68.4 (d), 67.8 (d), 63.5 (d), 22.2 (q), 21.1 (q), 20.9 (q), 20.8 (q). HRMS-ESI *m*/*z*: measured 505.1280 ($[M + 1]^+$, calc. 505.1275 for $C_{23}H_{25}N_2O_9S$).

MS-ESI *m*/*z* (relative intensity): 505 ([M + 1]$^+$, 100), 331 (9).

FTIR $\nu_{max}$ (KBr): 3057, 2932, 1746, 1469, 1439, 1370, 1225, 1175, 1131, 1093, 1042, 967 cm$^{-1}$.

UV ($CH_2Cl_2$) $\lambda_{max}$ (log $\varepsilon$): 229 (4.7), 245 (4.2), 264 nm (4.1).

**Synthesis of 1-β-D-glucopyranosylbrassilexin (222)**

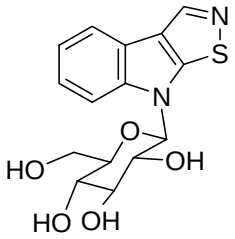


**222**

Sodium methoxide (0.1 M methanolic solution, 0.015 mmol) was added to a stirred solution of **89** (8.0 mg, 0.015 mmol) in dry MeOH (0.3 ml) and the reaction mixture was allowed to stir at room temperature for 45 min. After concentration under reduced pressure, the crude residue was chromatographed using a small Pasteur pipette containing reverse phase silica to yield 1-β-D-glucopyranosylbrassilexin (**222**) (5 mg, 94% yield) (Pedras and Hossain, 2006).

HPLC $t_R$ = 4.5 min;

$[\alpha]_D$ = +19 (*c* 0.22, $CH_3OH$).

$^1$H NMR (500 MHz, $CD_3OD$): δ 8.75 (s, 1H), 7.92 (d, *J* = 8 Hz, 1H), 7.69 (d, *J* = 8.5 Hz, 1H), 7.39 (ddd, *J* = 7.5, 8, 1 Hz, 1H), 7.27 (dd, *J* = 7.5, 8 Hz, 1H), 5.75 (d, *J* = 9 Hz, 1H), 3.94 (dd, *J* = 10, 1 Hz, 1H), 3.86 (dd, *J* = 9, 9 Hz, 1H) 3.76–3.67 (m, 3H), 3.49 (dd, *J* = 9, 9 Hz, 2H).

$^{13}$C NMR [125.8 MHz, $CD_3OD$]: δ 157.9 (s), 147.4 (d), 145.0 (s), 127.4 (s), 124.1 (d), 121.3 (d), 120.7 (s), 120.0 (d), 111.3 (d), 85.1 (d), 80.0 (d), 77.6 (d), 72.6 (d), 70.6 (d), 61.9 (d).

HRMS-ESI *m*/*z*: measured 337.0858 ($[M + 1]^+$, calc. 337.0858 for $C_{15}H_{17}N_2O_5S$).

MS-ESI *m*/*z* (% relative intensity): 337 ($[M + 1]^+$, 100)

FTIR $\nu_{max}$ (KBr): 3349, 3069, 2910, 1510, 1475, 1446, 1376, 1256, 1075, 742 $cm^{-1}$.

UV ($CH_3OH$) $\lambda_{max}$ (log $\varepsilon$): 221 (4.6), 245 (4.1), 265 nm (4.0).

### *4.4.5.2 Brassicanal A sulfoxide (229)*

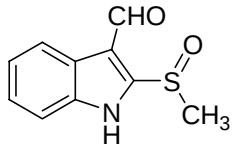


**229**

*m*-Chloroperbenzoic acid (20.7 mg, 0.12 mmol) was added to a stirred solution of brassicanal A (**34**, 19.5mg, 0.10 mmol) in MeOH (3 ml) at 0 °C. After 30 min stirring at 0 °C, the reaction mixture was treated with $Me_2S$ (200 µl), concentrated and subjected to FCC on silica gel ($CH_2Cl_2$-MeOH, 99/1) to afford brassicanal A sulfoxide (**229**, 18 mg, 85%) as an off white solid (Pedras and Khan, 1996).

HPLC $t_R$ = 6.3 min; $[\alpha]_D$ = −245 (*c* 0.33, $CH_3OH$).

$^1$H NMR (500 MHz, $CD_3OD$): δ 10.26 (s, 1H), 8.11 (d, *J* = 8 Hz, 1H), 7.59 (d, *J* = 8 Hz, 1H), 7.36 (ddd, *J* = 8, 8, 1 Hz, 1H), 7.31 (ddd, *J* = 8, 8, 1 Hz, 1H), 3.08 (s, 3H).

$^{13}$C NMR [125.8 MHz, $CD_3OD$]: δ 186.0 (s), 147.7 (s), 138.6 (s), 127.9 (s), 126.3 (d), 124.7 (d), 121.4 (d), 116.9 (s), 114.1 (d), 42.2 (q).

HRMSEI *m*/*z*: measured 207.0353 ($M^+$, calc. 207.0354 for $C_{10}H_9NO_2S$).

MS-EI *m*/*z* (% relative intensity): 207 ($M^+$, 21), 190 (100), 175 (14), 146 (16).

FTIR $\nu_{max}$ (KBr): 3166, 2925, 2854, 1656, 1488, 1448, 1391, 1095, 1035, 747 $cm^{-1}$.

#### *4.4.5.3 3-(Hydroxymethyl)indole-2-methylsulfoxide (230)*

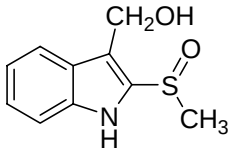

**230**

$NaBH_4$ (5.2 mg, 0.14 mmol) was added to a stirred solution of brasssicanal A sulfoxide (**229**, 10.6 mg, 0.05 mmol) in MeOH (2 ml) at room temperature. After 30 min stirring at room temperature, the reaction was quenched with water (0.5 ml) and the solvent was removed under reduced pressure. The crude product was purified by preparative TLC ($CH_2Cl_2$-MeOH, 99/5) to yield 3-(hydroxymethyl)indole-2-methylsulfoxide (**230**, 7 mg, 65%) as an off white solid (Pedras and Khan, 1996).

HPLC $t_R$ = 3.9 min.

$^1$H NMR (500 MHz, $CD_3CN$): δ 10.40 (br s, 1H $D_2O$ exchangeable), 7.69 (d, *J* = 8 Hz, 1H), 7.49 (d, *J* = 8 Hz, 1H), 7.28 (ddd, *J* = 7, 8, 1 Hz, 1H), 7.14 (ddd, *J* = 8, 7, 1 Hz, 1H), 4.88 (d, *J* = 13 Hz, 1H), 4.81 (d, *J* = 13 Hz, 1H), 2.9 (s, 3H).

$^{13}$C NMR [125.8 MHz, $CD_3OD$]: δ 139.3 (s), 134.5 (s), 127.8 (s), 126.1 (d), 121.3 (d), 121.1 (d), 120.7 (s), 113.3 (d), 55.1 (t), 41.1 (q).

HRMS-EI *m*/*z*: measured 209.0508 ($M^+$, calc. 209.0511 for $C_{10}H_{11}NO_2S$).

MS-EI *m*/*z* (% relative intensity): 209 ($M^+$, 54), 192 (87), 176 (100), 147 (68), 117 (52), 91 (28).

FTIR $\nu_{max}$ (KBr): 3268, 2929, 1711, 1667, 1450, 1212, 1023, 749 $cm^{-1}$.

### *4.4.5.4 Methyl (thianaphthen-3-yl-1-S-oxide)methyldithiocarbamate (296)*

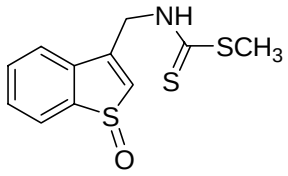


**296**

To a solution of thianaphthene-3-methanamine (**274**, 19 mg, 0.12 mmol) in $CF_3COOH$-$CH_2Cl_2$ (1:2, 0.75 ml), $H_2O_2$ (30%, 53 µl, 0.47 mmol) was added at 0 °C and the reaction mixture was stirred at the same temperature. After 3 hours, the mixture was neutralized with 10% $NaHCO_3$ and extracted with $CH_2Cl_2$ (2×10 ml). The combined organic extracts were dried over $Na_2SO_4$ and concentrated under reduced pressure. The residue was immediately dissolved in $CH_2Cl_2$ (0.5 ml), cooled to 0 °C, $Et_3N$ (50 µl) and $CS_2$ (50 µl) was added and the mixture was stirred at 0 °C. After 60 mins, $CH_3I$ (50 µl) was added and the reaction mixture was stirred for 30 mins at room temperature. The reaction mixture was poured into water (10 ml) and extracted with $CH_2Cl_2$ (2×10 ml). The combined organic extracts were dried over $Na_2SO_4$, concentrated under reduced pressure and the residue was applied for FCC on silica gel ($CH_2Cl_2$-MeOH, 99/1) to afford methyl (thianaphthen-3-yl-1-*S*-oxide)methyl-dithiocarbamate (**296**, 3 mg, 9%) as an off white solid.

HPLC $t_R$ = 10.8 min.

$[\alpha]_D$ = -252 (*c* 0.18, MeOH).

$^1$H NMR (500 MHz, $CD_3OD$): δ 7.97 (d, *J* = 7.5 Hz, 1H), 7.72 (d, *J* = 7.5 Hz, 1H), 7.67 (dd, *J* = 7.5, 7.5 Hz, 1H), 7.61 (dd, *J* = 7.5, 7.5 Hz, 1H), 7.01 (s, 1H) 5.05 (AB quartet, *J* = 17, 17 Hz, 2H), 2.65 (s, 3H).

$^{13}$C NMR [125.8 MHz, $CD_3OD$]: δ 201.1 (s), 146.3 (s), 145.6 (s), 136.8 (s), 132.7 (d), 131.7 (d), 129.7 (d), 126.4 (d), 123.4 (d), 44.0 (t), 17.2 (q).

HRMS-ESI *m/z*: measured 270.0079 ($[M+1]^+$, calc. 270.0075 for $C_{11}H_{12}NOS_3$).

MS-EI *m/z* (% relative intensity): 270 ($[M+1]^+$, 100).

FTIR $\nu_{max}$ (KBr): 3230, 3037, 2922, 1518, 1237, 1121, 1012, 935, 757 $cm^{-1}$.

UV ($CH_3OH$) $\lambda_{max}$ (log $\varepsilon$): 222 (4.4), 246 (4.1), 270 nm (4.0).

## 4.4.6 Spectral data of metabolites

### *4.4.6.1 7-Oxy-(O-β-D-glucopyranosyl)-1-methoxybrassinin (220)*

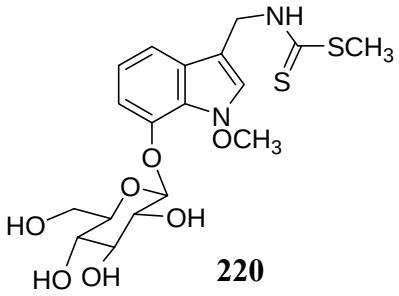


**220**

HPLC $t_R$ = 9.2 min

$[\alpha]_D$ = -55 (*c* 0.54, MeOH).

$^1$H-NMR (500 MHz, $CD_3CN$): δ 8.22 (br, s, 1H $D_2O$ exchangeable), 7.41 (s, 1H), 7.33 (d, *J* = 8 Hz, 1H), 7.06 (dd, *J* = 8, 8 Hz, 1H), 7.02 (d, *J* = 8 Hz, 1H), 5.14 (d, *J* = 8 Hz, 1H), 5.00 (d, *J* = 4.5 Hz, 2H), 4.14 (s, 3H), 3.42-3.84 (m, 10H, 4H $D_2O$ exchangeable), 2.59 (s, 3H).

$^{13}$C NMR (125.8 MHz, $CD_3CN$): δ 198.5 (s), 144.0 (s), 126.8 (s), 125.5 (d), 123.6 (s), 121.2 (d), 113.7 (d), 108.7 (d), 107.7 (s), 101.6 (d), 77.1 (d), 76.9 (d), 74.1 (d), 70.5 (d), 67.2 (q), 61.9 (d), 42.1 (t), 17.6 (q).

HRMS-ESI *m/z*: measured 445.1094 ($[M+1]^+$, calcd. 445.1097 for $C_{18}H_{25}N_2O_7S_2$).

MS-ESI *m/z* (% relative intensity): 445 ($[M+1]^+$, 58), 414 (72), 338 (100), 249 (25).

FTIR $\nu_{max}$ (KBr): 3347, 2926, 2855, 1698, 1578, 1496, 1249, 1077 $cm^{-1}$.

UV ($CH_3CN$) $\lambda_{max}$ (log ε): 221 (4.5), 270 (4.0).

### *4.4.6.2 1-(β-D-glucopyranosyl)cyclobrassinin (221)*

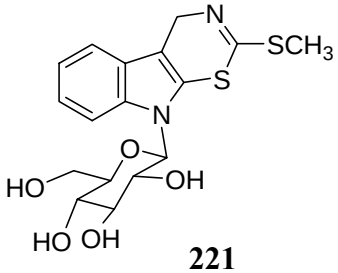


**221**

HPLC $t_R$ = 8.6 min

$[\alpha]_D$ = -14 (*c* 0.23, MeOH).

$^1$H NMR (500 MHz, $(CD_3)_2CO$): δ 7.57 (d, *J* = 8 Hz, 1H), 7.50 (d, *J* = 8 Hz, 1H), 7.09-7.16 (m, 2H), 5.48 (br, s, 1H), 5.32 (d, *J* = 18 Hz, 1H), 4.77 (d, *J* = 18 Hz, 1H), 4.66 (br, s, 1H, $D_2O$ exchangeable), 3.63-4.09 (m, 8H, 2H $D_2O$ exchangeable), 2.54 (s, 3H).

$^{13}$C NMR (125.8 MHz, $(CD_3)_2CO$): δ 152.5 (s), 137.0 (s), 125.5 (s), 121.9 (s), 121.8 (d), 120.4 (d), 117.3 (d), 111.1 (d), 104.5 (s), 86.1 (d), 80.4 (d), 78.1 (d), 72.7 (d), 70.8 (d), 62.4 (t), 48.5 (t), 14.7 (q).

HRMS-FAB *m/z*: measured 397.0881 ($[M+1]^+$, calcd. 397.0891 for $C_{17}H_{21}N_2O_5S_2$).

MS-FAB *m/z* (% relative intensity): 397 ($[M+1]^+$, 100), 396 (63), 395 (34), 329 (50).

FTIR $\nu_{max}$ (KBr): 3380, 2923, 2852, 1617, 1452, 1346, 1249, 1079, 901, 734 $cm^{-1}$.

UV ($CH_3CN$) $\lambda_{max}$ (log ε): 231 (4.4), 286 (3.9) nm.

### *4.4.6.3 6-Hydroxysinalexin (226)*

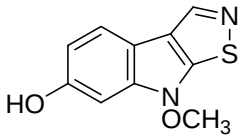


**226**

HPLC $t_R$ = 12.0 min.

$^1$H-NMR (500 MHz, $CD_3CN$): δ 8.63 (s, 1H), 7.74 (d, *J* = 8.5 Hz, 1H), 7.24 (br s, 1H $D_2O$ exchangeable), 6.98 (d, *J* = 2 Hz, 1H), 6.83 (dd, *J* = 8.5, 2 Hz, 1H), 4.14 (s, 3H).

HRMS-ESI *m*/*z*: measured 221.0377 ($[M+1]^+$, calc. 221.0379 for $C_{10}H_9N_2O_2S$).

MS-ESI *m*/*z* (% relative intensity): 221 ($[M+1]^+$ 100), 190 (56), 114 (34).

FTIR $\nu_{max}$ (KBr): 3353, 2928, 2857, 1611, 1460, 1248, 1203, 1075 $cm^{-1}$.

UV ($CH_3CN$) $\lambda_{max}$ (log ε): 228 (4.5), 266 (4.0) nm.

### *4.4.6.4 6-Oxy-(O-β-D -glucopyranosyl)sinalexin (227)*

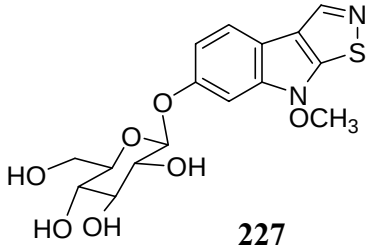


**227**

HPLC $t_R$ = 4.9 min.

$[\alpha]_D = -57$ (*c* 0.20, MeOH).

$^1$H NMR (500 MHz, $(CD_3)_2CO$): δ 8.73 (s, 1H), 7.86 (d, *J* = 8.5 Hz, 1H), 7.33 (d, *J* = 2 Hz, 1H), 7.06 (dd, *J* = 8.5, 2 Hz, 1H), 5.10 (d, *J* = 7.5 Hz, 1H), 4.23 (s, 3H), 3.94–3.47 (m, 8H, 2H $D_2O$ exchangeable).

$^{13}$C NMR (125.8 MHz, $(CD_3)_2CO$): δ 156.3 (s) 155.7 (s), 147.9 (d), 142.5 (s), 123.9 (s), 121.1 (d), 112.8 (s), 112.6 (d), 102.1 (d), 97.7 (d), 77.4 (d), 77.1 (d), 74.0 (d), 70.6 (d), 63.9 (q), 61.7 (t).

HRMS-ESI *m*/*z*: measured 383.0928 ($[M + 1]^+$, calc. 383.0912 for $C_{16}H_{18}N_2O_7S$).

MS-ESI *m*/*z* (% relative intensity): 383 ($[M + 1]^+$, 95), 185 (11), 114 (100).

FTIR $\nu_{max}$ (KBr): 3359, 2926, 2854, 1611, 1459, 1248, 1205, 1073 cm−1.

UV ($CH_3CN$) $\lambda_{max}$ (log ε): 228 (4.6), 267 (4.0) nm.

X-Ray crystal data: $C_{16}H_{18}N_2O_7S$, $M$ = 382.38, monoclinic, space group $P2_1$, $a$ = 13.8821(3), $b$ = 4.5502(2), $c$ = 14.6589(4) Å, $\beta$ = 109.8086(17)°, $U$ = 871.16(5) Å$^3$, $T$ = 173(2) K, $Z$ = 2, $\mu$(Mo-Kα) = 0.228 mm$^{-1}$, 10 196 reflections collected, 3438 independent reflections ($R_{int}$ = 0.0632), final $R$ values: $R_1$ = 0.0471, $wR_2$ = 0.1037 [$I > 2\sigma(I)$]; $R_1$ = 0.0559, $wR_2$ = 0.1090 (all data). CCDC reference number 603052.

### *4.4.6.5 1-Methyl-(oxy-O-β-D-glucopyranosyl)brassilexin (228)*

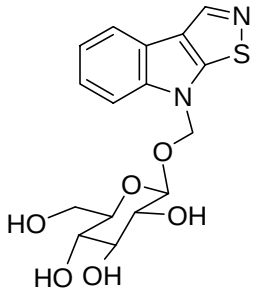


**228**

HPLC $t_R$ = 4.4 min.

$[\alpha]_D$ = −109 (*c* 0.06, MeOH).

$^1$H NMR (500 MHz, $(CD_3)_2CO$, after adding $D_2O$): δ 8.80 (s, 1H), 7.98 (d, $J$ = 8 Hz, 1H), 7.76 (d, $J$ = 8 Hz, 1H), 7.40 (ddd, $J$ = 7, 7, 1 Hz, 1H), 7.29 (dd, $J$ = 8, 7 Hz, 1H),

6.13 (d, $J$ = 11.5 Hz, 1H), 5.90 (d, $J$ = 11.5Hz, 1H), 4.39 (d, $J$ =7.5Hz, 1H), 3.86 (dd, $J$ =12, 3Hz, 1H), 3.70–3.60 (m, 3H), 3.58–3.48 (m, 2H).

$^{13}$C NMR (125.8 MHz, $(CD_3)_2CO$): δ 161.6 (s), 148.3 (d), 144.6 (s), 124.5 (d), 121.7 (d), 121.2 (s), 120.8 (s), 120.5 (d), 111.1 (d), 100.0 (d), 76.5 (d), 73.5 (d), 73.4 (t), 70.1 (d), 63.4 (d), 61.4 (d).

HRMS-FAB $m/z$: measured 367.0968 ($[M+1]^+$, calc. 367.0963 for $C_{16}H_{19}N_2O_6S$).

FTIR $\nu_{max}$ (KBr): 3350, 3068, 2910, 1509, 1476, 1446, 1375, 1257, 1073, 745 $cm^{-1}$.

UV ($CH_3OH$) $\lambda_{max}$ (log $\varepsilon$): 221 (4.4), 243 (3.9), 264 nm (3.8).

### *4.4.6.6 Spiro[3H-indole-3,5'-thiazolidin]-2(1H),2'-dione (231)*

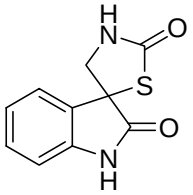


**231**

HPLC $t_R$ = 5.1 min.

$[\alpha]_D$ = −35 ($c$ 0.33, MeOH).

$^1$H-NMR (500 MHz, $CD_3CN$): δ 8.63 (br s, 1H $D_2O$ exchangeable), 7.53 (d, $J$ = 7.5 Hz, 1H), 7.31 (ddd, $J$ = 7.5, 7.5, 1 Hz, 1H), 7.10 (ddd, $J$ = 7.5, 8, 1.0 Hz, 1H), 6.95 (d, $J$ = 8 Hz, 1H), 6.40 (br s, 1H $D_2O$ exchangeable), 3.82 (d, $J$ = 11 Hz, 1H), 3.77 (d, $J$ = 11 Hz, 1H).

$^{13}$C-NMR (125.8 MHz, $CD_3CN$): δ 176.7 (s), 171.9 (s), 141.2 (s), 130.4 (d), 129.9 (s), 124.7 (d), 123.4 (d), 110.6 (d), 57.0 (s), 51.0 (t).

HRMS-EI $m/z$: measured 220.0304 ($M^+$, calc. 220.0306 for $C_{10}H_8N_2O_2S$).

MS-EI $m/z$ (% relative intensity): 220 ($M^+$, 48), 191 (59), 164 (36), 135 (27).

FTIR $\nu_{max}$ (KBr): 3273, 2919, 2854, 1719, 1619, 1472, 1328, 1247, 1185, 1079, 748 $cm^{-1}$.

UV ($CH_3CN$) $\lambda_{max}$ (log $\varepsilon$): 212 (4.4), 250 (3.7), 297 (3.2) nm.

#### *4.4.6.7 1-Methoxyspiro[3H-indole-3,5'-thiazolidin]-2(1H),2'-dione (232)*

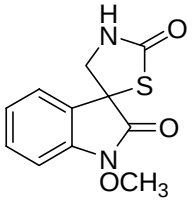

**232**

HPLC $t_R$ = 7.5min.

$[\alpha]_D$ = −7 (*c* 0.34, MeOH); ee 11% (calculated using chiral solvating agent by $^1$H NMR). $^1$H-NMR (500 MHz, $CD_3CN$): δ 7.59 (d, *J* = 7.5 Hz, 1H), 7.43 (dd, *J* = 7.5, 7.5 Hz, 1H), 7.20 (dd, *J* = 7.5, 7.5 Hz, 1H), 7.08 (d, *J* = 7.5 Hz, 1H), 6.45 (br s, 1H $D_2O$ exchangeable), 4.01 (s, 3H), 3.85 (d, *J* = 11 Hz, 1H), 3.80 (d, *J* = 11 Hz, 1H).

$^{13}$C-NMR (125.8 MHz, $CD_3CN$): δ 171.4 (s), 170.2 (s), 139.9 (s), 130.6 (d), 126.0 (s), 124.7 (d), 124.4 (d), 108.0 (d), 63.8 (q) 55.3 (s), 50.6 (t).

HRMS-EI *m*/*z*: measured 250.0410 ($M^+$, calc. 250.0412 for $C_{11}H_{10}N_2O_3S$).

MS-EI *m*/*z* (% relative intensity): 250 ($M^+$, 100), 194 (24), 163 (23), 162 (39), 148 (53), 131 (32).

FTIR $\nu_{max}$ (KBr): 3268, 2935, 2883, 1704, 1617, 1466, 1324, 1226, 1080, 750 $cm^{-1}$.

UV ($CH_3CN$) $\lambda_{max}$ (log $\varepsilon$): 212 (4.3), 256 (3.7) nm.

### *4.4.6.8 1-Methoxy-2'-thioxospiro[3H-indole-3,5'-thiazolidin]-2(1H)-one (233)*

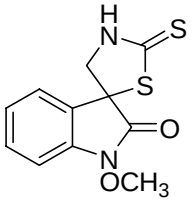

**233**

HPLC $t_R$ = 11.5 min.

$[\alpha]_D$ = −31 (*c* 0.10, MeOH); ee 30% (calculated using chiral solvating agent by $^1$H NMR).

$^1$H-NMR (500 MHz, $CD_3CN$): δ 8.18 (br s, 1H $D_2O$ exchangeable), 7.57 (d, *J* = 7.5 Hz, 1H), 7.41 (dd, *J* = 7.5, 7.5 Hz, 1H), 7.19 (dd, *J* = 7.5, 7.5 Hz, 1H), 7.05 (d, *J* = 7.5 Hz, 1H), 4.23 (d, *J* = 13 Hz, 1H), 4.20 (d, *J* = 13 Hz, 1H), 3.98 (s, 3H).

$^{13}$C-NMR (125.8 MHz, $CD_3CN$): δ198.3 (s), 169.6 (s), 139.9 (s), 130.8 (d), 124.8 (d), 124.5 (s), 124.3 (d), 108.2 (d), 63.9 (q) 59.5 (s), 58.7 (t).

HRMS-EI *m*/*z*: measured 266.0189 ($M^+$, calc. 266.0184 for $C_{11}H_{10}N_2O_2S_2$).

MS-EI *m*/*z* (% relative intensity): 266 ($M^+$, 100), 194 (36), 175 (26), 162 (44), 148 (36), 144 (37), 116 (19).

FTIR $\nu_{max}$ (KBr): 3220, 2935, 2859, 1731, 1617, 1503, 1463, 1291, 1058, 753 $cm^{-1}$.

UV ($CH_3CN$) $\lambda_{max}$ (log $\varepsilon$): 217 (4.4), 264 (4.2) nm.

### *4.4.6.9 1-Methylspiro[3H-indole-3,5'-thiazolidin]-2(1H),2'-dione (234).*

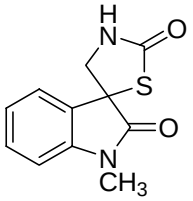

**234**

HPLC $t_R$ = 6.6 min.

$[\alpha]_D = -5$ ($c$ 0.20, $CH_3OH$).

$^1$H-NMR (500 MHz, $CD_3CN$): δ 7.57 (dd, $J$ =7.5, 0.5Hz, 1H), 7.39 (ddd, $J$ =8, 8, 1.1Hz, 1H), 7.15 (ddd, $J$ = 8, 8, 1 Hz, 1H), 6.98 (d, $J$ = 8 Hz, 1H), 6.39 (br s, 1H $D_2O$ exchangeable), 3.81 (d, $J$ = 11 Hz, 1H), 3.75 (d, $J$ = 11 Hz, 1H), 3.19 (s, 3H).

$^{13}$C-NMR (125.8 MHz, $CD_3CN$): δ 175.2 (s), 171.9 (s), 143.6 (s), 130.4 (d), 129.6 (s), 124.3 (d), 123.6 (d), 109.3 (d), 56.9 (s), 51.1 (t), 26.6 (q).

HRMS-EI $m/z$: measured 234.0459 ($M^+$, calc. 234.0463 for $C_{11}H_{10}N_2O_2S$).

MS-EI $m/z$ (% relative intensity): 234 ($M^+$, 44), 179 (11), 178 (100), 177 (17), 174 (18), 158 (11).

FTIR $\nu_{max}$ (KBr): 3263, 3058, 2935, 2883, 1706, 1611, 1470, 1372, 1347, 1247, 1133, 1077, 754 $cm^{-1}$.

UV ($CH_3CN$) $\lambda_{max}$ (log $\varepsilon$): 214 (4.5), 257 (3.9), 299 (3.3) nm.

### *4.4.6.10 1-Hydroxymethylspirobrassinin (235)*

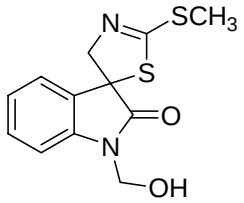


**235**

HPLC $t_R$ = 11.1 min.

$^1$H-NMR (500 MHz, $CDCl_3$): δ 7.45 (d, *J* = 8 Hz, 1H), 7.4 (dd, *J* = 8, 8 Hz, 1H), 7.20–7.14 (m, 2H), 5.35 (d, *J* = 11 Hz, 1H), 5.21 (d, *J* = 11 Hz, 1H), 4.76 (d, *J* = 14.5 Hz, 1H), 4.55 (d, *J* = 14.5 Hz, 1H), 2.82 (s, 3H).

$^{13}$C-NMR (125.8 MHz, $CDCl_3$): δ 176.9 (s), 164.7 (s), 140.8 (s), 130.6 (s), 130.3 (d), 124.7 (d), 124.6 (d), 110.0 (d), 75.4 (t), 64.8 (s), 64.7 (t), 16.1 (q).

HRMS-EI *m*/*z*: measured 280.0348 ($M^+$, calc. 280.0340 for $C_{12}H_{12}N_2O_2S_2$).

MS-EI *m*/*z* (% relative intensity): 280 ($M^+$, 26), 250 (49), 203 (40), 177 (100), 149 (51), 117 (47), 87 (57).

FTIR $\nu_{max}$ (KBr): 3311, 2935, 2854, 1739, 1620, 1583, 1464, 1086, 945, 743 $cm^{-1}$.

### *4.4.6.11 1-β-D-glucopyranosyl-3-phenylindole (299)*

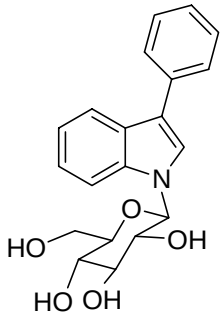


**299**

HPLC $t_R$ = 11.8 min.

$[\alpha]_D = -21$ (*c* 0.20, $CH_3OH$).

$^1$H-NMR (500 MHz, $CD_3CN/D_2O$, 5.0/0.01, v/v): δ 7.93 (d, *J* = 8 Hz, 1H), 7.74 (d, *J* = 7.5 Hz, 2H), 7.69 (s, 1H), 7.61 (d, *J* = 8 Hz, 1H), 7.49 (dd, *J* = 7.5, 7.5 Hz, 2H), 7.34-7.29 (m, 2H), 7.23 (dd, *J* = 7.5, 7.5 Hz, 1H), 5.54 (d, *J* = 9 Hz, 1H), 3.96 (dd, *J* = 9, 9 Hz, 1H), 3.79 (dd, *J* = 10, 2 Hz, 1H), 3.68-3.50 (m, 4H).

$^{13}$C-NMR (125.8 MHz, $CD_3CN$): δ 137.9 (s), 135.8 (s), 129.3 (d), 127.6 (d), 126.8 (s), 126.4 (d), 123.8 (d), 122.7 (d), 121.1 (d), 119.9 (d), 117.9 (s), 111.2 (d), 85.2 (d), 79.2 (d), 77.9 (d), 72.6 (d), 70.5 (d), 61.9 (t).

HRMS-ESI *m*/*z*: measured 354.1345 $[(M-1)^-$, calc. 354.1346 for $C_{20}H_{20}NO_5$).

FTIR $\nu_{max}$ (KBr): 3347, 2925, 1708, 1602, 1462, 1378, 1215, 1077, 1033, 746 $cm^{-1}$.

UV ($CH_3CN$) $\lambda_{max}$ (log $\varepsilon$): 202 (4.2), 224 (4.2), 267 (3.8) nm.

### *4.4.6.12 Methyl (7-oxy-**O**-β-D-glucopyranosylthianaphthen-3-yl)methyl-dithiocarbamate (297)*

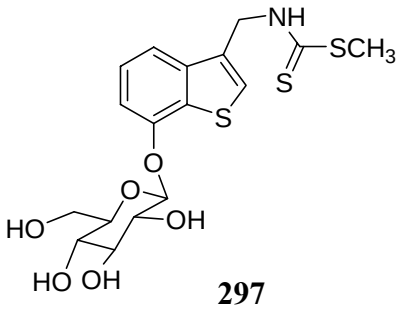


**297**

HPLC $t_R$ = 8.8 min.

$[\alpha]_D = -60$ (*c* 0.26, $CH_3OH$).

$^1$H-NMR [500 MHz, $(CD_3)_2CO$]: δ 9.33 (br, s, 1H), 7.61 (s, 1H), 7.58 (d, *J* = 8 Hz,1H), 7.36 (dd, *J* = 8, 8 Hz, 1H), 7.18 (d, *J* = 8 Hz, 2H), 5.23-5.21 (m, 3H), 3.90 (d, *J* = 10 Hz, 1H), 3.74-3.71 (m, 1H), 3.59-3.49 (m, 4H), 2.61 (s, 3H).

$^{13}$C-NMR (125.8 MHz, $(CD_3)_2CO$: δ 199.3 (s), 153.2 (s), 140.5 (s), 132.4 (s), 130.3 (s), 126.2 (d), 126.1 (d) 116.1 (d), 109.5 (d), 101.6 (d), 77.6 (d), 77.5 (d), 74.1 (d), 70.8 (d), 62.1 (t), 44.8 (t), 17.5 (q).

HRMS-ESI *m*/*z*: measured 430.0478 $[(M-1)^-$, calc. 430.0458 for $C_{17}H_{20}NO_6S_3$).

FTIR $\nu_{max}$ (KBr): 3335, 2925, 1710, 1602, 1552, 1462, 1378, 1216, 1078, 1032, 746 $cm^{-1}$.

UV ($CH_3CN$) $\lambda_{max}$ (log ε): 224 (4.4), 254 (4.1), 304 (3.5) nm.

### *4.4.6.13 Methyl (1-β-D-glucopyranosyl-3-hydroxylindol-2-yl)methyldithiocarbamate (295)*

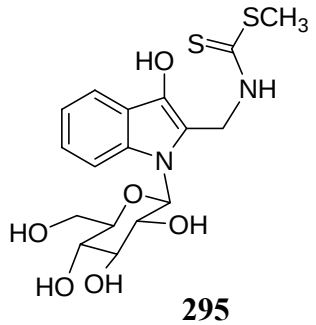


**295**

HPLC $t_R$ = 9.5 min.

$[\alpha]_D = -211$ (*c* 0.12, $CH_3OH$).

$^1$H-NMR (500 MHz, $CD_3CN/D_2O$, 5.0/0.01, v/v): δ 9.57 (br, s, $D_2O$ exchangeable, 1H), 9.25 (br, s, $D_2O$ exchangeable, 1H), 7.66 (d, *J* = 8 Hz,1H), 7.37 (d, *J* = 8 Hz,1H), 7.16 (dd, *J* = 8, 8 Hz, 1H), 7.08 (dd, *J* = 8, 8 Hz, 1H), 5.33 (d, *J* = 14.5 Hz, 1H), 4.86 (d, *J* = 14.5 Hz, 1H), 4.56 (d, *J* = 8 Hz, 1H), 3.93 (dd, *J* = 12, 2 Hz, 1H), 3.64 (dd, *J* = 12, 7 Hz, 1H), 3.45 (dd, *J* = 8, 8 Hz, 1H), 3.38 (dd, *J* = 8, 8 Hz, 1H), 3.31-3.24 (m, 2H), 2.62 (s, 3H).

$^{13}$C-NMR (125.8 MHz, $CD_3CN$): δ 201.6 (s), 135.2 (s), 133.9 (s), 126.6 (s), 123.6 (d), 121.6 (s), 120.2 (d), 118.6 (d), 112.9 (d), 105.9 (d), 77.3 (d), 77.1 (d), 74.4 (d), 71.2 (d), 62.7 (t), 41.2 (t), 18.4 (q).

HRMS-ESI *m*/*z*: measured 413.0840 $[(M-1)^-$, calc. 413.0846 for $C_{17}H_{21}N_2O_6S_2$).

FTIR $\nu_{max}$ (KBr): 3359, 2922, 1471, 1384, 1256, 1072 $cm^{-1}$.

UV ($CH_3CN$) $\lambda_{max}$ (log $\varepsilon$): 223 (4.5), 272 (4.2) nm.

## 4.5 Antifungal activity

The antifungal activity of compounds was determined using the following mycelial radial growth bioassay. First the isolate of *S. sclerotiorum* (clone # 33) was grown on potato dextrose agar (PDA) plates by inoculating one piece of sclerotia per plate and the plates were incubated for 3 days at 20±1 ºC in the dark. Solutions of each compound in DMSO (50 mM) were used to prepare assay solutions in minimal media (0.5, 0.3, 0.1, 0.05, and 0.02 mM) by serial dilution; control solutions contained 1% DMSO in minimal media. Sterile tissue culture plates (12-well, 23mm diameter) containing test solutions and control solution (1 ml per well) were inoculated with mycelium plugs (4 mm cut from 3-day-old PDA plates of *S. sclerotiorum*, clone # 33) placed upside down on the center of each plate and incubated under constant light for 3 days. All bioassay experiments were carried out in triplicate, at least two times.

## 4.6 Co-metabolism of brassinin, camalexins and potential brassinin detoxification inhibitors in *Sclerotinia sclerotiorum*

Six Erlenmeyer flasks (125 ml) each containing 50 ml minimal media were employed. Five of the flasks were each inoculated with three pieces of mycelial plugs (4-day old, 6 mm) of *S. sclerotiorum* clone # 33, the flasks were incubated at 22 ± 2º C on a shaker at 120 rpm in light. After four days of incubation potential inhibitors (final concentration 0.05 mM) in $CH_3CN$ [final concentration 0.5% (v/v)] were added to fungal cultures in two of the flasks (flasks 1 and 2). Similarly, the potential inhibitors (final concentration 0.1 mM) were added to fungal cultures in two other flasks (flasks 3 and 4). These four flasks (flasks 1, 2, 3 and 4) were incubated for 10 min and then brassinin (**9**, final concentration 0.05 mM) in $CH_3CN$ [final concentration 0.5% (v/v)] were added to each of the four flasks (flasks 1, 2, 3 and 4). To the flask 5, both

brassinin (**9**) (dissolved in $CH_3CN$, final concentration 0.05 mM) and potential inhibitors (dissolved in $CH_3CN$, final concentration 0.05 mM) were added to uninoculated medium (control 1). To the fungal culture in flask 6 (control 2) was added $CH_3CN$ (150 μl). Samples (5 ml each) were withdrawn from the flasks immediately after adding the compounds. Subsequently 5 ml samples were withdrawn after 2, 4, 6, 10, 12, 48 hours and so on until all the brassinin (**1**) was completely metabolized. Each sample was either frozen or immediately extracted with EtOAc (2 × 10 ml). The organic extracts were concentrated, dissolved in acetonitrile (500 μL), and filtered through a tight cotton plug into a HPLC vial for analysis.

## 4.7 Screening of potential brassinin detoxification inhibitors using crude cell free extracts

### 4.7.1 Preparation of crude cell free extracts

Erlenmeyer flasks (250 ml × 5) each containing 100 ml of PDB media were employed. All the flasks were inoculated with sclerotia (5 pieces) of *S. sclerotiorum* clone # 33. After seven days, a solution of camalexin (50 mM, 100 μl) in DMSO was added as an inducer to each of the five flasks (final concentration 0.05 mM) and incubated for 24 hours. The fungal mycelium was filtered off, washed with water, the remaining water squeezed out between filter paper and the mycelial pad frozen immediately. Frozen mycelia were mixed with ice-cold Tris HCl (50 mM, pH 8.0, containing 5% glycerol, 2 mM dithiothreitol, 2 mM PMSF, and 0.01% triton X-100) buffer (ca. 15 ml) and ground at 4 ºC using a mortar and pestle until a homogenous mixture was obtained. The mixture was then centrifuged at 58,545g (22,000 rpm) for 40 min to obtain the cell homogenate and the pellet was discarded.

### 4.7.2 Protein measurements

#### *4.7.2.1 Preparation of BSA calibration curve*

The Bradford protein assay was used to estimate the quantities of proteins in the cell homogenate using a calibration curve prepared from bovine serum albumin (BSA). A stock solution (1 mg/ml) of BSA in the extraction buffer was prepared from which five other concentrations (0.30, 0.25, 0.20, 0.15, and 0.10 mg/ml) were prepared by serial dilution using the same buffer. In a spectrophotometric cell (1 ml) were taken 100 μl of each solution and 1 ml of Bradford reagent. After mixing, the solution mixture was incubated for 5 min and the optical density was measured at 595 nm. A blank sample containing 100 μl extraction buffer and 1 ml Bradford reagent was used as control. All samples were prepared in triplicate and finally the calibration curve was obtained by plotting concentration vs. optical density.

#### *4.7.2.2 Protein measurements*

40 μl of cell homogenate was diluted to 1 ml using the extraction buffer. In a spectrophotometric cell (1 ml) were taken 100 μl of this diluted solution and 1 ml of Bradford reagent. After mixing, the solution mixture was incubated for 5 min and the optical density was measured at 595 nm. A blank sample containing 100 μl extraction buffer and 1 ml Bradford reagent was used as control. All samples were prepared in triplicate and finally the concentration of proteins was determined using the BSA calibration curve.

### 4.7.3 Enzyme assays

Enzyme assays were carried out at 25 ºC, using brassinin (**9**) (or other compounds as reported) as a substrate and UDPG as a glucose donor. The specific activity of cell-free extracts was defined as the amount (nmol) of 1-β-D-glucopyranosylbrassinin (**66**) product formed per min per mg of protein. The 0.5 ml

standard assay mixture contained 0.5 ml of cell free extract as enzyme source, 3 μl of 50 mM UDPG (final concentration 0.3 mM) solution in water, and 3 μl of 50 mM brassinin (final concentration 0.3 mM) in DMSO. The assay mixture was incubated at 25 ºC with constant shaking for 1 hour and EtOAc (2×2 ml) was used to extract the reaction product. After concentrating, the EtOAc extract was dissolved in 100 μl of $CH_3CN$ and analyzed by HPLC. Quantification of the reaction product was carried out using a standard calibration curve (Pedras et al. 2004c).

The screening of potential inhibitors was carried out in the following way. Each potential inhibitor (final concentration 0.3 and 0.6 mM) dissolved in DMSO was added to a vial containing 2.0 ml of cell-free extracts and UDPG (final concentration 0.3 mM, dissolved in water) and the mixture was incubated at room temperature for 30 min. After that, brassinin (**9**, 0.3 mM) was added in each vial and the mixture was immediately divided into four samples in separate vials (0.5 ml each). Three samples were incubated for one more hour and the remaining sample was extracted immediately with EtOAc. After 60 min of incubation the three samples were extracted separately with EtOAc (2×2 ml), the extracts were dissolved in $CH_3CN$ (100 μl) and analyzed by HPLC for the detection and quantification of the reaction product 1-β-D-glucopyranosylbrassinin (**66**). Control experiments containing only brassinin (**9**, 0.3 mM) were performed similarly.

# Chapter 5: REFERENCES


Acuna, I. A.; Strobel, G. A.; Jacobsen, B. J.; Corsini, D. L.; **2001**. Glucosylation as a mechanism of resistance to thaxtomin A in potatoes. *Plant Science* (Shannon, Ireland), 161, 77-88.

Adams, P.B.; Ayers, W.A.; **1979**. Ecology of *Sclerotinia* species. *Phytopathology*, 69, 96-899.

Agarwal, A.; Garg, G. K.; Singh, U. S.; Mishra, D. P.; **1994**. Detection and role of chlorotic toxin and phytohormones in the pathogenesis of Alternaria blight in *Brassica napus*. *Current Science*, 66, 442-443.

Arnoldi, A.; Merlini, L.; **1990**. Lipophilicity-antifungal activity relationships for some isoflavonoid phytoalexins. *Journal of Agricultural and Food Chemistry*, 38, 834-838.

Ayer, W. A.; Craw, P. A.; Yu-ting M.; Miao, S.; **1992**. Synthesis of camalexin and related phytoalexins. *Tetrahedron*, 48, 2919-2924.

Baerson, S. R.; Sanchez-Moreiras, A.; Pedrol-Bonjoch, N.; Schulz, M.; Kagan, I. A.; Agarwal, A. K.; Reigosa, M. J.; Duke, S. O.; **2005**. Detoxification and transcriptome response in Arabidopsis seedlings exposed to the allelochemical benzoxazolin-2(3H)-one. *Journal of Biological Chemistry*, 280, 21867-21881.

Bailey, B. A.; Larson, R. L.; **1989**. Hydroxamic acid glucosyltransferases from maize seedlings. *Plant Physiology*, 90, 1071-1076.

Bak, S.; Olsen, C. E.; Petersen, B. L.; Moller, B. L.; Halkier, B. A.; **1999**. Metabolic engineering of p-hydroxybenzylglucosinolate in Arabidopsis by expression of the cyanogenic CYP79A1 from *Sorghum bicolor*. *Plant Journal*, 20, 663-671.

Bennett, G. A.; Shotwell, O. L.; **1979**. Zearalenone in cereal grains. *Journal of the American Oil Chemists' Society*, 56, 812-819.

Bennett, R. N.; Wallsgrove, R. M.; **1994**. Secondary metabolites in plant defense mechanisms. *New Phytologist*, 127, 617-33.

Boland, G. J.; Hall, R.; **1994**. Index of plant hosts of *Sclerotinia sclerotiorum*. *Canadian Journal of Plant Pathology*, 16, 93-108.

Bowyer, P.; Clarke, B. R.; Lunness, P.; Daniels M. J.; Osbourn, A. E.; **1995**. Host-range of a plant-pathogenic fungus determined by a saponin detoxifying enzyme. *Science*, 267, 371-374.

Brady, W. T.; Giang, Y. F.; **1985**. Intramolecular (2 + 2) cycloadditions of phenoxyketenes. *Journal of Organic Chemistry*, 50, 5177-5179.

Brooks, C. J. W.; Watson, D. G.; **1985**. Phytoalexins. *Natural Product Reports*, 2, 427-59.

Brooks, C. J. W.; Watson, D. G.; **1991**. Terpenoid phytoalexins. *Natural Product Reports*, 8, 367-389.

Casimiro, S.; Tenreiro, R.; Monteiro, A. A.; **2006**. Identification of pathogenesis-related ESTs in the crucifer downy mildew oomycete *Hyaloperonospora parasitica* by high-throughput differential display analysis of distinct phenotypic interactions with *Brassica oleracea*. *Journal of Microbiological Methods*, 66, 466-478.

Cole, D. J. and Edwards, R., 2000; In: Roberts, T. (ed), *Metabolism of Agrochemicals in Plants*; John Wiley & Sons, LTD. p107.

Coutinho, P. M.; Deleury, E.; Davies, G. J.; Henrissat, B.; **2003a**. An evolving hierarchical family classification for glycosyltransferases. *Journal of Molecular Biology*, 328, 307-317.

Coutinho, P. M.; Stam, M.; Blanc, E.; Henrissat, B.; **2003b**. Why are there so many carbohydrate-active enzyme-related genes in plants? *Trends in Plant Science*, 8, 563-565.

Dickman, M.; Mitra, A.; **1992**. *Arabidopsis thaliana* as a model for studying *Sclerotinia sclerotiorum* pathogenesis. *Physiological and Molecular Plant Pathology*, 41, 255-263.

Dillard, H. R.; Ludwig, J. W.; Hunter, J. E.; **1995**. Conditioning sclerotia of *Sclerotinia sclerotiorum* for carpogenic germination. *Plant Disease*. 79, 411-415.

Elsner, J.; Boeckler, F.; Davidson, K.; Sugdenb, D.; Gmeinera, P.; **2006**. Bicyclic melatonin receptor agonists containing a ring-junction nitrogen: Synthesis, biological evaluation, and molecular modeling of the putative bioactive conformation. *Bioorganic & Medicinal Chemistry*, 14, 1949–1958.

Engelhardt, G.; Zill, G.; Wohner, B.; Wallnoefer, P. R.; **1988**. Transformation of the Fusarium mycotoxin zearalenone in maize cell suspension cultures. *Naturwissenschaften*, 75, 309-310.

Ferezou, J. P.; Riche, C.; Quesneau-Thierry, A.; Pascard-Billy, C.; Barbier, M.; Bousquet, J. F.; Boudart, G.; **1977**. Structures of two toxins isolated from cultures of the fungus *Phoma lingam* Tode: sirodesmin PL and deacetylsirodesmin PL. *Nouveau Journal de Chimie*, 1, 327-334.

Ford, C. M.; Boss, P. K.; Hoj, P. B.; **1998**. Cloning and characterization of *Vitis vinifera* UDP-glucose: flavonoid 3-*O*-glucosyltransferase, a homologue of the enzyme encoded by the maize *Bronze*-1 locus that may primarily serve to glucosylate anthocyanidins in vivo. *The Journal of Biological Chemistry*, 273, 9224-9233.

Frey, M.; Chomet, P.; Glawischnig, E.; Stettner, C.; Grun, S.; Winklmair, A.; Eisenreich, W.; Bacher, A.; Meeley, R. B.; Briggs, S. P.; Simcox, K.; Gierl, A.; **1997**. Analysis of a chemical plant defense mechanism in grasses. *Science*, 277, 696-699.

Fujita, M.; Yoshizawa, T.; **1990**. Metabolism of deoxynivalenol, a trichothecene mycotoxin, in sweet potato root tissues. *Shokuhin Eiseigaku Zasshi*, 31, 474-478.

Fukushima, K.; Arai, T.; Mori, Y.; Tsuboi, M.; Suzuki, M.; **1983**. Studies on peptide antibiotics, leucinostatins. II. The structures of leucinostatins A and B. *Journal of Antibiotics*, 36, 1613-1630.

Gachon, C. M. M.; Langlois-Meurinne, M.; Saindrenan, P.; **2005**. Plant secondary metabolism glycosyltransferases: the emerging functional analysis. *Trends in Plant Science*, 10, 542-549.

Gallant, M.; Link, J. T.; Danishefsky, S. J.; **1993**. A stereoselective synthesis of indole-β-*N*-glycosides: an application to the synthesis of rebeccamycin. *Journal of Organic Chemistry*, 58, 343-349.

Gilbert, J.; **1995**. Analysis of mycotoxins in food and feed: certification of DON in wheat and maize. *Natural Toxins*, 3, 263-268.

Godoy, G.; Steadman, J. R.; Dickman, M. B.; Dam, R.; **1990**. Use of mutants to demonstrate the role of oxalic acid in pathogenicity of *Sclerotinia sclerotiorum* on *Phaseolus vulgaris*. *Physiological and Molecular Plant Pathology*, 37, 179-191.

Gomez-Campo, C.; **1999**. In: *Biology of Brassica Coenospecies*, Amsterdam: Elsevier.

Gong, Z.; Yamazaki, M.; Sugiyama, M.; Tanaka, Y.; Saito, K.; **1997**. Cloning and molecular analysis of structural genes involved in anthocyanin biosynthesis and expressed in a forma-specific manner in *Perilla frutescens*. *Plant Molecular Biology*, 35, 915-927.

Goyal, B. K.; Kant, U.; Verma, P. R.; **1995**. Growth of *Albugo candida* (race unidentified) on *Brassica juncea* callus cultures. *Plant and Soil*, 172, 331-337.

Graniti, A.; **1991**. Phytotoxins and their involvement in plant diseases. *Experientia*, 47, 751-755.

Grayer, R. J.; Harborne, J. B.; **1994**. A survey of antifungal compounds from higher plants, 1982-1993. *Phytochemistry*, 37, 19-42.

Greenhalgh, J. R.; Mitchell, N. D.; **1976**. The involvement of flavor volatiles in the resistance to downy mildew of wild and cultivated forms of *Brassica oleracea*. *New Phytologist*, 77, 391-398.

GrootWassink, J. W. D.; Reed, D. W.; Kolenovsky, A. D.; **1994**. Immunopurification and immunocharacterization of the glucosinolate biosynthetic enzyme thiohydroximate *S*-glucosyltransferase. *Plant Physiology*, 105, 425-433.

Gross, D.; **1993**. Phytoalexins of Brassicaceae. *Zeitschrift fuer Pflanzenkrankheiten und Pflanzenschutz*, 100, 433-442.

Grubb, C. D.; Zipp, B. J.; Ludwig-Mueller, J.; Masuno, M. N.; Molinski, T. F.; Abel, S.; **2004**. Arabidopsis glucosyltransferase UGT74B1 functions in glucosinolate biosynthesis and auxin homeostasis. *Plant Journal*, 40, 893-908.

Guo, L.; Poulton, E.; **1994**. Partial purification and characterization of *Arabidopsis thaliana* UDPG: thiohydroximate glucosyltransferase. *Phytochemistry*, 36, 1133-1138.

Halkier, B. A.; Gershenzon, J.; **2006**. Biology and biochemistry of glucosinolates. *Annual Review of Plant Biology*, 57, 303-333.

Hall, J. C.; Hoagland, R. E.; Zablotowicz, R. M.; **2000**. In: *Pesticide Biotransformation in Plants and Microorganisms; ACS symposium Series*; ACS: Washington, DC, p. 432.

Hammerschmidt, R.; **1999**. Phytoalexins: what have we learned after 60 years? *Annual Review of Phytopathology*, 37, 285-306

Hans, J.; Brandt, W.; Vogt, T.; **2004**. Site-directed mutagenesis and protein 3D-homology modelling suggest a catalytic mechanism for UDP-glucose-dependent betanidin 5-*O*-glucosyltransferase from *Dorotheanthus bellidiformis*. *Plant Journal*, 39, 319-333.

Hansen, K. S.; Kristensen, C.; Tattersall, D. B.; Jones, P. R.; Olsen, C. E.; Bak, S.; Moller, B. L.; **2003**. The in vitro substrate regiospecificity of recombinant UGT85B1, the cyanohydrin glucosyltransferase from *Sorghum bicolor*. *Phytochemistry*, 64, 143-151.

Harborne, J. B.; **1999**. The comparative biochemistry of phytoalexin induction in plants. *Biochemical Systematics and Ecology*, 27, 335-367.

Harborne, J. B.; Baxter, H.; (Eds); **1999**. *The Handbook of Natural Flavonoids*, Volume 1. p 889. Chichester, UK: Wiley.

Heslin, M. C.; Stuart, M. R.; Murchu, P. O.; Donnelly, D. M. X.; **1983**. Fomannoxin, a phytotoxic metabolite of Fomes annosus: in vitro production, host toxicity and isolation from naturally infected Sitka spruce heartwood. *European Journal of Forest Pathology*, 13, 11-23.

Hirotani, M.; Kuroda, R.; Suzuki, H.; Yoshikawa, T.; **2000**. Cloning and expression of UDP-glucose: flavonoid 7-*O*-glucosyltransferase from hairy root cultures of *Scutellaria baicalensis*. *Planta*, 210, 1006-1013.

Hirotani, M.; O'Reilly, J.; Donnelly, D. M. X.; Polonsky, J.; **1977**. Fomannoxin - a toxic metabolite of *Fomes annosus*. *Tetrahedron Letters*, 651-652.

Hofmann, D.; Knop, M.; Hao, H.; Hennig, L.; Sicker, D.; Schulz, M.; **2006**. Glucosides from MBOA and BOA detoxification by *Zea mays* and *Portulaca oleracea*. *Journal of Natural Products*, 69, 34-37.

Hogan, M. E.; Manners, G. D.; **1990**. Allelopathy of small everlasting (*Antennaria microphylla*) phytotoxicity to leafy spurge (*Euphorbia esula*) in tissue culture. *Journal of Chemical Ecology*, 16, 931-939.

Hogan, M. E.; Manners, G. D.; **1991**. Differential allelochemical detoxification mechanism in tissue cultures of *Antennaria microphylla* and *Euphorbia esula*. *Journal of Chemical Ecology*, 17, 167-174.

Hu, X.; Bidney, D. L.; Yalpani, N.; Duvick, J. P.; Crasta, O.; Folkerts, O.; Lu, G.; **2003**. Overexpression of a gene encoding hydrogen peroxide-generating oxalate oxidase evokes defense responses in sunflower. *Plant Physiology*, 133, 170–181.

Hu, Y.; Walker, S.; **2002**. Remarkable structural similarities between diverse glycosyltransferases. *Chemistry & Biology*, 9, 1287-1296.

Huang, H.C., and Dueck, J. **1980**. Wilt of sunflower from infection by mycelial-germinating sclerotia of *Sclerotinia sclerotiorum*. *Canadian Journal of Plant Pathology*, 2, 47- 52.

Huang, J.-S.; **2001**. In: *Plant pathogenesis and resistance*: biochemistry and physiology of plant-microbe interactions. Dordrecht, Netherland: Kluwer Academic Publishers, p. 487 and 624.

Humenik, M.; Dzurilla, M.; Kutschy, P.; Solcaniova, E.; Kovacik, V.; Bekesova, S.; **2004**. Synthesis of 1-glycosyl derivatives of benzocamalexin. *Collection of Czechoslovak Chemical Communications*, 69, 1657-1674.

Humenik, M.; Kutschy, P.; Kovacik, V.; Bekesova, S.; **2005a**. 1,2-Anhydrosaccharides and 1,2-cyclic sulfites as saccharide donors in convergent synthesis of glucopyranosyl-, mannopyranosyl- and ribofuranosylbenzocamalexin. *Collection of Czechoslovak Chemical Communications*, 70, 487-506.

Humenik, M.; Kutschy, P.; Valkova, K.; Horvath, B.; Kovacik, V.; Bekesova, S.; **2005b**. Synthesis of β-D-glucopyranosides of 6-substituted 2-(indol-3-yl)benzothiazoles. *Collection of Czechoslovak Chemical Communications*, 70, 72-84.

Ibrahim, A.-R. S.; Galal, A. M.; Mossa, J. S.; El-Feraly, F. S.; **1997**. Glucose-conjugation of the flavones of *Psiadia arabica* by *Cunninghamella elegans*. *Phytochemistry*, 46, 1193-1195.

Inderjit; Duke, S. O.; **2003**. Ecophysiological aspects of allelopathy. *Planta*, 217, 529-539.

Ingham, J. L.; **1982**. Phytoalexins from the Leguminosae. In: Bailey, J. A.; Mansfield J. W. (eds) *Phytoalexins*, New York: John Wiley & Sons, p. 21-80.

Isayenkova, J.; Wray, V.; Nimtz, M.; Strack, D.; Vogt, T.; **2006**. Cloning and functional characterization of two regioselective flavonoid glucosyltransferases from *Beta vulgaris*. *Phytochemistry*, 67, 1598-1612.

Jadhav, S. J.; Mazza, G.; Salunkhe, D. K.; **1991**. Terpenoid phytoalexins in potatoes: a review. *Food Chemistry*, 41, 195-217.

Jasalavich, C. A.; Seguin-Swartz, G.; Vogelgsang, S.; Petrie, G. A.; **1993**. Host range of *Alternaria* species pathogenic to crucifers. *Canadian Journal of Plant Pathology*, 15, 314-315.

Jones, G.; Stanforth, S. P.; **1997**. The Vilsmeier reaction of fully conjugated carbocycles and heterocycles. *Organic Reactions*, 49, 1-330.

Jones, P. R.; Moller, B. L.; Hoj, P. B.; **1999**. The UDP-glucose:*p*-hydroxymandelonitrile-*O*-glucosyltransferase that catalyzes the last step in synthesis of the cyanogenic glucoside dhurrin in *Sorghum bicolor*. Isolation, cloning, heterologous expression, and substrate specificity. *Journal of Biological Chemistry*, 274, 35483-35491.

Jones, P.; Vogt, T.; **2001**. Glycosyltransferases in secondary plant metabolism: tranquilizers and stimulant controllers. *Planta*, 213, 164-174.

Kamila, S.; Biehl, E.; **2004**. Preparation of benzothiopyrano[2,3-b]indoles by the reaction of 1,3-dihydroindole-2-thiones with certain dienophiles. *Heterocycles*, 63, 2785-2795.

Kamimura, H.; **1986**. Conversion of zearalenone to zearalenone glycoside by Rhizopus sp. *Applied and Environmental Microbiology*, 52, 515-519.

Kashulin, I. A.; Nifant'ev, I. E.; **2004**. Efficient method for the synthesis of hetarenoindanones based on 3-arylhetarenes and their conversion into hetarenoindenes. *Journal of Organic Chemistry*, 69, 5476-5479.

Kawasaki, T.; Kodama, A.; Nishida, T.; Shimizu, K.; Somei, M.; **1991**. Preparation of 1-hydroxyindole derivatives and a new route to 2-substituted indoles. *Heterocycles*, 32, 221-227.

Kawase, M.; Kitamura, T.; Kikugawa, Y.; **1989**. Electrophilic aromatic substitution with *N*-methoxy-*N*-acylnitrenium ions generated from *N*-chloro-*N*-methoxyamides: synthesis of nitrogen heterocyclic compounds bearing a *N*-methoxyamide group. *Journal of Organic Chemistry*, 54, 3394-3404.

Kim, J. H.; Kim, B. G.; Ko, J. H.; Lee, Y.; Hur, H.-G.; Lim, Y.; Ahn, J.-H.; **2006**. Molecular cloning, expression, and characterization of a flavonoid glycosyltransferase from *Arabidopsis thaliana*. *Plant Science*, 170, 897-903.

Kim, Y.-J.; Uyama, H.; **2005**. Tyrosinase inhibitors from natural and synthetic sources: Structure, inhibition mechanism and perspective for the future. *Cellular and Molecular Life Sciences* 62, 1707-1723.

King, R. R.; Lawrence, C. H.; Calhoun, L. A.; **1992**. Chemistry of phytotoxins associated with *Streptomyces scabies* the causal organism of potato common scab. *Journal of Agricultural and Food Chemistry*, 40, 834-837.

King, R. R.; Lawrence, C. H.; Calhoun, L. A.; **2000**. Microbial glucosylation of thaxtomin A, a partial detoxification. *Journal of Agricultural and Food Chemistry,* 48, 512-514.

Ko, J. H.; Kim, B. G.; Hur, H.-G.; Lim, Y.; Ahn, J.-H.; **2006**. Molecular cloning, expression and characterization of a glycosyltransferase from rice. *Plant Cell Reports*, 25, 741-746.

Kohara, A.; Nakajima, C.; Hashimoto, K.; Ikenaga, T.; Tanaka, H.; Shoyama, Y.; Yoshida, S.; Muranaka, T.; **2005**. A novel glucosyltransferase involved in steroid saponin biosynthesis in *Solanum aculeatissimum*. *Plant Molecular Biology*, 57, 225-239.

Kuiper-Goodman, T.; Scott, P. M.; Watanabe, H.; **1987**. Risk assessment of the mycotoxin zearalenone. *Regulatory Toxicology and Pharmacology: RTP*, 7, 253-306.

Kutschy, P.; Sabol, M.; Maruskova, R.; Curillova, Z.; Dzurilla, M.; Geci, I.; Alfoeldi, J.; Kovacik, V.; **2004**. A linear synthesis of 1-(β-D-glucopyranosyl)brassinin, -brassenin A, -brassenin B and 9-(β-D-glucopyranosyl)cyclobrassinin. *Collection of Czechoslovak Chemical Communications*, 69, 850-866.

Kutschy, P.; Suchy, M.; Monde, K.; Harada, N.; Maruskova, R.; Curillova, Z.; Dzurilla, M.; Miklosova, M.; Mezencev, R.; Mojzis, J. **2002**. Spirocyclization strategy toward indole phytoalexins. The first synthesis of (±)-1-methoxyspirobrassinin, (±)-1-methoxyspirobrassinol, and (±)-1-methoxyspirobrassinol methyl ether. *Tetrahedron Letters*, 43, 9489-9492.

Laks, P. E.; Pruner, M. S.; **1989**. Flavonoid biocides: structure/activity relations of flavonoid phytoalexin analogs. *Phytochemistry*, 28, 87-91.

Lanot, A.; Hodge, D.; Jackson, R. G.; George, G. L.; Elias, L.; Lim, E.-K.; Vaistij, F. E.; Bowles, D. J.; **2006**. The glucosyltransferase UGT72E2 is responsible for monolignol 4-*O*-glucoside production in *Arabidopsis thaliana*. *Plant Journal*, 48, 286-295.

Lazarevic, M.; Dimova, V.; Gabor, D. M.; Kakurinov, V.; Ragenovic, K. C.; **2001**. Synthesis of some *N*1-aryl/heteroarylaminomethyl/ethyl-1,2,4-triazoles and their antibacterial and antifungal activities. *Heterocyclic Communications*, 7, 577-582.

Lefol, C.; Seguin-Swartz, G., Morrall, R. A. A.; **1997**. Resistance to *Sclerotinia sclerotiorum* in a weed related to canola. *Canadian Journal of Plant Pathology*, 19, 113 (Abstract).

Legault, C.; and Charette, A. B.; **2003**. Highly efficient synthesis of *O*-(2,4-dinitrophenyl)hydroxylamine. Application to the synthesis of substituted *N*-benzoyliminopyridinium ylides. *Journal of Organic Chemistry*, 68, 7119-7122.

Leighton, V.; Niemeyer, H. M.; Jonsson, L. M. V.; **1994**. Substrate specificity of a glucosyltransferase and an *N*-hydroxylase involved in the biosynthesis of cyclic hydroxamic acids in Gramineae. *Phytochemistry*, 36, 887-92.

Lemmens, M.; Scholz, U.; Berthiller, F.; Dall'Asta, C.; Koutnik, A.; Schuhmacher, R.; Adam, G.; Buerstmayr, H.; Mesterhazy, A.; Krska, R.; Ruckenbauer, P.; **2005**. The ability to detoxify the mycotoxin deoxynivalenol colocalizes with a major quantitative trait locus for fusarium head blight resistance in wheat. *Molecular Plant-Microbe Interactions*, 18, 1318-1324.

Lim, E.-K.; Bowles, D. J.; **2004**. A class of plant glycosyltransferases involved in cellular homeostasis. *EMBO Journal*, 23, 2915-2922.

Lim, E.-K.; Higgins, G. S; Li, Y.; Bowles D. J.; **2003**. Regioselectivity of glucosylation of caffeic acid by a UDP-glucose: glucosyltransferase is maintained in planta. *The Biochemical Journal*, 373, 987-992.

Lim, E.-K.; Li, Y.; Parr, A.; Jackson, R.; Ashford, D. A.; Bowles, D. J.; **2001**. Identification of glucosyltransferase genes involved in sinapate metabolism and lignin synthesis in Arabidopsis. *Journal of Biological Chemistry*, 276, 4344-4349.

Lunkenbein, S.; Bellido, M.; Aharoni, A.; Salentijn, E. M. J.; Kaldenhoff, R.; Coiner, H. A.; Munoz-Blanco, J.; Schwab, W.; **2006**. Cinnamate metabolism in ripening fruit. Characterization of a UDP-glucose: cinnamate glucosyltransferase from strawberry. *Plant Physiology*, 140, 1047-1058.

Manners, G. D.; Galitz, D. S.; **1986**. Allelopathy of small everlasting (*Antennaria microphylla*): identification of constituents phytotoxic to leafy spurge (*Euphorbia esula*). *Weed Science*, 34, 8-12.

Manzanares-Dauleux, M. J.; Barret, P.; Thomas, G.; **2000**. Development of a pathotype specific SCAR marker in *Plasmodiophora brassicae*. *European Journal of Plant Pathology*, 106, 781-787.

Marillia, E.-F.; MacPherson, J. M.; Tsang, E. W. T.; Van Audenhove, K.; Keller, W. A.; GrootWassink, J. W. D.; **2001**. Molecular cloning of a *Brassica napus* thiohydroximate *S*-glucosyltransferase gene and its expression in *Escherichia coli*. *Physiologia Plantarum*, 113, 176-184.

Matolcsy, G.; Nadasy, M.; Andriska, V.; **1988**. In *Pesticide Chemistry*, p. 354, New York: Elsevier.

Matsuo, M.; Underhill, E. W.; **1971**. Biosynthesis of mustard oil glucosides. XIII. Purification and properties of a UDP glucose: Thiohydroximate glucosyltransferase from higher plants. *Phytochemistry*, 10, 2279-2286.

Mehta, R. G.; Liu, J.; Constantinou, A.; Thomas, C. F.; Hawthorne, M.; You, M.; Gerhaeuser, C.; Pezzuto, J. M.; Moon, R. C.; Moriarty, R. M.; **1995**. Cancer-chemopreventive activity of brassinin, a phytoalexin from cabbage. *Carcinogenesis*, 16, 399-404.

Mesterhazy, A.; **2003**. In: *Fusarium head blight of wheat*, American Phytopathological society, St. Paul, MN. p. 363-380.

Meyer, M. D.; Kruse, L. I.; **1984**, Ergoline synthons: Synthesis of 3,4-dihydro-6-methoxybenz[cd]indol-5(1H)-one (6-methoxy-Uhle's ketone) and 3,4-dihydrobenz[cd]indol-5(1H)-one (Uhle's ketone) via a novel decarboxylation of indole-2-carboxylates. *Journal of Organic Chemistry*, 49, 3195-3199.

Milkowski, C.; Baumert, A.; Schmidt, D.; Nehlin, L.; Strack, D.; **2004**. Molecular regulation of sinapate ester metabolism in *Brassica napus*: expression of genes, properties of the encoded proteins and correlation of enzyme activities with metabolite accumulation. *Plant Journal*, 38, 80-92.

Milkowski, C.; Baumert, A.; Strack, D.; **2000a**. Cloning and heterologous expression of a rape cDNA encoding UDP-glucose: sinapate glucosyltransferase. *Planta*, 211, 883-886.

Milkowski, C.; Baumert, A.; Strack, D.; **2000b**. Identification of four Arabidopsis genes encoding hydroxycinnamate glucosyltransferases. *FEBS Letters*, 486, 183-184.

Miller, J. D.; Arnison, P. G.; **1986**. Degradation of deoxynivalenol by suspension cultures of the fusarium head blight resistant wheat cultivar Frontana. *Canadian Journal of Plant Pathology*, 8, 147-150.

Mithen, R. F.; Magrath, R.; **1992**. Glucosinolates and resistance to *Leptosphaeria maculans* in wild and cultivated Brassica species. *Plant Breeding*, 108, 60-68.

Moehs, C. P.; Allen, P. V.; Friedman, M.; Belknap, W. R.; **1997**. Cloning and expression of solanidine UDP-glucose glucosyltransferase from potato. *Plant Journal*, 11, 227-236.

Monde, K.; Takasugi, M.; Ohnishi, T.; **1994**. Biosynthesis of cruciferous phytoalexins. *Journal of the American Chemical Society*, 116, 6650-6657.

Mulichak, A. M.; Losey, H. C.; Lu, W.; Wawrzak, Z.; Walsh, C. T.; Garavito, R. M.; **2003**. Structure of the TDP-epi-vancosaminyltransferase GtfA from the chloroeremomycin biosynthetic pathway. *Proceedings of the National Academy of Sciences of the United States of America*, 100, 9238-9243.

Mulichak, A. M.; Losey, H. C.; Walsh, C. T.; Garavito, R. M.; **2001**. Structure of the UDP-glucosyltransferase GtfB that modifies the heptapeptide aglycone in the biosynthesis of vancomycin group antibiotics. *Structure*, 9, 547-557.

Mulichak, A. M.; Lu, W.; Losey, H. C.; Walsh, C. T.; Garavito, R. M.; **2004**. Crystal structure of vancosaminyltransferase GtfD from the vancomycin biosynthetic pathway: Interactions with acceptor and nucleotide ligands. *Biochemistry*, 43, 5170-5180.

Müller, K. O.; Börger, H.; **1940**. Experimentelle untersuchungen uber die *Phytophthora*-resistenz der Kartoffel. *Arb Biol Anst Reichsanst* (Berlin), 23, 189-231.

Nielek, S.; Lesiak, T.; **1982**. Chemistry of thiazole. I. Synthesis and properties of 2,3,5,6-tetrahydro-6-(3-methylbenzofuran-2-yl)imidazo[2,1-b]thiazole. *Chemische Berichte*, 115, 1247-1251.

Niemann, G. J.; **1993**. The anthranilamide phytoalexins of the Caryophyllaceae and related compounds. *Phytochemistry*, 34, 319-328.

Nukada, T.; Berces, A.; Zgierski, M. Z.; Whitfield, D. M.; **1998**. Exploring the mechanism of neighboring group assisted glycosylation reactions. *Journal of the American Chemical Society*, 120, 13291-13295.

Offen, W.; Martinez-Fleites, C.; Yang, M.; Eng, K.-L.; Davis, B. G.; Tarling, C. A.; Ford, C. M.; Bowles, D. J.; Davies, G. J.; **2006**. Structure of a flavonoid glucosyltransferase reveals the basis for plant natural product modification. *EMBO Journal*, 25, 1396-1405.

Ogata, J.; Kanno, Y.; Itoh, Y.; Tsugawa, H.; Suzuki, M.; **2005**. Plant biochemistry: Anthocyanin biosynthesis in roses. *Nature*, 435, 757-758.

Oh, S.-J.; Lee, K. C.; Lee, S.-Y.; Ryu, E. K.; Saji, H.; Choe, Y. S.; Chi, D. Y.; Kim, S. E.; Lee, J.; Kim, B.-T.; **2004**. Synthesis and evaluation of fluorine-substituted 1H-pyrrolo[2,3-b]pyridine derivatives for dopamine D4 receptor imaging. *Bioorganic & Medicinal Chemistry*, 12, 5505-5513.

Ohkubo, M.; Nishimura, T.; Jona, H.; Honma, T.; Ito, S.; Morishima, H.; **1997**. Synthesis of dissymmetric indolocarbazole glycosides using the Mitsunobu reaction at the glycosylation step. *Tetrahedron*, 53, 5937-5950.

Osbourn, A. E.; **1996**. Preformed antimicrobial compounds and plant defense against fungal attack. *Plant Cell*, 8, 1821-1831.

Osbourn, A. E.; **2003**. Saponins in cereals. *Phytochemistry*, 62, 1-4

Park, S. H.; Stierle, A.; Strobel, G. A.; **1994**. Metabolism of maculosin, a host-specific phytotoxin produced by *Alternaria alternata* on spotted knapweed (*Centaurea maculosa*). *Phytochemistry*, 35, 101-106.

Parker, D.; **1991**. NMR determination of enantiomeric purity. *Chemical Reviews* (Washington, DC, United States), 91, 1441-1457.

Pedras, M. S. C.; **1998**. Towards an understanding and control of plant fungal diseases in Brassicaceae, *Agricultural & Food Chemistry*, 2, 513-532.

Pedras, M. S. C.; **2001**. Phytotoxins from fungi causing blackleg disease on crucifers: isolation, structure determination, detection, and phytotoxic activity. *Recent Research Developments in Phytochemistry*, 5, 109-117.

Pedras, M. S. C.; Abrams, S. R.; Seguin-Swartz, G.; **1988**. Isolation of the first naturally occurring epimonothiodioxopiperazine, a fungal toxin produced by *Phoma lingam*. *Tetrahedron Letters*, 29, 3471-3474.

Pedras, M. S. C.; Abrams, S. R.; Seguin-Swartz, G.; Quail, J. W.; Jia, Z.; **1989**. Phomalirazine, a novel toxin from the phytopathogenic fungus *Phoma lingam*. *Journal of the American Chemical Society*, 111, 1904-1905.

Pedras, M. S. C.; Ahiahonu, P. W. K.; **2002**, Probing the phytopathogenic stem rot fungus with phytoalexins and analogues: unprecedented glucosylation of camalexin and 6-methoxycamalexin. *Bioorganic & Medicinal Chemistry*, 10, 3307-3312.

Pedras, M. S. C.; Ahiahonu, P. W. K.; **2004**. Phytotoxin production and phytoalexin elicitation by the phytopathogenic fungus *Sclerotinia sclerotiorum*. *Journal of Chemical Ecology*, 30, 2163-2179.

Pedras, M. S. C.; Ahiahonu, P. W. K.; **2005**. Metabolism and detoxification of phytoalexins and analogs by phytopathogenic fungi. *Phytochemistry*, 66, 391-411.

Pedras, M. S. C.; Ahiahonu, P. W. K.; Hossain, M.; **2004c**. Detoxification of the cruciferous phytoalexin brassinin in *Sclerotinia sclerotiorum* requires an inducible glucosyltransferase. *Phytochemistry*, 65, 2685-2694.

Pedras, M. S. C.; Borgmann, I.; Taylor, J. L.; **1992**. Biotransformation of brassinin is a detoxification in the "blackleg" fungus. *Phytochemistry*, 11, 1-7.

Pedras, M. S. C.; Chumala, P. B.; Quail, J. W.; **2004a**. Chemical Mediators: The remarkable structure and host-selectivity of depsilairdin, a sesquiterpenic depsipeptide containing a new amino acid. *Organic Letters*, 6, 4615-4617.

Pedras, M. S. C.; Chumala, P. B.; Suchy, M.; **2003b**. Phytoalexins from *Thlaspi arvense*, a wild crucifer resistant to virulent *Leptosphaeria maculans*: structures, syntheses and antifungal activity. *Phytochemistry*, 64, 949-956.

Pedras, M. S. C.; Hossain, M.; **2006**, Metabolism of crucifer phytoalexins in Sclerotinia sclerotiorum: detoxification of strongly antifungal compounds involves glucosylation. *Organic & Biomolecular Chemistry*, 4, 2581-2590.

Pedras, M. S. C.; Hossain, M.; Sarwar, M. G.; Montaut, S.; **2004d**. Determination of the enantiomeric purity of the phytoalexins spirobrassinins by 1H NMR using chiral solvation. *Bioorganic & Medicinal Chemistry Letters*, 14, 5469-5471.

Pedras, M. S. C.; Jha, M.; **2005**. Concise syntheses of the cruciferous phytoalexins brassilexin, sinalexin, wasalexins, and analogues: expanding the scope of the Vilsmeier formylation. *Journal of Organic Chemistry*, 70, 1828-1834.

Pedras, M. S. C.; Jha, M.; **2006**. Toward the control of *Leptosphaeria maculans*: Design, syntheses, biological activity, and metabolism of potential detoxification inhibitors of the crucifer phytoalexin brassinin. *Bioorganic & Medicinal Chemistry*, 14, 4958-4979.

Pedras, M. S. C.; Jha, M.; Ahiahonu, P. W. K.; **2003a**. The synthesis and biosynthesis of phytoalexins produced by cruciferous plants. *Current Organic Chemistry*, 7, 1635-1647

Pedras, M. S. C.; Jha, M.; Okeola, O. G.; **2005b**. Camalexin induces detoxification of the phytoalexin brassinin in the plant pathogen *Leptosphaeria maculans*. *Phytochemistry*, 66, 2609-2616.

Pedras, M. S. C.; Khan, A. Q., **1996**. Biotransformation of the brassica phytoalexin brassicanal A by the blackleg fungus. *Journal of Agricultural and Food Chemistry*, 44, 3403-3407.

Pedras, M. S. C.; Khan, A. Q.; Smith, K. C.; Stettner, S. L.; **1997**. Preparation, biotransformation, and antifungal activity of methyl benzyldithiocarbamates. *Canadian Journal of Chemistry*, 75, 825-828.

Pedras, M. S. C.; Khan, A. Q.; Taylor, J. L.; **1998**. The phytoalexin camalexin is not metabolized by *Phoma lingam*, *Alternaria brassicae*, or phytopathogenic bacteria. *Plant Science*, 139, 1-8.

Pedras, M. S. C.; Liu, J.; **2004**. Designer phytoalexins: probing camalexin detoxification pathways in the phytopathogen *Rhizoctonia solani*. *Organic & Biomolecular Chemistry*, 2, 1070-1076.

Pedras, M. S. C.; Montaut, S.; **2003**. Probing crucial metabolic pathways in fungal pathogens of crucifers: biotransformation of indole-3-acetaldoxime, 4-hydroxyphenylacetaldoxime, and their metabolites. *Bioorganic & Medicinal Chemistry* 11, 3115-3120.

Pedras, M. S. C.; Montaut, S.; Suchy, M.; **2004b**. Phytoalexins from the crucifer rutabaga: Structures, syntheses, biosyntheses, and antifungal activity. *Journal of Organic Chemistry*, 69, 4471-4476.

Pedras, M. S. C.; Montaut, S.; Zaharia, I. L.; Gai, Y.; Ward, D. E.; **2003c**. Transformation of the host-selective toxin destruxin B by wild crucifers: probing a detoxification pathway. *Phytochemistry*, 64, 957-963.

Pedras, M. S. C.; Okanga, F. I.; **1999**. Strategies of cruciferous pathogenic fungi: detoxification of the phytoalexin cyclobrassinin by mimicry. *Journal of Agricultural and Food Chemistry*, 47, 1196-1202.

Pedras, M. S. C.; Okanga, F. I.; Zaharia, I. L.; Khan, A. Q.; **2000**. Phytoalexins from crucifers: synthesis, biosynthesis, and biotransformation. *Phytochemistry*, 53, 161-176.

Pedras, M. S. C.; Sarwar, M. G.; Suchy, M.; Adio, A. M.; **2006b**, The phytoalexins from cauliflower, caulilexins A, B and C: Isolation, structure determination, syntheses and antifungal activity. *Phytochemistry*, 67, 503-1509.

Pedras, M. S. C.; Sorensen, J. L.; **1998**. Phytoalexin accumulation and antifungal compounds from the crucifer wasabi. *Phytochemistry*, 49, 1959.

Pedras, M. S. C.; Suchy, M.; **2005**. Detoxification pathways of the phytoalexins brassilexin and sinalexin in Leptosphaeria maculans: Isolation and synthesis of the elusive intermediate 3-formylindolyl-2-sulfonic acid. *Organic & Biomolecular Chemistry* 3, 2002-2007.

Pedras, M. S. C.; Suchy, M.; Ahiahonu, P. W. K.; **2006a**. Unprecedented chemical structure and biomimetic synthesis of erucalexin, a phytoalexin from the wild crucifer *Erucastrum gallicum*. *Organic & Biomolecular Chemistry*, 4, 691-701.

Pedras, M. S. C.; Taylor, J. L.; Nakashima, T. T.; **1993**. A novel chemical signal from the "blackleg" fungus: beyond phytotoxins and phytoalexins. *Journal of Organic Chemistry*, 58, 4778-4780.

Pedras, M. S. C.; Yu, Y.; Liu, J.; Tandron-Moya, Y. A.; **2005a**. Metabolites produced by the phytopathogenic fungus *Rhizoctonia solani*: Isolation, chemical structure determination, syntheses and bioactivity. *Zeitschrift fuer Naturforschung*, C: *Journal of Biosciences*, 60, 717-722.

Pedras, M. S. C.; Zaharia, I. L.; **2000**. Sinalbins A and B, phytoalexins from *Sinapis alba*: elicitation, isolation, and synthesis. *Phytochemistry*, 55, 213-216.

Pedras, M. S. C.; Zaharia, I. L.; **2001**. Unprecedented Vilsmeier formylation: expedient syntheses of the cruciferous phytoalexins sinalexin and brassilexin and discovery of a new heteroaromatic ring system. *Organic Letters*, 3, 1213-1216.

Pedras, M. S. C.; Zaharia, I. L.; Gai, Y.; Zhou, Y.; Ward, D. E.; **2001**. In planta sequential hydroxylation and glycosylation of a fungal phytotoxin: Avoiding cell death and overcoming the fungal invader. *Proceedings of the National Academy of Sciences of the United States of America*, 98, 747-52.

Perrin, D. R.; Bottomley, W.; **1962**. Studies on phytoalexins. V. The structure of pisatin from *Pisum sativum*. *Journal of the American Chemical Society*, 84, 1919-1922.

Pflugmacher, S.; Sandermann, H. J.; **1998**. Taxonomic distribution of plant glucosyltransferases acting on xenobiotics. *Phytochemistry*, 49, 507-511.

Pirkle, W. H.; Hoover, D. J.; **1982**. NMR chiral solvating agents. *Topics in Stereochemistry*, 13, 263-331.

Poppenberger, B.; Berthiller, F.; Bachmann, H.; Lucyshyn, D.; Peterbauer, C.; Mitterbauer, R.; Schuhmacher, R.; Krska, R.; Gloessl, J.; Adam, G.; **2006**. Heterologous expression of Arabidopsis UDP-glucosyltransferases in *Saccharomyces cerevisiae* for production of zearalenone-4-*O*-glucoside. *Applied and Environmental Microbiology*, 72, 4404-4410.

Poppenberger, B.; Berthiller, F.; Lucyshyn, D.; Sieberer, T.; Schuhmacher, R.; Krska, R.; Kuchler, K.; Gloessl, J.; Luschnig, C.; Adam, G.; **2003**. Detoxification of the Fusarium mycotoxin deoxynivalenol by a UDP-glucosyltransferase from *Arabidopsis thaliana*. *Journal of Biological Chemistry*, 278, 47905-47914.

Preobrazhenskaya, M. N.; Korbukh, I. A.; **1988**. The synthesis and reactions of pyrrole, pyrazole, triazole, indole, indazole, and benzotriazole nucleosides and nucleotides. *Chemistry of Nucleosides and Nucleotides* (Ed. By Townsend, L. B.), Plenum Press, New York, 3, 1-97.

Radominska-Pandya, A.; Little, J. M.; Czernik, P. J.; **2001**. Human UDP-glucuronosyltransferase 2B7. *Current Drug Metabolism*, 2, 283-298.

Reed, D. W.; Davin, L.; Jain, J. C.; Deluca, V.; Nelson, L.; Underhill, E. W.; **1993**. Purification and properties of UDP-glucose: thiohydroximate glucosyltransferase from *Brassica napus* L. seedlings. *Archives of Biochemistry and Biophysics*, 305, 526-32.

Richman, A.; Swanson, A.; Humphrey, T.; Chapman, R.; McGarvey, B.; Pocs, R.; Brandle, J.; **2005**. Functional genomics uncovers three glucosyltransferases involved in the synthesis of the major sweet glucosides of *Stevia rebaudiana*. *Plant Journal*, 41, 56-67.

Rodriguez, J. G., Lafuente, A. and Garcia-Almaraz, P., **2000**. Synthesis and structural analysis of (*E*)-2-(2'-nitrovinyl)indoles from the corresponding 2-formylindole derivatives. *Journal of Heterocyclic Chemistry*, 37, 1281-1288.

Rogers, E. E.; Glazebrook, J.; Ausubel, F. M.; **1996**. Mode of action of the *Arabidopsis thaliana* phytoalexin camalexin and its role in Arabidopsis-pathogen interactions. *Molecular Plant-Microbe Interactions*, 9, 748-757.

Roshchin, A. I.; Kel'chevski, S. M.; Bumagin, N. A.; **1998**. Synthesis of benzofurans via $Pd^{2+}$-catalyzed oxidative cyclization of 2-allylphenols. *Journal of Organometallic Chemistry*, 560, 163-167.

Rouxel, T.; Kollmann, A.; Balesdent, M.-H.; **1995**. Phytoalexins from the crucifers. In: Daniel, M.; Purkayastha, R. P. (eds). *Handbook of Phytoalaexin Metabolism and Action*. New York: Macel Dekker, p. 229-261.

Sandermann, H. J.; Haas, M.; Messner, B.; Pflugmacher, S.; Schroder, P.; Wetzel, A.; **1997**. The role of glucosyl and malonyl conjugation in herbicide selectivity. *NATO ASI Series, Series 3: High Technology*, 37 (Regulation of Enzymatic Systems Detoxifying Xenobiotics in Plants), 211-231.

Schnabel, M.; Rompp, B.; Ruckdeschel, D.; Unverzagt, C.; **2004**. Synthesis of tryptophan *N*-glucoside. *Tetrahedron Letters*, 45, 295-297.

Schneweis, I.; Meyer, K.; Engelhardt, G.; Bauer, J.; **2002**. Occurrence of zearalenone-4-beta-D-glucopyranoside in wheat. *Journal of Agricultural and Food Chemistry*, 50, 1736-1738.

Schulz, M.; Wieland, I.; **1999**. Variation in metabolism of BOA among species in various field communities. Biochemical evidence for co-evolutionary processes in plant communities? *Chemoecology*, 9, 133-141.

Schulze-lefert, P.; Panstruga, R.; **2003**. Establishment of biotrophy by parasitic fungi and reprogramming of host cells for disease resistance. *Annual Review of Phytopathology*, 41, 641-667.

Sewald, N.; Lepschy von Gleissenthall, J.; Schuster, M.; Mueller, G.; Aplin, R. T.; **1992**. Structure elucidation of a plant metabolite of 4-desoxynivalenol. *Tetrahedron: Asymmetry*, 3, 953-960.

Shao, H.; He, X.; Achnine, L.; Blount, J. W.; Dixon, R. A.; Wang, X.; **2005**. Crystal structures of a multifunctional triterpene/flavonoid glycosyltransferase from Medicago truncatula. *Plant Cell*, 17, 3141-3154.

Sicker, D.; Frey, M.; Schulz, M.; Gierl, A.; **2000**. Role of natural benzoxazinones in the survival strategy of plants. *International Review of Cytology*, 198, 319-346.

Sicker, D.; Hao, H.; Schulz, M.; **2004**. Benzoxazolin-2(3H)-ones: Generation, effects and detoxification in the competition among plants. *Allelopathy*, 77-102.

Sicker, D.; Schneider, B.; Hennig, L.; Knop, M.; Schulz, M.; **2001**. Glycoside carbamates from benzoxazolin-2(3H)-one detoxification in extracts and exudates of corn roots. *Phytochemistry*, 58, 819-825.

Sippell, D. W.; Davidson, J. G. N.; Sadasivaia, R. S.; **1985**. *Rhizoctonia* root rot of rapeseed in the Peace region of Alberta. *Canadian Journal of Plant Pathology*, 7, 184-186.

Smith, C. J.; **1996**. Accumulation of phytoalexins: defense mechanism and stimulus response system. *New Phytologist*, 132, 1-45.

Sokolova, T. N.; Shevchenko, V. E.; Preobrazhenskaya, M. N.; **1980**. Interaction of indoles with glycosyl halides in the presence of silver oxide. *Carbohydrate Research*, 83, 249-61.

Sonnenbichler, J.; Bliestle, I. M.; Peipp, H.; Holdenrieder, O.; **1989**. Secondary fungal metabolites and their biological activities, I. Isolation of antibiotic compounds from cultures of Heterobasidion annosum synthesized in the presence of antagonistic fungi or host plant cells. *Biological Chemistry Hoppe-Seyler*, 370, 1295-1303.

Stierle, A. C.; Cardellina, J. H. II; Strobel, G. A.; **1988**. Maculosin, a host-specific phytotoxin for spotted knapweed from Alternaria alternata. *Proceedings of the National Academy of Sciences of the United States of America*, 85, 8008-8011.

Strobel, G. A.; Hess, W. M.; **1997**. Glucosylation of the peptide leucinostatin A, produced by an endophytic fungus of European yew, may protect the host from leucinostatin toxicity. *Chemistry & Biology*, 4, 529-536.

Strobel, G. A.; Torczynski, R.; Bollon, A.; **1997**. Acremonium sp.-a leucinostatin A producing endophyte of European yew (*Taxus baccata*). *Plant Science* (Shannon, Ireland), 128, 97-108.

Suchy, M.; Kutschy, P.; Monde, K.; Goto, H.; Harada, N.; Takasugi, M.; Dzurilla, M.; Balentova, E.; **2001**. Synthesis, absolute configuration, and enantiomeric enrichment of a cruciferous oxindole phytoalexin, (*S*)-(-)-spirobrassinin, and its oxazoline analog. *Journal of Organic Chemistry*, 66, 3940-3947.

Sue, M.; Ishihara, A.; Iwamura, H.; **2000**. Occurrence and characterization of a UDP-glucose: hydroxamic acid glucosyltransferase isolated from wheat (Triticum aestivum) seedlings. *Zeitschrift fuer Naturforschung*, C: *Journal of Biosciences*, 55, 701-707.

Suu, V. T.; Buu-Hoi, N. P.; Xuong, N. D.; **1962**. Some properties of 2-formylbenzofuran. *Bulletin de la Societe Chimique de France*, 1875-1877.

Suzuki, T.; Kim, S.-J.; Yamauchi, H.; Takigawa, S.; Honda, Y.; Mukasa, Y.; **2005**. Characterization of a flavonoid 3-*O*-glucosyltransferase and its activity during cotyledon growth in buckwheat (*Fagopyrum esculentum*). *Plant Science*, 169, 943-948.

Taguchi, G.; Ubukata, T.; Hayashida, N.; Yamamoto, H.; Okazaki, M.; **2003**. Cloning and characterization of a glucosyltransferase that reacts on 7-hydroxyl group of flavonol and 3-hydroxyl group of coumarin from tobacco cells. *Archives of Biochemistry and Biophysics*, 420, 95-102.

Takasugi, M.; Katsui, N.; Shirata, A.; **1986**. Isolation of three novel sulfur-containing phytoalexins from the Chinese cabbage *Brassica campestris* L. ssp. pekinensis (Cruciferae). *Journal of the Chemical Society*, *Chemical Communications*, 1077-1078.

Takasugi, M.; Monde, K.; Katsui, N.; Shirata, A.; **1988**. Studies on stress metabolites. 7. Novel sulfur-containing phytoalexins from the Chinese cabbage *Brassica campestris* L. ssp. pekinensis (Cruciferae). *Bulletin of the Chemical Society of Japan*, 61, 285-289.

Tanaka, Y.; Yonekura, K.; Fukuchi-Mizutani, M.; Fukui, Y.; Fujiwara, H.; Ashikari, T.; Kusumi, T.; **1996**. Molecular and biochemical characterization of three anthocyanin synthetic enzymes from *Gentiana triflora*. *Plant and Cell Physiology*, 37, 711-716.

Theologis, A.; Ecker, J. R.; Palm, C. J.; Federspiel, N. A.; Kaul, S.; White, O.; Alonso, J.; Altafi, H.; Araujo, R.; Bowman, C. L.; Brooks, S. Y.; Buehler, E.; Chan, A.; Chao, Q.; Chen, H.; Cheuk, R. F.; Chin, C. W.; Chung, M. K.; Conn, L.; Conway, A. B.; Conway, A. R.; Creasy, T. H.; Dewar, K.; Dunn, P.; Etgu, P.; Fedlblyum, T. V.; Feng, J.; Fong, B.; Fujii, C. Y.; Gill, J. E.; Goldsmith, A. D.; Haas, B.; Hansen, N. F.; Hughes, B.; Hulzar, L.; Hunter, J. L.; Jenkins, J.; Johnson-Hopson, C.; Khan, S.; Khaykin, E.; Kim, C. J.; Koo, H. L.; Kremenetskala, I.; Kurtz, D. B.; Dwan, A.; Lam, B.; Langin-Hooper, S.; Lee, A.; Lee, J. M.; Lenz, C. A.; Li, J. H.; Li, Y.; Lin, X.; Liu, S. X.; Liu, Z. A.; Luros, J. S.; Malti, R.; Marziall, A.; Militscher, J.; Miranda, M.; Nguyen, M.; Nierman, W. C.; Osborne, B. I.; Pal, G.; Peterson, J.; Pham, P. K.; Rizzo, M.; Rooney, T.; Rowley, D.; Sakano, H.; Salzberg, S. L.; Schwartz, J. R.; Shinn, P.; Southwick, A. M.; Sun, H.; Tallon, L. J.; Tambunga, G.; Toriumi, M. J.; Town, C. D.; Utterback, T.; VanAken, S.; Vaysberg, M.; Vysotskala, V. S.; Walker, M.; Wu, D.; Yu, G.; Fraser, C. M.; Venter, J. C.; Davis, R. W.; **2000**. Sequence and analysis of chromosome 1 of the plant *Arabidopsis thaliana*. *Nature*, 408, 816-820.

Thorson, J. S.; Hosted, T. J. Jr.; Jiang, J.; Biggins, J. B.; Ahlert, J.; **2001**. Nature's carbohydrate chemists: the enzymatic glycosylation of bioactive bacterial metabolites. *Current Organic Chemistry*, 5, 139-167.

Tohge, T.; Nishiyama, Y.; Hirai, M. Y.; Yano, M.; Nakajima, J.-I.; Awazuhara, M.; Inoue, E.; Takahashi, H.; Goodenowe, D. B.; Kitayama, M.; Noji, M.; Yamazaki, M.; Saito, K.; **2005**. Functional genomics by integrated analysis of metabolome and transcriptome of Arabidopsis plants over-expressing an MYB transcription factor. *Plant Journal*, 42, 218-235.

Tomiyama, K.; Sakuma, T.; Ishizaka, N.; Sato, N.; Katsui, N.; Takasugi, M.; Masamune, T.; **1968**. New antifungal substance isolated from resistant potato tuber tissue infected by pathogens. *Phytopathology*, 58, 115-116.

Unligil, U. M.; Rini, J. M.; **2000**. Glycosyltransferase structure and mechanism. *Current Opinion in Structural Biology*, 10, 510-517.

VanEtten, H.; Temporini, E.; Wasmann, C.; **2001**, Phytoalexin (and phytoanticipin) tolerance as a virulence trait: why is it not required by all pathogens? *Physiological and Molecular Plant Pathology*, 59, 83-93.

Veronese, P.; Nakagami, H.; Bluhm, B.; AbuQamar, S.; Chen, X.; Salmeron, J.; Dietrich, R. A.; Hirt, H.; Mengiste, T.; **2006**. The membrane-anchored botrytis-induced kinase1 plays distinct roles in Arabidopsis resistance to necrotrophic and biotrophic pathogens. *Plant Cell*, 18, 257-273.

Vogt, T.; Grimm, R.; Strack, D.; **1999**. Cloning and expression of a cDNA encoding betanidin 5-*O*-glucosyltransferase, a betanidin- and flavonoid-specific enzyme with high homology to inducible glucosyltransferases from the Solanaceae. *Plant Journal*, 19, 509-519.

Vogt, T.; Jones, P.; **2000**. Glycosyltransferases in plant natural product synthesis: characterization of a supergene family. *Trends in Plant Science*, 5, 380-386.

Vogt, T.; Zimmermann, E.; Grimm, R.; Meyer, M.; Strack, D.; **1997**. Are the characteristics of betanidin glucosyltransferases from cell-suspension cultures of *Dorotheanthus bellidiformis* indicative of their phylogenetic relation ship with flavonoid glucosyltransferases? *Planta*, 203, 349-361.

von Rad, U.; Huttl, R.; Lottspeich, F.; Gierl, A.; Frey, M.; **2001**. Two glucosyltransferases are involved in detoxification of benzoxazinoids in maize. *Plant Journal*, 28, 633-642.

Wahlroos, O.; Virtanen, A. I.; **1959**. The precursors of 6-methoxybenzoxazolinone in maize and wheat plants, their isolation and some of their properties. *ACTA Chem Scand* 13, 1906-1908.

Walter, M. H.; Fester, T.; Strack, D.; **2000**. Arbuscular mycorrhizal fungi induce the non-mevalonate methylerythritol phosphate pathway of isoprenoid biosynthesis correlated with accumulation of the 'yellow pigment' and other apocarotenoids. *Plant Journal*, 21, 571-578.

Wenzel, T. J.; **2000**. Lanthanide-chiral solvating agent couples as chiral NMR shift reagents. *Trends in Organic Chemistry*, 8, 51-64.

Weston, L. A.; Duke, S. O.; **2003**. Weed and crop allelopathy. *Critical Reviews in Plant Sciences,* 22, 367-389.

Weymouth-Wilson A. C.; **1997**. The role of carbohydrates in biologically active natural products. *Natural Product Reports*, 14, 99-110.

Wieland, I.; Kluge, M.; Schneider, B.; Schmidt, J.; Sicker, D.; Schulz, M.; **1998**. 3-β-D-glucopyranosyl-benzoxazolin-2(3H)-one -a detoxification product of benzoxazolin-2(3H)-one in oat roots. *Phytochemistry*, 49, 719-722.

Yamazaki, M.; Gong, Z.; Fukuchi-Mizutani, M.; Fukui, Y.; Tanaka, Y.; Kusumi, T.; Saito, K.; **1999**. Molecular cloning and biochemical characterization of a novel anthocyanin 5-*O*-glucosyltransferase by mRNA differential display for plant forms regarding anthocyanin. *Journal of Biological Chemistry*, 274, 7405-7411.

Zaidlewicz, M.; Chechlowska, A.; Prewysz-Kwinto, A.; Wojtczak, A.; **2001**. Enantioselective synthesis of 2- and 3-benzofuryl β-amino alcohols. *Heterocycles*, 55, 569-577.

Zill, G.; Ziegler, W.; Engelhardt, G.; Wallnoefer, P. R.; **1990**. Chemically and biologically synthesized zearalenone-4-β-D-glucopyranoside: comparison and convenient determination by gradient HPLC. *Chemosphere*, 21, 435-42.

Zweimuller, M.; Antus, S.; Kovacs, T.; Sonnenbichler, J.; **1997**. Biotransformation of the fungal toxin fomannoxin by conifer cell cultures. *Biological Chemistry*, 378, 915-921.